DECLARATION

I declare that all work included in this thesis is my own except where otherwise stated. No part of this work has been or will be submitted for any other degree of professional qualification.

Karen Sherwood

2008

Centre for Infectious Diseases
University of Edinburgh
Summerhall
Edinburgh
EH9 1QH

ACKNOWLEDGEMENTS

My deepest thanks must first go to my supervisor, **Professor John Fazakerley**, without whom this thesis would never have happened. I have learnt an incredible amount working with John and it has been an honor to have completed this project with him. Thank you also to **Dr. Mark Head**, for his unwavering belief, support and understanding, through all the bad times and until the bitter end. I could not have asked for two better supervisors. I have been incredibly lucky that they saw the potential in me and gave me chance, allowing me to develop as a scientist and as a person. I hope this thesis justifies all their hard work.

I am enormously grateful to **Dr. Rennos Fragkoudis**, your help and jokes were invaluable and we have become strong friends along the way. A match made in cake heaven, as baking was my sanctuary while cake-eating is yours. And to **Dr. Alex Peden**, who has probably only ever heard me start a sentence with 'Could I ask you a question?" and for never once saying "No". I would also like to thank all the other PhD students and Post-Docs in the CID and NCJDSU. As sources of information and amusement, sometimes at the same time, it was a pleasure to work alongside all of you.

A huge thank you to my family. To **Daddy**, even when working 67 hour weeks in Abu Dhabi, you were still able to find the time to proof-read. To **Mommy**, for phone calls and never letting me give up, and for at least one unannounced arrival at my flat 'just to check I was ok'. To **Ed** and **Fi**, my wonderful siblings, for always being there and going through all the ups and downs with me. Your unfailing love has made all this possible. My best friend, **Ros**, who, although is many miles away, was always close enough to cheer me up and keep me grounded. And last but by no means least, to **Sash**, my patient, supportive and loving boyfriend. You held me together and stuck by me. Without you I would not have made it this far and it is with all my love and appreciation that I thank you.

To all these special people and others I have not been able to mention, this is dedicated to you.

ABBREVIATIONS

ACDP	Advisory Committee on Dangerous Pathogens
AcOH	Acetyl hydroxide
AD	Alzheimer's disease
AFS	Agonal Factor System
AFS	Agonal factors
ANOVA	Analysis of Variance
AP-SA	Alkaline phosphatase-conjugated streptavidin
AS	Agonal state
Biotinylated-UTP	Biotinylated-uracil triphosphate
Bis-Tris	1,3-bis(tris(hydroxymethyl)methylamino)
BSE	Bovine Spongifrom Encephalopathy
CCD	Charged Coupled device
CD	Complement defence
cDNA	copy Deoxyribonucleic acid
CI	Confidence interval
CL	Category Laboratory
CNS	Central nervous system
cRNA	Copy RNA
CSF	Cerebrospinal fluid
DEPC	Diethylpyrocarbonate
dH20	Distilled water
dNTP	Deoxyribonucleotide triphosphate
DRC	Dose-response curve
DTT	Dithiothreitol
E.Coli	*Escherichia coli*
ECL	Electrochemiluminescence
EDTA (TAE)	Ethylenediaminetetraacetic acid
FDR	False discovery rate
FI	Freezer interval
FTC	Freeze-thaw cycles
GD	Gravity-displacement
GTC	Guanidium thiocyanate
GdmSCN	Guanidinium
GLP	Good laboratory practise
H & E	Hematoxylin and eosion
HEPA	High efficiency particulate absorption
HG	Hazard group
hPrP	Human prion protein
HRP	Horseradish peroxidase
i.c.	Inter-cranial
ID_{50}	Infectious Dose to 50 Percent of Exposed Individuals
IHC	Immunohistochemisty
IAS	Index of agonal state
IL	Interleukin
IPA	Incubation period assay

IPTG	Isopropyl-beta-D-thiogalactopyranoside
JC viruses	John Cunningham viruses
kGy	KiloGray (radation unit of measure)
KSCN	Potassium thiocyanate
LB	Lysogeny Broth/ Luria-Bertani
LD_{50}	Lethal Dose 50
MeOH	Methyl alcohol
$MgCl_2$	Magnesium Chloride
MRC	Medical Research Council
mRNA	Messenger ribonucleic acid
MSC	Microbiological safety cabinets
NaCl	Sodium chloride
NaOCl	Sodium hypochlorite
NaOH	Sodium hydroxide
NCJDSU	National Creutzfeldt-Jakob Disease Surveillance Unit
NRIE	New Royal Infirmary
NND	Non-neurological disease
OD	Optical density
OND	Other neurological disease
PCR	Polymerase chain reaction
PD	Parkinson's disease
PDVF	Polyvinylidene difluoride
PID	Prion Inactivating Detergent
PL	Porous-displacement
PLP	Paraformaldehyde-lysine-periodate
PM	Post-mortem
PMI	post mortem interval
PPE	Personal protective equipment
PK	proteinase K
PrP	Prion protein
QRT-PCT	Quantitative Real Time Polymerase chain reaction
RI	Refrigeration interval
RIN	RNA Integrity Number
RNA	Ribonucleic acid
rpm	Revolutions per minute
rRNA	Ribosomal ribonucleic acids
SAM	Significance Analysis of Microarrays
SCN	Thiocyanate
SDS	Sodium dodecyl sulfate
SEAC	Spongiform Encephalopathy Advisory Committee
SOC	Super Optimal Catabolite
ss/dsDNA	Single/double-stranded deoxyribonucleic acid
TBS-T	Tris-buffered saline with Tween
TE-buffer	Tris-EDTA buffer
tRNA	Transfer ribonucleic acid
TSE	Transmissible spongiform encephalopathy

UV	ultra violet
Vcjd	Variant Creutzfeldt-Jakob disease
w/v	Weight per volume
WHO	World Health Organisation
X-Gal	5-bromo-4-chloro-3-inodlyl-β-D-galactopyranoside
β-ME	β-mercaptoethanol

List of TSE strain nomenclature

STRAIN	SOURCE
22A	Mouse-passaged scrapie
139A	Mouse-passaged scrapie
ME7	Mouse-passaged scrapie
Chandler/SWRj	Mouse-passaged scrapie
263K	Hamster-passaged scrapie
Sc237	Hamster-passaged scrapie
301V	Mouse-passaged BSE
Fukuoka-1	Mouse-passaged CJD
Kitasoto-1	Mouse-passaged CJD
SY	Hamster-passaged CJD
K.Fu	Hamster-passaged CJD
S.Co	Guinea pig-passaged CJD

List of Figures

Chapter 1

Chapter 2

Chapter 4

Chapter 5

Chapter 6

Chapter 8

List of Tables

Chapter 1

Chapter 2

Chapter 3

Chapter 4

Chapter 5

Chapter 6

Chapter 8

Appendix

ABSTRACT

The pathological mechanisms of variant Creutzfeldt-Jakob disease (vCJD) in the human brain remain poorly understood. Gene expression data may provide insight into the molecular mechanisms involved. This requires analysis of human post-mortem brain tissue however; the variability in RNA preparations from human brain material is a concern. A method for the isolation of RNA from vCJD brains which minimized infectivity and reduced Proteinase K resistant prion protein levels to undetectable by biochemical assay was developed. RNA preparations were made from sample of the frontal parasagital cortex, sub-frontal cortex and cerebellum of 78 human autopsy cases; 21 vCJD, 26 other neurological disease (OND) and 31 non-neurological disease (NND).

Suitable RNA metrics for these human brain RNA preparations were evaluated and the intra- and inter-case variability of RNA preparations was determined. There was marked intra- and inter-case variability in RNA integrity number (RIN), $A_{260:280}$ absorbance ratio and RNA yield. In particular, RIN and $A_{260:280}$ showed little variation intra-patient, although RNA yield was more variable. The effects of post-mortem interval, tissue pH, age at death, gender, freeze-thaw cycles (including storage method and temperature) and agonal state were investigated; none of these parameters correlated with the marked variability observed.

Parameters for matching vCJD and OND/NND cases were considered and RNA from three age and gender matched comparison groups, each containing one OND, one NND and one vCJD case, were used for gene expression analysis. Data was generated using Superarray GEArray® Focused DNA Microarray and analysed using the GEArray Expression Analysis Suite and Significance Analysis of Microarray software. A comparison between matched vCJD and NND control cases identified 26 up-regulated and 16 down-regulated genes, showing >1.5-fold change with a false discovery rate of 9%. The modulated genes were involved in cell signaling, cell death, cholesterol and lipid metabolism. Involvement of these pathways is consistent with findings in other transmissible spongiform encephalopathy studies.

1 INTRODUCTION

1.1 TRANSMISSIBLE SPONGIFORM ENCEPHALOPATHIES

Transmissible Spongiform Encephalopathies (TSE) or prion diseases are a biologically unique group of rare and fatal neurodegenerative diseases which include Creutzfeldt-Jakob disease and kuru in humans, bovine spongiform encephalopathies in cattle, scrapie in sheep and goats and chronic wasting disease in elk and deer. TSEs have previously been described as subacute spongiform encephalopathies, slow virus diseases and transmissible dementias. Animal TSEs have been recognized for well over 200 years (McGowan, 1922). The prototypic disease is scrapie, a naturally occurring disease affecting sheep and goats which is endemic in most of Europe and North America. Since scrapie was first described, various forms of human prion diseases have been reported, including kuru, Creutzfeldt-Jakob disease (CJD), Gerstmann-Sträussler-Scheinker syndrome (GSS) and fatal familial insomnia (FFI). More recently new forms of animal prion disease have emerged, such as bovine spongiform encephalopathy (BSE) in cattle, transmissible mink encephalopathy (TME) in mink, chronic wasting disease (CWD) in deer and elk, feline spongiform encephalopathy (FSE) in cats and exotic ungulate encephalopathy (EUE) in several antelope species including nyala and kudu.

Prion diseases in humans can be sporadic, familial or acquired in origin (Ironside, 1996; Prusiner, 1998). Currently, there is no epidemiological evidence for the causes of sporadic prion diseases, and no association established between disease and mutant PrP alleles (Will, 1993; Harries-Jones *et al.*, 1988). Alternative hypotheses have suggested exposure to an unidentified virus, spontaneous generation of a non-viral agent through somatic cell mutations and stochastic initiation of spontaneous PrP^{res} formation without PrP mutation as possible causes. Inherited forms account for 10-15% of all human prion diseases and are associated with an autosomal dominant change (mutation or insertion) in the prion protein gene that predisposes to abnormal folding of the protein, resulting in disease. Transmission of human TSEs from infected individuals is relatively rare, accounting for less than 1% of total CJD cases

worldwide. TSEs are not naturally transmissible via airborne droplets, skin contact or most other forms of casual contact although experimentally, intra-nasal transmission has been proven (Hamir *et al.*, 2008). However, transmission is possible through contact with infected tissue, body fluids, or contaminated medical instruments. Normal sterilization procedures such as steam sterilization or irradiation do not fully inactivate the infectivity, and difficulties in detecting and inactivating infectivity has led to iatrogenic transmission of CJD (Powell-Jackson *et al.*, 1985; Heckmann *et al.*, 1997). More recently and worryingly, there have been three confirmed transmissions of vCJD through blood transfusions. With the lack of a non-invasive pre-clinical diagnostic assay, there opens up the real possibility of a world-wide public health issue regarding iatrogenic spread of vCJD (Llewelyn *et al.*, 2004; Peden *et al.*, 2004).

In recent years, public interest and media attention has brought TSEs to centre stage. In 1987, the Central Veterinary Laboratory in England reported the first formal diagnosis of a novel prion disease in cattle, known as bovine spongiform encephalopathy (BSE) (Wells *et al.*, 1987). With the discovery of yet another novel spongiform encephalopathy in 1996 (vCJD), this time in humans, epidemiological studies indicated a potential for interspecies transmission of BSE to humans. The suspected exposure was believed to be food chain contamination with infected meat and other bovine-derived products (Will *et al.*, 1996). This discovery had significant implications for human health, as well as other animals, including felines (Wyatt *et al.*, 1991) and zoo animals (Sigurdson & Miller, 2003). Molecular strain-typing studies and experimental transmission studies into transgenic and conventional mice with BSE and vCJD have established that the two diseases are caused by the same agent, with biological properties distinct from those in scrapie and sCJD (Collinge *et al.*, 1996; Bruce *et al.*, 1997). Since the emergence of vCJD in 1995, a total of 166 cases have been reported in the UK and 41 further cases worldwide, in countries including Japan, France and USA (www.cjd.ed.ac.uk, 2008).

1.1.1 Creutzfeldt-Jakob Disease

Clinical and pathological descriptions of what is now referred to as CJD first appeared in the 1920's. Hans Gerhard Creutzfeldt first described ' a new and unusual type of neurological disease' of a progressive mental and neurological disturbance in a 22-year-old woman (Creutzfeldt, 1920). Although Creutzfeldt is credited with the first description of the disorder, it has since been suggested that his patient did not suffer from a TSE and the case would not now meet the diagnostic criteria for CJD. One year later, a German neurologist, Alfons Maria Jakob, described four further cases of defects in the motor systems, of which at least two had clinical features suggestive of the entity now recognised as CJD. Over the decades, considerable debate over the nature, identity and clinico-pathological features of these disorders have persisted. It was not until the direct experimental transmission of CJD from a human to a chimpanzee (Gibbs *et al.*, 1968), that a unique disease entity was assigned to this neurodegenerative disorder.

In 1996, neuropathologists and neurologists at the National CJD Surveillance Unit (NCJDSU) in the United Kingdom identified a new variant form of CJD, which has since been found in several other European countries as well as Japan and the United States (www.cjd.ed.ac.uk, 2008). The presenting symptoms of the variant form were distinct from those of classic CJD, striking features being the younger age of the patients compared to classical forms of the disease. Research suggests that this new variant form of the disease may have resulted from human consumption of beef from cattle with a TSE disease, as opposed to sheep with scrapie, since scrapie has been endemic in the UK for over 400 years and epidemiological studies show no association between sheep scrapie and the occurrence of CJD in humans (Brown *et al.*, 1987). The emergence of BSE in UK cattle in 1984 however, has been widely attributed to scrapie transmission to cattle via contaminated feed prepared from rendered sheep carcasses, a practice introduced in the 1950's (Wilesmith, 1988). An alternative hypothesis suggests the 1986 BSE epidemic was a result of recycling cattle carcasses of rare sporadic BSE cases for meat and bone meal (MBM) cattle feed. Whether or not BSE originated from sheep scrapie or by other means, it became clear by 1990, with the occurrence of novel spongiform encephalopathies

among domestic cats and eventually humans, that its host range was drastically different from that of scrapie.

1.2 NATURE OF THE INFECTIOUS AGENT

The cellular prion protein (PrP), isolated from normal individuals is protease-sensitive, and is traditionally termed PrP^{c} (for cellular) or PrP^{sen} (for sensitive to protease digestion). Modifications of PrP can result in a protease-resistant isoform, termed PrP^{res}, or a disease-associated PrP, termed PrP^{Sc} or PrP^{d}. As protease resistance does not specify that the isoform is capable of transmitting disease, PrP^{Sc} is used to denote the pathogenic, infectious isoforms and PrP^{res} the proteinase resistance isoforms.

The hypothesis first put forward by Alper to define the increasingly confusing etiology of 'slow-virus' diseases described the unit of TSE pathogenesis and transmissibility as a specific aberrantly folded host protein (Alper *et al.*, 1966). By the late 1970's, Prusiner had formulated the protein-only hypothesis, or 'prion', denoting '**pro**teinaceous **in**fectious particle', postulating that the aberrant protein- PrP^{Sc}- is the sole infectious component of the agent and is sufficient to be responsible for prion propagation. In this hypothesis, normally folded PrP^{c} is induced to a misfolded conformation by exposure to aberrant PrP, precipitating an autocatalytic conversion cascade. Indeed, evidence of highly purified PrP^{Sc} producing disease when inoculated into wild-type mice and the observation that PrP knockout mice are resistant to infection support the prion hypothesis (Prusiner, 1982; Bueler *et al.*, 1993). Further research however, raised a number of issues regarding the prion hypothesis. For example, recombinant mammalian prions harbouring mutations found in familial TSE-affected patients, although exhibiting similar properties to PrP^{Sc}, were not infectious when inoculated into wild-type hosts (Lehmann & Harris, 1996; Chiesa *et al.*, 1998). Recently, a recombinant PrP fragment lacking the N-terminal one-third of the polypeptide was assembled *in vitro* into amyloid

fibrils and found to induce TSE-like disease in transgenic mice over-expressing the same truncated portion of PrP (Legname *et al.*, 2004), although this is not conclusive evidence that PrP amyloid alone transmits the disease since transgenic animals overexpressing PrP can spontaneously develop prion-like diseases (Chiesa *et al.*, 1998; Westaway *et al.*, 1994).

Nonetheless, it is generally considered that pure *in vitro* generation of infectivity by misfolding of (recombinant) prion protein would provide definitive proof of the prion hypothesis (Chesebro, 1998; Soto & Castilla, 2004). A new technique may provide this. Protein misfolding cyclic amplification (PMCA) is analogous to polymerase chain reaction (PCR) and involves cell free conversion of PrP^{sen} to PrP^{res} using only purified constituents (Saborio *et al.*, 2001). Data obtained using this method have been challenged because large amounts of same species infectious PrP^{res} are required as the seeding substrate, thereby precluding demonstrating the infectiousness of any resulting aberrant PrP produced (Hill *et al.*, 1999). Advances in the method have resulted in critical studies showing *in vitro* generation of PrP^{Sc} capable of infection and de novo formation and propagation of infectious PrP^{Sc} (Castilla *et al.*, 2005; Deleault *et al.*, 2007).

Even though the body of evidence in favour of the prion hypothesis is compelling, there is still ongoing controversy. Studies of animal brain tissues containing high titres of TSE infectivity but undetectable levels of PrP^{res} (Barron *et al.*, 2007; Lasmezas *et al.*, 1997) and the presence of high levels of accumulated PrP^{res} without infectivity (Piccardo *et al.*, 2007) throw doubt on the protein-only theory. Alternative models based on viruses, virinos and other infectious agents containing small RNAs have been proposed (Narang, 2002; Rohwer, 1984a; Bellinger-Kawahara *et al.*, 1988; Manuelidis *et al.*, 1988; Bellinger-Kawahara *et al.*, 1988; Rohwer, 1991). Evidence that retroviral RNA co-precipitates with PrP^{Sc} and that short (>4 kb) RNA fragments are released after nuclease digestion from purified infectious fractions lends weight to these models (Murdoch *et al.*, 1990; Akowitz *et al.*, 1990; Akowitz *et al.*, 1994). Moreover the addition of polyanions such as RNA promotes PMCA (Deleault *et al.*, 2007).

1.3 THE PRION PROTEIN GENE (PRNP)

The prion protein gene (*PRNP*) is a single-copy gene, located on the short arm of chromosome 20 in man, spans 16 Kb and contains two exons, encoding 253 amino acid residues (Kretzchmar *et al.*, 1986). The translation product of *PRNP* is processed by the removal of an amino terminal signal peptide of 22 amino acids and a carboxy terminal hydrophobic peptide of 23 amino acids. A C-terminal glycosylphosphatidylinositol (GPI)-anchor is added post-translationally and permits attachment to the surface of neurones and other cell types (Prusiner, 1991; Stahl *et al.*, 1987). In addition, asparagine residues 181 and 197 also contain highly branched glycosyl groups, resulting in PrP being found as a mixture of three forms – unglycosylated, with one glycosyl-, and with two glycosyl-groups. Glycoform analysis of PrP^{res} as determined by Western blot constitutes the current method of classification of CJD subtypes, although glycoform ratios can vary and should be interpreted with caution (Telling *et al.*, 1996). The biochemical properties of the cellular prion protein differ radically from the properties of the disease-associated isoform, even though to date, no identifiable primary structure or covalent modification differences have been described for the two isoforms. The difference in tertiary structure though, is striking. PrP^{c} is a monomeric protein with a globular C-terminal domain rich in α-helical structure, whereas PrP^{Sc} is rich in β-sheet, highly aggregated and contains a C-terminal core with considerable resistance to proteolytic degradation in non-denaturing conditions (Pan *et al.*, 1993). Because the amino acid sequences of PrP^{c} and PrP^{Sc} are identical (apart from the genetic forms), the contrasting properties of the two molecules, and to an extent the strain phenomenon of TSEs, is generally believed to be due to conformation difference (Bessen & Marsh, 1994). Figure 1.1 shows the genetic features of the cellular prion protein.

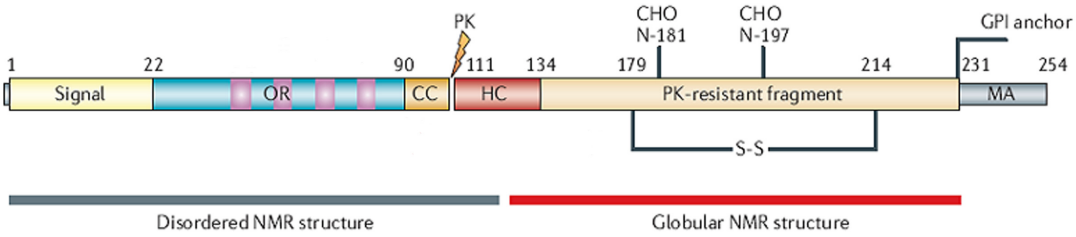

Figure 1.1. Structural features of the cellular prion polypeptide. The primary structure of the cellular prion protein including post-translational modifications. A secretory signal peptide resides at the extreme N-terminus. The numbers describe the position of the respective amino acids. CC (orange) defines the charged cluster. OR, octapeptide repeats. HC (red) defines the 'hydrophobic core'. S-S indicates the single disulphide bridge. The proteinase K (PK) resistant core of PrP^{Sc} is depicted in gold and the approximate cutting site of PK within PrP is indicated by the lightening signal. MA denotes the hydrophobic peptide cleaved when the GPI anchor is attached. Modified from **(Aguzzi & Heikenwalder, 2006)**.

1.3.1 Cellular Prion Protein

The cellular prion protein is highly conserved among mammals and is expressed in most tissues, although the highest level of PrP^{c} expression is found in the CNS, where it is localized to synaptic membranes of neurons and astrocytes (Manson *et al.*, 1992; Moser *et al.*, 1995). The physiological function of the cellular form is still undetermined, although current hypotheses include; copper-related oxidative stress resistance (Brown *et al.*, 2001), circadian rhythms (Tobler *et al.*, 1996), copper metabolism (Brown *et al.*, 1997a), cell signaling (Mouillet-Richard *et al.*, 2000), synaptic function (Maglio *et al.*, 2004) and alterations in superoxide dimutase activity (Brown *et al.*, 1997b; Klamt *et al.*, 2001). However, PrP^{c} has yet to be proven to be essential for normal neurological development and function. PrP null mouse lines were observed to develop normally and PrP knockout mice survive with no apparent phenotypic abnormalities. These results suggest that PrP is not essential for development, as loss of PrP is physiologically tolerated and the pathophysiology seen in prion diseases is not due to loss of normal PrP function (Bueler *et al.*, 1993; Mallucci *et al.*, 2002; Manson *et al.*, 1994). Figure 1.2 illustrates the structural features of PrP.

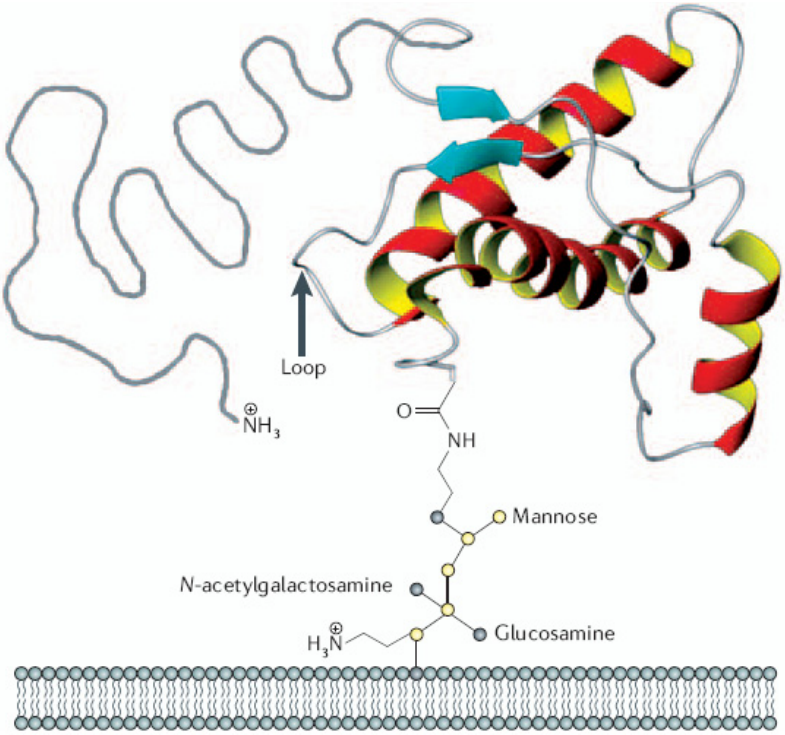

Figure 1.2. Tertiary structure of the cellular prion protein. The prion protein is inserted into a lipid bilayer, as deduced from NMR spectroscopy, including the 'unstructured' N-terminal tail (grey) and the glycosylphosphatidylinositol (GPI) anchor. The ribbon schematic represents the α-helices in red, the β-strands as blue arrows and the loop regions connecting the second β-sheet and the third α-helix is indicated by the black arrow. Taken from (Aguzzi & Heikenwalder, 2006).

1.3.2 Disease-Associated Prion Protein

While PrP^{c} is a soluble, protease-sensitive protein, pathological isoforms are insoluble in non-ionic detergents and partially resistant to protease treatment, leaving an indigestible carboxyterminal fragment which tends to aggregate, termed PrP^{res} or PrP27-30 (Chesebro, 1998). However, these hallmark properties of PrP^{Sc}, i.e. resistance to proteases and insolubility in non-ionic detergents, which have been traditionally linked to the presence of prion infectivity are not absolute (Bolton *et al.*, 1984). In some experimental systems, protease-resistance and detergent-insolubility are not associated with prion infectivity (Shaked *et al.*, 1999) and protease-resistant PrP cannot be found in samples containing prion infectivity (Lasmezas *et al.*, 1997; Barron *et al.*, 2007).

1.3.3 Conversion of PrP^{c} to PrP^{Sc}

The key difference between TSEs and other amyloidoses is the ability of aggregated PrP to promote the rearrangement of unmutated protein thereby allowing transmission of disease. Two models have been proposed to explain PrP^{Sc}-induced conversion of PrP^{c} to PrP^{Sc}; the template-directed refolding model (Gajdusek, 1988; Prusiner & DeArmond, 1990) and the noncatalytic nucleated polymerization model (Come *et al.*, 1993). The first mechanism hypothesises that a PrP^{Sc} monomer acts as a template, promoting the conversion of PrP^{c} to PrP^{Sc} or a partially destabilized intermediate (PrP*) and involves only a conformational change. In this model PrP^{Sc} is inherently more stable but kinetically inaccessible. Refolding of PrP^{c} would have to overcome a high activation energy barrier, preventing spontaneous conversion. Heterodimeric complexes would lower the activation energy barrier or might require a chaperone and/or an energy source. α-lytic proteases have been observed to behave in this manner. Interconversion of a globule-like intermediate, I, to the more stable native form, N, is extremely slow, representing an energy barrier of ~25 kcal/mol. However, conversion is greatly accelerated by the addition of a naturally-occurring propeptide region, which reduces energy requirement to 14 kcal/mol (Baker & Agard, 1994). An alternative modified model supposes the existence of an ancillary factor, protein X. PrP^{c} is in equilibrium with PrP* which binds to the putative protein X. PrP^{Sc} interacts with the PrP*-protein X complex and induces the conversion of PrP* to PrP^{Sc} (Telling *et al.*, 1995).

The model most widely accepted has been referred to as the 'seeded polymerization' or noncatalytic nucleated polymerization of PrP^{c} by aggregated PrP^{Sc} in a two-step process (binding and conversion). In this model, PrP^{Sc} is less stable than PrP^{c} but is stabilized upon binding to the PrP^{Sc} aggregate (Jarrett & Lansbury, 1993; Gajdusek, 1988), consistent with observations of cell-free conversion studies that indicate PrP^{Sc} aggregates are able to convert PrP^{c} into a protease-resistant PrP isoform (Caughey *et al.*, 1997; Kocisko *et al.*, 1994). Here the energy barrier exists at the initial nucleation step, where formation of small aggregates is unfavourable because the free energy gained from intermolecular interactions does not overcome the entropic cost of binding until the energy threshold determined by a minimum size nucleus is attained.

Introduction of a seed, i.e. infection with PrP^{Sc}, would circumvent the slow step of nucleation. There are biological precedents of such models. Flagellin is a monomeric unit and is incorporated into the growing end of a flagellum. Monomers in solution are conformationally unfavorable to spontaneous nucleation but if a seed of fragmented flagellum is added, then polymerization rapidly ensues. Interestingly, the polymerizing monomers can assume the conformation of even heterologous seed material, reflecting the template 'behaviour' (Asakura *et al.*, 1964; Asakura *et al.*, 1966).

How this process might result in neurodegeneration is currently unknown but it is possible that the PrP^{c} has an antioxidant effect which is lost, accompanied by the addition of a gain of cytotoxicity (Giese & Kretzchmar, 2001). A recent structural study compared the Doppel protein (a PrP paralog which is topologically identical to PrP but does not undergo structural rearrangements) with disease-associated PrP. The results indicated that the prion protein contains at least two sequence fragments with highly unusual intrinsic properties, PrP (114–125) and helix B. Also, it was possible to determine that most PrP mutations associated with neurodegenerative disorders had increased local hydrophobicity. It was therefore suggested that the observed increase in hydrophobicity may facilitate PrP-to-PrP and/or PrP-to-cofactor interactions, and thus promote structural conversion (Kuznetsov & Rackovsky, 2004). In reality, it is highly possible that the models may not be mutually exclusive, biological precedent indicating overlapping aspects of both. Figure 1.3 is a schematic of possible mechanisms and sites of PrP^{c} synthesis and PrP^{c}-PrP^{Sc} conversion.

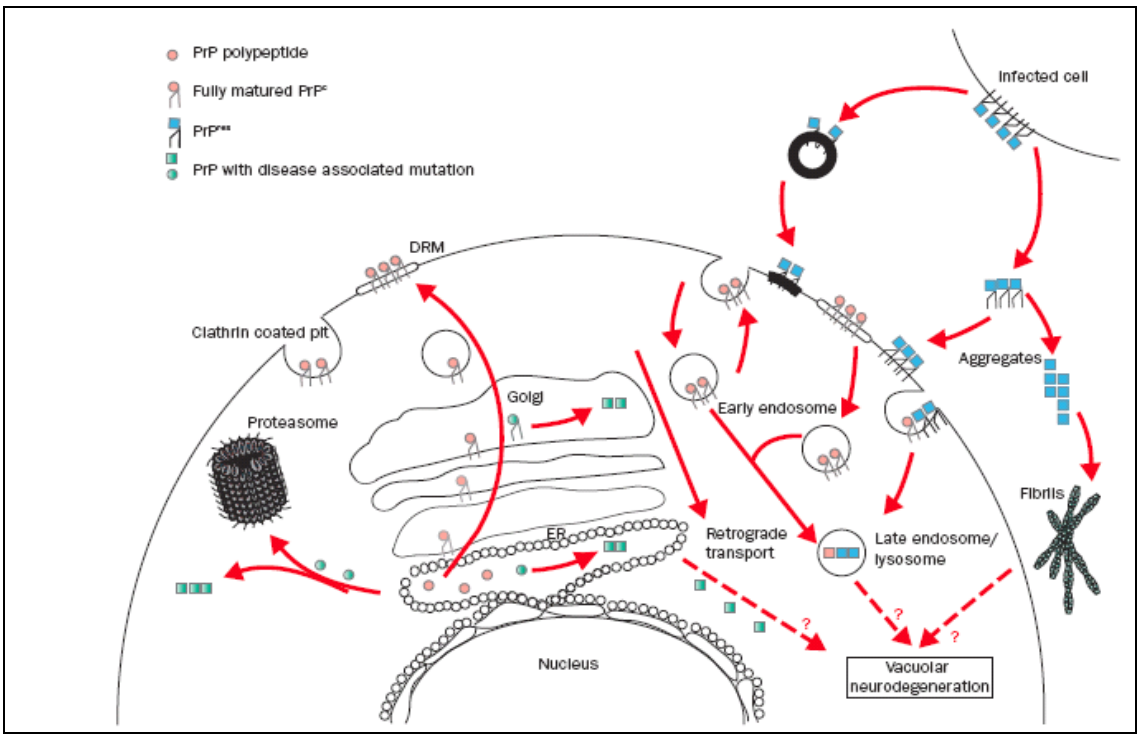

Figure 1.3. Normal PrP^{c} synthesis and cell turnover with possible sites of conversion to PrP^{Sc}. Although mechanisms of toxicity and neurotoxicity remain unresolved, it is known that PrP accumulating in the cytosol forms aggregates, and once present, continue to persist. PrP^{Sc} synthesis followed by degradation and clearance of misfolded proteins from the ER must be kept in complete control and is a finely balanced function. Compromise of quality control in endoplasmic reticulum protein synthesis mean that this harmful soluble conformer are allowed to accumulate. DRM, detergent-resistant microdomains. Taken from (Collins et al., 2004).

1.4 PATHOLOGICAL MECHANISMS

1.4.1 Clinical Features of vCJD

Particular combinations of clinical features distinguish the different forms of CJD. The most common form is classical (sporadic) CJD, which exhibits diverse clinical features according to the particular physical and chemical properties of PrP^{Sc} and the codon 129 genotype of the patient. In contrast, vCJD displays a relatively consistent clinical phenotype distinct from all other human prion diseases. sCJD onset generally occurs at a mean age of 66 years (range 20-95), whereas cases of vCJD show a downward shift in average age, with a relatively young age of onset for neurodegenerative diseases (mean 29 years, range 14-74). sCJD symptoms progress

extremely rapidly, over days or weeks. vCJD has a significantly longer pre-clinical phase and relatively slow progression. Initial symptoms are usually psychiatric; patients present with depression, delusions, anxiety and withdrawal. Within a median of 6 months, multiple clear neurological features develop, including cognitive impairment, progressive cerebellar syndrome with gait and limb ataxia and myoclonic jerks, always eventually leading to dementia and death occurring a median 14 months from onset (range 6-39mnths) (Will *et al.*, 2000).

1.4.2 Histopathology of vCJD

The pathological features of TSE diseases have long been characterized and neuropathological assessment has remained the definitive tool to providing a diagnosis. For surveillance purposes, confirmation of diagnosis is done by neuropathological examination, and in research, it has allowed the discovery of new disease subtypes. A range of investigative techniques, including PrP gene analysis, PrP immunocytochemistry and detection by Western blot, histoblot and immunoblot techniques, prion rod/SAF detection by electronmicroscopy and transmissibility to both wild-type and transgenic laboratory animals are all used as diagnostic applications. However, the underlying mechanisms leading to this pathology are not understood.

CNS neuropathology of human prion diseases are characterised by five features; spongiform change in the CNS, neuronal loss, astrocytosis, microglial proliferation (gliosis) and amyloid plaque formation. Histological analysis can be complicated by age-associated histological abnormalities and must be distinguished from any coexisting CNS disorder. Table 1.1 lists the neuropathological features generally observed in TSE infected patients.

CLASSICAL CHANGES CONSISTENTLY OBSERVED IN TSE's	Spongiform change
	Neuronal loss
	Gliosis
	Abnormal PrP deposition*
OTHER OCCASIONAL FEATURES	PrP amyloid plaques *
	Status spongiosus
	Neuronal swelling
	Abnormal neuritic dendrites
	White matter necrosis and cavitation
	Beta amyloid protein deposition

Table 1.1. Histopathological changes in human prion diseases. *Indicates histopathological feature specific to TSE's. Taken from (Ironside, 1996).

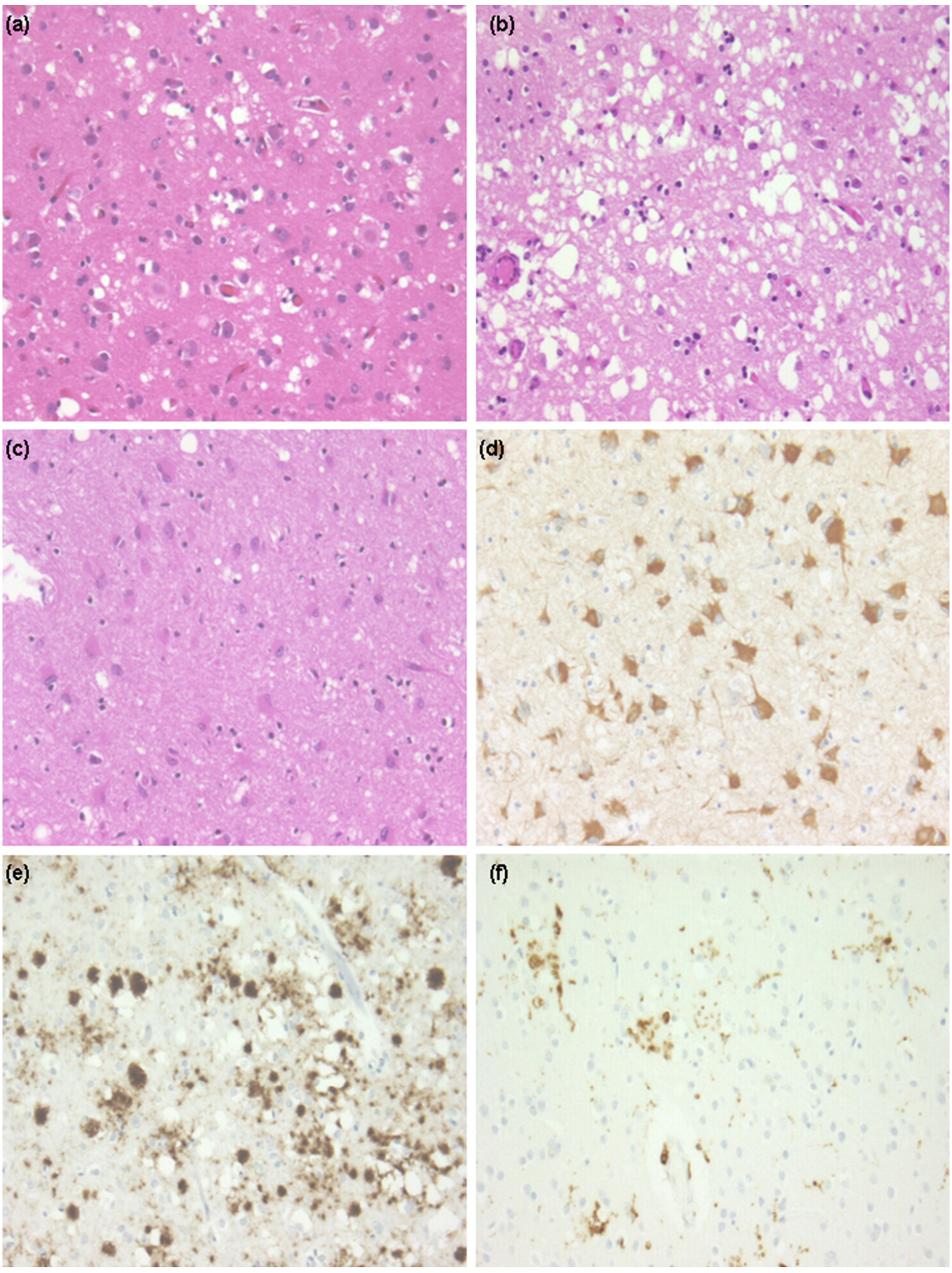

Figure1.4. Characteristic neuropathological changes observed in vCJD. (a) A distinctive diagnostic neuropathological abnormality observed in vCJD cases is the florid plaque. These comprise an eosinophilic core and a pale radial periphery and are most frequently observed in the occipital , cerebral and cerebellar cortexes. This section of the frontal cortex from a case of vCJD shows several florid plaques and patchy spongiform change (Haematoxlin and eosin, x 200 **(b)** The spongiform change occurs in many forms of human TSE and in vCJD is usually most severe within the basal ganglia, thalamus and cerebellar cortex. Vacuoles may also coalesce resulting in complete collapse of the cytoarchitecture. Confluent spongiform change from a case of vCJD is evident in the basal ganglia

(Haematoxlin and eosin, x100) **(c).**Marked neuronal loss can be extensive in vCJD and occurs in all layers of the cerebellar and cerebral cortex but is most severe in the anterior and medail thalamus. This section of the dorsomedial nucleus of the thalamus in vCJD shows almost total neuronal loss and marked astrocytosis (Haematoxlin and eosin, x200) **(d).** Immunohistochemical staining using an antibody to GFAP as a marker for active astrocytes shows widespread gliosis in this section of the dorsomedial nucleus of the thalamus in vCJD (GFAP, x200) **(e).** Immunohistochemistry for prion protein in vCJD shows intense labelling of the florid plaques and smaller cluster plaques, with widespread pericellular positivity within the frontal cortex (KG9 anti-PrP antibody with Haematoxylin counterstain, x 200). **(f).**Immunohistochemical staining using an anti-CD68 antibody demonstrates activated microglia from a section of the occipital cortex. Some of the fine cellular processes are located towards the periphery of the florid plaques (PGM1(anti-CD68 antibody) with haematoxylin counterstain, x100).

Spongiform change, as distinct from non-specific vacuolation which occurs in a multitude of disorders as a consequence of neuronal loss, was first characterised as being a CJD specific neuropathy by Masters (Masters & Rishardson, 1978). In vCJD, spongiform change is most prominent within the cerebral cortex, occipital and inferior frontal cortex. Confluent spongiform change is rare in these regions but more common in the caudate nucleus and putamen, often without numerous amyloid plaques. Florid plaques, defined as diffuse or focally clustered (morula-type) small discrete round or oval vaculoles in the neuropil of the whole depth or deep layers of the cerebral cortex, cerebellar cortex (predominantly molecular and granular layer) and subcortical grey matter (Budka *et al.*, 1995), were seen previously only in scrapie and are a particularly unusual but highly consistent feature. Florid plaques are readily identifiable on haematoxylin and eosin staining as lesions comprising of an eosinophilic central core with radiating fibrils in the periphery of the plaque, which are surrounded by a rim of spongiform change in an otherwise intact neuropil (Figures 1.4a). PrP deposition patterns in vCJD are quite unique to the disease. Amorphous PrP deposition is mainly observed in a pericellular (neuronal and astrocytic) pattern in all areas of the cerebral and cerebellar cortex and around capillary walls, with additional synaptic accumulation evident in the thalamus (Figure 1.4e). PrP accumulation is less evident in other cortical regions. Astrocytosis is widespread and does not correlate with the presence of amyloid plaques but rather with neuronal loss. Posterior thalamic gliosis is particularly marked in vCJD. Neuronal loss is most evident in the occipital cortex and the cerebellum, with severe loss in the posterior thalamic nuclei and the dorsomedial nucleus, accompanied by severe astrocytosis. As described, these pathological features do not occur uniformly throughout the brain, but are consistently focused at certain neuronal regions, a

phenomenon called neuropathological targeting (Bell & Ironside, 1993). Western blot analysis of PrP^{res} from vCJD brain shows a highly consistent pattern, termed type 2B, and is characterized by a 19kDa non-glycosylated fragment with a predominance of the diglycosylated form (Collinge *et al.*, 1996; Parchi *et al.*, 1997).

1.4.3 Pathological Mechanisms

Many of the key issues of how PrP^{Sc} or PrP^{c} carrying mutations might cause neurodegeneration are still unclear. Numerous studies show that abnormal forms of the prion protein play a predominant role in both the etiology and the pathogenesis of all forms of prion disorders. Neuronal loss caused by the accumulation and/or conversion of PrP is the pivotal event of neurodegeneration, but how the process of conversion and aggregation causes neurodegeneration is unknown. Proposed mechanisms of neurodegeneration include; loss of cytoprotective properties associated with PrP^{c} , acquisition of cytotoxicity properties of PrP^{Sc} (Giese & Kretzchmar, 2001), increased oxidative stress (Gotz *et al.*, 1994; Beal, 1995), dysfunction of iron (Gerlach *et al.*, 1994), copper (Jobling *et al.*, 2001; Quaglio *et al.*, 2001) and calcium metabolism (Thellung *et al.*, 2000; Florio *et al.*, 1996).

GAIN OF FUNCTION

Many of the pathogenic properties of PrP^{Sc}, such as neurotoxicity, proteinase-resistance and induction of hypertrophy and proliferation of astrocytes, have been attributed to the peptide fragment corresponding to residues 106–126 (PrP[106–126]) (Forloni *et al.*, 1993). Neurotoxicity studies use either this fragment or purified PrP^{Sc}, although it must be noted that PrP [106-126] may not fully encapsulate normal PrP physiological or structural properties. Neuronal expression of PrP^{c} is essential for cellular neurotoxic damage; neurons not expressing PrP^{c} are resistant to *in vitro* PrP[106-126] toxicity (Brown *et al.*, 1994) and *in vivo* neurodegeneration (Bueler *et al.*, 1993). Additionally, overexpression of PrP^{c} increases cellular toxic sensitivity to the fragment (Brown, 1998). Investigations have also revealed that in culture, microglia mediate neurotoxic cell damage; neurons are resistant to fragment mediated cell-death after depletion of contaminating microglia (Brown *et al.*, 1996).

However, this has only been observed *in vitro* and needs to be reproduced *in vivo* to validate its biological relevance.

Toxic gain of function properties possessed by PrP^{Sc} unrelated to the normal physiological function of PrP^{c} may be causative of neuronal death. Indeed co-localisation of accumulated PrP^{Sc} and neuropathy indicates a toxic effect is exerted by PrP^{Sc}. It has been suggested that the toxic effects arise from blocked axonal transport, interference with synaptic function or activation of apoptotic pathways. Mice expressing a PrP mutation without the N-terminal ER-targeting signal sequence spontaneously developed neurodegeneration when the mutant protein was synthesised in the cytosolic compartment (cytoPrP) (Ma *et al.*, 2002). cytoPrP neurotoxicity is dependent on association with intracellular membranes and Bcl-2 (an antiapoptotic protein present at the cytosolic side of ER and mitochondrial membranes) (Wang *et al.*, 2006; Rambold *et al.*, 2006). It has also been shown that PrP^{Sc} inhibits the 26S proteosome and causes dysfunction of the ubiquitin-proteosome system (UPS) in prion infected mice (Kristiansen *et al.*, 2007) and compromised proteosome activity increases PrP accumulation in the cytosol, via retrograde transportation out of the ER, and generates amorphous partially PK resistant PrP aggregates (Ma & Lindquist, 2001). Interestingly, inherited human pathogenic PrP mutants are partially mis-targeted to the cytosol (Zanusso *et al.*, 2000). However, the recent demonstration of PK-resistant PrP core fragments in non-CJD brains argues against PrP^{Sc} neurotoxicity; small quantities of abnormal prion may not be pathogenic and these might be lying dormant in many human brains (Yuan *et al.*, 2006).

LOSS OF FUNCTION

Prenatal ablation of PrP confers resistance to prion infection (Bueler *et al.*, 1993) whereas postnatal depletion of neuronal PrP can prevent neuronal loss and reverse early spongiform change with no progression to clinical disease (Mallucci *et al.*, 2003). These observations argue against a loss of function being causative for pathology. However it is possible PrP^{c} may possess a biological activity that is lost upon conversion into PrP^{Sc}, or the loss of function exacerbates pathology caused by

toxic gain or other functional mechanism, leading to neurodegeneration. Evidence for this was first observed in cell culture experiments with primary neurons. *Prnp*$^{-/-}$ cells underwent apoptosis within 4 days when serum was removed from cell cultures, but showed greater survival after transfecting with PrP^{c} expression vectors (Kuwahara *et al.*, 1999). *In vivo* experiments demonstrated larger infarct volumes after ischaemic brain injury in PrP^{c}-knockout mice (McLennan *et al.*, 2004). Anti-apoptotic function of PrP^{c} has also been proven in *in vivo* and *in vitro* modeling systems (Roucou & LeBlanc, 2005). Figure 1.5 is a schematic representation of possible consequences of cellular interactions with PrP^{Sc} within the brain.

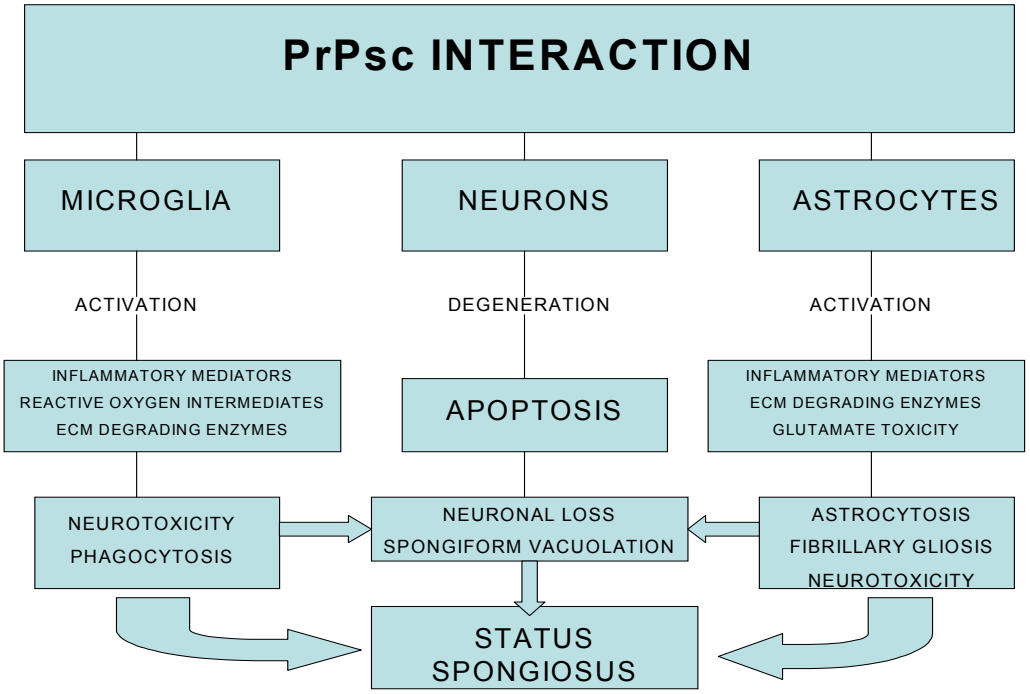

Figure 1.5. Possible implication of neuronal death in prion diseases. Schema representing the processes underlying prion pathology. Three types of cells that are known to be involved in the pathophysiology of prion diseases, but the exact involvement and method of cell death have yet to be determined. ECM, extracellular matrix. Modified from (Rezaie & Lantos, 2001).

OXIDATIVE STRESS AND ANTIOXIDANT STRESS DEFENCE

Oxidative stress induced by reactive oxygen species (ROS) or free radicals has been suggested as a causal factor in the pathogenesis of Alzheimer's as well as prion diseases (Guentchev *et al.*, 2000). The CNS is particularly vulnerable to oxidative stress; low levels of antioxidants, high oxygen consumption, and the presence of

large amounts of lipids and metals capable of free-radical formation, all increase susceptibility to damage (Halliwell *et al.*, 1992). Dysfunction of any of several interconnected cellular pathways is sufficient to cause oxidative stress in the brain, including impaired mitochondrial function, increased oxidative damage, defects in the ubiquitin-proteosome system, presence of aggregated proteins, excitotoxicity and inflammation. Neurodegenerative disorder brain tissues have been observed to have higher levels of oxidant by-products (Gotz *et al.*, 1994; Beal, 1995). The potential link between oxidative stress and prion diseases is marked by two pathophysiological events; 1) enhanced production of ROS and reactive nitrogen species (RNS), 2) impairment of the cellular oxidative stress defense.

Primary neuronal cultures were only affected by PrP [106-126] toxicity when activated microglia were present to respond by production of oxygen radicals (Brown *et al.*, 1996). In scrapie-infected mice, increased free radical generation, including superoxide anion (O_2^-), was coupled with an increase in oxidative stress markers, malondialdehyde (MDA) and heme oxygenase-1 (HO-1). Conversely, an antioxidant enzyme (Cu/ZN-superoxide dimutase (SOD)) remained unaffected, while a mitochondrial enzyme (Mn-SOD) involved in scavenging O_2^- was markedly decreased (Choi *et al.*, 1998; Choi *et al.*, 2000; Lee *et al.*, 1999). Although the latter observation has not been reproduced (Waggoner *et al.*, 2000; Hutter *et al.*, 2003). The accumulation of iron has also been linked to brain pathology, as iron potentiates oxygen toxicity via a reaction termed the iron-catalyzed Harber-Weiss reaction. For example, in the presence of iron, superoxide anion and hydrogen reoxide can easily be converted into more dangerous species, such as highly reactive hydroxyl ($^{\cdot}OH$) radicals (Halliwell *et al.*, 1992). Evidence for this was observed in scrapie mice models, where levels of total iron and ferric iron ($Fe3^+$) were significantly increased (Kim *et al.*, 2000). The presence of high levels of ferric iron may exacerbate oxidative damage as it induces hydroxyl radical formation and lipid peroxidation (Ben-Shachar *et al.*, 1991). Elevated ROS generation, changes in iron levels and in iron redox states, in conjunction with lowered scavenging activity in mitochondria might lead to free radical damage to neuronal cells in neurodegenerative disorders.

PrP^c has been shown to have direct antioxidative protective effects as seen by comparison of wild type and PrP null mouse lines. Cell cultures derived from $PrP^{0/0}$ mice have increased susceptibility to agents that induce oxidative stress and brain tissue from $PrP^{0/0}$ mice also exhibits biochemical changes indicative of oxidative stress (Brown *et al.*, 1997b; Brown *et al.*, 2002; Wong *et al.*, 2001). PrP^c itself has been reported as having intrinsic SOD-line activity, which can be inhibited by the addition of PrP [106-126], although this observation may not be biologically relevant, as supra-physiological concentrations of copper were required for enzymatic activation (Brown *et al.*, 2001). PrP^c may also act indirectly to protect cells from oxidative stress by up-regulating the activities of ROS detoxifying proteins, such as Cu-Zn or Cu-dependent SOD. $PrP^{0/0}$ mice have 10-50% less Cu-Zn SOD activity (Brown *et al.*, 1997b; Klamt *et al.*, 2001), although these observations have failed to be reproduced by others (Waggoner *et al.*, 2000; Hutter *et al.*, 2003). PrP^c contains a unique octapeptide-repeat sequence at its N-terminal region (51-90). ROS provoke cleavage of the cellular prion at the octagon repeat, which is also the region at which copper-binding occurs (McMahon *et al.*, 2001). Defects in copper metabolism may affect copper-dependent SOD, diminishing its enzymatic ability to detoxify ROS (Brown *et al.*, 2001; Brown *et al.*, 1999) although again, these findings have not been replicated (Jones *et al.*, 2005). Figure 1.6 illustrates potential roles of oxidative stress pathways in neurodegeneration.

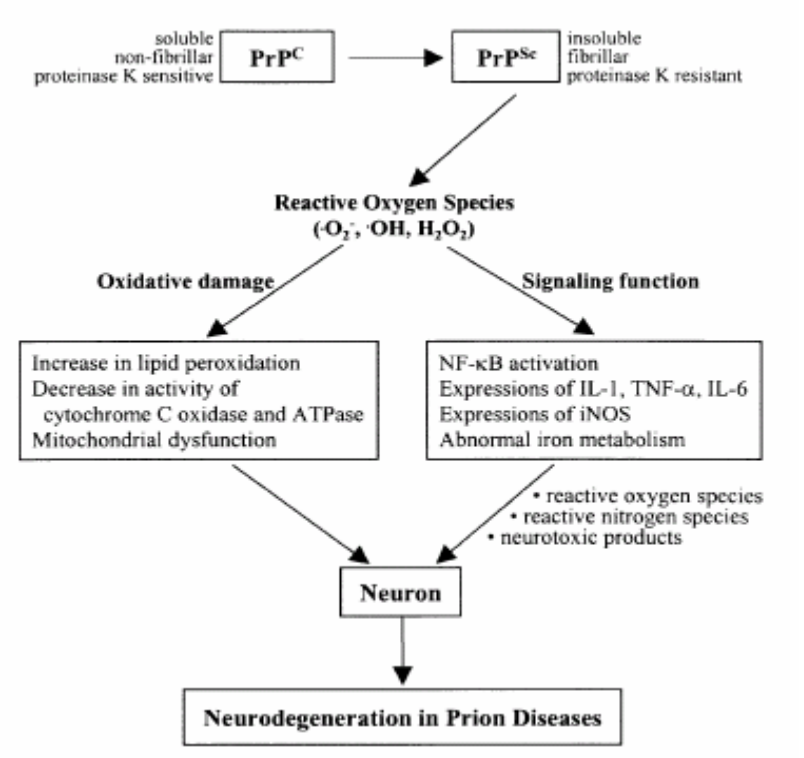

Figure 1.6. Possible role of oxidative stress in neurodegeneration in prion diseases. Exact mechanisms remain undetermined, but recent studies have suggested the involvement of reactive oxygen species in neurodegeneration. A link between oxidative stress and neurodegeneration has also been suggested and is being investigated for other neurodegenerative diseases, including Alzheimer's and Parkinson's diseases (Kim et al., 2001).

ENDOPLASMIC RETICULUM STRESS

The endoplasmic reticulum (ER) carries out numerous fundamentally important functions including; post-translation modification, folding and assembly of newly synthesized proteins, biosynthesis of proteins, steroids, cholesterol and other lipids and calcium storage and calcium signaling. Critically, it also discriminates between normal (native) and abnormal proteins, initiating retro-translocation of misfolded proteins for degradation. Therefore, the ER is extremely sensitive to changes that may affect its structure, integrity and function. Dysfunction or loss of integrity of the ER leading to stress can be caused, for example, by accumulation of unfolded proteins and by changes in calcium homeostasis within the ER. Such stress elicits cellular responses which confer protective effects against the toxic buildup of misfolded protein. If accumulation is excessive or if ER dysfunction is severe or prolonged, a signaling cascade termed the unfolded protein response (UPR) becomes activated, increasing expression of chaperones and folding enzymes that decrease unspecific aggregation or targets misfolded proteins to proteasome-mediated degradation (Sitia & Braakman, 2003). If the UPR is unable to rectify ER folding capacity, death pathways mediators are induced, ultimately leading to organelle dysfunction and cell death (Breckenridge *et al.*, 2003). Cell culture studies have suggested that PrP^{c}-PrP^{Sc} conversion occurs post-translationally on the cell surface or in the endocytic pathway, although the precise subcellular compartments, the molecular mechanisms of this process and the pathways that links ER stress to programmed cell death remain poorly understood (Borchelt *et al.*, 1992; Caughey & Raymond, 1991).

Wild-type PrP staining patterns suggests localization to an intracellular compartment, most likely the perinuclear Golgi. In contrast, mutant PrP localized in a more widespread pattern, largely with the ER marker protein disulphide isomerase, where delayed biosynthesis and export out of the ER resulted in increased protein concentrations within the ER (Ivanova *et al.*, 2001; Piccardo *et al.*, 1990). It is possible that the delayed transportation of mutant PrP within the ER is due to post-translational modifications conferring proteinase K (PK) resistance and detergent insolubility properties to PrP^{Sc} (Caughey *et al.*, 1991). In addition, retrotransport of

PrP^{c} from *trans*- Golgi compartments toward the ER occurs in scrapie -infected neuroblastoma cells (Taraboulos *et al.*, 1992). However brefeldin A, an ER-Golgi trafficking inhibitor, results in decreased levels of PrP^{Sc}, suggesting that the ER alone is insufficient for PrP^{c}-PrP^{Sc} conversion and requires transition via the endocytic pathway to the Golgi (Taraboulos *et al.*, 1992; Hetz *et al.*, 2007).

Several ER-related chaperones are up-regulated and the ER-related intrinsic apoptotic pathway mediator caspase-12 is activated *in vitro* in human and experimental prion diseases. PKR-like endoplasmic reticulum kinase (PERK) and its downstream effector, eukaryotic translation initiation factor 2α (eIF2α), are both activated in AD pathology but have normal expression levels in prion pathology (Unterberger *et al.*, 2006). Glucose-regulated proteins (GRPs) are Ca^{2+}-binding chaperones with ER protective properties. In scrapie murine models, accumulation of PrP^{Sc} was closely followed by induction of the ER chaperone Grp58, but not Grp78 or GADD153/CHOP, indicating that Grp58 induction is a specific response to prion replication (Rao & Bredesen, 2004). Figure 1.7 illustrates the ER stress pathways which may be modulated during prion infection.

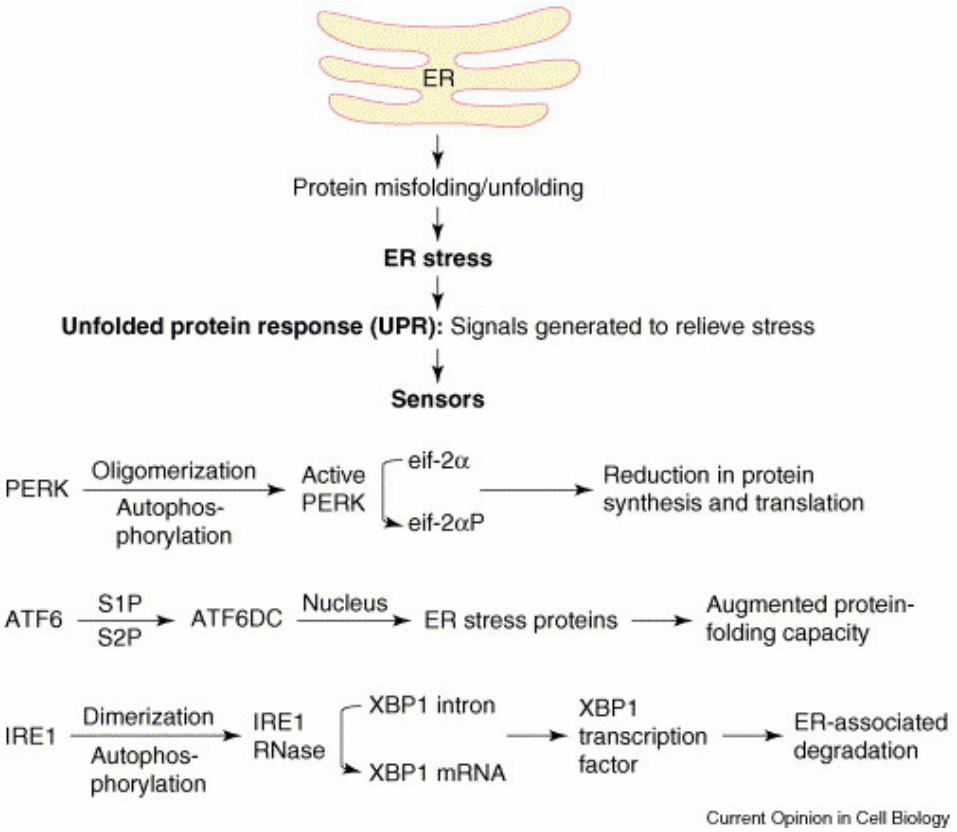

Figure 1.7. Signal transduction events associated with ER stress. Accumulation of misfolded proteins in the ER can disrupt ER function resulting in 'ER stress'. The ER responds by triggering specific signaling pathways including the unfolded protein response (UPR). The UPR is co-ordinately regulated by the three proximal sensors, IRE1, PERK and ATF6. The activation of all three proximal sensors results in reduction in the amount of new protein translocated into the ER lumen, increased degradation of ER-localized proteins and increased protein folding capacity of the ER. ATF6DC represents the 50 kDa cytosolic bZIP-containing fragment that translocates to the nucleus to activate transcription. Taken from (Rao & Bredesen, 2004).

SIGNAL TRANSDUCTION

PrP^c attaches to the lipid bilayer membrane via a GPI-anchor and resides in lipid raft domains which serve as molecular scaffolds for signal transduction (Mouillet-Richard *et al.*, 2000). Since the PrP^c polypeptide chain is entirely extracellular, transmission of signals into the cytoplasm would require interaction with transmembrane adaptor proteins. This has raised interest in identifying PrP cell-surface signaling or cell adhesion functions, and whether loss, gain or subversion of these functions accounts for the pathological outcome. PrP^c may mediate signal transduction pathways directly, although to date it has not been possible to elucidate how this may occur, or indirectly by activating transmembrane signaling pathways, either constitutively or by interaction with specific ligands. One example of this is

activation of a tyrosine kinase (Fyn) by PrP^c. Serotoninergic or noradrenergic neurons exhibit Fyn activity under the mediation of caveolin-1 and possibly clathrin (Williams *et al.*, 1994). Activated glial cells are a prominent feature of prion diseases; these are generally confined to regions of vacuolation and PrP deposition (Brown *et al.*, 1996). This is consistent with the observation that PrP neurotoxicity requires microglial cells (Diedrich *et al.*, 1991a). Time course experiments have established that microglial activation precedes neuronal death and prion protein is known to accumulate in astrocytes prior to neuropathological changes in scrapie (Williams *et al.*, 1997; Giese *et al.*, 1998). Therefore glial activation is not just a sequelae of cell destruction (Peyrin *et al.*, 1999). Induction of proinflammatory microglial cytokines have been shown (IL1β, IL6 and TNFα) and actrocytes up-regulate glial fibrillary acidic proteins (GFAP) (Kim *et al.*, 1999; Campbell *et al.*, 1994; Williams *et al.*, 1994), however results show that the aging brain displays a pro-inflammatory gene expression profile similar to prion-infected brain, therefore the role of glial cells and the interactions of PrP with signal transduction pathways in TSE disease remain unclear.

Reactive oxygen species (ROS) have been suggested as intracellular effectors in gene regulation and may be involved in signal transduction pathways. Among the most important pathways affected by oxidants are the NF-κB signalling pathways (Kim *et al.*, 1999). The NF-κB/Rel family of transcription factors is important in the regulation of numerous genes involved in mediating inflammatory and immune responses to stress (Vassallo *et al.*, 2005; Weise *et al.*, 2006). Immunostaining for activated NF-κB localizes with reactive astrocyte and PrP-amyloid plaques (Ju *et al.*, 1998). Representative target genes for NF-κB pathway activation also show significant increases in scrapie models (Baeuerle & Henkel, 1994). PrP^c may also activate the PI3/Akt pathway to modulate neuroprotective effects during stress. $Prnp^{-/-}$ mouse brain tissue shows reduced Akt pathway activity relative to $Prnp^{+/+}$ brain tissue when subjected to ischemic brain injury. Moreover, pharmacological inhibition of Akt reduced the ability of PrP^c to protect cells against oxidative insult (Mironov *et al.*, 2003).

PrP TRAFFICKING AND CHOLESTEROL

When PrP accumulates in the cytosol, neurotoxicity and neurodegeneration are observed (Magalhaes *et al.*, 2002; Ma *et al.*, 2002). The exact mechanism of how this occurs has not been elucidated, but provides a possible explanation as to how heritable and transmissible forms of the same disease can share certain characteristic pathological changes. Access of PrP to the cytoplasm of neurons and the endocytic processes involved would be a commonality between all forms of the disease. Internalisation of PrP^{c} co-localises with endosomal markers and FM4-64 (Borchelt *et al.*, 1992). Involvement of the endocytic recycling pathway adds evidence to findings that the initial steps in conversion may take place on the plasma membrane or immediately following internalisation of PrP^{c} (Shyng *et al.*, 1994; Shyng *et al.*, 1995; Madore *et al.*, 1999).

Surprisingly, clathrin coated pits and vesicles are primarily responsible for the endocytic uptake of PrP^{c}. GPI-anchored proteins lack cytoplasmic domains and are unable to directly interact with adapter proteins and clathrin. Nonetheless, uptake of PrP^{c} is mediated by recognition of the N-terminal sequence; deletions in this region diminish internalisation efficacy (Gauczynski *et al.*, 2001; Horonchik *et al.*, 2005; Hijazi *et al.*, 2005; Zanata *et al.*, 2002). It is highly likely that there is a putative PrP^{c} receptor containing a transmembrane domain, a localisation signal within its cytoplasmic domain and a extracellular domain binding the N-terminal of PrP^{c}. Currently this putative ligand has not been identified, although candidates have been suggested including laminins and glycoaminoglycans (Madore *et al.*, 1999; Parkyn *et al.*, 2008).

PrP^{c}, like other GPI-anchored proteins, resides in raft-like microdomains of the plasma membrane believed to be foci for signal transduction events (Hugel *et al.*, 2004; Tarraboulos *et al.*, 1995). Indeed, raft location of PrP^{c} is a prerequisite for its involvement in signal transduction (Vey *et al.*, 1996). In addition, there is growing evidence to suggest an integral role of lipid rafts with PrP^{Sc} conversion; first, both PrP^{c} and PrP^{Sc} co-localise to rafts (Taraboulos *et al.*, 1995b; Bate *et al.*, 2004); second, cholesterol depletion and thus lipid raft dissociation redistributes PrP^{c}

outside rafts, decreases formation of PrP^{Sc} and reduces PrP^{c} degradation in prion infected cell lines (Kaneko *et al.*, 1997); and thirdly, recombinant transmembrane forms of PrP^{c} which do not localised to rafts are not substrates for the formation of PrP^{Sc} (Kazlauskaite & Pinheiro, 2005; Taylor & Hooper, 2006).

Previous links between cholesterol levels and/or metabolism and AD development indicated the possibility of a similar link in prion disease pathogenesis. Low-density lipoprotein (LDL) receptor-related protein (LRP) is involved in the clearance of amyloid deposits (Kazlauskaite *et al.*, 2003). Studies have shown that modifying cholesterol levels disrupts lipid raft formation and thereby prion conversion. Furthermore, binding of PrP to lipid membrane causes structural changes to PrP depending on the environmental conditions. Membrane-induced alteration in conformation can lead to amporphous protein aggregation or formation of amyloid fibrils and can cause integrity destabilization of the lipid bilayer (Chandler, 1961; Chandler & Turfrey, 1972).

1.5 MODEL SYSTEMS

Transgenic models have been fundamental in understanding the normal and abnormal function of the PrP protein. TSE transmission experiments to mice were first introduced in the 1960's and to hamsters in the 1970's (Nonno *et al.*, 2006). Experimental scrapie models have typically been used as representative of TSE diseases, although experimental CJD models have also been developed. More recently, bank voles have been described as being susceptible to CJD (Bruce *et al.*, 1991; Bruce, 2003). Availability of inbred mouse strain has enabled standardisation of brain lesion profiling and characterisation of TSE strain types (Bueler *et al.*, 1993; Bruce *et al.*, 1991; Moore *et al.*, 1995; Manson *et al.*, 1994; Sakaguchi *et al.*, 1996). Two approaches to generating transgenic mice have been described; 1) by homologous recombination of defined genetic alterations or gene of interest introduced at the defined site of integration in the mouse genome of transfected

murine stem cells or 2) by direct microinjection of a transgenic DNA sequence encoding the gene of interest into the pronucleus of a mouse oocyte which leads to insertion of the transgene randomly into the mouse genome. Transgenic mice harbouring modifications of the endogenous murine PrP gene (produced by gene targeting) permits modifications to be introduced *in situ*. Therefore, the gene can be altered within its natural context, being in the correct genomic location and under the control of the normally regulated expression components. This is particularly useful as any alteration in the disease must therefore be attributed to the modification and this is essential for the direct comparison of different transgenic lines.

A number of PrP knockout mouse lines have been produced using gene targeting to investigate the role of PrP^{c} in normal and diseased tissues. Phenotypically, $PrP^{0/0}$ are overtly normal at the macroscopic, microscopic and behavioural levels, with subtle differences which may be attributed to other genes compensating for lack of PrP rather than the absence of the endogenous/original PrP. All four extant lines of null mice are resistant to scrapie (Fischer *et al.*, 1996). Furthermore, when a murine PrP^{c} transgene is reintroduced into these mice, they become susceptible to infection (Westaway *et al.*, 1991; Scott *et al.*, 1989). Mutant PrP expression models which over- or under-express either the endogenous or heterologous species of prion have demonstrated a link between expression levels of PrP and disease progression. Over-expression of the PrP gene leads to shorter incubation times, provided the inoculating strain is compatible with the origin of the transgene. The efficiency of transmission is affected by the donor PrP versus recipient PrP compatibility but may also be influenced by strain specific effects. This observation has prompted development of a wide range of transgenic mouse lines expressing human, mink, bovine, ovine, caprine, cervid and mouse PrP^{c} (Hsiao *et al.*, 1990; Westaway *et al.*, 1994). Over-expression can also result in spontaneous disease, which can be transmissible (Manson, 1996; Bueler *et al.*, 1993). The effects of under-expression of PrP have emerged from observation of heterozygous offspring from the production of $PrP^{0/0}$ mice. Such offspring contain only one functional copy of murine *Prnp* gene, and when inoculated with various TSE strains, have exhibited relatively longer incubation times than wild-type controls (Xiang *et al.*, 2004; Skinner *et al.*, 2006;

Baker & Manuelidis, 2003; Brown *et al.*, 2004; Brown *et al.*, 2005a; Sorensen *et al.*, 2008; Dandoy-Dron *et al.*, 2000; Booth *et al.*, 2004; Riemer *et al.*, 2004).

Recent transcription-profiling studies have found distinct gene-expression patterns in diseased tissue of a number of model systems, shedding light on the principal mechanisms involved in TSE disease (Vuong *et al.*, 2000; Brown *et al.*, 2004; Brown *et al.*, 2005a; Huber, 2003; Fountolakis, 2004). Comprehensive genome-wide studies screen for molecular changes associated with TSEs and identify host genes which exhibit modified expression patterns. The expression pattern of a gene or gene product during disease may provide insight into cellular processes which are a cause or a consequence of disease. The human genome encodes >30,000 genes and it is the selective expression of a specific subset of these genes under defined conditions which gives the cell or tissue type its phenotype. Dynamic gene expression can be studied using two approaches. Quantification of mRNA levels, or transcriptome analysis, identifies the particular response of the cells to an insult (i.e. TSE infection) by modification of the transcriptional program. However, the expression of many genes is regulated after transcription, so an increase in mRNA concentration need not always increase expression. In addition, analysis of relative mRNA expression levels can be complicated by the fact that relatively small changes in mRNA expression can produce large changes in the total amount of the corresponding protein present as there is no strict linearity between gene expression and steady-state protein level. Alternatively, proteomic analysis measures the entire complement of proteins expressed at a given time point under defined conditions. It is estimated that the average protein undergoes between 2 and 20 post-translational modifications such as amino- and carboxyl-terminal cleavage, phosphorylattion, glycosylation and myristoylation, greatly increasing the protein isoforms present in cells and complicating proteome studies (Gorg *et al.*, 2004; Santoni *et al.*, 2000). Proteomics is a relatively new field and has certain disadvantages; technologically, it is not suited to high-throughput methodologies, is much harder to standardise and requires large amounts of protein. Proteins, and particularly their modifications, are less stable than RNA and are susceptible to degradation. Detection methods are not as sensitive as RNA methods and, confounded by the unavailability of amplification method like

PCR, are unable to detect certain classes of proteins i.e. hydrophobic membrane bound and low or high molecular weight . Nonetheless, transcriptomics and proteomics are complementary technologies, combining genotype and phenotype data to further the understanding of the neurobiology of disease.

Previously published mouse and human brain gene expression studies have identified commonly altered pathways during TSE infection. Oxidative and ER stress, activated ER and mitochondrial apoptosis pathways and activated cholesterol biosynthesis were identified in ME7/CV mouse scrapie models (Brown *et al.*, 2005a). Increased mRNA levels for inflammatory response, proteolysis and signal transduction genes were also observed (Riemer *et al.*, 2004; Xiang *et al.*, 2004). In sCJD human brain, similar genes involved in stress-response factors and elements involved in cell death and down-regulation of genes encoding synaptic proteins have been identified (Xiang *et al.*, 2005). The large data volumes generated from gene expression studies can be confusing; however fundamental changes which are causative in TSE pathology should be common to all types of TSE. The finding that scrapie responsive genes are comparably altered in BSE-infected mouse brain suggests common pathogenic events occur in different TSEs (Dandoy-Dron *et al.*, 2000). Comparative transcriptome analysis of brains from experimental mouse TSE, BSE, sheep scrapie and human TSEs are therefore warranted and needed. A number of gene expression studies on TSE infected mouse brain exist as does a study of sCJD brain (Brown *et al.*, 2004; Brown *et al.*, 2005a; Riemer *et al.*, 2004; Xiang *et al.*, 2004; Xiang *et al.*, 2005). Studies on the BSE infected cow brain and the scrapie infected sheep brain are in progress. This project investigates the feasibility of studying the transcriptome of the human vCJD brain.

AIM:

Extract and characterize RNA from human autopsy vCJD and control brains, determine pre- and post-mortem factors affecting quality and quantity of this RNA and carry out preliminary studies to determine its suitability for gene expression studies.

OBJECTIVES

- Establish safe protocols for the extraction of RNA from human post-mortem vCJD and control brain material;
- Determine whether it is possible to remove infectivity, as defined by PK resistant PrP detection, from RNA preparations derived from TSE infected human brain material;
- Determine suitable assays for assessment of yield and quality of this RNA;
- Assess the quality and quantity of RNA isolated from human autopsy brain material.
- Assess whether pre- and post-mortem parameters affect RNA yield and quality;
- Identify RNA preparations (case control and RNA quality) suitable for comparative transcriptome analysis;
- Carry out preliminary studies to compare gene expression in vCJD and control brains.

HYPOTHESES:

This study addresses two hypotheses:

1. That the quality and yield of RNA preparations from human post-mortem brain material are related to pre- and post-mortem factors.
2. That RNA preparations isolated from human autopsy material is suitable for microarray comparison of gene expression in vCJD and control brain.

2 MATERIALS AND METHODS

2.1 RNA EXTRACTION PROTOCOL

2.1.1 RNA Extractions

All procedures were conducted entirely in the Class 1 microbiological safety cabinet in the Category 3* high risk lab wearing standard gown and disposable high-risk over-gown, protective footwear, protective eyewear and double gloves.

Tissues were removed from RNAlater (Ambion Biosystems, Warrington, UK) and 80 – 100 mg dissected for homogenisation. A freezer cooled, RNase-free plastic micro-pestle (Eppendorf, Cambridge, UK) was used to homogenise the sample. RNA was extracted using the Rneasy lipid tissue mini kit (Qiagen, Crawley, UK), with an extra phenol:chloroform extraction as described by Maniatis et al (Maniatis *et al.*, 1982). RNA was stored at –80ºC in RNase/ DNase-free TE-buffer pH 8.0 (Sigma-Aldrich, Dorset, UK).

Qiagen RNeasy Lipid tissue RNA Extraction
Total cellular RNA was isolated from the samples using the RNeasy Lipid Tissue mini kit (Qiagen, Crawley, UK) according to the manufacturer's instructions. Briefly, 1000 µl of Qiazol was added to a 100 mg sample, and the mixture was homogenised using a pre-chilled RNase-free plastic micro-pestle (Eppendorf, Cambridge, UK) for cell lysis. After homogenation, 200 µl chloroform (Sigma-Aldrich, Dorset,UK) was added and the mixture was vortexed. The subsequent aqueous and organic layers were separated by centrifugation (FastPrep-120; Q BIOgene) at 12,000 x *g* for 15 minutes at 4°C. The upper aqueous phase containing the RNA was removed and 200 µl of 70% ethanol (Sigma-Aldrich, Dorset, UK) was added to adjust binding conditions. The mixture was applied to the silica-gel matrix and centrifuged through at 8,000 x *g* for 15 seconds to allow RNA to adsorp to the membrane (Qiagen, Crawley, UK). Contaminants were washed through by wash spins (8,000 x *g* for 15

seconds) using wash buffers supplied with the kit (RW1 and RPE). RNA is then eluted in > 30 µl RNase-free H_2O (supplied in kit).

Phenol:chloroform RNA extraction

Total RNA samples were then re-extracted using phenol:chloroform extraction protocol as described by Maniatis et al (Maniatis *et al.*, 1982). Briefly, RNA sample were made up to 300 µl using RNase-free TE-buffer (Sigma-Aldrich, Dorset, UK) and carrier transfer RNA (tRNA) (final concentration 0.1mg/ml) (Sigma-Aldrich, Dorset, UK). 300 µl phenol:chloroform:isoamyl alcohol was added and vortexed. The subsequent aqueous and organic phases were separated by centrifugation at 12,000 x *g* for 15 seconds at room temperature. The upper aqueous phase containing the RNA was removed and reserved. The organic phase was back-extracted by adding an equal volume of TE-buffer (pH 8.0) (Sigma-Aldrich, Dorset, UK) and vortexing. The aqueous and organic phases were separated by centrifugation at 12,000 x *g* for 15 seconds and the upper aqueous phases was removed and combined with the first. An equal volume of chloroform (Sigma-Aldrich, Dorset, UK) was added to the aqueous phase and vortexed. The phases were again separated by centrifugation at 12,000 x *g* for 15 seconds. The upper aqueous phase was removed and ammonium acetate solution was added to a final concentration of 2M. In order to recover the RNA, 2.5-3 volumes of cold (-20°C) 100% ethanol was added and the RNA prepitated overnight at -20°C. The precipitate was spun at 12,000 x *g* for 15 minutes, all excess ethanol was removed and the pellet was allowed to air-dry in a microbiological safety cabinet for <2 hours to ensure no carry over of contaminating organic solvents. The pellet was then resuspended in 100 µl TE-buffer (pH 8.0) (Sigma-Aldrich, Dorset, UK) and stored at -80°C.

2.1.2 Nucleic Acid Quantification and Quality Assessment

RNA quantification and quality assessments were carried out at the Centre of Infectious Diseases, Summerhall.

The RNA samples quality were analysed on an Agilent 2100 Bioanalyzer (Agilent Technologies, Edinburgh, UK). In this system, micro-channels on an Agilent chip are filled with a gel matrix, which acts as a sieving polymer. Sample components are electrophoretically separated and detected by their fluorescence and visualised on a gel-like image and an electropherogram (Figure 2.1). This determines the quantity and quality of the RNA extracted from the sample and the ratio of 28S rRNA to 18S rRNA. The Bioanalyzer also produces a RNA Integrity Number (RIN), a software algorithm developed by Agilent Technologies in order to standardise the assessment of RNA quality. The RIN scales between N/A or 0.0 (completely degraded, undetectable RNA) and 10.0 (completely intact RNA).

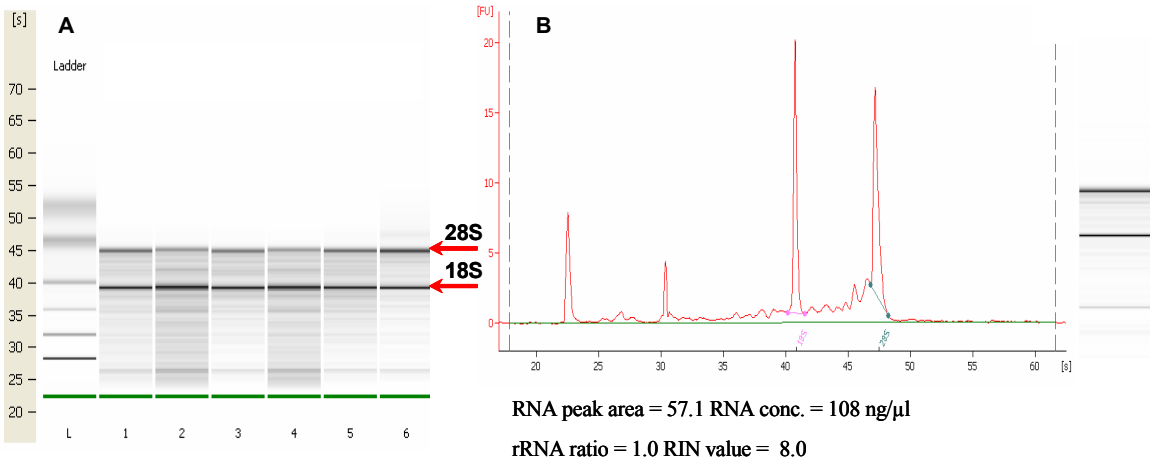

RNA peak area = 57.1 RNA conc. = 108 ng/µl

rRNA ratio = 1.0 RIN value = 8.0

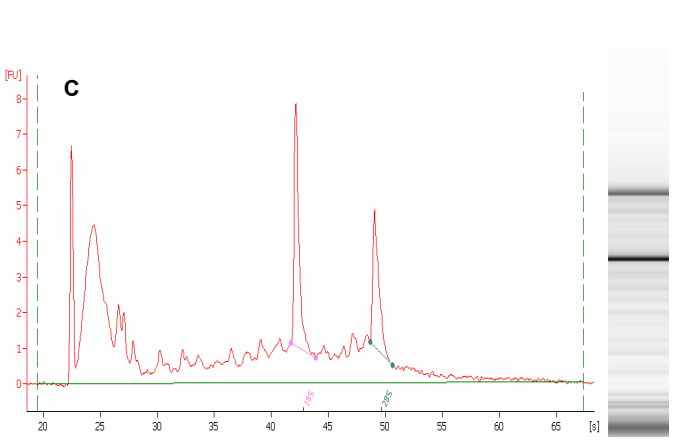

RNA peak area = 104.1 RNA conc. = 104 ng/µl

rRNA ratio = 0.6 RIN value = 6.3

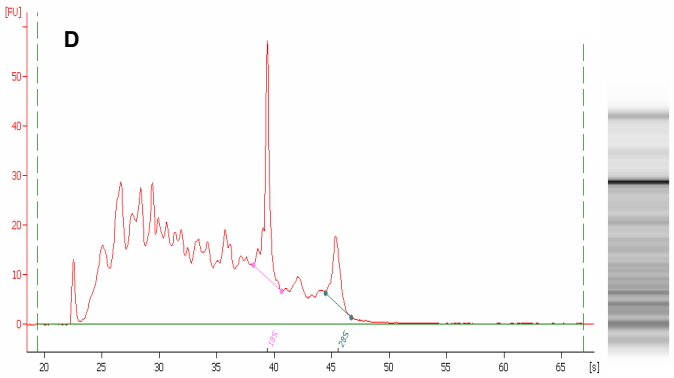

RNA peak area = 999.2 RNA conc. = 473 ng/µl

rRNA ratio = 0.4 RIN value = 4.8

Figure 2.1. Electropherogram and gel-like image from Agilent 2100 Bioanalyzer output. A. Agilent gel-like image shows the two major bands corresponding to 28S and 18S rRNA bands (arrows). Each sample can be visualised as an electropherogram. B. This sample is an excellent example of RNA which is not degraded. The 5S peak (30 sec) is just visible along with the 18S and 28S rRNA peaks. There is no evidence of degraded RNA because the base line is flat. In some tissues the 28S peak has twice the RNA content of the 18S peak. The 28S species is highly susceptible to degradation- hence any degradation can be seen as a reduction in the 18S:28S ratio. C. This electropherogram highlights a partially degraded sample. Notice the 28S peak is reduced and degraded RNA is visible as peaks in the base line emerging at time frames 30-40 sec. D. This electropherogram shows a degraded RNA sample. Notice the peaks at 25-30 sec, indicative of small RNA fragments.

The RNA sample quantities were analysed on a Nanodrop ND-1000 Spectrophotometer (Nanodrop Technologies, Washington, USA). In this system, 1 µl of sample is pipetted directly on to the end of a fibre optic cable (receiving fibre). A second fibre optic cable (source fibre) is brought into contact with the liquid sample and a liquid column is formed, bridging the gap between the two fibres. A pulsed xeon flash lamp provides the light source and a spectrometer utilizing a linear CCD array is used to analyse the light after it has passed through the sample.

All DNA samples were quantified on the Nanodrop ND-1000 spectrophotometer using the same method discussed for RNA samples.

2.2 Assessing RNA preparation

2.2.1 Sample Preparation for Western Blot Analysis

Standardised brain reference sample preparations were carried out as described below. Wet tissue weighing of ~80-100 mg was taken from frozen samples. A freezer cooled, RNase-free plastic micro-pestle (Eppendorf, Cambridge, UK) was used to homogenise this in 4ºC extraction buffer, to obtain a 10 % (w/v) brain homogenate. A non-ionic detergent insoluble pellet (nucleocytoskeletal fraction) was collected by centrifugation at 2,000 x *g* for 5 minutes at 4ºC (Eppendorf 5417R). 200 µl of the detergent soluble (cytoplasmic and membrane fraction) supernatant was digested using proteinase K (VWR International, Leicestershire, UK) at a final concentration of 50 µg/ml at 37ºC for 1 hour. Protease digestion was terminated by the addition of Pefabloc (Roche, Hertfordshire, UK) to a final concentration of 1 mM and the sample was stored at –20ºC or used immediately for analysis.

RNA sample preparations were carried out as described below. 10 µl of the RNA extract or human recombinant PrP was digested using proteinase K (VWR International, Leicestershire, UK) at a final concentration of 50 µg/µl at 37ºC for 1 hour. Protease digestion was terminated by the addition of Pefabloc (Roche,

Hertfordshire, UK) to a final concentration of 1 mM and the sample was stored at –20ºC or used immediately for analysis.

An equal volume of 2X sample buffer (Invitrogen, Paisley, UK) was added to an aliquot of sample and heated to 100ºC for 10 minutes. Samples were collected at the bottom of the tube by a brief spin. The samples were run at 200 V constant current for 50 minutes, using 10% Bis-Tris pre-set gel cassettes (Invitrogen) and NuPAGE MES-SDS 1X running buffer (Invitrogen). A pre-stained benchmarker (Invitrogen) was run in conjunction with the samples.

The gel was blotted onto a polyvinylidene difluoride (PVDF) membrane (Hybond-P, Amersham, UK). The membrane was first wet in MeOH, incubated in dH_2O for 10 minutes and equilibrated for 20 minutes in transfer buffer (Invitrogen). 4-6 pieces of blotting paper were wet in transfer buffer for 20 minutes. The transfer cell was assembled; 2-3 pieces of pre-soaked padding, followed by 1 piece 3MM blotting paper (Hybond), the gel (dye side up), pre-soaked PVDF membrane, 1 piece 3MM blotting paper and finally 2-3 pieces of pre-soaked padding. The cell was assembled and covered in transfer buffer, and the outer tank was filled with water. The transfer was run at 30V constant current for 1 hour.

For detection, the PDVF membrane was washed twice in 40 ml TBS-T (Sigma-Aldrich, Dorset UK) for 3 minutes. The membrane was then blocked by incubation in 50 ml 5 % non-fat powdered milk (Safeway, Bradford, UK) in TBS-T (Tris-buffered saline; 10 mM Tris, pH 7.4, 150 mM NaCl containing 0.1 % Tween 20) for 45 minutes. The membrane was then washed three times for 3 minutes each, in 40 ml TBS-T and incubated with a mouse monoclonal antibody 6H4 (epitope hPrP144-152) (100 µg, Prionics, Schileren, Switzerland) at 1:20,000 (2 µl) in 40 ml of TBS-T for 45 minutes. Another three washes were carried out using 40 ml TBS-T for 3 minute incubations. A secondary antibody incubation of horseradish peroxidase-HRP-conjugated anti-mouse (from sheep, GE Lifesciences, Buckinghamshire,UK) at 1:40,000 (1 µl) in 40 ml TBS-T for 45 minutes was followed by a final three washes of 3 minute incubations in 40 ml TBS-T. Chemiluminescent substrate was prepared

by combining 4 ml ECL PLUS reagent A with 100 µl reagent B (Lumigen, Amersham, Buckinghamshire, UK), dispensed onto drained membrane and incubated for 5 minutes. Transfers were visualised using Hyperfilm ECL film (GE Lifesciences) and developed using the Hyperprocessor (GE Lifesciences), with exposure times of 30 seconds, 3 minutes and 30 minutes. All reagent recipes are given in Appendix 9.1.

2.3 Oligo GEarray Protocol

2.3.1 cRNA Preparations and Labelling

TrueLabeling-AMP 2.0 kits (SuperArray Bioscience, Maryland, USA) were used to amplify and label antisense RNA (aRNA) for hybridisation to the Oligo GEArray from SuperArray Bioscience. Briefly, annealing mixtures were prepared for each RNA sample by combining the following in a sterile, RNase-free PCR tube: 0.1 – 3.0 µg total RNA, 1.0 µl component G1 and RNase-free H_2O to a final volume of 10 µl. The annealing mixture was then incubated at 70°C for 10 minutes and then placed on ice.

cDNA synthesis master mixes were prepared by mixing the following in a sterile, RNase-free PCR tube for each reaction: 4 µl RNase-free H_2O, 4 µl 5X cDNA synthesis buffer (G3), 1 µl RNase inhibitor (RI), 1 µl cDNA synthesis enzyme mix (G2). 10 µl cDNA synthesis master mix was added to each tube containing 10 µl annealing mixture and mixed well. The reaction was incubated at 42°C for 50 minutes followed by 72°C for 5 minutes then cooled to 37°C. Amplification master mixes were prepared by mixing the following in a sterile, RNase-free PCR tube for each reaction: 16 µl 2.5X RNA polymerase buffer (G24), 2 µl biotinylated-UTP (10Mm) (Sigma Aldrich, Dorset, UK), 2 µl RNA polymerase enzyme (G25). 20 µl of amplification master mix was added to 20 µl cDNA synthesis mix, mixed well and incubated for at least 1 hour and up to overnight at 37°C.

cRNA PURIFICATION

60 µL RNase-free H_2O was added to each cRNA synthesis reaction to a final volume of 100 µl and transferred to a 1.5 ml RNase-free microcentrifuge tube. 350 µl lysis and binding buffer (G6) was added to each reaction mixture and mixed well. 350 µl room temperature ACS-grade 100% ethanol (Sigma Aldrich) was added to the reaction tubes and mixed well. Each sample was pipetted directly onto the centre of a spin column and centrifuged at 8000 x *g* for 30 seconds. The flow through was discarded and 600 µl washing buffer (G17 with ethanol) was pipetted directly onto the spin column filter. The sample was centrifuged at 8000 x *g* for 30 seconds and the flow through was discarded. Another 200 µl of washing buffer was pipetted directly onto the spin column filter and centrifuged at 11000 x *g* for 60 seconds, followed by 11000 x *g* for 2 minutes, ensuring all wash buffer was spun through. The spin columns were transferred to a new sterile, RNase-free microcentrifuge tube and 50µl of room temperature RNase-free 10 mM Tris buffer pH 8.0 (G26) was pipetted directly onto the spin column filter and left to incubate at room temperature for 2 minutes. The sample was then centrifuged at 8,000 x *g* for 60 seconds and collected. The purified cRNA was stored at -20°C.

2.3.2 cRNA Quantification and Quality Assessment

Quantification was done by two methods: Agilent 2100 Bioanalyzer (Agilent Technologies, Edinburgh, UK) and NanoDrop ND-1000 spectrophotometer (Nanodrop Technologies, Washington, USA). Both methods are described in Chapter 5.

2.3.3 RNeasy Mini Protocol for RNA Cleanup

For cRNA samples that did not fall within set criteria (concentration $A_{260} \geq 11$ ng/µl; $A_{260:280} \geq 2.0$; $A_{260:230} \geq 1.7$ and clear 18S and 28S rRNA peaks as analysed by Agilent 2100 Bioanalyzer (Figure 2.1)), the RNeasy mini RNA cleanup protocol (Qiagen, Crawley, UK) was followed. Briefly, β-mercaptoethanol (β-ME) was added to buffer RLT and ethanol was added to buffer RPE before use, as per kit instructions. Sample volumes were adjusted to 100 µl with RNase-free water. 350 µl

buffer RLT was added and mixed. 250 µl ethanol (96-100%) was added to RNA sample and mixed thoroughly. Immediately, 700 µl of the sample was applied to the RNeasy mini column in a 2 ml collection tube, and centrifuged for 15 seconds at 8,000 x *g*. The flow-through was discarded and the rest of the sample was spun through in the same manner, until completed. The column was transferred to a new 2 ml collection tube, 500 µl buffer RPE was applied to the column and centrifuged for 15 seconds at 8,000 x *g*. The flow-through was discarded, another 500 µl buffer RPE was applied to the column and centrifuged for 2 minutes at 8,000 x g, to dry the silica membrane. The RNeasy column was placed in a new 2 ml collection tube and centrifuged for 1 minute at full speed. The RNA was eluted by transferring the column to a new 1.5 ml collection tube, and 30-50 µl RNase-free water was applied directly to the silica-gel membrane. This was centrifuged for 1 minute at 8,000 x g.

2.3.4 Hybridisation Protocol

PRE-HYBRIDISATION

To pre-wet array membranes, 5 ml of deionised water was added to the hybridization tubes, inverted and incubated for 5 minutes. The GEAhyb hybridization solution was warmed to 60ºC. 2 ml of hybridization solution was added to the hybridization tubes and vortexed briefly. At least 2 µg of biotin-labelled cRNA was added to 0.75 ml of pre-warmed hybridization solution, and kept at 60ºC. The pre-hybridization solution was discarded and the target hybridization solution containing the labelled cRNA target was added to the tube. Hybridization was carried out overnight, with continuous but slow agitation at 5 to 10 rpm.

WASHING

5 ml of wash solution 1 and 5 ml of wash solution 2 were prepared for each array (Appendix 9.1) and pre-warmed to 60°C. 5 ml of wash solution 1 was added to the hybridization tube, vortexed and placed in to the incubator at 60°C with 20 to 30 rpm

agitation for 15 minutes. Wash solution 1 was then discarded and 5 ml of wash solution 2 was added to the hybridization tube, vortexed briefly and placed back in the incubation oven for exactly 15 minutes at 60°C with 20 to 30 rpm agitation. Wash solution 2 was immediately discarded and the tubes were resealed to prevent the membranes drying out and allowed to cool to room temperature in the hybridisation oven.

CHEMILUMINESCENT DETECTION

2 ml GEAblocking solution Q was added to the hybridisation tube, vortexed briefly and incubated for 40 minutes with continuous agitation at 20 to 30 rpm. 16 ml 1X buffer F was prepared for each array membrane, and 16 ml 1X buffer F was prepared to dilute alkaline phosphatase-conjugated streptavidin (AP-SA) buffer. After appropriate incubation, buffer Q was discarded and 2 ml dilute AP-SA buffer was added, vortexed and incubated for exactly 10 minutes with continuous 5 to 10 rpm agitation. The membranes were then washed four times, each time using 4 ml 1X buffer F for 5 minutes with gentle agitation. After the final wash, the membranes were rinsed twice, using 3 ml buffer G. 1 ml CDP-Star chemiluminescent substrate was added to the hybridisation tube and placed in room temperature rotating oven for 5 minutes. After incubation, the arrays were removed, dried of excess CDP-Star solution without drying out membrane and placed in a plastic sheet protector, array face up, for image acquisition.

2.3.5 Microarray Analysis

Image acquisition was carried out using an Epson Perfection 1640SU (Epson, Herts, UK) flatbed scanner. Images were uploaded onto SuperArray proprietary web-based analysis software (SuperArray GEArray Expression Analysis Suite. http://geasuite.superarray.com/). Probe signal and background signal were determined using the GEArray Expression Analysis Suite (Superarray, Washington, USA). To normalise signal intensity across the array slide, arrays were intra-normalised using the GEArray Expression Analysis Suite (Superarray, Washington, USA) in the following manner; background correction was based on the lowest

average density spot on the array. Summation correction was based on the total density divided by the number of pixels. Arrays were then inter-normalised by comparing the interquartile values (between 25 -75%) of all probe signals. The values were converted to log base 10. Detailed information about this oligonucleotide array including description of gene probes, experimental protocol, and data analysis method can be obtained at the supplier's website (www.superarray.com).

2.4 POLYMERASE CHAIN REACTIONS (PCR)

2.4.1 Primer Design

A set of 5 primers was designed for use in the quantitative PCR machine (Rotogene 3000, Corbett Research, Australia) (Table 2.1). All primers were designed using Primer3 software (available online @: http://frodo.wi.mit.edu/cgi-bin/primer3/primer3_www.cgi) and verified for low spontaneity to form duplexes and hairpin loops using Netprimer software (available online @: http://www.premierbiosoft.com/netprimer/netprlaunch/netprlaunch.html).

Primer specifications:

- Primer length between 18 – 22 base pairs (optimum 20 base pairs)
- GC content of between 45 – 55% (optimum 50%)
- Maximum self complementarity predictions less than 3 were favoured, where software could predict suitable primer oligo, otherwise higher complementarity was allowed.
- Maximum 3' self complementarity predictions less than 2 were favoured, where software could predict suitable primer oligos otherwise higher complementarity was allowed.
- (ΔG) values similar for both sense and antisense primers were favoured.
- Melting temperature of primer oligos between 58 – 62°C (optimum 62°C)

- BLAST analysis (http://www.ncbi.nlm.nih.gov/BLAST/) carried out for each primer set to ensure specificity to gene of interest within E value >1.0.

Gene name	UniGene	Symbol	Forward primer	Reverse primer	Annealing temp (C°)	Start	End	PCR product size
glyceraldehyde-3-phosphate dehydrogenase	Hs.544577	GAPDH	*TCATCATCTCTGCCCCCTCT*	*CCATCACGCCACAGTTTCC*	60	458	698	241
Beta-actin	Hs.520640	ACTB	*ATTCCTATGTGGGCGACGAG*	*GCTGGGGTGTTGAAGGTCTC*	60	225	465	241
Cyclophilin A	Hs.356331	PPIA	GGCAAGACCAGCAAGAAGA	GGGAGGGAACAAGGAAAAC	58	520	718	179
Ubiquitin C	Hs.520348	UBC	*TGGGTCGCAGTTCTTGTTTG*	*GGGTGGACTCTTTCTGGATGTT*	58	403	647	245
18S rRNA	X03205[a]	18S rRNA	TCAAGAACGAAAGTCGGAGG	GGACATCTAAGGGCATCACA	60	1025	1513	468

Table 2.1. Forward and reverse primer sequences and product size of primers used for PCR and QRT-PCR analysis. [a] is accession number.

2.4.2 Reverse Transcription of RNA for cDNA Synthesis

In 0.2 ml thin-walled PCR tubes (Axygen Scientific Inc, California, USA), the following were added: 1 µl random pentadecamer primer (MWG Biotech, Ebersberg, Germany), 5 µl total RNA, 1 µl 10 mM dNTPs (Promega, Mannheim, Germany) and DNase/RNase- free, DEPC-treated water to make a final volume of 12 µl. An Express Thermohybaid cycler (Thermo Fischer Scientific, Epsom, UK) was used to heat samples for 5 minutes at 65ºC, before chilling tubes on ice for at least 1 minute. The following were added to the tubes: 4 µl 5X first strand buffer (Invitrogen, Paisley, UK), 2 µl 0.1 M DTT (Invitrogen), 1 µl RNAsin Recombinant Ribonuclease Inhibitor (Promega) and tubes were incubated at 25ºC for 2 minutes. After incubation, 1 µl of Superscript III Rnase H^- reverse transcriptase enzyme (Invitrogen) was added and tubes incubated at 50 minutes at 50ºC. Samples were inactivated by heating at 70ºC for 15 minutes before storage at –20ºC.

2.4.3 PCR Amplification

Amplification of the cDNA was carried out in 0.2 ml thin-walled PCR tubes (Axygen). To these tubes, reaction mixtures of 50 µl containing the following were added: 5 µl 10X PCR reaction buffer, 1 µl dNTPs, 7 µl $MgCl_2$ (25 mM), 0.25 µl Upstream primer (50 pM), 0.25 µl Downstream primer (50 pM), 1 µl sample cDNA, 0.25 µl *Taq* DNA polymerase and Dnase/Rnase-free, DPEC-treated water to make a final volume of 50 µl. Rnase/Dnase-free water was substituted for sample cDNA and used as negative controls. An Express Thermohybaid cycler (Thermo Fischer Scientific) was used to heat samples at 95ºC for 2 minutes. The samples were then denatured during cycling at 95ºC for 30 seconds, followed by primer annealing at 60ºC for 35 seconds. A primer extension cycle was run at 72ºC for 1 minute, and for 30 cycles. The final extension stage was at 72ºC for 15 minutes. Non-template (H_2O) controls were run in parallel with every PCR to test for reagent contamination.

2.4.4 Agarose Gel Electrophoresis for PCR Products

DNA and RNA were analysed by agarose gel electrophoresis. Briefly, 0.7 - 2 % gels were prepared using 0.5 M Tris acetate EDTA (TAE) buffer with 0.5 µg/ml ethidium bromide for visualisation under UV. Samples were mixed with 6 X loading buffer and loaded into wells. Depending on the size and agarose percentage of the gel, an electrical current of between 100-130 volts was applied, for approximately 1 hour. This allowed separation of nucleic acid fragments. A 100 bp ladder (New England Biolabs) or 1 kb ladder (Invirtrogen) was run in parallel as a size reference marker. The gel was then viewed under the UV transilluminator (UltraViolet Products, UK). PCR products were stored at -20°C for further analysis.

2.4.5 PCR Product Purification from Agarose Gel

High pure PCR purification kits (Roche Applied Science, Mannheim, Germany) were used to isolate PCR products from amplification reactions. The process' principle is based on PCR amplified DNA binding selectively to special glass fibres pre-packed in the High Pure Filter Tube when in the presence of the chaotrophic salt guanidine thiocyanate. The glass fibres only bind to DNA fragments with a minimum length of 100 bp, thus oligonucelotides and dimerized primers from PCR reactions are selectively removed. Bound DNA is purified in a series of rapid wash-and-spin steps to remove contaminating primers, nucleotides, and salts, and then eluted using a low salt solution. The simple method eliminated the need for organic solvent extractions and DNA precipitation. Two PCR product purification methods are possible; from solution after amplification or alternatively purification of DNA fragments from agarose gel.

For purification of DNA fragments from agarose gel, the desired DNA band was cut from the gel using a sterile scalpel and placed into a 1.5 ml DNase-free microcentrifuge tube. 300 µl binding buffer was added for every 100 mg agarose gel slice. The gel and buffer was incubated at 56°C for 10 minutes or until the gel was completely dissolved. 150 µl isopropanol was added for every 100 mg agarose gel slice in the tube and vortexed thoroughly. The solution was pipetted directly onto a

High Pure Filter and centrifuged at 13,000 x *g* at room temperature, for 60 seconds. The flow-through was discarded and 500 µl Wash buffer was pipetted directly onto the filter and centrifuged as above. This was repeated with 200 µl Wash buffer, twice. The flow-through was discarded each time and the spin column was placed in a clean 1.5 ml DNase-free microcentrifuge tube. 50 µl Elution buffer was pipetted directly onto the filter and centrifuged at 13000 rpm at room temperature for 60 seconds, and the purified DNA was collected and stored at -20°C.

For purification of PCR products in solution after amplification, the PCR reaction volume was adjusted to 100 µl using DNase-free H_2O. 500 µl Binding Buffer was added and mixed well. The sample was applied to the filter column and centrifuged at 13,000 x *g* for 1 minute. The flow through was discarded, 500 µl Wash Buffer was applied directly to the filter membrane and centrifuged again at 13,000 x *g* for 1 minute. An additional 200 µl Wash Buffer was added and centrifuged at 13,000 x g for 1 minute to ensure complete removal of Wash Buffer from the membrane. The spin column was placed in a clean 1.5 ml DNase-free microcentrifuge tube. To elute the DNA, 50 µl Elution Buffer was applied directly to the filter membrane and centrifuged at 13,000 x *g* for 1 minute. The purified DNA was collected and stored at -20°C.

2.4.6 Molecular Cloning

pGEM-T Easy Cloning

PCR fragments were cloned into the pGEM®-T Easy vector according to the manufacturer's instructions. Briefly, 5 µl of 2X Rapid Ligation buffer, 1 µl (50 ng) pGEM-T-Easy vector, 1 – 3 µl PCR product (calculated from the measured DNA concentration), 3 Weiss units of T4 DNA ligase (1 µl) and molecular grade H_2O to a final volume of 10 µl were mixed together. The reaction was incubated for approximately 16 hours at 4°C for maximum transformations. Following incubation,

3 µl of the ligation reaction were used to transform subcloning efficiency DH5α and JM 109 chemically competent *E.coli* cells.

BACTERIAL TECHNIQUES

All bacterial protocols were performed under aseptic conditions.

Bacterial Culture

Various laboratory strains of *E.Coli* were grown in Luria-Bertani (LB) medium or on LB agar plates (1.5% agar). Media was sterilized and agar melted by autoclaving. Media was supplemented with appropriate antibiotics (100 µl/ml ampicillin) prior to use. LB agar was poured into 10 cm diameter Petri dishes. Bacteria were plated on the surface of LB agar by spreading with a glass spreader, inverted and incubated at 37°C for approximately 16 hours. Single colonies from agar plates were used to inoculate liquid medium. Liquid cultures were incubated for approximately 16 hours with constant shaking at 225 rpm in an orbital shaker at 37°C.

Transformation of One Shot® DH5α™ Chemically Competent cells

One Shot DH5α – T1 chemically competent cells were transformed with the products of the pGEM-T-Easy cloning reaction. Briefly, a 50 µl aliquot of competent cells were thawed on ice for approximately 10 minutes. 2 µl of the cloning reaction was added to the cells, mixed gently and incubated on ice for 30 minutes. The cells were then heat-shocked for 20 seconds at 37°C. 950 µl pre-warmed SOC medium was added to the cells and incubated for 1 hour at 37°C with constant shaking at 225 rpm in an orbital shaker. 50 µl or 150 µl of the transformation reaction was then plated on LB agar plates supplemented with 100 µg/ml ampicillin and incubated, inverted, at 37°C for approximately 16 hours.

pGEM-T-Easy vectors allow blue/white colony screening for selection of colonies containing recombinant plasmids. Briefly, pGEM-T-Easy vectors contain the β-galactosidase gene. Insertion of the PCR fragment into the plasmid disrupts the

coding sequence of β-galactosidase. Colonies containing recombinant plasmids therefore appear white on indicator plates. Indicator plates were made by spreading 100 µl of 100 mM isopropyl-beta-D-thiogalactopyranoside (IPTG) and 20 µl of 50 mg/ml 5-bromo-4-chloro-3-inodlyl-β-D-galactopyranoside (X-Gal) on the surface of LB agar plates supplemented with 100 µg/ml ampicillin. Plates were allowed to absorb IPTG/X-Gal for 30 minutes at 37°C. To allow development of colour, these plates were incubated, inverted, for approximately 17 hours at 37°C.

Transformation of JM109™ Chemically Competent cells

JM109™ chemically competent cells were transformed with the products of the pGEM-T-Easy cloning reaction. Briefly, a 50 µl aliquot of competent cells were thawed on ice for approximately 10 minutes. 2 µl of the cloning reaction was added to the cells, mixed gently and incubated on ice for 30 minutes. The cells were then heat-shocked for 35 seconds at 42°C. 950 µl pre-warmed SOC medium was added to the cells and incubated for 1 hour at 37°C with constant shaking at 225 rpm in an orbital shaker. 50 µl or 150 µl of the transformation reaction was then plated on LB agar plates supplemented with 100 µg/ml ampicillin and incubated, inverted, at 37°C for approximately 16 hours.

Plasmid DNA Extraction (Miniprep)

QIAprep Spin Miniprep kits were used according to the manufacturer's instructions, for isolation of small amounts of plasmid DNA. Briefly, a single colony was isolated from an LB agar plate and used to inoculate 5 ml of LB medium supplemented with 100 µl/ml ampicillin in universal tubes. Inoculations were then incubated for approximately 16 hours at 37°C, shaking at 225 rpm in an orbital shaker. Cultures were then centrifuged at 1500 x g for 6 minutes. Pelleted bacterial cells were resuspended in 250 µl Buffer P1 and transferred into a sterile microcentrifuge tube. 250 µl of Lysis buffer P2 was added and mixed gently by repeated inversions. Lysis

was allowed to proceed for 5 minutes and 350 µl Buffer N3 added and again gently mixed by repeated inversions. The mixture was centrifuged at 17,900 x *g* for 10 minutes and the supernantant transferred to a QIAprep Spin column. The spin column was centrifuged for 1 minute at 17,900 x *g* to bind the DNA to the silica-gel membrane. The membrane was then washed using 500 µl Buffer PB and centrifuged at 17,900 x *g* for 1 minute. An additional wash step using 750 µl Buffer PE was carried out, followed by centrifugation at 17,900 x *g* for 1 minute. The column was then centrifuged for an additional minute to remove any residual wash buffer. To elute DNA, 50 µl DNase-free H_2O was added directly to the silica-gel membrane and was allowed to incubate for 1 minute at room temperature. The column was centrifuged at 17,900 x *g* for 1 minute to elute the DNA. DNA samples were quantified and checked for quality as described in section 1.1.2 and stored at -80°C.

Large Scale Plasmid DNA Extraction (Maxiprep)

Qiagen EndoFreePlasmid Maxi Kits were used according to the manufacturer's instructions, for isolation of large amounts of high quality plasmid DNA. Briefly, a single colony was isolated from an LB agar plate and used to inoculate 5 ml of LB broth supplemented with 100 µl/ml ampicillin in universal tubes. The starter culture was incubated for 6 – 8 hours at 37°C, shaking at 225 rpm in an orbital shaker. 500 µl of the starter culture was used to inoculate 250 µl LB medium supplemented with 100 µl/ml ampicillin. The culture was grown for 14 – 16 hours at 37°C, shaking at 225 rpm in an orbital shaker. Bacterial cells were harvested by centrifugation at 6,000 x *g* for 15 minutes at 4°C. The bacterial pellet was resuspended in 10 ml of Buffer P1 and 10 ml of Buffer P2 was added. The mixture was mixed gently by repeated inversions and lysis was allowed to proceed for no more than 5 minutes. 10 ml of chilled Buffer P3 was added to the lysate and poured into the barrel of the QIAfilter Cartridge and incubated for 10 minutes at room temperature. Cell lysate was filtered into a 50 ml tube and 2.5 ml Buffer ER was added. The tube was inverted 10 times to mix and incubated on ice for 30 minutes. A QIAGEN-tip 500 was equilibrated by applying 10 ml Buffer QBT; Buffer was allowed to flow through

by gravity flow. The filtered lysate was added to the equilibrated QIAGEN-tip and allowed to enter the resin. The QIAGEN-tip was washed twice using 30 ml Buffer QC. 15 ml Buffer QN was used to elute the DNA. DNA was precipitate by the addition of 0.7 volumes of isopropanol and centrifuged at 15,000 x g for 30 minutes at 4°C. The pellet was washed with 5 ml of 70% ethanol and centrifuged at 15,000 x *g* for 10 minutes. The supernatant was removed and the pellet was allowed to air-dry. Once dry, the pellet was resuspended in 300 µl DNase-free H_2O and stored at -80°C.

Preparation of frozen stocks of transformed bacteria

A single colony from an LB agar plate was used to inoculate 5 ml of LB medium containing 100 µl/ml ampicillin. The culture was grown for approximately 16 hours at 37°C at 225 rpm in an orbital shaker. Cells were pelleted by centrifugation at 1500 x *g* for 6 minutes and the pellet resuspended in 1 ml 50% glycerol in H_2O. The sample was transferred to a sterile eppendorf tube and snap frozen on dry ice. Samples were stored at -80°C.

Plasmid DNA Restriction Digestion

Restriction endonucleases were used to digest plasmid DNA. A number of different restriction endonucleases were used for this project. Generally restriction digestion reactions contained: 2 µl digestion buffer, 2 µl 10X BSA, 1 µl restriction endonucleases, plasmid DNA (volumes adjusted depending on the required amount needed in subsequent reactions) and DNase-free H_2O to a final volume of 20 µl. The reactions were incubated for 2 – 4 hours at the optimum temperature for the restriction endonuclease in use.

Purification of Restriction Digestion Products

QIAquick PCR purification Kits were used to purify DNA fragments from restriction digestion reactions, according to the manufacturer's instructions. Briefly, 5 volumes of Buffer PB was added to 1 volume of digestion reaction and missed by pippeting. The DNA sample was applied directly to the QIAquick spin column and centrifuged for 1 minute at 17,900 x *g*. All flow-through was discarded and 750 µl Buffer PE was added. The column was spun at 17,900 x *g* for 1 minute and again any flow-through was discarded. An additional centrifugation at 17,900 x *g* for 1 minute was carried out to remove any residual buffer. 30 µl DNase-free H_2O was applied directly to the silica-gel membrane and DNA was eluted by centrifugation at 17,900 x *g* for 1 minute. DNA samples were stored at -20°C.

Sequencing of Plasmid DNA and Sequence analysis

To verify that the gene of interest was amplified and cloned successfully into the pGEM-T-Easy vector, approximately 300 ng in 15 µl DNase-free H_2O was sent to for sequencing at The Sequencing Service (School of Life Sciences, University of Dundee, Scotland, www.dnaseq.co.uk) using the M13 forward and reverse primers.

DNA sequencing was performed by The Sequencing Service (School of Life Sciences, University of Dundee, Scotland, www.dnaseq.co.uk) using Applied Biosystems Big-Dye Ver 3.1 chemistry on an Applied Biosystems model 3730 automated capillary DNA sequencer. Sequences were analysed using BLAST (http://www.ncbi.nlm.nih.gov/blast/Blast.cgi) and the BIOEDIT software package.

2.5 QUANTITATIVE POLYMERASE CHAIN REACTION (Q-PCR)

2.5.1 Reverse Transcription of RNA for QRT-PCR

cDNA was synthesised from total RNA by reverse transcription using the method previously described in section 1.4.2.

2.5.2 Quantitative PCR assay

cDNA was amplified using a Rotor-Gene Version 5 (Corbett Research, Australia) QRT-PCR machine. In 0.1 ml PCR tubes, the following was added: 0.4 µl of Upstream primer (50 pM), 0.4 µl of Downstream primer (50 pM), 0.4 µl dNTPs, 2.8 µl MgCl2 (25 mM), 2 µl 10X PCR reaction buffer, 11.15 µl Dnase/Rnase-free, DPEC-treated water, 0.7 µl of 1:100 diluted SYBR green (Biogene, USA), 0.15 µl Taq Faststart (Roche, Switzerland) and 2 µl sample cDNA. Rnase/Dnase-free water was substituted for sample cDNA and used as negative controls. An initial denaturation step of 95ºC for 10 minutes was followed by 40 cycles of: 30 seconds at 95ºC, 20 seconds at 62ºC and 20 seconds at 72ºC. Fluorescence was measure at the end of each 72°C stage.

At the end of the PCR cycle, a melt curve analysis was performed according to the manufacturer's instructions: measuring fluorescence during the incremental increase in temperature from 65°C to 94°C. A standard curve was generated from a series of 10-fold dilutions of its corresponding gene-inserted plasmid of known concentration. Analysis was carried out using Rotogene software.

2.6 STATISTICAL ANALYSIS

All statistical analysis was carried out using Microsoft excel (with SAM add-on programs for microarray data analysis), Minitab 14, Graph Pad Prism and SigmaPlot 10.0.

2.7 MOUSE TISSUE SAMPLING

Mouse tissue was obtained from the Animal Unit, Centre for Infectious Diseases, University of Edinburgh. All mice were 10 week old males, of mixed genotype. The mice were carbon monoxide gas chamber euthanized and tissues were harvested immediately.

3 ASSESSMENT OF RISK AND DECONTAMINATION

3.1 STABILITY OF TSE AGENTS TO INACTIVATION PROCEDURES

TSE agents exhibit exceptional stability and resistance to conventional chemical and physical decontamination methods. In addition, decontamination issues are complicated by the fact that the material or surface to be treated, the type of contaminating organism present and the circumstance of use (for example, allowing contamination to dry or treatment with formalin) affect the efficacy of decontamination. This project requires evidence-based guidelines for decontaminating CJD infectivity and in particular RNA preparations derived from CJD material (Asher *et al.*, 1986; Asher *et al.*, 1987; Taylor & McBride, 1987; Taylor & McConnell, 1988).

It is well documented that different strains of TSE vary in their resistance to inactivation, but there is limited information on the properties of human disease agents. As the longest recognised and most intensively studied of the TSEs, scrapie is the acknowledged model for the majority of decontamination studies. The two strains most commonly used for comparative studies are; 263K hamster-passaged scrapie, a strain which contains the highest infectivity levels in the brain and 22A, mouse-passaged scrapie which is considered one of the most thermal stable of the TSE agents. It is generally assumed that decontamination studies with these scrapie isolates are applicable to human TSE infected material. However, there remains the possibility that human TSE agents are more or less resistant; the former has particular implications for risk assessments.

3.1.1 Factors Affecting Efficacy of Decontamination

Although the precise molecular nature of TSE agents is unknown, there have been a significant number of important studies relating to their inactivation. The uncertainty surrounding the exact nature of TSE infectivity has however complicated data interpretation and comparisons. Host species, strain of agent, origin of agent, prion concentration in test material, sample preparation (e.g. macerate, homogenate and partially purified preparations), test animals, duration of follow-up of inoculation test animals and route of infection are all issues that affect how an agent will react to decontamination and quantification of agent inactivation.

To date, highly purified native infectious agent has not been achieved to a standard that eliminates the possibility of co-purification (Hunter & Millson, 1967; Caughey & Baron, 2006; Silveira *et al.*, 2005). Without a suitable technique to purify native infectious agent, decontamination studies rely on the use of high-titre infected tissues (usually brain). The interpretation of TSE agent infectivity titres is a significant aspect of decontamination studies. Western blot analysis of immunoreactive PrP^{Sc}, as assessed by staining with antibodies, is commonly used in diagnostics and has been used to evaluate the removal of PrP^{Sc} in decontamination studies (McLeod *et al.*, 2004). The sensitivity of western blots is however a potential problem. Currently the gold standard for measuring prion infectivity is animal bioassay based on intracerebral inoculation of mice, which is slow (~140 days). The dose of infectious agent administered and the resulting incubation period in rodents follows a precise relationship, therefore allowing titres of infectivity to be measured from a standard dose-response curve (DRC) for any particular strain of agent within a specific host genotype (Dickinson *et al.*, 1968; Kimberlin & Walker, 1977; Kimberlin & Walker, 1986).

Incubation period assays (IPA) can be used to titre the concentration of infectious agent extrapolation from a DRC. However, IPAs cannot be relied upon to measure infectivity which survives chemical or physical treatments. Some treatments (including heat, sodium dodecyl sulphate and sodium deoxycholate) can modify the pathogenesis independently of titre, altering the relationship between infectivity dose

and incubation period. This can modify the DRC, causing delays when compared with equivalent titres of untreated infectivity, and lead to under estimation of titre. Full titration assays involving a range of dilutions are considered more accurate and would be most suitable for decontamination studies (Dickinson & Fraser, 1969; Kimberlin, 1977; Somerville & Carp, 1983; Kimberlin & Walker, 1977; Lax *et al.*, 1983; Taylor & Fernie, 1996).

The successful transmission of CJD from human to rodents has provided a suitably cheap and reproducible bioassay for accurate titrations of infectivity (Tateishi *et al.*, 1981; Bruce *et al.*, 1997; Manuelidis, 1975; Manuelidis *et al.*, 1977). Even with the development of suitable rodent assays, a number of factors make direct comparisons of inactivation data difficult. The chosen route of infection may affect the pathogenic pattern and incubation period. If using IPAs, only a limited number of dilutions are assayed. Therefore, it requires a prediction of the amount of inactivation which might be achieved and a suitable dilution selected. This can be problematic if an unsuitable dilution is assayed and used to extrapolate results from a DRC. With regards to titrations of infectivity, extending the observation times of test animals to at least 200 days beyond that of the usual dose-response end-point, so as not to miss late developing cases, would diminish overestimations of titre loss. Titrations are most often carried out by the inter-cranial (i.c.) route, the most efficient for detecting small amounts of infectivity. However, the loss of titre on treatment may in part be due to an impaired ability of residual agent to infect by the i.c. route but not by other routes (Dickinson & Fraser, 1969; Bruce *et al.*, 1997). Therefore titre changes may not reflect exactly the physicochemical destruction of the agent. Organ specific modifications of pathogenic characteristics have also been demonstrated, highlighting the level of complexity of the disease agent and the importance of experimental rationale of strain choice and titre quantification (Robinson *et al.*, 1990).

Tissue types vary in their infectivity levels. Peripheral tissues have lower titres of infectivity per gram of wet tissue than brain tissue (WHO guidelines; 2006). Infectivity levels also vary according to the host species. Although Brown et al

demonstrated that infectivity levels in two CJD models (guinea-pig and mouse) were comparable to human tissue infectivity levels and inferred that the levels observed were substantially lower than in mouse or hamster scrapie, inactivation of guinea-pig and mouse passaged CJD agent were not studied (Brown *et al.*, 1982). It would be reasonable to assume that agents adapted to a different species might possess different characteristics from the human CJD agent. Most inactivation studies are therefore based on the well known thermostable 301V or the high titre 263K strains, so as to be more likely to overestimate than to underestimate inactivation requirements.

Different strains of agent vary in their resistance to inactivation methods (Kimberlin *et al.*, 1983; Taylor *et al.*, 2002; Dickinson & Taylor, 1978). It is well established that PrP^{Sc} is an excellent surrogate marker of prion infectivity but in certain circumstances, infectivity and PrP^{Sc} have different characteristics. A number of TSE strains, on application of heat, have a significant reduction in infectious titre with little or no reduction in the level of PrP^{Sc}, as quantifiable by western blot (Somerville *et al.*, 2002). To conclusively prove complete inactivation, the decontamination protocol must demonstrate activity against PrP^{Sc} and also requires verification by bioassay for infectivity.

Decontamination becomes progressively more difficult as infectivity titre and concentration of tissue debris increases (Rohwer, 1984b). As TSE agents cannot be purified to homogeneity, and as the relevant risk material is frequently tissue samples, decontamination studies are generally done using crude tissue homogenates. This adds further problems. The exact concentration of brain tissue inoculum is difficult to quantify and can vary between inoculations and studies. Additionally, most inactivation studies use brain homogenate or brain macerate, a tissue that contains very high levels of lipid membrane. It is possible that the TSE agent is protected from assaults of chemical or thermal inactivation by binding to lipid membranes. This may explain how resistant sub populations of agent exist and display persistent infectivity in bioassays. The propensity of PrP^{Sc} to aggregate may also have a protective effect. These factors may allow the prion protein to survive

harsh conditions (Rohwer, 1984a; Rohwer, 1984b) and may also account for reports of reversible inactivation (Prusiner *et al.*, 1981; Shaked *et al.*, 2001). Regardless of the assumed protection from decontamination, there is no doubt that the agent's relative resistance to chemical and physical inactivation is several orders greater than that for conventional micro-organisms.

3.1.2 Current Recommendations for Decontamination

The safest method of dealing with the issue of spread of TSE infectivity by instruments and devices is to make them single-use and dispose of them by incineration. This option is not always possible; therefore methods of disinfection are needed. It is difficult to gain a consensus opinion on what constitutes optimal and practical conditions for inactivation of TSE infectivity on medical instruments and devices. Different protocols are employed by different agencies. Table 3.1 consolidates the recommended methods from the Advisory Committee on Dangerous Pathogens (ACDP), the Spongiform Encephalopathy Advisory Committee (SEAC) and the World Health Organisation (WHO) into ineffective and recommended methods of decontamination of TSE agents, specifically CJD.

To distinguish the terminology used for this project, they are defined as: Disinfection, for general cleaning of the work area and as good laboratory practise (GLP). The use of Virkon (a widely used anti-viral detergent) for disinfection is not suitable for decontamination of TSE agents; Decontamination, specific for TSE work and must follow the decontamination protocol as set out in Appendix 9.6. Sterilisation, involves the removal of microbiological infectious agent from devices or surfaces; and Inactivation, the process of inactivating the infectious agents so that it no longer has the ability to transmit disease.

CHEMICAL DISINFECTANTS	**GASEOUS DISINFECTANTS**	**PHYSICAL PROCESSES**
INEFFECTIVE Alcohol Ammonia β-propiolactone Chlorine dioxide Formalin Glutaraldehyde and related compounds Hydrochloric acid Hydrogen peroxide Iodophores Peracetic acid Phenolics Sodium dichloroisocyanurate (‘presept’) Sodium dodecyl sulphate (SDS) (5%) 10,000 ppm sodium hypochlorite	INEFFECTIVE Ethylene oxide Formaldehyde	INEFFECTIVE Boiling Dry heat (<300˚C) Ionising, UV or microwave radiation Nucleases Proteases Autoclaving at 121°C for 15 minutes and pourous load autoclaving for extended cycles and times ‘Prion Cycle’ on some bench top autoclaves
VARIABLY OR PARTIALLY EFFECTIVE Chlorine dioxide Glutaraldehyde** Guanidinium thiocyanate (4 M) Iodophores** Sodium dichloro-isocyanurate** Sodium metaperiodate Urea (6 M)		VARIABLY OR PARTIALLY EFFECTIVE Boiling in 3% sodium dodecyl sulfate (SDS)
RECOMMENDED 20,000 ppm available chlorine or sodium hypochloride for 1 hour 2M sodium hydroxide for 1 hour		RECOMMENDED
**WHO states as effective, while UK advisory committee states as ineffective		

Table 3.1. Ineffective and recommended effective methods of decontamination of TSE agents. Modified from (1996; Advisory Committee on Dangerous Pathogens & Spongiform Encephalopathy Advisory Committee, 2003).

3.2 CONCLUSIONS FOR DECONTAMINATION PROCEDURES

The results of numerous studies designed to define conditions for inactivation of TSE infectivity have concluded that protein denaturants are effective at reducing infectivity but that complete inactivation requires extremely harsh conditions. The majority of published recommendations suggest a combination of soaking in NaOH or NaOCl, followed by autoclaving at either 121°C or 134°C. It is important to note that these conditions, on which some current guidelines are based, were determined for rodent strains, before it was known that prion strains may exhibit different stabilities to denaturation by heat, as well as chaotropes (Taylor *et al.*, 2002; Peretz *et al.*, 2001).

In 2000, the WHO published updated recommendations on how to deal with surgical equipment used on people with confirmed or suspected CJD. The guidelines offered a number of different options, identifying incineration of suspect instruments as being the safest method. The WHO also listed six rigorous decontamination methods; three of the chemical and autoclave sterilization methods outlined in Annex 3 of the WHO infection control guidelines are given in Appendix 9.7. The WHO also suggests a list of general considerations when considering an effective policy for TSE agent decontamination. Firstly, that decontamination is context-dependent and may not be completely effective under all circumstances. Secondly, that the chosen method of cleaning facilitates decontamination by reducing infectivity and organic load. The policy must use the best-validated methods available and it is advisable to use an orthogonal strategy—two different methods—whenever possible (WHO guidelines, 1996).

The UK ACDP and SEAC guidelines suggest using ambient temperature and 2 M NaOH for 1 hour, or 20,000 ppm available chlorine of NaOCl for 1 hour, as the most

effective chemical methods. Unfortunately, this concentration of chlorine is impractical for most uses, requiring respirator protection or evacuation of the immediate area. In addition, chemical breakdown of stock solutions and difficulties in establishing actual free chlorine levels make this approach difficult to implement. The use of 10,000 ppm hypochlorite is stated as being ineffectual against TSE agents and is not recommended. There are no current recommendations with regards to autoclaving (Advisory Committee on Dangerous Pathogens & Spongiform Encephalopathy Advisory Committee, 2003).

The NCJDSU laboratory decontamination and risk management protocols (Table 3.2) are in accordance with UK ACDP and SEAC guideline recommendations. The principle of all work is containment followed by decontamination. Training for this project was carried out by the NCJDSU Chief Biomedical Scientist and Health and Safety Advisor (Linda McCardle). All personnel underwent a probationary period which was signed off by the supervisor, before being permitted to work within Category laboratory (CL) 3* laboratory.

ITEM	CONCENTRATION	CONTACT TIME
Disposable PPE, paper tissues, etc	Double bag, I.D. tag and incinerate[2].	
Disposable sharps and instruments	Decontaminate with 2M NaOH. Collect in sharpsafe or similar container with safety signs and incinerate.	Minimum 60 minutes
Non-disposable metal instruments	Steam autoclave at 134°C – 136°C (GD or PL).	GD – 60 minute cycle PL – 18 minute cycle
Work surfaces	Flood with 2 M NaOH. Rinse before next usage*.	Minimum 60 minutes
Class 1 cabinets[1]	Wipe with excess 2 M NaOH. Fumigation with formalin prior to contract servicing. Dispose of high efficiency particulate	Minimum 60 minutes

	absorption (HEPA) and dust filters by double bagging and incineration.	
Contaminated fluids	Decontaminate in a container of 1 litre of 2 M NaOH (at final concentration). When 1/3 full, absorb in sawdust, double bag and incinerate.	Minimum 60 minutes
Contaminated organic solvents	Absorb small amounts in sawdust in a falcon tube with lid, double bag and incineration.	Minimum 60 minutes
* 2 M NaOH will damage aluminum or zinc surfaces.		

Table 3.2. Decontamination procedures to be used in this project. This protocol is in accordance with UK ACDP and SEAC guideline recommendations. 1. Decontamination of class 1 microbiological safety cabinets. From evidence provided by decontamination studies, it has been established that conventional methods of safety cabinet fumigation using formalin or vaporised formaldehyde are not effective against TSE agents. Nonetheless, fumigation is still necessary as a precaution against other infectious agents that may be present within the cabinet or on the surface of the HEPA filter. Also, fumigation is a requirement of contracted service engineers, even though contract companies are fully aware of it being ineffectual on TSE agent. Service personnel will be informed of TSE work with the cabinet in advance of visits. Full fumigation protocol is supplied in Appendix 9.8. 2. Disposal of waste. Disposal of all waste is in accordance with the statutory requirements under the Controlled Waste Regulations 1992. Incineration is completed by a verified, dedicated waste contractor via the Health Trust.

3.3 ASSESSMENT OF RISK FOR THIS PROJECT

Due to their unique biological and biochemical properties and their human disease potential, safety considerations are particularly important in working with the TSE agents derived from humans, or which are known to be capable of infecting and causing disease in humans. The nature of this project means that RNA preparation protocols need to take into account the necessity for removal of the infectious agent, as molecular studies are to be carried out in a CL2 laboratory. Transfer of the work was necessary since specialist equipment required was only available at the CL2 laboratory. How to work with infectious tissues, how to remove infectious material

from tissues while leaving RNA intact and how to decontaminate equipment and utensils that have come into contact with infectious material are the main considerations.

The NCJDSU receives fixed and frozen tissue samples from autopsies of neurological patients suspected of CJD. Due to the TSE agent's resistance to most normal processes of inactivation, tissue received is considered highly infectious. Risk assessments and safe working procedures were already in place at the NCJDSU, but as this project introduced a number of new techniques, updated and revised proposals were needed.

3.3.1 Hazards and Risks Associated with Workplace Exposure to TSE Agents.

The factors to be considered when working with TSEs are set out by the Advisory Committee on Dangerous Pathogens (ACDP) and the Spongiform Encephalopathy Advisory Committee (SEAC) and include or comprise the following:

i. Is intention to work with the agent deliberate
ii. Hazard categorisation of the agent
iii. Origin of the agent
iv. Type of tissue handled
v. Knowledge of expression of the agent in any experimental model and whether the work is likely to result in a high titre of infectivity
vi. Assessment of the type of task (e.g. concentration/purification)
vii. Frequency of contact with the agent or materials likely to contain them
viii. Potential for inoculation injury and other possible routes of exposure.

(Advisory Committee on Dangerous Pathogens & Spongiform Encephalopathy Advisory Committee, 2003)

At the NCJDSU, multiple organ samples are handled and stored. Within the scope of this project, only frozen human brain tissue will be accessed. Infectivity of the TSE agent varies according to the agent strain, host and tissue type (Table 3.3). Based on

accumulated data, the WHO issued updated guidelines on tissue infectivity in naturally occurring disease or in primary experimental infections by the oral route. Tissues, regardless of the stage of disease, are categorised as having high, low or undetectable levels of infectivity (WHO guidelines,2006).

Tissue	**HUMAN TSEs**			
	vCJD		***Other TSEs***	
	Infectivity[1]	PrP^{TSE}	Infectivity	PrP^{TSE}
Brain	+ P	+	+	+
Spinal cord	+ P	+	+	+
Spinal ganglia	+	+	+	+
Dura mater[3]	NT	-	+	-
Cranial nerves	+	+	+	+
Cranial ganglia	+	+	+	+
Retina	NT	+	+	+
Optic nerve[2]	NT	+	NT	+
Spinal ganglia	+	+	NT	+
Trigeminal ganglia	+	+	NT	+
Pituitary gland[3]	NT	+	+	+

Table 3.3. High infectivity tissues. Generally, CNS tissues and certain tissues anatomically associated with the CNS, attain a high titre of infectivity in the later stages of TSE. Modified from WHO guidelines on tissue infectivity distribution in transmissible spongiform encephalopathies and guidelines from Advisory Committee on dangerous pathogens and the Spongiform Encephalopathy Advisory Committee. The detection of misfolded host prion protein (PrP^{TSE}) has proven to be a reliable indicator of infectivity and has been presented in parallel with bioassay data. Data entries are shown as follows: + Presence of infectivity or PrP^{TSE}; - Absence of detectable infectivity or PrP^{TSE}; NT Not tested. P Infectivity has been proven in experimental transmission studies.
[1]. Infectivity bioassays of human tissues have been conducted in either primates or mice (or both). [2]. In experimental models of TSE, the optic nerve has been shown to be a route of neuroinvasion and contains high titres of infectivity. [3]. No experimental data about infectivity in human pituitary gland or dura mater have been reported, but cadaveric dura mater allograft patches, and growth hormone derived from cadaveric pituitaries have transmitted disease and are therefore included in the category of high-risk tissues. Modified from (WHO guidelines, 2006).

Human CNS tissues are considered to contain the highest titres of infectivity and require stringent precautionary handling protocols. Based on accumulated evidence, as a frame of reference, brain typically contains about 10^6 LD_{50}/g, spleen up to 100 LD_{50}/g and blood generally < 100 LD_{50}/ml (Brown & Abee, 2005; WHO guidelines,2006). For the purpose of this project, it is assumed that human brain tissue contains high levels of infectivity. It is important to point out that categories of infectivity are distinct from categories of risk. The latter requires consideration not only of the level of infectivity but also of the amount of material to which a person is exposed, and the potential route(s) of transmission.

Extraction of RNA from tissues is generally based on phenol-chloroform extraction (Maniatis *et al.*, 1982). The RNA extraction protocol will include the use of guanidinium thiocyanate (GTC, a strong protein denaturant and a known inactivator of TSE agents) and phenol. The lysis reagent contains GTC concentrations of ~ 4 M and phenol concentrations of ~ 2M. Based on evidence discussed in section 1.1.3, > 2.5 M GTC should be effective at reducing even high titres of CJD in brain tissue and although phenolics are considered ineffective at inactivating PrP^{Sc}, the monophasic purification steps should retain PrP^{Sc} within the organic phases. Thus, the agent should be inactivated by two separate mechanisms; 4 M GTC should denature the proteinaceous material and inactivate PrP^{Sc}; the additional phenol extraction should retain all remaining PrP/PrP^{Sc}. RNA should fractionate into the aqueous phases and the proteinaceous fractions will be retained in the phenol and discarded. Since TSE infectivity co-purifies with the proteinaceous fraction of brain material (Bolton *et al.*, 1982), this should therefore remove the majority, if not all, of the infectious material. After this stage, the infectivity risk should be considerably reduced.

Having considered the criteria set out by ACDP and SEAC, the main risk in this project lies prior to phenol-chloroform extraction of the brain homogenate. The majority of the brain sampling will be carried out by trained experienced staff, which will further minimise sharp and inoculation risks and sample preparation work will be carried out in a microbiological class 1 hood within the high risk CL3* laboratory,

to protect against aerosol and volatile chemical inhalation. Subsequent work with the extracted RNA samples represents minimal risk and can be carried out in a CL2 laboratory.

3.3.2 Transport of RNA Preparations

All RNA extractions were required to be carried out in the NCJDSU CL3* high-risk laboratory. After RNA extraction (as described in Chapter 2), RNA samples were deemed safe for transportation to the CL2 laboratories at Summerhall.
For transportation, government regulation standards set by the Department of Health in conjunction with the ACDP and SEAC were followed.

CLASSIFICATION AND PACKAGING
Clinical samples known or suspected to contain disease-form prions (e.g. CJD, vCJD etc) are a Category B infectious substance under the transport regulations. Based on the nature of the materials and purpose for which they are being transported, they are assigned to UN3373 with the proper shipping name Biological Substances Category B. This UN number and proper shipping name identifies and classifies the substances under the international system.

All materials transported to and from the NCJDSU were packaged using a triple layer packaging system. This comprises a leak proof primary receptacle, a leak proof secondary packaging and an outer packaging. Absorbent material, in sufficient quantity to absorb the entire contents of any leakage from the primary, was placed between the primary and the secondary layers. The primary receptacle was placed in the secondary in such a way that under normal conditions it cannot be punctured or leak. The secondary was secured or supported in the outer with suitable cushioning material. This system was in line with the packaging instructions published by the Department of Transport, Carriage of Dangerous Goods ADR 650. A sticker stating UN 3373 was displayed on the outer box and a warning sticker stating ‘DO NOT OPEN EXCEPT IN LABORATORY CONDITIONS’ was displayed on the surface

of the receptacles. An emergency procedures protocol and a packaging procedure information sheet were packaged with the samples.

3.4 ETHICAL STATEMENT FOR ANIMAL WORK

All mice were derived from stock bred in the Animal Unit, Centre for Infectious Diseases, University of Edinburgh and were used at less than 10 weeks of age. Mice were healthy, and were used for control brain tissue for assay optimisation. All procedures involving animal work complied with the Animals (Scientific Procedures) Act 1986, and were carried out under the authority of a UK Home Office License.

3.5 ETHICAL STATEMENT FOR HUMAN WORK

With regard to the removal of tissues, the main ethical principles from the donor's point of view are:

- respect for the human body, even after the person's death
- respect for the autonomy of the donor; thus, tissue may not be removed whenever the person refuses. For deceased persons, this implies that tissues may not be removed if the person refused consent during her/his lifetime
- protection of vulnerable people, namely people unable to give consent
- respect for private life and medical confidentiality, which is a fundamental right
- the right to prior information on the conditions of removal and the expected use of the tissues
- the right not to be subjected to unfair discrimination, which could result from the revelation of data collected from the donor, or the family, to third parties (e.g. employers and insurance companies).

All procedures involving the use of human tissues comply with the Human Tissue Act (2004). The Certificate of Ethical Review code for this research project was allocated LREC\2000\4\157.

3.6 DISCUSSION

An extensive number of decontamination studies and reviews have been undertaken in response to concerns about CJD transmission associated with blood transfusion, dura mater and cadaver derived growth hormone contamination (Llewelyn *et al.*, 2004; Esmonde *et al.*, 1993; Powell-Jackson *et al.*, 1985). Even so, it has still not been possible to reach a consensus as to which method of decontamination is most suitable, within clinical, pharmaceutical or research settings. There is ongoing dispute as to whether the prion protein is the only infectious component of the TSE agent (Manuelidis *et al.*, 1987). It seems unlikely that current decontamination issues will be resolved in the near future.

The different experimental systems and methodologies employed to compare decontamination and differences between TSE agents, make direct comparison of decontamination results difficult. Direct comparison of TSE agents in different hosts would make it easier to evaluate which model is the best predictor of CJD in humans. The biological relevance of scrapie for CJD, given that strains exhibit such variation in thermostability for example, is an issue that also requires attention.

Decontamination studies which use high titre strains of TSE have been criticised for being prone to recommending extreme inactivation protocols. While some may consider the use of high titre agents ($10^{10\text{-}11}$ infectious units per gram of brain tissue for many scrapie strains) to infer appropriate decontamination procedures for lower titre agents, such as BSE and/or vCJD or sCJD agents (infectivity titres of

approximately 10^{8-9} infectious units per gram of brain tissue) as excessive, it is probably preferable to overestimate the resistance of TSE agent, especially with relevance to human strains, for fear of increased iatrogenic spread. The direct use of low titre agents as a study model may be problematic as large log reductions in infectivity cannot be demonstrated and arguably may not provide sufficient evidence of decontamination. Consequently, while some researchers may consider scrapie models unsuitable for testing decontamination methods for CJD, testing on CJD material is not plausible unless more sensitive infectivity detection methods are developed (Peretz *et al.*, 2006).

There has been controversy as to whether the protease-resistant and detergent-insoluble characteristic of prion proteins is necessarily associated with prion infectivity (Shaked *et al.*, 1999). If this is indeed the case then protease sensitive and/or detergent soluble agent could remain infective. This holds significant consequences for decontamination studies that have assumed that the absence of residual PrP^{res} or detergent-insoluble PrP has proven successful inactivation. This is another reason why it is very important to carry out full end point titration bioassays as they are currently the most sensitive method of detecting infectivity (Shaked *et al.*, 1999).

Inactivation methodologies involving the use of heat would seem to be highly specific for a particular agent, having clear evidence of thermostable variation and the ability to acquire resistance (Taylor *et al.*, 1998). While this may pose complications for inactivation and kinetic studies, fortunately as yet there have been no reported differences in the chemical susceptibility between TSE agents; leading to the conclusion that chemical inactivation of infectious agents may be more practical. For this project, Qiagen RNA extraction kits containing a lysis buffer with ~4 M GTC and ~2 M phenol at a pH of 5.0 were used. These concentrations have been observed to reduce CJD titre by > 99.7% and increased acidity increases inactivation of the scrapie agent when using GTC as a denaturant (Manuelidis, 1997; Caughey *et al.*, 1997). Inactivation studies often state incomplete tissue penetration as a reason for incomplete inactivation. Strong chaotropic ions such as GTC are extremely

disruptive and should significantly enhance tissue penetration, an issue of more importance when working with high lipid tissues such as brain.

Although phenolics have been specified as being ineffective for complete inactivation of TSE agents, retention of the proteinaceous infectious material within the phenol phase and the denaturing action of the GTC should be sufficient to remove infectivity from the RNA preparations. Nonetheless, the absolute inactivation of CJD agent from human brain cannot yet be guaranteed, and although these evidence-based guidelines provide a good basis to assume CJD inactivation >99.7% was achieved, it was necessary to treat RNA preparations as low risk samples. RNA preparations were tested for the presence of PrP^{Sc}, to determine the RNA extraction protocol (refer to Chapter 2) efficacy of protein removal and the results are discussed in detail in Chapter 5.

4 CASE SELECTION

4.1 OBJECTIVES

- Evaluate suitable case selection criteria and select suitable cases.

4.2 CONCEPT

Tissues were supplied for this project from two brain banks; the National Creutzfeldt-Jakob Disease Surveillance Unit (NCJDSU) and the Medical Research Council (MRC) Sudden Death Brain and Tissue bank. The purpose was to acquire brain material from cases of variant Creutzfeldt-Jakob disease (vCJD), non-neurological disease (NND) and other neurological disease (OND), to prepare TSE agent decontaminated RNA preparations from human autopsy brain material, to evaluate human RNA quality and quantity and to determine sample suitability for a comparative study of gene expression. vCJD and OND cases were obtained from the NCJDSU Brain Bank and NND cases were obtained from the MRC Sudden Death Brain Bank. vCJD diagnosis was confirmed by histopathology. OND cases in the NCJDSU constitute suspected CJD cases, which were subsequently shown by histopathology not to be prion disease. NND control case diagnosis is based on the tissue analysis report completed by a consultant neuropathologist.
Material was obtained from cases in which consent for research had been obtained from relatives. The NCJDSU Brain Bank and MRC Sudden Death Brain Bank have ethical approval to store and use autopsy brain tissues for research (NCJDSU LREC: 2000/4/157. MRC LREC: 2003/8/37.)

4.3 NATIONAL CREUTZFELDT-JAKOB DISEASE BRAIN BANK

The NCJDSU was set up in response to recommendations from the Report of the Working Party (The Southwood Committee) on Bovine Spongiform Encephalopathy (BSE), following the discovery that UK cattle were infected with this transmissible spongiform encephalopathy. The NCJDSU is directly funded by the Department of Health and the Scottish Executive Health Department and is a member of the BrainNet Europe consortium (Bell *et al.*, 2008). The primary aim of the NCJDSU is to identify and monitor all suspected cases of CJD within the UK, and identify patterns of disease epidemiology and risk factors that may be linked to the emergence of vCJD. Each suspected CJD case is investigated thoroughly by clinical examination, clinical investigations, neuropathological examinations, genetic analysis, molecular biological investigations, and the acquisition of basic epidemiological data. Current surveillance involves three types of referrals; clinical, death certificate and other sources. At the point of referral, cases are classified according to established criteria (Appendix 9.2). Whenever possible, all referrals to the NCJDSU categorised as 'definite CJD', 'probable CJD', 'possible CJD' and ' diagnosis unclear' are visited in life by a NCJDSU neurologist, at which point physical examination, a blood specimen and clinical information are collected and the classification is re-assessed. If the case classification requires it, a final review form is opened for each suspect case and is held as an 'opened' case file at the NCJDSU. All incoming clinical and laboratory data is recorded and stored on file until the patient's death, at which point a post-mortem may be performed if consent is granted. If this is the case, all investigational data, reports and pathological materials are also logged and stored in the case file. Referrals for probable or definite genetic CJD or iatrogenic CJD are not followed up by the NCJDSU, unless the diagnosis is unclear or a specific request is made by the local clinician for a visit by a neurologist from the NCJDSU. Professor Michael Preece, Institute of Child Health, London, follows up cases of growth hormone related iatrogenic CJD and the investigation of cases of familial CD is undertaken by staff at the National Prion Clinic, London.

Following appropriate consent, post-mortems are performed by a neuropathologist. For diagnostic purposes, the brain is examined macroscopically by a neuropathologist and the whole organ or regionally defined specimens of it are retained in fixative. The samples are decontaminated in formic acid, processed to paraffin blocks, cut and stained immunohistochemically, primarily for prion protein. The neuropathologist then examines the slides for microscopic changes and either confirms or makes an alternative final diagnosis. If consent has been obtained and frozen brain tissue is available, a western blot is carried out to detect abnormal prion protein and to determine prion protein isotype. This is based on the Parchi classification system (Parchi *et al.*, 1999). If specific consent for genetic analysis is obtained from the family, prion protein gene codon 129 determination and in some cases full sequencing of the gene is also carried out, usually on a blood specimen taken in life, but this can also be performed from frozen tissue obtained at autopsy. Cases stored at the Brain Bank include; sporadic, familial and variant CJD, as well as suspected cases of CJD, which diagnostic tests have shown not to be CJD. The latter form the majority of the OND controls in this study.

4.3.1 Autopsy Protocol (NCJDSU)

A full, informed, written consent post-mortem is requested for each patient, and use of tissues for research purposes requires specific permission from the family of the deceased. Post-mortems must be carried out in a mortuary with high-risk facilities. In Edinburgh, the registered neuropathology centre with a high-risk mortuary is sited at the New Royal Infirmary (NRIE), Little France. Patients suspected of having CJD within the north of England and the East of Scotland are normally referred to NRIE. Post-mortems can be organized for these patients at the NRIE, to be performed by consultant neuropathologists (Prof. J. Ironside, Prof. J. Bell, and Dr. C. Smith). In these cases, it is possible to collect and store tissues of specific interest at the brain bank, once full consent has been obtained.

4.3.2 Arrangements for Post-Mortems (NCJDSU)

There are two types of post-mortem: Hospital post-mortems and Coroner post-mortems. Coroners can request a post-mortem examination and do not need relative's authorization. Hospital post-mortems can only be carried out with fully informed consent from the relatives. In order for full informed consent, relatives only complete the authorization form having been made aware of the meaning of its various sections particularly with regards to the retention of tissue and individual organs for diagnosis and/or teaching and research. All requests for hospital post-mortem include a correctly completed request form. This form includes space for full patient identification and brief clinical summary. This is a legal requirement and must be completed before the post-mortem can commence.

4.3.3 Tissue Storage (NCJDSU)

The NCJDSU has been involved in the surveillance of CJD cases, in particular (new) variant CJD cases within the UK from its establishment in 1990. This involves the collection and storage of tissues in a purpose-built brain bank and laboratory, as well as the accumulation of clinical, pathological and epidemiological data on each case. Tissue samples can come from local autopsies or from autopsies carried out elsewhere. In-house autopsies have a PM protocol (Appendix 9.3), which standardizes the types of samples collected. Autopsies carried out at one of the other 27 registered neuropathology centres in the UK means samples can vary in tissue type, sample size and post-mortem interval and are therefore less predictable and uniform. At all local autopsies, samples are collected by identical methods and stored using one of three techniques. Whole half-brains and 29 specified regional brain samples are frozen by immediately placing them in a -80°C freezer. Prior to changes in the health and safety regulations of the NCJDSU, small samples were snap frozen by immersion in liquid nitrogen. This is no-longer the procedure as it was deemed to involve unnecessary risk. Since 2000, specimen requests at post-mortem have included nine specified brain areas collected and fixed in paraformaldehyde-lysine-periodate (PLP) for histological analysis. Samples of other organs, blood and cerebral spinal fluid are also collected and frozen at -80°C. For the purpose of this study, the specimen request was extended to include an additional 12 specified samples from the frontal cortex and cerebellum. These 12 samples were taken adjacent to the samples already routinely taken for

histology, to allow comparative histological and molecular studies. Six of these were placed immediately into RNAlater, and six were frozen at -80°C (Appendix 9.4).

4.3.4 Histology (NCJDSU)

Sections processed from all specimens taken for histological analysis undergo hematoxylin and eosion (H & E) staining. A select few tissue samples also have PrP immunohistochemisty tests (IHC), using a variety of PrP antibodies. Selected tissues that are H & E stained and IHC stained and used to identify any morphological and pathological changes, are referred to as the 'immuno-set'. These are used at the NCJDSU for diagnostic purposes.

4.4 MEDICAL RESEARCH COUNCIL SUDDEN DEATH BRAIN BANK

Non-neurological control cases were provided for this study by the MRC Sudden Death Brain and Tissue bank, also a member of BrainNet Europe (Bell *et al.*, 2008). The purpose of the MRC Brain Bank is to retain, store and make available for research use, post-mortem tissue samples from victims of sudden death. All samples are authorised and ethically approved for research (ethical code LREC: 2003\8\37). Tissue samples date back to the start of the bank's inception in 1990. Tissue that is authorised for retention from hospital and medicolegal post-mortem examinations are collected, with the majority of post-mortem tissues having been obtained 8-27 hrs after death. Brain pH measurements are made on coronally cut whole brains and a hand held digital pH meter with glass electrode is inserted into the lateral ventricle. Tissue is retained from all regions of the brain and spinal cord, peripheral nervous system and many non-CNS organs and tissues and is stored both in formalin fixed, paraffin embedded blocks and in snap frozen samples. For snap- frozen samples, tissues are sampled at post-mortem, frozen in liquid nitrogen and stored at -80°C. Non-neurological disease (NND) control case diagnosis is based on the tissue analysis report completed by a consultant neuropathologist.

4.5 TISSUE SAMPLING PLAN

A prospective and retrospective tissue sampling system was defined. At the NCJDSU for autopsies carried out after the start of this project, 12 specified samples from the frontal cortex (sub frontal cortex) and cerebellum, adjacent to the samples already routinely taken for histology were requested. Tissue supplied by the MRC Brain Bank (autopsy samples and stored tissues) was sampled from the frontal cortex (frontal parasaggital, 2nd gyrus from midline). Retrospective tissue sampling from frozen whole half brains stored at the NCJDSU corresponded to the areas sampled at autopsy from the NCJDSU and supplied by the MRC bank. Neuroregional matching was carried out to limit the effect of regional variation. Figure 4.1 illustrates the areas sampled for this project.

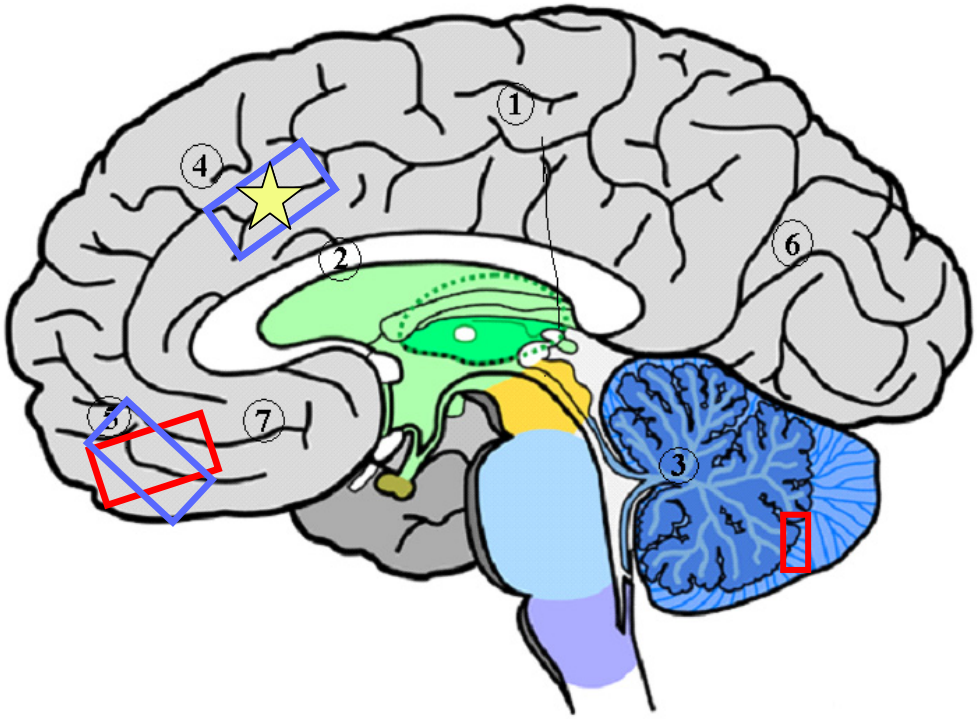

Figure 4.1. Sagittal view of human brain indicating area of sampling as determined by post-mortem protocol. The decision to study mainly areas in the frontal region of the brain is based on evidence that significant pathological change is seen in this particular region of the human brain in vCJD patients. In order to reduce regional disparity of gene expression, attempts were made to ensure that tissue samples were taken from corresponding regions. 1. Cerebral hemisphere; 2. corpus callosum; 3. cerebellum; 4. superior frontal gyrus; 5. sub frontal cortex; 6. occipital lobe; 7. temporal pole. Red box represent anatomical region taken by NCJDSU neuropathologist at autopsy and either snap frozen or stored in RNAlater (sub frontal cortex, dentate nucleus of cerebellum). Blue boxes represent the anatomical regions sampled from frozen half brains for regional study (sub frontal cortex and frontal parasaggital, 2nd gyrus left of frontal gyrus midline). The star represents the anatomical region provided by the MRC Brain Bank for this study (frontal parasaggital, 2nd gyrus left of frontal gyrus midline).

4.6 CLINICAL HISTORY AND CONSENT

Medical records and information for individual cases was accessed at the NCJDSU, Western General Hospital, Edinburgh. Due to the importance of patient confidentiality, all research carried out respected patient anonymity by using coded samples for this study, and protected the rights of the patient and their families. All clinical data was obtained with permission from the NCJDSU Director.
Tissues stored at the brain bank may or may not have consent for use for research purposes, and only those cases with full consent for research use were available for this study.
The procurement of human tissues requires the prior, informed and free consent of the person concerned or their proxy. The information provided to the donor should concern:

- The procurement arrangements, in particular concerning the free nature of the donation, and the extent of its anonymity.
- Possible tissue storage time and conditions, and conditions of registration of data in databases, in conformity with requirements of private life protection and medical confidentiality.
- Foreseeable use of the tissues (diagnostic, allograft or autograft, pharmaceutical products, research, production of cellular lines etc.).
- The donor may at any time withdraw her/his consent.

4.6.1 Index of Agonal State Scoring System

Agonal factors (AF) are defined as the condition of the patient and the circumstances immediately preceding the time of death. The agonal state is determined by the length of time AFs have been present. Certain AFs are suggested to significantly impact on RNA quality, including hypoxia, dehydration and seizures. It was necessary to establish a system which could evaluate the agonal state of a patient, to allow comparisons between samples to be carried out. For the purpose of this study, the Index of Agonal State (IAS) was developed as a graduated scoring system from 0-20. This system incorporates more detail than the Agonal Factor System (AFS) developed by Tomita et al (Tomita *et al.*, 2004), because the cause as well as the duration of the

conditions leading to death is accounted for. Clinical case histories, histology reports, autopsy reports and histopathological slides were examined for all NCJDSU cases and a list of 10 factors was scored in the following manner;

- Duration (1 score per 9 mnth duration)
- Mode of death (0 - 4, as described by (Hardy *et al.*, 1985) (see Table 4.5)
- Seizures (0 for absent, 1 for present)
- Coma (0 for absent, 1 for present)
- Hypoxic and/or ischaemic change (0 for none, 1 for evidence of, 2 for severe) (see Figure 4.2)
- Pyrexia (0 for absent, 1 for present)
- Dehydration (0 for none, 1 for evidence of, 2 for severe)
- Hypoglycemia (0 for none, 1 for evidence of, 2 for severe)
- Multiple Organ Failure (0 for absent, 1 for present)
- Neurotoxic substances (0 for absent, 1 for present)

The sum of each factor gives the IAS for each case. Where possible, assessment of all case information was done with discussion with the registrar and nurse practitioner involved in the case and the neuropathologist involved in the autopsy and histology reports. For details for each score break-down, refer to Appendix 9.9.

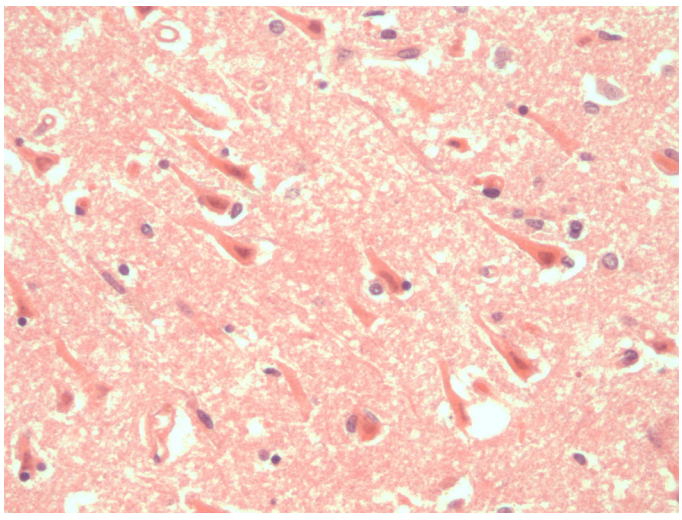

Figure 4.2. Microscopic photographs of a representative example of severe (grading 2) ischemic changes observed in brain tissue. Eosinophilic shrunken neurones in the hippocampus from a case of global cerebral hypoxia in a 56 year old male. The affected cells also show nuclear shrinkage, but not fragmentation. Images courtesy of Prof. J. Ironside

4.7 ASSESSMENT OF CASE SELECTION REQUIREMENTS

4.7.1 Difficulties in Studying Gene Expression in Human Brain Tissue

Identification of differentially expressed genes in CJD versus control brains could be affected by a huge range of pre- or post-mortem factors that can affect the outcome of the measurements. This is a major disadvantage to studying human tissues instead of experimental animal tissue. For experimental animals, rigid controls are in place, both during the animal's lifetime and at death. Human studies have uncontrollable variables during life, illness and death, which increase the potential of change in gene expression levels unrelated to the disease pathology.

A DNA-RNA hybridization study in rodents indicates that gene expression in the brain may exhibit a greater level of variation than any other region of the body (Hahn & Laird, 1971). It seems reasonable to extrapolate this to humans. Furthermore, the heterogeneity of cell sub-types and their function, for example, in areas of cognition, is so diverse that controlling for brain region in gene expression studies is only practical to a limited extent. Gene expression levels are dynamically regulated by developmental times, spatial positioning (e.g. cell-type specific manner), environmental factors (e.g. activity-dependent gene expression) and disease states (Sporns *et al.*, 2000; Tononi *et al.*, 1994).

While it is entirely possible that disease relevant genes are expressed differentially throughout the brain, it is equally possible that disease related genes are only expressed differentially in a specific brain region. As it is impractical to study the human brain as a single entity, to choose areas to study one can make the assumption that the most disease affected area of the brain, according to neuropathological and biochemical criteria, are the areas most likely to show pathology related changes in gene expression. Although this approach is practical, the selected brain region chosen on the basis of neuropathology, neuroimaging or biochemical studies, may not coincide with the brain region(s) having the greatest changes in gene expression relevant to the pathophysiology of CJD. Disease specific gene expression may only

occur within certain timeframes in disease progression and may not be observed in areas of greatest pathology at post-mortem. If this is the case, then gene expression studies may not identify causative genes, but secondary and subsequent changes in gene expression. However, these secondary changes may still be crucial for understanding the effects of the disease on the brain, as well as potential marker for diagnostics and development of pharmacological therapies.

Concerns about brain region sampling were raised when significant genetic variation was observed between different samples within the BSE-infected bovine caudal medulla (Brown, 2005). Recently, region specific patterns of gene expression in the human brain were demonstrated using microarrays (Ernst *et al.*, 2007; Roth *et al.*, 2006). Studies based on regional patterns of gene expression in human and chimpanzee brains give insight into the gene expression differences between brain regions. Observed transcriptome variation was greater between individuals than within individuals and notably, the sets of genes selectively expressed in the cerebellum were particularly large and diverse (Khaitovich *et al.*, 2004; Enard *et al.*, 2002). To appreciate the vast heterogeneous nature of the brain, studies generating RNA profiles extracted from single cell nuclei were able to show comparable degrees of variation. Expression patterns, while consistent for a single type of brain nuclei, showed significant differences between different nuclei (Bonaventure *et al.*, 2002; Kacharmina *et al.*, 1999; Kacharmina *et al.*, 1999). This has implications for gene expression studies based on tissue samples containing an array of cell types; endogenous variation between cell types may confound any gene expression alterations identified. Such heterogeneity would therefore make accurate analysis of the brain region necessary (Colantuoni *et al.*, 2000; Watakabe *et al.*, 2001).

The NCJDSU has three neuropathologists that routinely carry out autopsies on referred cases. Although specimens will be from as close to the same region as is possible, slight discrepancies in the exact region that is dissected may affect gene expression levels and lead to identification of differences that are caused by regional variation rather than between individuals. The distinctive pattern of expression in each region of the brain requires precise dissection of the tissue at post-mortem, in order to limit significant intra-regional gene differences. Morphological variation between individual human brains and irregularities of anatomy might cause problems in

identifying correct spatial positioning for sampling. When tissue is dissected from larger pieces or from the whole organ, for example, it is possible a sample may contain a cross section of cortical ribbon and white matter, while another sample may contain no white matter. If these two samples were to be compared, differences that would be observed would not be due to the disease, but in fact to the differences of the material included in the dissection.

Post-mortem gene expression in the brain of each individual is likely to be affected by a unique combination of variables, including immediate cause of death, temperature and interval between death and refrigeration of the body (refrigeration interval, RI), or removal of the brain tissue and freezing or fixing it (post-mortem interval, PMI) and the interval of storage before the tissue is used for research purposes, freezer interval (FI). While it is possible to control post-mortem factors to some extent, inevitably variations in tissue handling happen. It is not feasible to control for these pre-mortem variables, although the consensus opinion within the literature is that these factors are likely to have the greatest impact on RNA populations in brain tissue. Pre-mortem variables considered to have an effect on mRNA stability and integrity include; age, gender, ethnicity, medication, agonal state, disease severity and laterality of the brain, and are discussed below.

Addressing the issue of high mRNA variance observed in human post-mortem brain, Preece et al evaluated whether mRNA transcripts within a single brain were degraded in an ordered system, either by confounding factors or as a function of time. If degradation of transcriptomes occurred in a highly randomized manner, the post-mortem mRNA representation would bear no resemblance to the *in vivo* situation and inferred differences in mRNA levels due to pathology would not be distinguishable from post-mortem changes and would render expression data worthless (Preece *et al.*, 2003). While absolute levels of mRNA showed high variance between individuals (>1000-fold), relative mRNA (3 positive and 3 reference genes) levels had insignificant (<0.001) mean change. Evidence of such an ordered degradation of transcriptome allows for the removal of inter-individual variation from the statistical model and infers a more authoritative gene expression profile.

It is possible to limit the amount of background genetic variation by using a genetically homogenous population of subjects. While theoretically possible, say, if studying familial forms of E200K CJD in Jews of Libyan descent (Sachs & Bat-Miriam, 1957; Kahana *et al.*, 1974), this would drastically limit the sample size (for example, at the NCJDSU, sample size would be limited to less than 8 cases) and therefore the statistical strength of the study. Thus it was not possible for this study to match for genetics in the most general sense. However for certain disease specific genes implicated in CJD, this is possible. All frozen tissue from the NCJDSU has a record of the codon 129 genotype of the prion protein gene, although the gene may not be completely sequenced, if consent was not obtained. All 21 vCJD cases included in this study were MM at codon 129 and of these, 18 cases were tested for, and did not contain, any other disease-related polymorphisms within the *prnp* gene. But this criterion is not considered of high relevance when selecting cases, since there is limited evidence that differences in the genotype would have an effect on the disease pathogenesis gene expression profile.

4.7.2 Analysis of Available Samples

The NCJDSU has the largest collection of CJD and non-CJD infected tissue in Britain, dating from the Oxford study by Professor Robert Will and Professor Bryan Matthews in 1980's. Tissues are stored frozen (-80°C), snap frozen (historical; liquid nitrogen, recent; -80°C) and PLP fixed. The types and amounts of tissues stored vary, as the brain bank receives samples collected from autopsies all over Britain. Therefore it may not be possible to use cases from other neuropathology centers if frontal cortex and cerebellum have not been supplied, or if only small amounts of tissue were provided. Non-neurological control cases provided by the MRC Sudden Death Brain Bank are requested based on the availability of suitable cases within the NCJDSU. Since a peak in the number of vCJD cases in 2000, there has been a decrease in the number of cases referred to the NCJDSU. This may in part be due to better diagnosis and more family members unwilling to consent to tissue use for research, making it difficult to find suitable cases for this study. The scarcity of donor tissue and the restrictions on sample size places limits on the power and resolution of any statistical analysis. If the sample size is too limited, any inferences that are drawn from the data may not be representative of the population. Therefore, it is important to consider the

number of samples available and not to limit the sample size by insisting on matching cases based on too many restrictive and unnecessary criteria.

4.7.3 Stability of Archived Material

Liquid nitrogen snap frozen tissue, -80°C freezer stored tissue and RNAlater treated tissues were compared in order to identify the most suitable method of storing tissue while retaining RNA quality and quantity, in an unbiased manner. Retrospective and prospective comparisons were also carried out to determine the utility of archived material. Tissue samples from the 1970's exist at the brain bank at the NCJDSU. It is not known whether the RNA in these tissues is still suitable for RNA profiling. Once removed or collected, tissues are subject to a series of operations:

- processing
- preserving and storage
- registration (to collect the data which will enable in particular the source of the tissues to be traced)
- distribution and delivery.

Older samples may have been removed from the freezer a number of times and potentially have been subjected to numerous freeze-thaw cycles. The effects on mRNA stability of long-term storage of tissue in the frozen state and therefore the subsequent damage to the integrity of the RNA will be an important aspect to the case selection criteria.

4.7.4 Inclusion and Exclusion Criteria

For a genetic comparison to be successful, case matching must be done to a high standard. Therefore, an assessment of relevant inclusion and exclusion criteria was undertaken. As human tissue is scarce, it was imperative to make informed decisions and not waste material. Pre-mortem and post-mortem factors that can affect RNA integrity may have implications for downstream analysis. Every individual is a composite of many different factors; variations in brain RNA levels are necessarily going to be the net result of an exceedingly complex set of underlying conditions. Ultimately gene expression analysis will be carried out, using two types of control cases. The purpose of two control groups is to establish TSE-specific modulated

genes from non-specific alterations. NND cases were used as normal control cases, allowing identification of any neurological disease modulation, whereas OND cases, being a pooled collection of various non amyloidgenic diseases, would allow a comparative list to be compiled and help identify TSE-specific gene changes. Clinical backgrounds of all patients are accessible from patient records. Based on the classical clinical features of vCJD, case matching for two control types (NND and OND) becomes a complicated matter. vCJD clinical features include; long disease duration (~ 12 months), young age of onset (~ 27 years), and neurological presentation. Typically OND cases have an older age of onset, variable lengths of disease duration and may or may not have neurological presentation depending on the individual case selected. NND cases have no known disease and therefore, at a minimum, would be matched by age and sex. In the MRC Sudden Death Brain Bank, a significant percentage of the cases are of a younger age group, overlapping with the young onset age of the vCJD group.

CONFOUNDING FACTORS

Factors such as age at death and pH of the brain are confounding variables (or covariates). These factors correlate with both the dependent variable (i.e. altered gene expression) and the independent variable (i.e. disease). Factors such as species are fixed factors. For accurate data analysis, confounding variables must be removed so that observed effects are not attributed to a confounder rather than the independent variable (i.e. vCJD). There are two methods of removing confounding variables in a study; matching for them or measuring them and using stratification or multivariate analysis (or both). Matched or case-controlled studies are slightly better than controlling by multivariate analysis because while multivariate analysis can accommodate some of the differences in confounding variable (i.e. age and sex), so many other variables depend on age and sex, it is simpler if the groups have similar profiles.

A large proportion of CJD patients normally succumb to a respiratory infection of the bronchi, or starvation and thirst. Dehydration and hypoglycaemic effects on RNA would therefore be relevant when studying vCJD patients. Co-infected individuals could exhibit different gene expression profiles, if this “secondary” infection affects mRNA expression in the brain. This may vary according to the infection and the

immune response at the time of death. For example, infections such as broncopneumonia would alter peripheral cytokine levels which could also affect gene expression in the brain. Cytokines such as interleukin (IL)-10, -1 and -6 have been shown to regulate microglia maturation and activation. Extraneural complement activation in response to infection may also affect RNA expression within the brain (Mabbott, 2004; Kovacs *et al.*, 2004; John *et al.*, 2003; Gasque *et al.*, 2000; Singhrao *et al.*, 2000). Viruses can target the CNS and routine post-mortem human specimens are frequently infected by a range of viruses, including; hepatitis, herpes and JC viruses (Sanders *et al.*, 1996; Shapshak *et al.*, 1986; White *et al.*, 1992). Viruses are able to induce apoptosis and other host responses and also infect and affect regions of the brain differently, potentially complicating vCJD gene expression studies (Kumar *et al.*, 2007; Allsopp & Fazakerley, 2000; Kristensson, 1992). Patients with simultaneous infections of the brain are useful control cases. Neuropathological gene expression changes may be confounded by other factors, for example age of patient.

PRE-MORTEM FACTORS

Although pre-mortem factors have been evaluated for their effect on RNA integrity, the published data are contradictory. Brain pH and agonal state are thought to exert the most damage to RNA and are interdependent factors. Prolonged agonal state causes an increase of lactic acid in the brain, thereby reducing the pH. Studies on pH from the frontal cortex indicate a long terminal phase of disease results in a lower pH than rapid death. The low pH (6.0-6.5) observed corresponded to lactic acid concentrations (20-25 mM) known to be neurotoxic (Kingsbury *et al.*, 1995). This effect has been observed to alter RNA yield, mRNA integrity and enzymatic activity (Harrison *et al.*, 1995; Johnston *et al.*, 1997; Barton *et al.*, 1993; Harrison *et al.*, 1991; Hardy *et al.*, 1985; Taylor *et al.*, 1986; Yates *et al.*, 1990; Perry *et al.*, 1982). Individuals who suffer prolonged agonal states, such as respiratory arrest, multi-organ failure or coma, or who have an increased age at death, tend to have lower brain pH, whereas those who experienced quick death, accidents, cardiac events or asphyxia, generally have normal pH. Lower pH brain samples generally contain degraded mRNA while brain samples from higher pH tissue contain more intact mRNA; pathological brain samples are comparable to control material of similar pH (Hardy *et al.*, 1985; Harrison *et al.*, 1991; Morrison & Griffin, 1981; Harrison *et al.*, 1995; Kingsbury *et al.*, 1995). Tissue pH is therefore likely to be a good indicator of mRNA

preservation. Hypoxia often leads to metabolic acidosis and lactic acid accumulation but brain tissue pH does not always correlate with the histological presence of hypoxic change (Harrison *et al.*, 1995). The cerebellar cortex and the hippocampus are particularly vulnerable to hypoxic damage (Graham & Lantos, 1997). Therefore it was decided that for this study the dentate nucleus within the cerebellum would be sampled, as this region would be less likely to be affected by hypoxic changes. Irrespective of agonal state, brain tissue pH stabilises post-mortem. Animal studies have shown that although there may be a rapid drop in pH in the initial 10 mins after death, brain tissue pH then remains stable for 24-36 hrs (Johnston *et al.*, 1997; Kingsbury *et al.*, 1995; Ravid *et al.*, 1992; Trotter *et al.*, 2002; Hardy *et al.*, 1985). In addition, brain tissue pH has been shown to be unaffected during freezer storage and is remarkably consistent across different brain regions (Johnston *et al.*, 1997). Table 4.1 lists previously published pre- and post-mortem parameters which may affect brain tissue pH.

	SIGNIFICANT CONTRIBUTION TO BRAIN pH	**NO OR LITTLE CONTRIBUTION TO BRAIN pH**
PATHOLOGY	Brain pH lower in AD brains than controls	
GENDER		No pH difference
AGE AT DEATH		No correlation in brain pH
AGONAL STATE		Poor predictor of brain pH
POSTMORTEM INTERVAL	AD correlation with pH	Controls not correlated to brain pH
mRNA	Brain pH correlation with mRNA amount	Not applicable
TOTAL RNA YIELD		No difference in pathology or gender
RNA YIELD AND pH		No correlation of total RNA to pH

Table 4.1. Factors contributing to variation in human brain tissue pH. Modified from (Preece & Cairns, 2003).

Treatment plans are prescribed based on the nature of the illness. The types of palliative medication prescribed to vCJD patients and OND patients will differ and older patients are often prescribed many different medications, which may further confound analysis. The drug history of the patient and preceding medical history are both relevant for gene expression studies. The use of opiates or other pain-relief medicines, prior blood transfusions, neurosurgery, viral encephalitis and previous childbirth are all factors which warrant consideration when selecting cases. It is highly unlikely that all these criteria will be matched for each case. It is unclear which medications might be most likely to affect CNS transcriptome profiles. Figure 4.3 defines the pre- and post-mortem situations of tissues before research use.

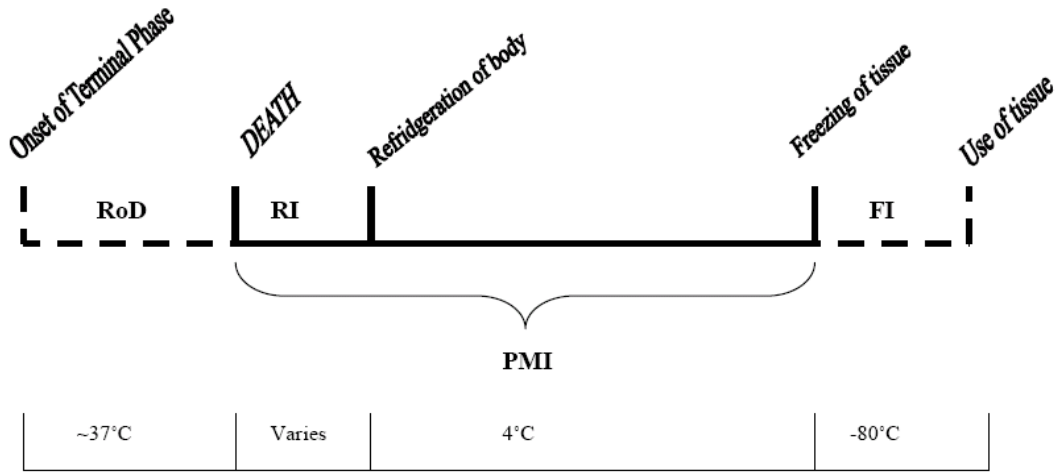

Figure 4.3. Handling of bodies and tissues used in study. RoD: rapidity of death. RI: refrigeration interval. PMI: post mortem interval. FI: freezer interval. Modified from (Johnston *et al.*, 1997).

POST-MORTEM FACTORS

Post-mortem factors have an adverse effect on the integrity of mRNA, although they are considered less important than pre-mortem factors (Tomita *et al.*, 2004; Barton *et al.*, 1993; Hynd *et al.*, 2003; Burke *et al.*, 1991). While a number of studies have indicated that agonal factors significantly affect the integrity of RNA and that post-mortem factors have only a relatively small effect, this is not always the case (Bahn *et al.*, 2001; Barton *et al.*, 1993; Harrison *et al.*, 1995; Kingsbury *et al.*, 1995; Perrett *et al.*, 1988). Studies have shown a relationship between PMI and RNA quality (Lipska

et al., 2006). However, other studies have concluded that there is at best a modest relationship (Barton *et al.*, 1993; Lukiw *et al.*, 1990; Harrison *et al.*, 1995) or no relationship (Cummings *et al.*, 2001; Kobayashi *et al.*, 1990; Johnson *et al.*, 1986; Morrison & Griffin, 1981; Heinrich *et al.*, 2007; Miller *et al.*, 2006; Schramm *et al.*, 1999; Watakabe *et al.*, 2001), with the Heinrich et al studies testing PMI up to 118 hrs, and the Schramm et al studies testing PMI up to 4 days. Given the contradictory reports, it cannot be concluded that RNA quality and yield are impervious to PMI. Just because overall RNA or mRNA content may not be affected markedly by PMI, it cannot be assumed that individual transcripts are all unaltered. If RNAs are selectively degraded post-mortem, then the pool of RNA can only be representative of a disordered system and would not resemble the *in vivo* situation. If RNAs are degraded in a random manner as a function of time, the pool of RNA remains in quantitative order and it is still possible to determine biologically relevant changes in post-mortem brain tissue. It has been shown that the pool of post-mortem human mRNA is essentially an ordered system. Such quantitative order of variation means that mRNAs are retained in the relative representative states that existed before death (Preece *et al.*, 2003). For practical and ethical reasons, a PMI of at least 1 hour and usually considerably longer is inevitable.

Storage method and freeze-thaw cycles may have more influence on mRNA preservation than agonal state or PMI. Although mRNA remains stable for extended periods of time within the body (<48 hrs), this greatly depends on the temperature of storage (Barton *et al.*, 1993; Leonard *et al.*, 1993; Schramm *et al.*, 1999). Once tissue has been harvested from the human body, it comes under a barrage of assaults and RNA can easily become degraded. Preservation techniques used in the NCJDSU have previously included liquid nitrogen freezing, but this is no longer permitted for health and safety reasons. Currently, tissue is stored frozen at –80˚C, either as small specimens or as whole half brains. Small tissue pieces freeze relatively quickly, whereas large organs take longer. Tissue storage time must also be considered. There is evidence that storage of human brain material at –70˚C for up to 15 years results in little or no degradation of RNA until it is thawed (Yasojima *et al.*, 2001). In contrast, in another study, RNA degradation was observed in human post-mortem brain stored at -70°C for more than 5 yrs (Leonard *et al.*, 1993). While the total amount of RNA that can be isolated from freezer-stored tissues may not vary significantly, the quality

of the RNA may deteriorate over time, affecting biological activity but not quantification of mRNA. Full length RNA is more vulnerable to degradation and fragmentation with extended PMI. Modern PCR techniques are able to tolerate partial RNA degradation. If enough full-length and partial transcripts (which are observed to Be more stable) remain for amplification, it is possible to use post-mortem tissue isolated RNA to study RNA transcript levels (Johnson *et al.*, 1986; Schramm *et al.*, 1999). Gene transcript levels from tissue stored by overnight refrigeration or 4 hrs at room temperature and then overnight refrigeration were similar to levels in tissue processed immediately (Trotter *et al.*, 2002). A decrease in transcipts was observed only after 8-24 hrs at room temperature and overnight refrigeration, but even then 90-95% of detected transcripts were within 40% of baseline levels.

Preservation of the messenger fraction of RNA is of particular importance. Directly after tissue harvesting, changes in gene expression may occur due to specific and nonspecific RNA degradation as well as due to transcriptional induction. Such changes need to be avoided for all reliable quantitative gene expression analyses. Long term storage of tissues for gene expression studies can only be done by freezing. The freezing procedures may affect the RNA that can subsequently be isolated. This may be due to autolysis of tissue, ice crystal formation and cellular dehydration. Whole organ freezing results in non-uniform freezing condition throughout the tissue. Cryopreservation using liquid nitrogen vapor results in less macroscopic artifact of anatomical structure and less friable frozen tissues, whereas liquid nitrogen or liquid nitrogen cooled isopentane is more prone to cracks or disintegration. With regards to gene expression investigations, tissue stored using any method of liquid nitrogen freezing shows minimal effects on DNA and RNA (Vonsattel *et al.*, 1995). Sample preparation requires thawing tissues from -80°C to at least 0°C. The number of freeze-thaw cycles can have serious adverse affects on the resulting isolated RNA, disrupting the cellular membrane and allows mixing of cellular enzymes and substrates which are normally segregated. The addition of chemical additives may help to minimize cellular stresses during freezing. Although the exact mechanism is unknown, the agents may protect the cell against harmful electrolyte concentrations which arise when water molecule crystallize (Hardy & Dodd, 1983; Leal-Klevezas *et al.*, 2000; Bischof, 2000; Karlsson & Toner, 1996). The RNA stabilization reagent 'RNALater' (Ambion, Warrington,UK) is designed for stabilization and protection of cellular RNA in animal tissues.

Table 4.2 summarizes the criteria to be considered when selecting cases for this study. It will not be possible to match all these criteria and not all information is available for all cases. Having considered all the literature, the table indicates the importance of each factor and ranks them in descending order of importance. The foremost factor for selecting tissue for inclusion in this study is neuropathological verification of the clinical diagnosis (if possible). This is especially critical for disorders such as CJD, where the final diagnosis can only be made neuropathologically.

RANK OF RELEVANCE	CRITERIA	IMPORTANCE	POSSIBILITY
1	**TYPE OF CJD** (sporadic/ variant/ iatrogenic/ familial)	*5*	**HIGH**
2	**REGION OF BRAIN ANALYSED** (frontal cortex and cerebellum)	*5*	**HIGH**
3	**TISSUE STORAGE METHOD**	*3*	**HIGH**
4	**POST MORTEM INTERVAL (PMI)**	*2*	**LOW**
5	**AGE**	*4*	**MEDIUM/HIGH**
6	**AGONAL STATE**	*3*	**HIGH**
7	**pH OF BRAIN**	*2*	**LOW**
8	**SEX**	*5*	**HIGH**
9	**DURATION OF ILLNESS**	*2*	**MEDIUM**
10	**MEDICAL HISTORY**; i.e. drugs prescribed, clinical trials, final diagnosis	*2*	**MEDIUM**
11	**BACKGROUND; i.e vegetarian, ethnic origin, familial medical history**	*1*	**LOW**

12	**LENGTH OF TIME OF TISSUE STORAGE**	*2*	**HIGH**
13	**CODON 129 GENOTYPE**	*1*	**HIGH**

Table 4.2. Case selection criteria. IMPORTANCE- indicates how suitable it will be to case match for this criteria (1-5, 1= unsuitable to attempt to match this criteria, 5= suitable to match for this criteria). POSSIBILITY- indicated how possible it would be to obtain the necessary information in order to match the samples (HIGH- MEDIUM- LOW).

The exclusion of certain cases will be necessary to ensure that selections for case matches are as appropriate as possible. Table 4.3 lists the exclusion factors in order of descending importance.

RANK OF RELEVANCE	CRITERIA	DESIRABILITY OF EXCLUSION
1	**OLDER SAMPLES that have been free-thawed**	**MEDIUM**
2	**CLINICAL TRIAL CASES**	**HIGH**
3	**NEUROSURGERY PATIENTS**	**HIGH**
4	**ALZHEIMER DISEASE PATHOLOGY/ DIAGNOSIS**	**HIGH**
5	**VIRAL INFECTIONS especially encephalopathies**	**MEDIUM**
6	**STATE OF DIAGNOSIS; must be definite diagnosis, i.e. category 1.0 or 4.3**	**HIGH**
7	**AGE-ASSOCIATED HISTOLOGICAL ABNORMALITIES, GENDER-SPECIFIC DIFFERENCES**	**LOW**

Table 4.3. Exclusion criteria for case selection.

4.8 DEMOGRAPHICS OF SELECTED CASES

Based on the inclusion and exclusion criteria, brain samples from a total of 78 cases were requested from the NCJDSU and MRC Brain Banks. The selected cases were then matched for as many parameters as possible.

4.8.1 Demographics of the Patients Studied

The demographic details of the cases selected for inclusion in this project are summarized in Table 4.4 and Table 4.5. There are two control groups; other neurological disease (OND) and non-neurological disease (NND). The NND control cases had no history of neurological disorders, the recorded cause of death was unrelated to neurological disorders and no neuropathological changes were observed by a consultant neuropathologist. OND control cases obtained at the NCJDSU are patients with neurological disorders, usually suspected CJD. The final diagnosis however was not CJD or other human prion disease, as established by a consultant neuropathologist. For experimental purposes, Alzheimer disease cases were excluded due to pathological and biochemical similarities to vCJD. vCJD cases were confirmed diagnostically by western blot and immunohistochemical staining and reported as vCJD cases by a consultant neuropathologist.

Table 4.4 shows the age range of cases, the ratios of male to female cases and the range of PMI from each cohort group. Brain pH was only recorded from the MRC post-mortems and is therefore only available for NND cases.

	NND (n= 31)	**OND (n= 26)**	**vCJD (n= 21)**
Age at death (yrs)	40.3 ± 1.7 (16-82)	65.5 ± 1.4 (25-86)	30.8 ± 1.0 (17-53)
Onset of symptoms (months)	-	-	12.8 ± 1.3(7-33)
Sex (M:F)	21:10	17:9	12:9
PMI (hrs)	64.1 ± 2.6 (37-115)	68.6 ± 4.5 (6-288)	50.4 ± 2.5 (24-120)
Brain pH	6.56 ±0.05 (5.55-7.50)	-	-

Table 4.4. Demographic details of NND, OND and vCJD groups. Values are mean ± SEM, with range in parentheses. Age; p-value >0.0001. PMI: p-value = 0.277.

One way ANOVA analysis for the three groups reveals a significant difference in the median age, with the 95 % CI for the means being most different for the OND group. vCJD and NND CI overlap demonstrating greater age similarity between these two groups than with the OND group. This result is expected because the majority of NND are sudden death cases, where healthy young adults die unexpectedly and vCJD typically affects young adults. The median age of onset in vCJD is 28 years with median illness duration of ~ 14 months. Table 4.4 shows the age of the patients at time of death, not time of onset. If the median age of onset (28 years) and duration of illness (~ 1 year) are extrapolated to time of death, a median time of death of ~ 29 years would be expected. This is essentially similar to the 30.8 ± 1.0 years (Table 4.4), in agreement with this data.

The spread of age at death (yrs) for male and female patients is shown in Figure 4.4.

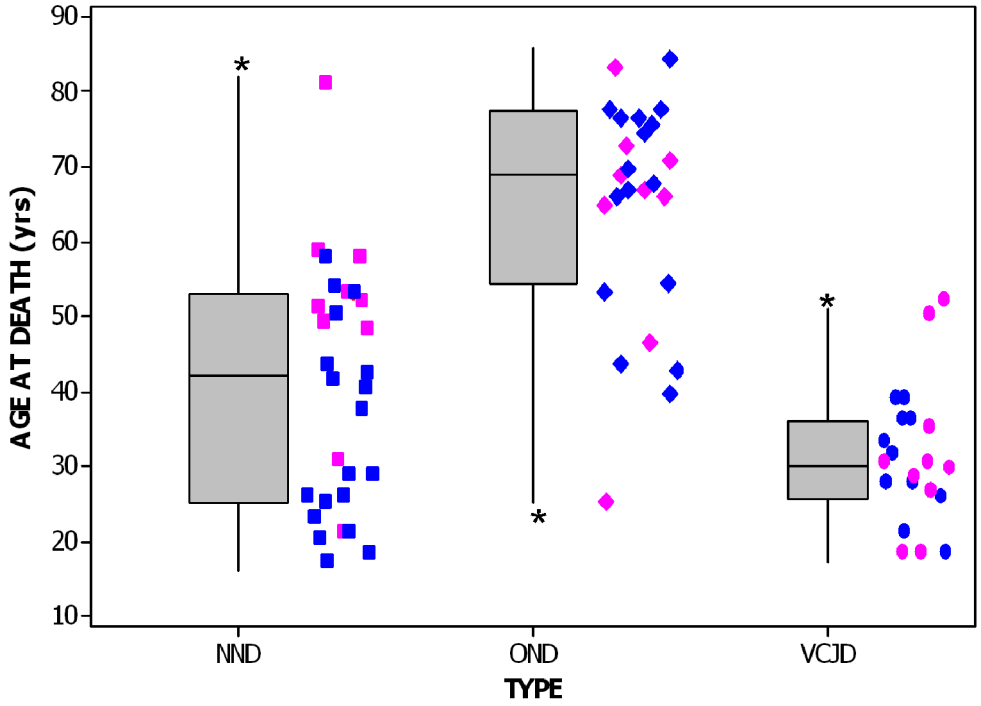

Figure 4.4. Combined scatter and box and whisker plots showing age range and gender proportion for each group. Compares the sample distribution of (■) non-neurological disease patients (NND), (◆) other neurological disease patients (OND) and (●) vCJD disease patients. Blue symbols are male and pink symbols are female. The boxes represent the 25th – 75th quartiles, divided horizontally by the median. The whiskers represent the range and the adjacent scatter plots represent the individual values from which the box and whiskers are derived. Outliers are denoted by (*). Male to female ratio of cases are; 21:10 (NND), 17:9 (OND) and 12:9 (vCJD).

Modes of death were classified into four groups by examination of clinical notes and autopsy reports. Using a modification of the method described by Hardy et al (Hardy *et al.*, 1985). Table 4.5 details the cause of death, mode of death and drug regime for each case. Mode of death was classified as follows;

1. Violent fast death. Death was due to shooting (accidental, homicidal or suicidal) or blunt force trauma. Typical cases are trauma sustained in road traffic accidents.
2. Fast death of natural cause. Death was sudden, unexpected deaths of otherwise healthy individuals. Typical cases are suspension by ligature.
3. Intermediate death. Death of patients suffering from illness but whose death was unexpected. These cases could neither be classified as sudden deaths (above) nor as slow deaths (below). Most of these cases died in hospital. Typical cases include myocardial infarctions.
4. Slow deaths. Death of patients suffering from a long period of illness with a prolonged terminal phase.

Sex	Age	Cause of death/associated diseases	PMI (hrs)	pH	FTC	IAS (including MOD)	Notes/ Mode of death (MOD)
M	28	Suspension by ligature	39	7.5	1	-	2
M	53	Suspension by ligature	37	6.4	1	-	2
M	54	Ischaemic heart disease. Severe coronary artery atheroma. COPD.	70	6.34	1	-	3
F	53	Suspension by a ligature	87	6.14	1	-	2
F	58	Haemopericardium. Left ventricle rupture. Acute myocardial infarct. Coronary artery thrombosis.	47	6.25	1	-	3
M	50	GI haemorrhage & liver failure	61	7.2	1	-	3
M	24	Fatal poisoning with alcohol	51	6.3	1	-	2
F	52	Acute myocardial infarct	64	6.4	1	-	3
M	40	Acute myocardial infarct	48	6.2	1	-	3
M	41	Dilated cardiomyopathy	48	6.4	1	-	3
M	37	Acute myocardial infarction	92	?	1	-	3
M	25	Internal bleeding. Rupture of thoracic aorta.	92	6.6	2	-	3
M	58	Internal bleeding. Rupture of an abdominal aorta aneurysm.	67	6.4	2	-	3

Sex	Age	Cause of death/associated diseases	PMI (hrs)	pH	FTC	IAS (including MOD)	Notes/ Mode of death
M	20	Hyperglycaemic coma	37	5.55	2	-	4
F	20	Combined drug poisoning	95	6.39	2	-	3
M	53	Acute myocardial infarct	51	6.3	2	-	3
M	25	Acute hydrocarbons poisoning	55	6.63	2	-	2
F	59	Subarachnoid haemorrhage	48	?	1	-	3
M	16	Suspension by a ligature	48	6.3	1	-	2
M	17	Severe head and neck trauma	55	6.63	2	-	1
M	43	Ischaemic heart disease	76	7.3	1	-	3
F	51	Hypertensive heart disease & cirrhosis	115	6.4	1	-	3
M	53	Combined effects of ischaemic heart disease and hypertensive heart disease	44	6.4	2	-	3
F	48	Pulmonary thromboembolism	50	6.5	1	-	3
M	42	Pulmonary thromboembolism	98	7.1	1	-	3
F	49	Congestive cardiac failure and acute intoxication with alcohol	111	?	1	-	3

Sex	Age	Cause of death/associated diseases	PMI (hrs)	pH	FTC	IAS (including MOD)	Notes/ Mode of death
F	30	Positional asphyxia	71	6.4	1	-	2
M	22	Suspension by a ligature	101	6.56	1	-	2
M	28	Multiple injuries	48	7.3	1	-	1
M	19	Fatal amitriptyline poisoning	51	6.26	1	-	2
F	82	Bronchopneumonia	44	?	1	-	4
F	**28**	**Bilateral bronchopneumonia**	**72**	**-**	**13**	**5**	**4**
M	**26**	**Bronchopneumonia**	**48**	**-**	**17**	**7**	**4**
F	**30**	**Bilateral bronchopneumonia**	**24**	**-**	**14**	**6**	**4**
M	**27**	**Acute bronchopneumonia and pulmonary congestion**	**48**	**-**	**18**	**9**	**4**
F	**17**	**Bronchopneumonia**	**24**	**-**		**7**	**4**
M	**27**	**Bronchopneumonia**	**24**	**-**	**3**	**7**	**4**
M	**17**	**Bronchopneumonia**	**120**	**-**	**3**	**8**	**4**
F	**53**	**Acute bronchopneumonia with severe oedema and congestion**	**48**	**-**	**12**	**6**	**4**

Sex	Age	Cause of death/associated diseases	PMI (hrs)	pH	FTC	IAS (including MOD)	Notes/ Mode of death
F	30	Bronchopneumonia	48	-	11	8	4
F	35	Bronchopneumonia	72	-	3	8	4
M	31	Bronchopneumonia	?	-	23	7	4
M	25	?	24	-	7	8	4
M	36	Bronchopneumonia	24	-	7	7	4
M	20	Bilateral bronchopneumonia and immobility	72	-	13	9	4
M	36	Acute bronchopneumonia	96	-	23	8	4
M	39	Bronchopneumonia	24	-	4	9	4
F	17	Bronchopneumonia	24	-	6	10	4
M	33	Bronchopneumonia	48	-	8	7	4
F	51	Bronchopneumonia and pulmonary odema	48	-	7	11	4
M	39	Bronchopneumonia and immobility and testicular tumour (pending histology investigation)	24	-	16	8	4
F	29	Bronchopneumonia and cerebral palsy	96	-	15	8	4

Sex	Age	Cause of death/associated diseases	PMI (hrs)	pH	FTC	IAS (including MOD)	Notes/ Mode of death
M	*71*	*Bronchopneumonia and liver cirrhosis with periportal fibrosis, artheriosclerosis with severe ischaemic damage to basal ganglia.*	*120*	*-*	*2*	*-*	*4*
M	*68*	*Bronchopneumonia with infective necrotising meningoencephalitis.*	*48*	*-*	*2*	*5*	*4*
F	*25*	*Bilateral thromboemboli, deep vein thrombosis, Guillan-Barre syndrome, possible Degos' disease*	*120*	*-*	*3*	*5*	*4*
M	*67*	*Bronchopneumonia and mild cerebral atrophy, generalised muscle wasting, healed tracheostomy.*	*48*	*-*	*6*	*11*	*4*
M	*40*	*Familial Alzheimer's disease (?)*	*6*	*-*	*5*	*7*	*3*
M	*86*	*Bronchopneumonia and arteriosclerosis and lacunar infarction.*	*96*	*-*	*4*	*5*	*4*
F	*70*	*Widespread small vessel cerebrovascular disease, bilateral bronchopneumonia*	*24*	*-*	*2*	*6*	*4*
F	*85*	*B-cell lymphoma*	*96*	*-*	*2*	*8*	*4*
F	*66*	*Vascular dementia. Bronchopneumonia to immobility*	*72*	*-*	*3*	*8*	*4*
M	*76*	*Road accident- was ix factor defective hemophiliac, therefore at high risk from use of blood product.*		*-*	*2*	*-*	*1*
M	*43*	*Bronchopneumonia and Lewy Body dementia*	*6*	*-*	*1*	*7*	*4*

Sex	Age	Cause of death/associated diseases	PMI (hrs)	pH	FTC	IAS (including MOD	Notes/ Mode of death
F	*74*	*Diffuse Lewy Body disease and congophilic angiopathy*	*24*	*-*	*2*	*6*	*4*
M	*?*	*Bronchopneumonia, myocardial hypertrophy and fibrosis*	*288*	*-*	*2*	*-*	*4*
M	*69*	*Malignant angioendotheliosis*	*24*	*-*	*1*	*5*	*4*
M	*54*	*Multifocal calcifying leucoencephalopathy and artheriosclerosis*	*96*	*-*	*2*	*10*	*4*
F	*44*	*No significant abnormalities*	*24*	*-*	*2*	*-*	*2*
F	*68*	*No evidence of primary neurodegenerative disorder. Oedema and gliosis, artheriosclerosis. Speticemia and cerebral hypoxia.*	*96*	*-*	*5*	*11*	*4*
F	*47*	*Multifocal hypoxic/ischaemic brian damage and cerebrovascular dementia*	*72*	*-*	*1*	*6*	*4*
M	*72*	*Bronchopneumonia, severe emphysemia. Chronic obstructive airways disease.*	*48*	*-*	*2*	*11*	*4*
F	*77*	*Bronchopneumonia and Lewy Body dementia*	*48*	*-*	*1*	*7*	*4*
M	*67*	*Bilateral severe bronchopneumonia with abscess formation. Metastatic carcinoid tumour.*	*48*	*-*	*7*	*6*	*4*

Sex	Age	Cause of death/associated diseases	PMI (hrs)	pH	FTC	IAS (including MOD	Notes/ Mode of death
M	*79*	*Severe artheriosclerosis*	*96*	*-*	*5*	*10*	*4*
M	*78*	*Multifocal calcifying leucoencephalopathy*	*72*	*-*	*8*	*-*	*4*
M	*78*	*Bronchopneumonia and Lewy Body dementia*	*24*	*-*	*3*	*7*	*4*
M	*79*	*Bronchopneumonia and pulmonary oedema*	*48*	*-*	*3*	*-*	*4*
M	*55*	*Bronchopneumonia and Lewy Body dementia*	*72*	*-*	*12*	*6*	*4*

Table 4.5. Detailed individual case information for all NND, vCJD and OND cases included in this study. Normal = non neurological cases. Bold = variant CJD cases. Italics = other neurological disease cases.

4.8.2 Case matched comparison groups for gene expression

Table 4.6 summarises the matched comparison groups, suitable for gene expression analysis, which were possible based on the inclusion and exclusion criteria for case selection and matching for sex and age (within 10 years).

NND			**vCJD**			*OND*		
STATUS (control)	AGE (yrs)	SEX	**STATUS**	**AGE (yrs)**	**SEX**	*STATUS (control)*	*AGE (yrs)*	*SEX*
1 NND	18	M	**1 vCJD**	**17**	**M**	*1 OND*	*19*	*M*
2 NND	54	M[1]	**2 vCJD**	**39**	**M**	*2 OND*	*41*	*M*
3 NND	18	M	**3 vCJD**	**27**	**M**	*3 OND*	*28*	*M*
4 NND	18	M	**4 vCJD**	**27**	**M**	*4 OND*	*25*	*M*
5 NND	25	F	**5 vCJD**	**30**	**F**	*5 OND*	*31*	*F*
6 NND	43	M	**6 vCJD**	**30**	**M**	*6 OND*	*25*	*M*
7 NND	43	M	**7 vCJD**	**33**	**M**	*7 OND*	*37*	*M*

Table 4.6. Summary of comparison groups, matched by age and sex. All ages are ± 10years with the exception of 1.

7 matched comparison groups possible from tissues stored at the NCJDSU (vCJD and OND) and the MRC brain bank (NND). These cases are suitable for gene expression analysis, as they fulfilled the RNA quality criteria set by this project. Briefly the criteria were; RIN value ≥ 5.0, $A_{260:280}$ nm absorbance ≥ 2.0 and $A_{260:230}$ nm absorbance ≥ 1.7. This is discussed further in Chapter 5.

4.9 DISCUSSION

Brain bank organizations are established to provide clinically and neuropathologically well-documented specimens for research purposes. Although there is no consensus on how to prepare, categorise and store the specimen, appropriate strategies for tissue preservation and data collection are important for successful and reproducible application of quantitative competitive RT-PCR, western blotting, microarray and proteomic assays of unfixed tissues. It can also help link the clinical, pathological and scientific aspects of research. Prospective harvesting and storing of tissues gives researchers access to an invaluable resource. A worrying continuous decline in autopsy rates worldwide is serious cause for concern (Anderson & Hill, 1989), further limiting this precious and scarce source of tissue. Therefore it is imperative that maximum use is made of the tissue, by retaining samples with biochemical, molecular and structural integrity. Furthermore, the use of standardized tissue methods promotes multicentre collaborations. As new genetic techniques have emerged, there is an increased demand for post-mortem tissue. Brain banking will need to accommodate the requirements of these techniques.

In order for studies to be meaningful, optimized tissue collection and storage methods should limit post-mortem variability, and in depth pre-mortem data collection will help identify and adjust for pre-mortem confounding factors. While the list of pre- and post-mortem factors discussed earlier in this chapter is by no mean exhaustive, a balance must be struck between matching for the various factors and building a sufficiently large sample population. Interpretation of the results of post-mortem studies requires fastidious consideration of these factors in order to separate changes due to disease from epiphenomena. Without pre-mortem data, it would be difficult to separate disease-related changes from changes unrelated to disease and/or artefact. Post-mortem measurements therefore need to be complemented by pre-mortem data.

An important consideration is to separate disease-specific changes from the non-specific effects of factors, such as PMI and AS that may contribute to RNA quality and quantity and which may affect gene expression analysis. Pre-mortem variation is inevitable, not only age and gender but every individual is subjected to many different

factors. By matching cases based on pre-mortem factors, confounding effects are minimized. The question is which pre-mortem factors have the greatest effect and are most important to match? Pre-mortem factors which correlate with RNA quality and/or quantity would be important as would pre-mortem factors which affect CNS gene expression. Post-mortem variation can be more easily controlled. For example, regional differences in human brain can be minimized by careful selection of suitable regions. The choice of frontal cortex and cerebellum for this study is based on data indicating that CJD generally affects these areas of the brain. It is however, possible that these regions do not have gene expression changes related to disease pathology, or there is considerable variation in gene expression, even in control brains, within these regions. One approach to address this is to study as many samples as possible within a region; another is to use pooled samples. Using pooled samples also reduces the problem of case matching. The advantages of this method would be to eliminate a source of inter-patient variation. The disadvantage is that it may reduce the magnitude of observed changes in gene expression. Further complications are introduced by the common practise of using one hemisphere for biochemical analysis and the other for pathological examination.

Based only on age (± 10 yrs) and gender, from a total of 78 cases, it was possible to match cases across the 3 cohort groups, and to generate 7 comparison groups, each containing one vCJD, one NND and one OND case. This is a promising sign that future studies will not be constrained by limited samples, and that close adherence to case selection criteria is possible without restricting the strength of any potential findings.

While it has been found in this project that it is possible to study RNA from a large number of post-mortem brains, it has not been possible to account for the variability between samples. Chapter 5 covers this is more detail. By using multivariate analysis methods, it may be possible to identify a variety of potentially important covariates on RNA transcript levels that can help researchers devise appropriate tissue collection methods and analysis plans.

5 PREPARATION AND ASSESSMENT OF RNA FROM HUMAN BRAINS

5.1 OBJECTIVES

- Assess the quality and quantity of RNA extracted from human brain autopsy material.
- Identify the level of intra- and inter-case variability of RNA quality and yield.
- Evaluate retrospective and prospective tissue storage methods.
- Identify post-mortem variables which impact on RNA quality.
- Identify metrics which could be used to prospectively screen samples prior to their use for gene expression analysis.

5.2 RNA EXTRACTION AND ANALYSIS

RNA is traditionally isolated from tissues by homogenisation in guanidinium thiocyanate (GTC), phenol extraction and ethanol precipitation. Different organic solvents, alcohols and salts have been used. The selection of these is determined by the future work required. For example, a common method of removing proteinaceous material from nucleic acid solutions is to extract first with phenol-chloroform followed by chloroform. The use of both organic solvents is more effective than use of phenol alone because; 1) deproteinization is more efficient when two organic solvents are used, 2) although phenol denatures proteins efficiently, it does not completely inhibit RNase activity and it is a solvent for RNA molecules that contain long tracts of poly(A) (Brawerman *et al.*, 1972) and 3) subsequent extraction with chloroform removes residual traces of phenol from the nucleic acid preparation.
A mixture of phenol:chloroform:isoamyl alcohol (25:24:1) is the most commonly used solvent. Following extraction, nucleic acids are then generally precipitated in the presence of monovalent cations, recovered by centrifugation and redissolved in

an appropriate buffer. Ammonium acetate was selected for use in this project because other commonly used salts can inhibit downstream processes. For example, sodium or lithium chlorides are unsuitable as chloride ions suppress the activity of RNA-dependent DNA polymerase. Carrier RNA, for example yeast tRNA, is frequently added before precipitation to improve the recovery of small amounts of RNA.

When working with RNA, care must be taken to avoid degradation by RNases, which are extremely stable and active. Intracellular RNases are released during the lysis step of the RNA isolation procedure and must be rapidly and thoroughly inactivated to obtain high quality RNA. Proteins dissolve readily in solutions containing potent denaturing agents such as GTC. Cellular structures disintegrate and nucleoproteins dissociate from nucleic acids as protein secondary structure is lost (Cox, 1968; Sela *et al.*, 1957). Phenol also has denaturing properties, but is less effective at inactivating RNases than GTC. Nevertheless, phenol phase extraction is efficient at de-polarising proteins and partitioning the phenol-soluble proteins within the phenol phase (Kickhoefen & Buerger, 1962). GTC and phenol in combination are therefore generally the method of choice to separate nucleic acids from proteins and inhibit RNase activity (Chirgwin *et al.*, 1979).

In recent years these empirical methods have been replaced by kits based on a single-step RNA isolation method using acid GTC as first described by Chomczynski and Sacchi (Chomczynski & Sacchi, 1987). One such commercially available kit is the Qiagen RNeasy lipid tissue extraction kit, designed for high lipid tissues such as brain. A specialized buffer included with the Qiagen RNA isolation kit contains ~ 4 M GTC, to inactivate RNases. The Qiagen kit extraction method includes the use of a silica-gel based membrane spin column, which selectively binds RNA >200 bp length. This process partially enriches for mRNA since the majority of small RNA such as 5.8S rRNA, 5S rRNA and tRNAs, which together comprise 15-20% of total RNA, do not bind to the membrane. A specialised high-salt buffer system allows up to 100 µg of RNA >200 bases to bind to the RNeasy silica-gel membrane. Proteins, lipids, DNA and small RNA molecules do not bind to the membrane and are spun out of the columns, see www.qiagen.co.uk for more details.

One aim of this project is to investigate gene expression in vCJD brains. Analysis of gene expression is dependent upon the quality of the RNA that can be isolated. Minimally degraded RNA yields reliable microarray data, although this depends on the method of evaluating degrees of degradation (Schoor *et al.*, 2003).

To obtain RNA samples suitable for gene expression analysis it is necessary to consider RNA quantity, quality and purity. RNA quantity is generally assessed by UV spectrophotometric analysis, although it is susceptible to interference from contaminants (Sambrook & Russel, 2001). Nanodrop ND-1000 Spectrophotometer (Nanodrop Technologies, Washington, USA) measures the optical density of a sample over a continuous spectrum of wavelengths from 200 – 750 nm. In this system, 1 µl of sample is directly scanned without the use of cuvettes or capillaries. Nucleotides, RNA and ss/dsDNA will absorb at 260 nm and contribute to the total absorbance. A_{280} readings estimate the degree of protein material. A_{260} readings and the ratios of absorbance at 260 nm and 280 nm are usually used to asses the purity of RNA. Although it is possible to have $A_{260:280}$ ratios of ~1.8, the purity can vary greatly, especially when using organic solvents during extraction. A peak at 230 nm may be evidence of contamination with organics, thiocyanates, phenolate ions, ethanol or isopropanol. $A_{260:230}$ ratios are much more variable but generally, ratios ~ 1.7 indicate good purity and no contamination.

Quality assessment of total RNA is traditionally determined by reference to the size of 28S and/or 18S rRNA bands on ethidium bromide gels. Good quality RNA is based on subjective interpretation of > 2:1 ratio of 28S rRNA to 18S rRNA. The 28S:18S rRNA ratio is however inconsistent and unlikely to be > 2.0 for RNA isolated from dense connective tissue (Reno *et al.*, 1997), RNase-rich tissue (Monstein *et al.*, 1995) or tumour tissue (Skrypina *et al.*, 2003).

There is currently no gold standard to define the RNA quality prior to gene expression analysis. Using a single simple feature to judge RNA integrity has been shown to be insufficient (Miller *et al.*, 2006). No single method fully reflects all the

properties of the degradation process. Using several features which complement each other, an enhanced profile of the degradation 'fingerprint' of RNA preparation can be achieved, reducing the error to a minimum value which is in the order of the natural noise of the target data.

Recently two computer methods; the degradometer software (Auer *et al.*, 2003) and the Agilent RNA integrity number (RIN) algorithm (Schroeder *et al.*, 2006) have been described. Agilent Bioanalyzers generate electropherograms which visualise many more components of total RNA than was previously possible on standard gel electrophoresis.

The Agilent 2100 Bioanalyzer is a platform designed for electrophoretic analysis of RNA samples. The molecular weights of RNA species are determined by their migration distance, as on a gel, and the Bioanalyzer plots an electropherogram of each sample (Figure 5.1). The quantity and quality of RNA are determined in three ways; RNA integrity number (RIN), the ratio of 28S to 18S rRNA and the concentration of total RNA.

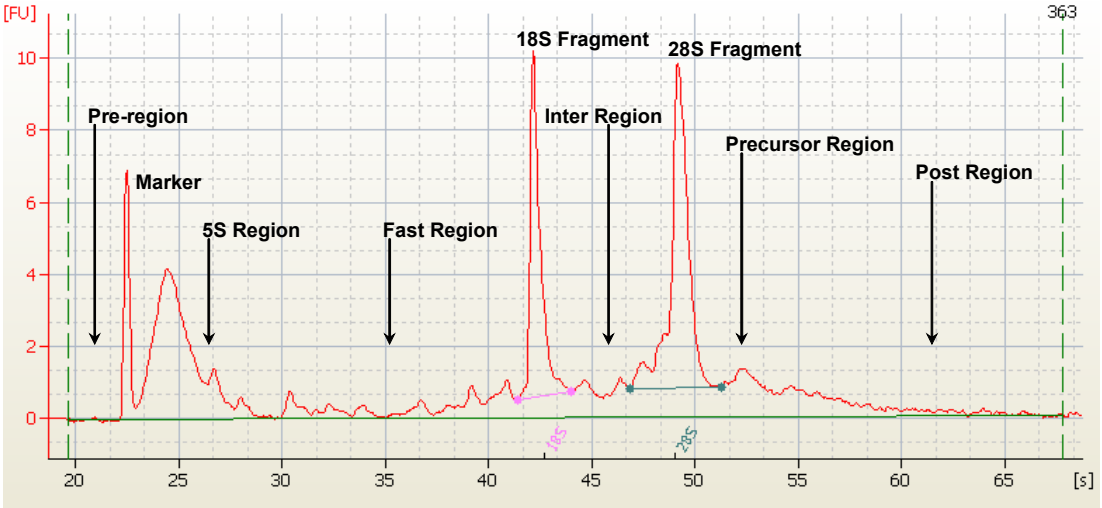

Figure 5.1. Electropherogram detailing the regions indicative of RNA quality. The area preceding the lower marker is the pre-region. The lower marker peak is an internal standard used to align the ladder data with the data from the sample wells. The marker region coincides with the area occupied by the marker peak. These two regions are not accounted for in the RIN algorithm. The 5S-region covers the smaller rRNA fragments (5S, 5.8S rRNA and tRNA).

The most distinct features on the electropherogram are the 18S and 28S ribosomal RNA peaks. Intact mRNA migrates between these two ribosomal peaks and for good quality RNA the trace here is smooth and lacks distinct peaks. For good quality RNA, the baseline between ~25 seconds and the 18S rRNA is relatively flat and free of peaks (corresponding to smaller RNA molecules). Qiagen RNA extraction kits remove smaller RNA molecules and should leave the mRNA and two large rRNA peaks. The RIN value is described in detail by Schroeder et al (Schroeder *et al.*, 2006). Briefly, the algorithm primarily utilizes the area of the 28S peak, the area of the 18S peak (the percent of total electropherogram area represented by both is proportional to RIN) and the area of the fast region (which is inversely proportional to RIN). The RIN values range from N/A or 0.0, completely degraded, undetectable RNA to 10.0, completely intact RNA.

Figure 5.2 details a standard operating procedure (SOP) for RNA quality assessment for this study. It has been suggested that this working procedure be integrated into the NCJDSU Brain Bank SOP. An RNA integrity database would provide valuable information for future molecular studies and facilitate case selection. A similar system is under review at the MRC Sudden Death Tissue Bank.

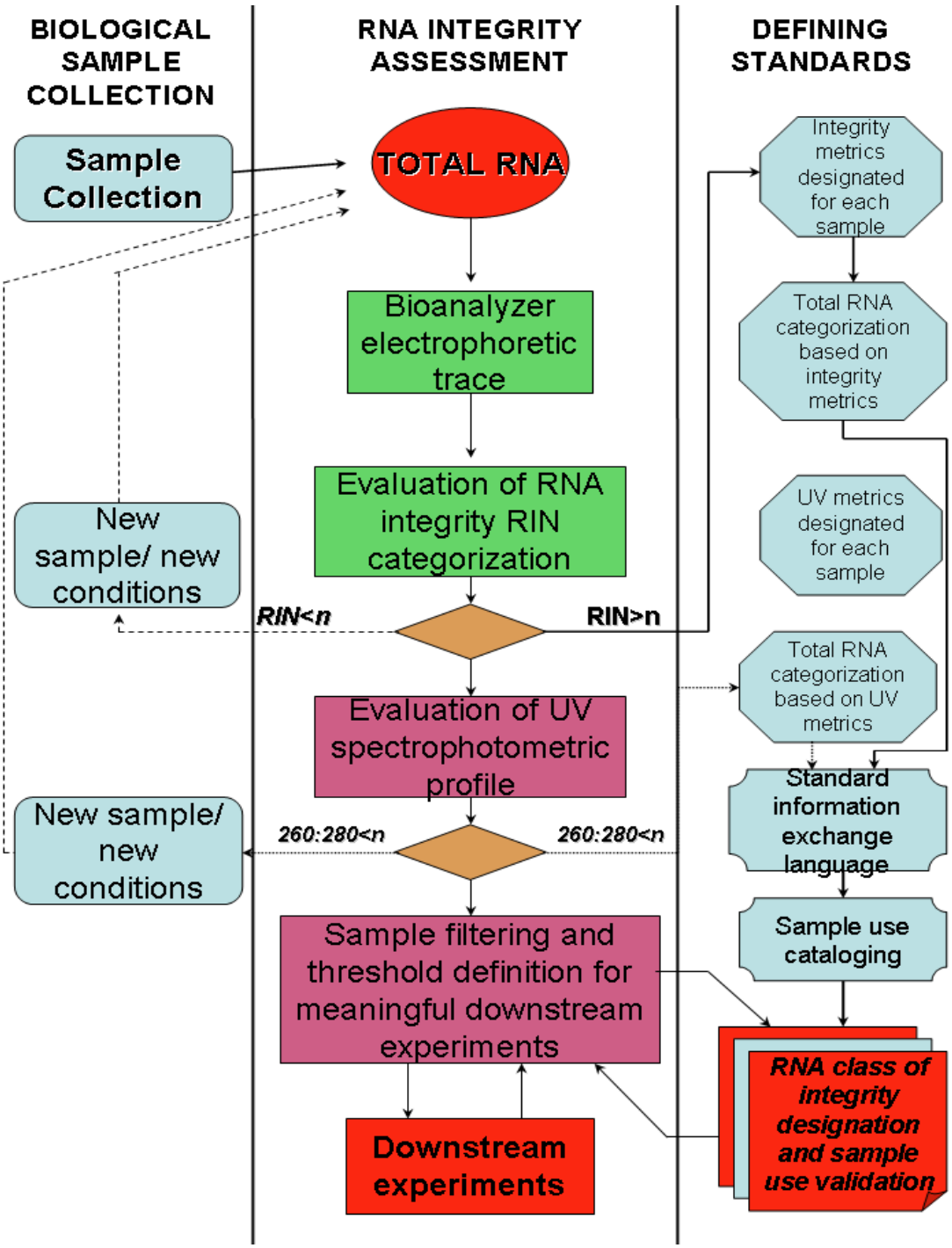

Figure 5.2. Work flow of operational procedure for RNA quality assessment. Integrity of the RNA, once extracted and purified from tissue samples, is controlled from the bioanalyzer electrophoretic traces. As standard, the Agilent software RIN metric is calculated, scoring each RNA sample into 10 numerically predefined categories of integrity (RIN, from 1 to 10; n is the users predefined threshold value). As an independent control, UV absorbance readings will also be recorded. Such double classification will improve documentation of RNA integrity and degradation, and data can be stored alongside clinical, genetic and histological information at the NCJDSU. This will aid in future projects for case selection, as cases of comparable RNA integrity would be recorded, thereby limiting unnecessary tissue usage. A standard operating procedure would be beneficial and feedback information would help users to define threshold integrity metrics based on the results of any RNA-based analyses (modified from (Imbeaud *et al.*, 2005).

For this study it was decided to use the Qiagen RNeasy lipid tissue extraction kit for the isolation of brain RNA. This method contains ~ 4 M GTC and ~ 2 M phenol, which should be sufficient to inactivate TSE agents (see Chapter 3); however for safety, it was decided to carry out a further double phenol-chloroform extraction to remove any remaining protein (infectious material). RNA quantity, quality and purity will be assessed by measuring the 28S:18S rRNA ratio, $A_{260:280}$ ratio and the RIN.

5.3 ASSESSING THE QUALITY AND QUANTITY OF RNA PREPARATIONS

5.3.1 Pilot Study on Mouse Brains

To test the RNA isolation protocol, RNA was extracted from 8 mouse brain samples using the Qiagen RNeasy lipid tissue kit. The RIN, 28S:18S rRNA ratio and total RNA yield were determined. Samples were then processed through a double phenol-chloroform extraction and the RIN, 28S:18S rRNA ratio and RNA yield again measured. The results for RIN and RNA yield after Qiagen kit processing and after double phenol-chloroform processing are shown in Table 5.1.

AFTER QIAGEN EXTRACTION			**AFTER SECOND PHENOL-CHLOROFORM EXTRACTION**		
RIN	***28S:18S RATIO***	***Yield (µg)***	***RIN***	***28S:18S RATIO***	***Yield (µg)***
8.8 ± 0.49 (8.2-9.9)	1.3 ± 0.08 (1.2-1.4)	96.8 ± 37.7 (51.0-186.6)	8.9 ± 0.32 (8.4-9.6)	1.1 ± 0.16 (0.9-1.3)	46.7 ± 17.8 (21.3-82.5)

Table 5.1. RNA Integrity Number (RIN), 28S:18S rRNA ratio as determined by Agilent 2100 Bioanalyzer. Concentration readings (ng/µl) were also determined and used to calculate RNA yield (µg) per 100 mg starting brain material. Aliquots of RNA from after Qiagen extraction and after a second phenol-chloroform extraction were tested for RNA integrity and concentration. Values are mean ± SD with range in parentheses. Average difference: RIN= 0.1, 28S:18S ratio= 0.2, Yield (ng) = 50.0. P-values, RIN= 0.321, 28S:18S ratio= 0.003, RNA yield< 0.0001. n=12. (Significance level= 0.05).

Paired dependent t-test analysis showed no significant difference between the RIN value of samples after Qiagen extraction or after the additional phenol-chloroform step. However, there was a significant difference between the 28S:18S ratio and the RNA yields. Approximately 50% RNA was lost in the phenol-chloroform extraction. The reduction in yield of RNA was considered acceptable in the interest of the additional safety.

5.3.2 Comparison of Extraction From Human and Mouse Brains

To determine the quantity, quality and reproducibility of the RNA isolation protocol for mouse and human brain material, RNA preparations were compared from mouse and human brains. Samples were coded to anonymize them and eliminate bias and all extractions were carried out in parallel. Figure 5.3 shows the Agilent Bioanalyzer analysis of 6 mouse and 6 human brain RNA samples.

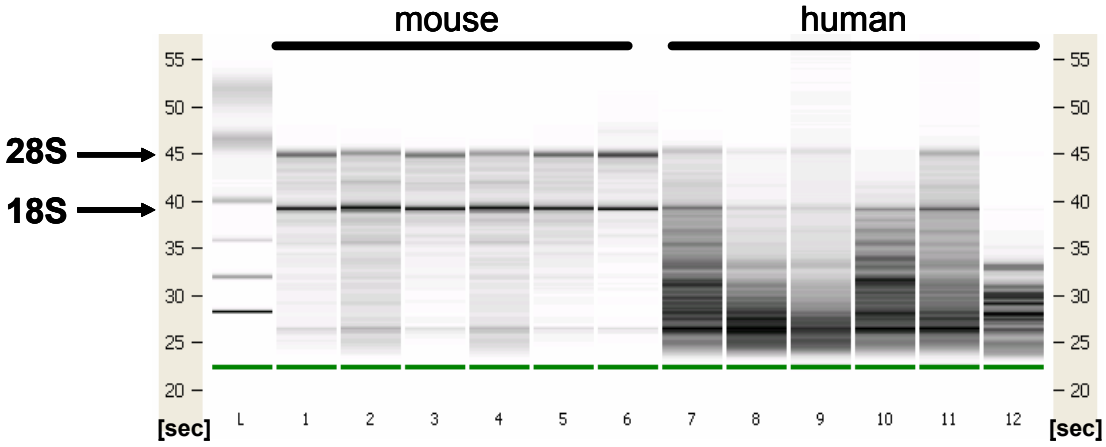

Figure 5.3. Agilent Bioanalyzer gel image using the RNA LabChip (1 µl RNA extract). Lane L. 150 ng RNA ladder. Lanes 1-6, RNA from the brains of 10 week old mice. Lane 7-12, RNA preparations from human brains. Most samples have two clearly resolved bands which correspond to the 28S and 18S ribosomal RNA bands (elution times ~ 40 secs and 45 secs, respectively).

Figure 5.4 represents the electropherogram and gel-like image of RNA isolated and assayed on the Agilent 2100 Bioanalyzer.

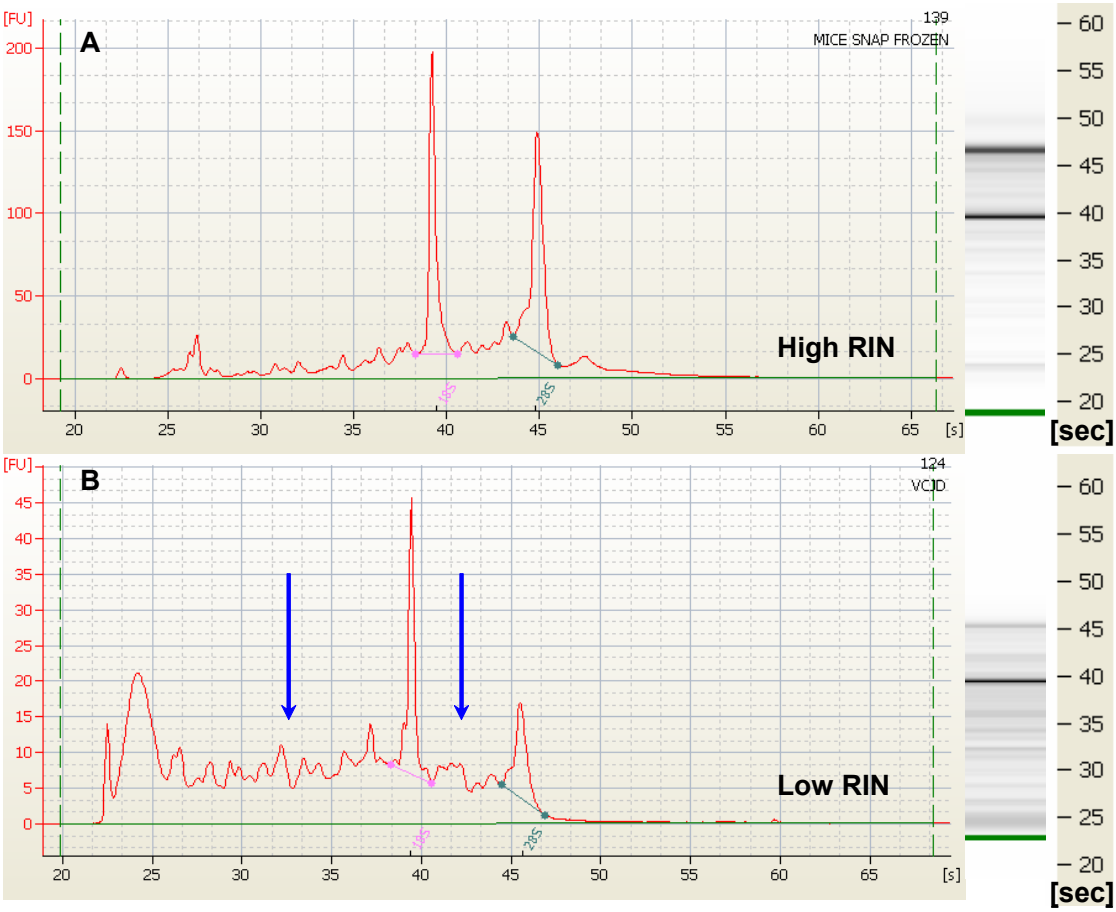

Figure 5.4. Examples of Agilent Bioanalyzer profiles. RNase degradation of total RNA samples produces a shift in the RNA size distribution towards smaller fragments and a decrease in fluorescence signal. Profile A; typical electrophoretic trace and gel-like image of total RNA extracted from mouse brain, a. RIN value of 7.5. Profile B; typical electrophoretic trace and gel-like image of total RNA extracted from human brain material, a RIN value of 5.3 is typical. 18S rRNA baselines corresponding to florescent peaks are labeled with a pink line. The 28S rRNA baselines corresponding to the florescent peaks are labeled with a green line. Blue arrows indicate regions where smaller fragments of RNA appear, indicative of degradation of mRNA.

The RNA isolated from mouse brains contained fewer small RNA fragments (< 35secs) than RNA isolated from human brains. This is evident from the reduced number of bands eluting during the fast region and a clear separation in 28S and 18S rRNA bands. In human RNA samples, the banding pattern was less well resolved and a higher level of small RNA fragments was detected. These smaller fragments are indicative of RNA degradation and show that all the RNA preparations from human brains were more degraded than those from mouse brains.

Panel A is an example of a mouse RNA sample with little evidence of degradation. The flat baseline and lack of peaks eluting at the < 40 sec timeframe indicates there are few small RNA fragments in the sample. Panel B is an example of a human RNA sample with degradation. Although two main RNA bands or peaks corresponding to the 28S and 18S rRNA species are still visible, degradation products are observed as ragged peaks eluted during the fast and mid-regions.

As RNA degrades;

- The peaks begin to shift towards the left of the electropherogram
- The baseline between and to the left of the ribosomal bands becomes jagged and more defined looking peaks appear.
- The intensities of the ribosomal peaks decrease relative to the peaks resulting from their degradation.
- The intensity of smaller degraded RNA increases. The most highly degraded products have a migration time between 22 and 24 seconds.

All RNA preparations were also tested by UV spectrometry using the Nanodrop ND-1000 Spectrophotometer. Optical density (OD) measurements were taken over a full spectrum of UV wavelengths. This can be represented graphically, as below (Figure 5.5).

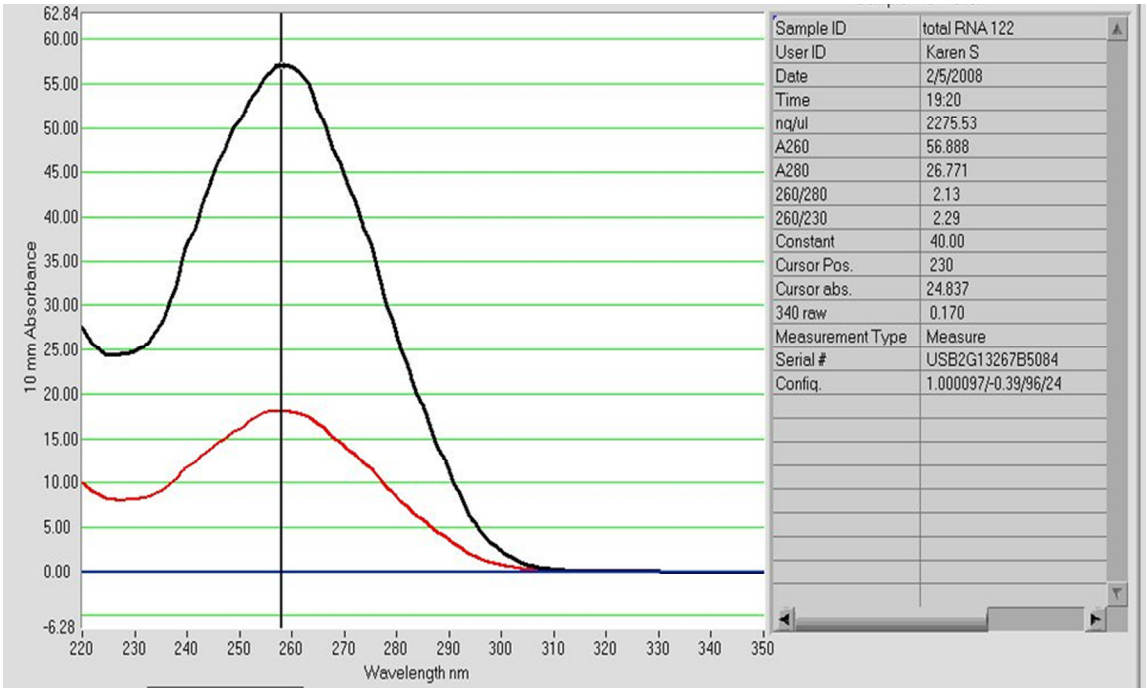

Figure 5.5. Nanodrop spectrophotometeric full wavelength profile scan. Comparison of high purity RNA preparation and low purity RNA preparation. Black profile corresponds to RNA sample with A260:280 of 1.8 and A260:230 of 2.0, indicative of high purity RNA, free from organic solvent, protein or genomic DNA contamination. Red profile corresponds to RNA sample with A260:280 of 0.3 and A260:230 of 3.4, indicative of significant organic solvent contamination and would be evaluated as a low purity sample and excluded from further analysis.

For this project, GTC and phenol-chloroform were used for RNA extractions. UV measurements are greatly affected by phenol contamination, even at low concentrations. 0.5% w/v results in a 300% error in concentration measurements (Lightfoot, 2002). Residual GTC and phenol absorb at ~230 nm, consequently altering the 260:230 ratio. Therefore, this method is highly sensitive to phenol or GTC contamination of the samples. Contaminated preparations are unsuitable for RT or PCR amplification reactions, since carryover reduces the efficacy of or inhibits enzymatic activity.

5.3.3 Reproducibility

To determine the reproducibility of the extraction method and the Agilent Bioanalyzer, a single tissue sample was split into two and both samples were extracted and measured on the Agilent Bioanalyzer (Figure 5.6A). A single sample was also extracted and then measured on the Agilent Bioanalyzer twice (Figure 5.6B).

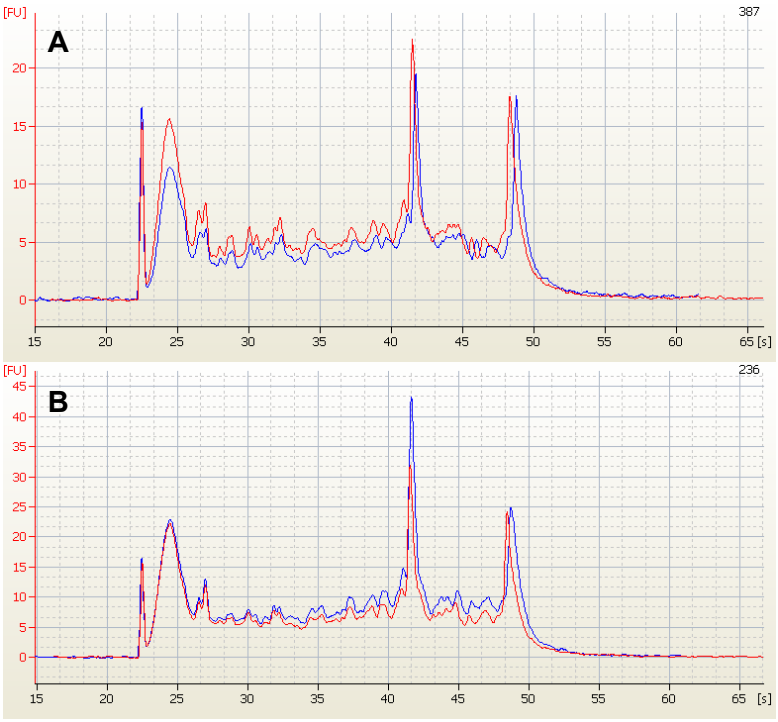

Figure 5.6. Reproducibility of the RNA extraction procedure and of Agilent Bioanalyzer measurements. A. A single brain sample was separated into two and RNA extracted. Each of the extractions was assayed by the Agilent Bioanalyser once. Red profile; RIN =4.7, 28s:18S ratio = 1.7, total RNA concentration (ng/µl) =272. Blue profile; RIN =5.1, 28S:18S ratio= 1.4, total RNA concentration (ng/µl) = 447. B. Single brain RNA preparation assayed on the Agilent Bioanalyzer twice. Red profile; RIN =5.5, 28s:18S ratio = 0.4, total RNA concentration (ng/µl) =266. Blue profile; RIN =5.5, 28S:18S ratio= 0.7, total RNA concentration (ng/µl) = 383.

As expected, the level of variation when comparing two separate extractions is marginally greater than when comparing the same sample twice. However, it should be noted that when comparing the same sample although the RIN value didn't change there was a considerable difference in the 28S:18S ration and the concentration, showing that differences in the latter values must be interpreted with caution. A more detailed analysis of yield measurements is presented in section 5.5.

The extraction reproducibility was also tested on the Nanodrop. A single tissue sample was split into two and both samples were processed through the extraction protocol and measured on the Nanodrop (Figure 5.7A). In addition, the Nanodrop

reproducibility was tested by measuring a single RNA preparation, twice (Figure 5.7B).

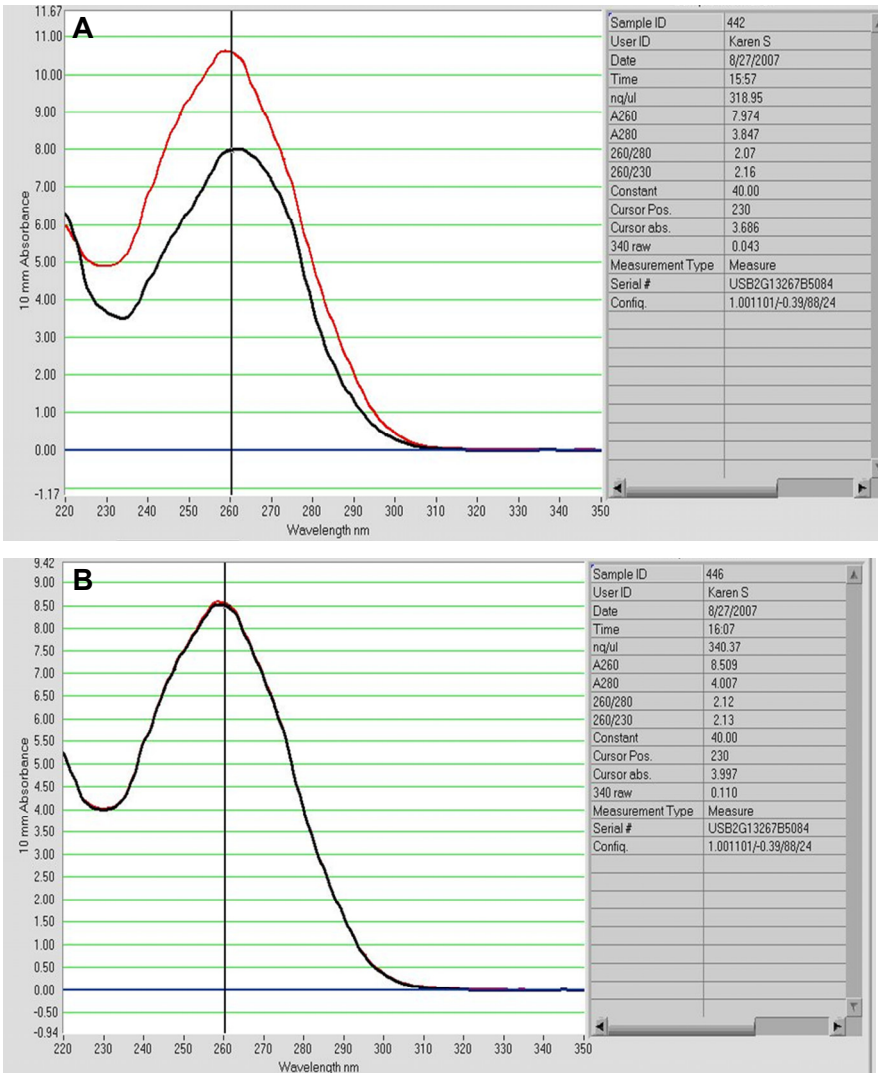

Figure 5.7. Nanodrop spectrophotometeric full wavelength profile scan. Panel A. Superimposed profiles of adjacent tissue samples, RNA isolated individually and measured. Red profile. A260:280 = 2.11. A260:230 = 2.17. Black profile. A260:280 = 2.07. A260:230 = 2.16. Panel B. Superimposed profiles of a single RNA preparation measured on the Nanodrop twice. Red profile.A260:280 = 2.12. A260:230 = 2.13. Black profile. A260:280 = 2.12. A260:230 = 2.13.

Figure 5.7A superimposes the full wavelength profiles from the Nanodrop 2100 spectrophotometer of repeated preparations. Figure 5.7A shows the variation within the extraction protocol as well as variation within the Nanodrop. Figure 5.7B indicates the level of variability within the Nanodrop measurement only. Figure 5.7B demonstrates the high level of reproducibility of the Nanodrop measurements. This indicates that the variation identified in Figure 5.7A, while limited, is mostly due to processing variation and/or human error. When compared to the Agilent Bioanalyzer results (Figure 5.6), Nanodrop quantification of RNA preparations is more reproducible.

5.4 SAFETY ANALYSIS OF PROCEDURES DEVELOPED

After assessment of risk, an evidence based protocol for RNA preparations was developed (see Chapter 3). This was deemed suitable for inactivating and removing PrP and infectivity from human brain material. RNA preparations were only handled by expert personnel (Karen Sherwood) and transported as if low risk infectious specimens. In order to assess whether the RNA extraction protocol efficiently removed PrP , PrP^{res} levels were investigated by western blot.

5.4.1 Presence of Detectable Protein

To determine the sensitivity of the western blot, dilutions of brain homogenates from a vCJD brain were investigated (Figure 5.8, 5.9). PrP protein was assessed by immunoblotting using 6H4 antibodies (50 ng /ml) on a half log serial dilution of 10 % (w/v) human brain homogenate. 6H4 antibody was used because it recognises an epitope within helix 1 of the prion protein, considered to be a prerequisite for infectivity (Heller *et al.*, 1996). The sequence DYEDRYYRE is present on both human PrP^{c} and PrP^{Sc} (144-152) and is highly conserved in mammalian PrP proteins.

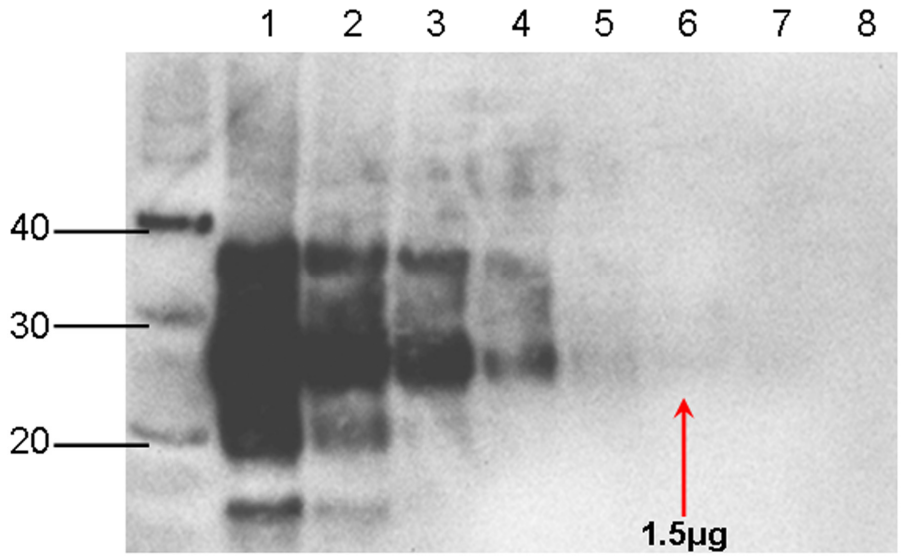

Figure 5.8. Western blot dilution end point assay of half log serial dilution of 10 % (w/v) frontal cortex sample from vCJD patient brain tissue, with proteinase K treatment. The supernatant of 10% centrifuged homogenate from frontal cortex of human autopsy brain material was incubated with 6H4 antibodies. Precipitate was analysed on a western blot for the presence of PrP using a HRP-conjugated sheep anti-mouse IgG. For each lane, corresponding amounts of brain material are: lane 1, 500 µg;

lane 2, 158 µg; lane 3, 50 µg; lane 4, 15 µg; lane 5, 5 µg; lane 6, 1.5 µg; lane 7, 0.5 µg, lane 8, 0.15 µg. Red arrow indicates the limit of detection. Numbers of the left correspond to molecular weight markers in kilodaltons (kDa).

From this assay, it was possible to detect PrP^{res} in > 0.5 µg vCJD brain equivalent.

5.4.2 Presence of Detectable PrP Protein After Protocol

Human brain RNA preparations were assessed for levels of PrP^{res} by western blot (Figure 5.9).

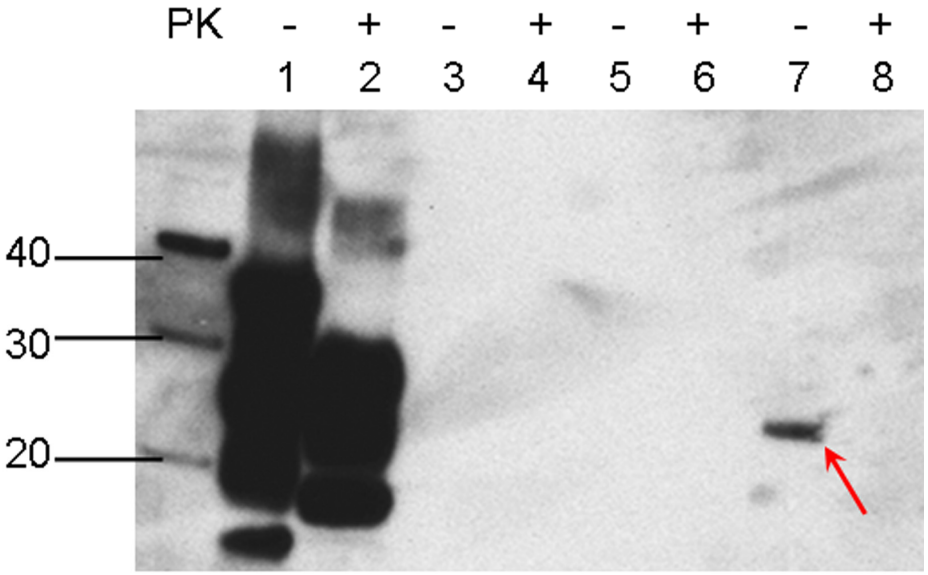

Figure 5.9. PrP western blot analysis of RNA preparations from human, with (+) or without (-) proteinase K treatment. Lane 1 and 2, type 2B vCJD (0.5 mg brain equivalent); lane 3 and 4, type 2B vCJD RNA extracts (10 mg brain equivalent); lane 5 and 6, NND RNA extracts (10 mg brain equivalent); lane 7 and 8, human recombinant PrP (0.1 µl). Immunoblot profiles in lanes 1 and 2 are characteristic of type 2B CJD. Red arrow indicates band of molecular weight of 23 kilodaltons, which is the expected molecular size of human recombinant PrP-PURE (Alicon). PrP-PURE is completely digested by proteinase K. Numbers on the left correspond to molecular weight markers in kilodaltons.

Lanes 3 and 4 were loaded with 20-fold more brain equivalent of the RNA extract than un-extracted brain loaded in lanes 1 and 2. Since the detection limit of western blot is ~ 1 µg brain equivalent, and 10 mg of brain homogenate equivalent from RNA extracts were loaded, the negative result would indicate the level of PrP^{res} is at least 10,000-fold less than in the starting brain homogenate. From this data, it is possible to conclude that the following RNA extraction protocol, when assessed by

western blot, the levels of PK resistant PrP^{Sc} have been reduced by at least 10^4 fold. Assuming that the infectious agent is indeed the proteinase-K resistant PrP isoform, the RNA extraction protocol was able to remove sufficient PrP^{Sc} from infectious brain material as to be immeasurable and was therefore considered a suitable method of sample preparation.

5.4.3 Presence of PrP Protein in Control Cases

To establish that NND control brain did not contain detectable amounts of PK-resistant PrP, brain homogenate and RNA extracts were tested for PrP^{res} by western blot (Figure 5.10).

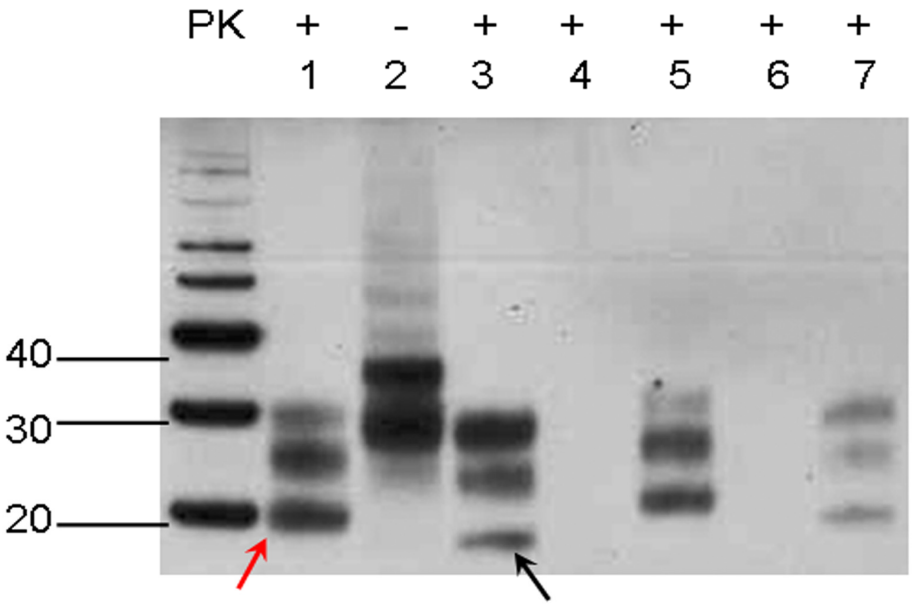

Figure 5.10. Western blot analysis of NND human frontal cortex samples from 10 % (w/v) human brain homogenate (lanes 1-3, 5, 7) or RNA extract (lanes 4 and 6), with (+) or without (-) PK treatment. Lane 1, type 1 CJD; lane 2, NND; lane 3, type 2B CJD; lane 4, NND (RNA extract); lane 5, type 1 CJD; lane 6, NND (RNA extract); lane 7, type 2B CJD. Red arrow indicates the lower band of molecular weight ~21 kDa, characteristic of type 1 CJD PrP immunoblot profiles. Black arrow indicated the lower band of molecular weight ~19 kDa, characteristic of type 2B CJD PrP immunoblot profiles. Numbers on the left correspond to molecular weight markers in kilodaltons**.**

In conclusion, NND brain homogenate contains significant amounts of PrP^{c}, but undetectable amounts (> 0.5 µg brain equivalent) of PK resistant PrP^{Sc}. Also, from the two NND cases tested, RNA extract preparations contain undetectable amounts of PK resistant PrP^{Sc}.

5.5 ISOLATION OF RNA FROM HUMAN BRAIN MATERIAL

Following the pilot comparison of RNA quantity and quality from human and mouse brain and the analysis of PrP in the human preparations from vCJD brains, it was decided to prepare RNA from a large number of human brains in order to compare the quality and yield and determine parameters that affect these values. It was necessary to carry out these preparations on different days and as positive controls, samples of mouse brain tissue were included in each batch of RNA prepared. RNA was prepared from 78 cases, selected from the NCJDSU and MRC brain banks based on criteria set out in Chapter 4. RNA preparations were measured for quality and quantity using a variety of techniques; RIN value, concentration and 28S:18S rRNA ratio as measured by the Agilent 2100 Bioanalyzer and full UV spectrum absorbance, specifically the $A_{260:280}$ and $A_{260:230}$ ratios and concentrations as measured by the Nanodrop ND-1000 spectrophotometer. The most reliable parameters for assessing RNA quality and quantity were determined by comparing all methods and evaluating suitability. 78 cases were included in this evaluation (unless otherwise stated). From the 78 cases, selected cases were used to determine the intra-patient variation between neurological distinct regions and adjacent samples and are detailed in section 5.6. Inter-patient variation due to a number of pre- and post-mortem parameters were also evaluated and are detailed in section 5.7. Analysis of all inter-patient variation was based on the Agilent and Nanodrop measurements taken from all 78 cases (unless otherwise stated). Clinical and histological notes used for IAS analysis in section 5.7.7 were included for cases, where available.

5.5.1 Variation in RNA Quantification Assay Method

Bland-Altman plots are generally used to describe the agreement between two quantitative measurements. Figure5.11 shows a Bland-Altman plot between two methods of measuring total RNA concentration; Agilent 2100 Bioanalyzer and Nanodrop ND-1000 spectrophotometer.

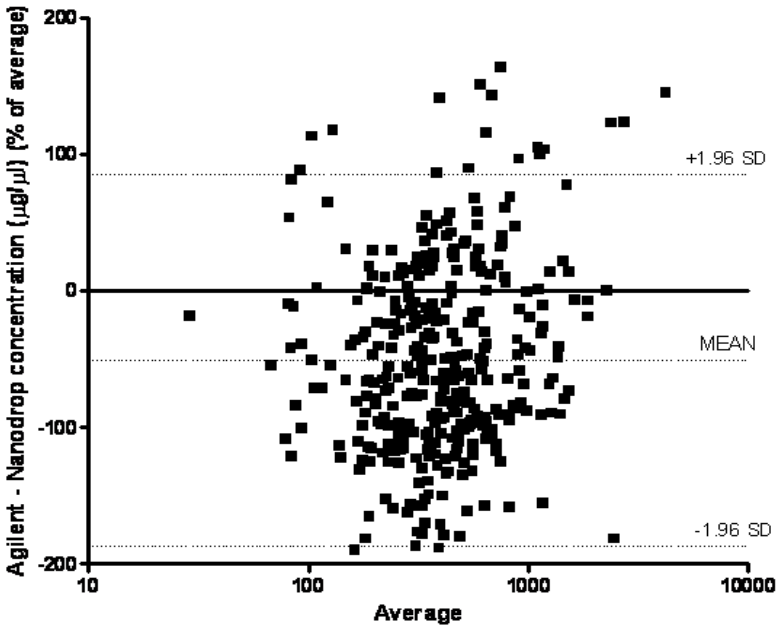

Figure 5.11. Bland-Altman plot to determine agreement between two quantitative measurements; instrument A (Agilent) and instrument B (Nanodrop), when measuring the quantity of total RNA (ng/µl). Bias = -50.67. SD of bias = 69.32. 95% confidence = -186.53, + 85.19**.**

The difference of the paired measurements is plotted against the mean of the two measurements. A good concordance in the measurements is present when 95% of the data points lie within ± 2SD of the mean difference. The data points should cluster around the 'difference = 0' line. Any large variations were checked, as anomalies could have been due to wrong data-entry. From the plot, it is observed that 18/361 (4.9%) of the points are beyond the ± 2SD lines which gives 95.1% corroboration between the two assays measurements, within 2SD agreement tolerance. As observed by the greater number of points below the 'difference = 0' line, instrument A (Agilent) is measuring lower than instrument B (Nanodrop) the majority of the time.

UV spectrophotometeric quantitation of RNA has generally been the standard method of RNA quantitation. The use of intercalating fluorescent dyes to detect RNA is more specific and sensitive, but much less reproducible due to additional mixing and incubation steps. UV spectrophotometeric analysis is much more reproducible, largely due to the simplicity of the method. Although Agilent quantitation accuracy is ± in the range of 35% of UV measured values, it was decided to base all further quantitation of RNA samples on Nanodrop measurements. In addition, UV spectrophotometric analysis allows for sample retrieval, whereas Agilent analysis requires minimal, but consumed samples.

5.5.2 Correlation Between Individual Abs or rRNA Ratios and RIN Values

Potential correlation between individual measurements made with the Nanodrop Spectrophotometer ($A_{260:280}$, $A_{260:230}$) and the Agilent Bioanalyzer (RIN, 28S:18S ratio) were examined (Figure 5.12). 431 samples were analysed on the Bioanalyzer and 316 samples were analysed on the spectrophotometer (72% human, 28% mice).

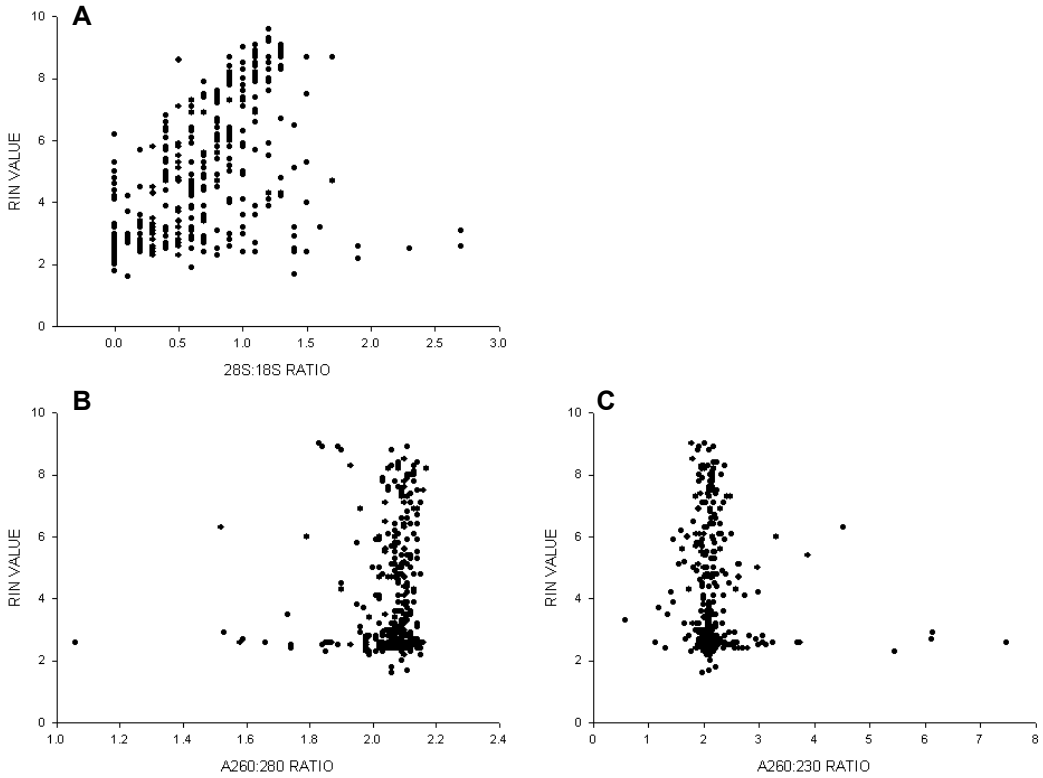

Figure 5.12. Correlation between individual absorbance A260:280 nm ratios, A260:230 nm ratios, 28S:18S rRNA ratios and RIN. Spearman rank correlation analysis; A: r2 = 0.69, p-value <0.0001. n = 431. B: r2 = 0.12, p-value = 0.022. n = 316. C: r2 = -0.11, p-value = 0.047. n = 316. (Significance level = 0.05).

Spearman rank correlation analysis shows a highly significant, positive correlation between 28S:18S ratios and RIN values, as would be expected. Both $A_{260:280}$ and $A_{260:230}$ show no correlation with RIN values. Clustering of data around the ~2.0 point in figures B and C is expected if the majority of samples constitute uncontaminated, high purity RNA. In addition, low $A_{260:280}$ correlated with low $A_{260:230}$ (data not shown).

5.5.3 RNA Preparation Characteristics

Figure 5.13 graphically represents the distribution of 368 human and 102 mouse brain RNA preparations.

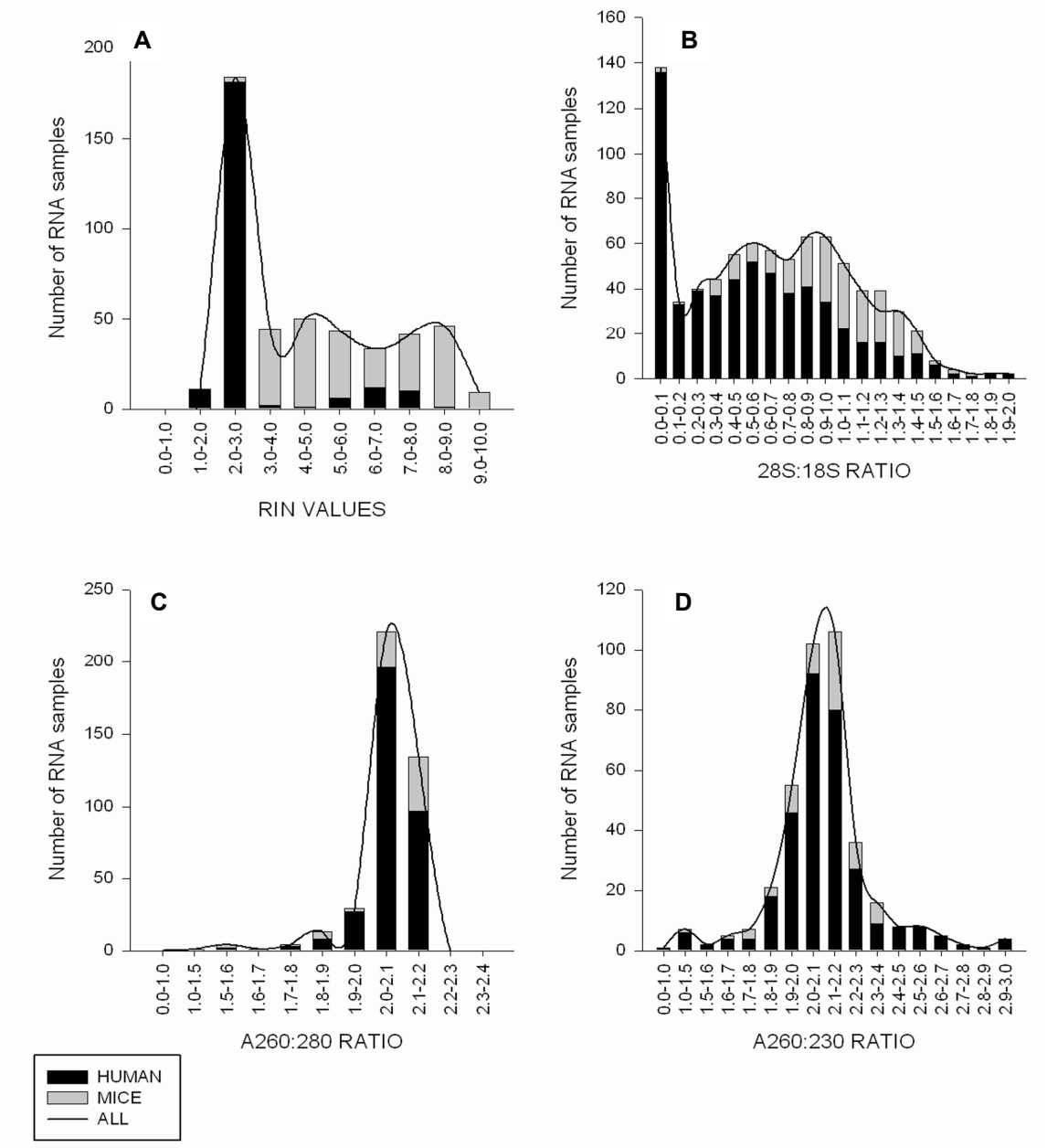

Figure 5.13. Characterisation of RNA preparations and their distributions. A. 441 RIN values were returned by the Agilent Bioanalyzer. B. 28S:18S rRNA ratios were automatically assigned by the Agilent software for 458 samples. C and D. $A_{260:280}$ and $A_{260:230}$ ratios for 365 samples were calculated automatically by the Nanodrop Spectrophotometer software, from a full UV spectrum profile reading. The distribution of all samples was plotted. Black human. Grey mouse. The lines are the mean distribution of both.

Overall, RIN analysis was successful on 441 samples. Data from 19 samples was not obtained due to software default anomaly parameters. In each case, the reading was flagged as error corresponding to critical anomalies including unexpected data in sample type, (or) ribosomal ratio, (or) baseline and signal in 5S region. The average RIN value was 4.46 (Confidence Intervals (IC) 4.25-4.67). 28S:18S readings were automatically calculated for 458 samples, with a mean value of 0.56 (IC 0.51-0.60). Although due to software programming, 28S:18S ratio readings were not considered to be accurate. Software recognition of the 28S and 18S rRNA peaks was inflexible and limited. Agilent software recognises peaks with the 35-40 second time frame as 18S rRNA and peaks within the 45-50 second time frame as 28S rRNA. If peaks are out-with these time frames, the software will assign the sample a 28S:18S value of 0.0. Atypical migration of peaks generally occurs with degraded samples, which results in 28S:18S values of 0.0. This low 28S:18S ratio assessment done by the Agilent has been recorded in other published literature, where < 44% of samples were within expected range (Imbeaud *et al.*, 2005). In addition, 28S:18S reading can be highly variable (see Figure 5.13) and it is suggested that 28S:18S ratio of 2.0 is an unsuitable and outdated calibrator of RNA (see discussion).

Nanodrop readings were carried out on 365 samples in total, with 100% success rate. The expected range for $A_{260:280}$ ratios is 1.8-2.1 and an average $A_{260:280}$ ratio of 2.06 was observed (IC 2.05-2.09) with 94% of the values falling within the expected range. The expected range for $A_{260:230}$ ratios is 1.7-2.2 and an average $A_{260:230}$ ratio of 2.16 was observed (IC 2.09-2.24) with ~80% of the values falling within the expected range. This result is similar to published data on RNA quality characterization (Imbeaud *et al.*, 2005).

Table 5.2 shows the percentage of RNA preparations that would fit the various definitions of good quality RNA suitable for subsequent analysis.

	RIN ≥5.0*	**28S:18S RATIO ≥2.0***	**$A_{260:280}$ RATIO ≥2.0**	**$A_{260:230}$ RATIO ≥1.7**
% HUMAN SAMPLES	20	0.9	97	95
% MOUSE SAMPLES	93	0	92	97

Table 5.2. Percentage of samples which fulfil either the Agilent assessment of RNA quality or the UV spectrophotometer assessment of RNA quality. Human samples; Agilent criteria* n=342, Nanodrop criteria n= 297. Mice samples; Agilent criteria* n= 97, Nanodrop criteria n= 66.

Depending on which method is used, different numbers of cases would be considered suitable for genetic analysis. Generally $A_{260:280}$ ratios > 1.8 and $A_{260:230}$ ratios > 1.7 should provide sufficient evidence of high purity RNA samples uncontaminated with organic solvents or proteinaceous material. Pure RNA should have equivalent $A_{260:280}$ and $A_{260:230}$ ratios which are ≥ 1.8 (Manchester, 1996; Manchester, 1995; Glasel, 1995).

The majority of samples have ≥ 1.7 $A_{260:230}$ ratios suggesting that very few samples were contaminated by GTC or phenol-chloroform. From this data, there is sufficient evidence to indicate that 28S:18S ratio determination of RNA quality is unsuitable for total RNA isolated from brain tissue. The use of 28S:18S rRNA ratio would have incorrectly excluded most samples.

Mouse tissues were processed in parallel with human tissues. The quality of the RNA preparations from each was compared (Table 5.3).

	RIN	**28S:18S rRNA ratio**	**$A_{260:280}$ ratio**	**Yield (µg)**
MOUSE	7.57 ± 1.47	0.93 ± 0.32	2.05 ± 0.18	129 ± 105
HUMAN	3.59 ± 1.45	0.46 ±0.48	2.06 ±0.08	52 ± 29.8
P-value	*<0.0001*	*<0.0001*	*0.325*	*<0.0001*

Table 5.3. Comparison of human and mouse brain RNA preparations. Values are mean ± SD.

With the exception of the $A_{260:280}$ ratio, there is a highly significant difference between the two groups. There is more degradation in the human than the mouse RNA preparations as determined by RIN and the median 28S:18S rRNA ratio which is higher for the mouse brain RNA preparations. Interestingly, even for mouse brains, where tissue has been handled in near optimal conditions, the 28S:18S ratio is rarely near 2.0, confirming the suggestion that 28S:18S ratios are unsuitable for assessing RNA isolated from brain tissue. RNA yields achievable from mouse brain material are approximately 30-48 % greater that RNA yields achievable from human brain material. Similar differences in the range of yields for mice and human tissues are observed in the literature (Johnson *et al.*, 1986). Mouse and human samples were extracted in parallel, but only human cases had low values, therefore either the RNA extraction process only adversely affects human brain RNA samples or there are other issues that affect RNA quality and yield.

5.5.4 Cases Suitable For Downstream Processing

For this project, human RNA samples with a RIN ≥ 4.5 were considered suitable for microarray and qRT-PCR (Table 5.4). Previous studies have recommended a RIN ≥ 5.0 as being good total RNA quality and ≥ 8.0 as perfect RNA for downstream applications (Fleige *et al.*, 2006; Fleige & Pfaffl, 2006). If these criteria were used within the scope of this project, the sample size would be too small to provide any reasonable statistical strength.

	NND	**OND**	**vCJD**	***MICE***
Cases tested [samples]	31 [83]	26 [160]	21 [110]	*[101]*
RIN ≤ 4.4	18 [48]	20 [104]	16 [98]	*[6]*
RIN ≥ 4.5 and $A_{260:280}$ ≥ 1.8	13 [31]	6 [53]	5 [9]	*[90]*
YIELD RNA (µg)	38.23 ± 2.44 (5.9-101.5)	48.29 ± 2.32 (2.9-159.4)	62.64 ± 3.37 (4.4-183.5)	*128.6 ± 10.59 (3.7-614.3)*
Suitable for downstream processing (e.g. microarray or qRT-PCR)	50%	23%	24%	*91%*

Table 5.4. Summary of cases from which RNA was extracted. Yield values are mean ± SEM, with range in parentheses.

NND cases have a greater number of samples (42%) which fulfil the RIN and UV absorbance criteria than diseased cases (OND or vCJD) (23%). Samples were selected for transcriptional analysis if the following criteria were fulfilled;

- RIN value ≥ 5.0
- $A_{260:280}$ nm absorbance ≥ 1.8
- $A_{260:230}$ nm absorbance ≥ 1.7

Samples with 4.5 < RIN ≤4.9 were reserved for contingency.

5.6 INTRA-PATIENT VARIATION

To investigate intra-patient variation of RNA a whole half human brain was sampled from three anatomically distant regions and RNA extracted and tested for quality and quantity (Table 5.5).

REGION	RIN	TOTAL RNA YIELD (µg)	28S:18S RATIO	$A_{260:280}$ RATIO
CB (n=2)	6.40 (0.283)	4.32 (1.98)	1.000 (0.141)	-
FPS (n=6)	4.03 (1.145)	76.86 (38.26)	0.567 (0.308)	2.082 (0.012)
SFC (n=11)	5.09 (1.503)	58.53 (50.01)	0.72 (0.316)	2.080 (0.020)[a]
P-VALUE	*0.049*	*0.056*	*0.126*	*1.000*

Table 5.5. Intra-patient variation. Results of Kruskal- Wallis analysis for RNA variable and brain region within a single organ. Means are shown with SD in brackets.

The results indicate that there is no evidence for a difference between the means of each region, regardless of RNA parameter. The p-values for RIN and yield are approaching significance, but given the power of the small sample size, the results are difficult to draw conclusions from. However, it is suggested here that there is no difference in the quality or yield of the RNA derived from different areas of the same brain.

For each NCJDSU case sampled, a minimum of three contiguous tissue samples were taken at a single sampling. For MRC cases, a minimum of two contiguous tissue samples were supplied. All RNA preparations were measured on the Agilent to obtain a RIN value and on the Nanodrop for quantitation. To determine the inter- and intra-patient variation in RNA quality (based on RIN values only) and quantity (based on Nanodrop values), samples were categorised by status (vCJD, NND and

OND) and replicate (1, 2 or 3 contiguous tissues samples) and data analysed by one-way ANOVA (Table 5.6). 67 brains (284 samples) were included in this analysis (21 from MRC, 46 from NCJDSU).

	ALL		**VCJD**		**NND**		**OND**	
	RIN	***YIELD (µg)***	RIN	YIELD (µg)	RIN	YIELD (µg)	RIN	YIELD (µg)
INTER- **BRAIN EFFECT**	***1.2***	***15.3***	1.0	18.1	1.2	13.3	1.4	10.8
INTRA- **BRAIN EFFECT**	***0.7***	***19.5***	0.4	24.8	0.7	15.2	0.7	19.3

Table 5.6. Variation of RIN value and total RNA yield (µg) due to inter-brain effect or intra-brain effect. Values are the estimated standard deviation in the RIN values or the total RNA yield (µg). All n = 184. vCJD n = 56. NND n = 83. OND n = 45.

Approximately 65% of the variability of RIN values is due to inter-patient differences. The vCJD cases show the least amount of RNA quality variation intra-patient, while the OND cases showed the greatest variation. This may be due to the agonal state of the patient and the pathogenesis occurring within the brain. All vCJD patients generally have a very similar agonal state (see Chapter 4, Table 4.5), respiratory infection being the most common cause of death. The cause of death of OND patients is not as uniform, with vastly differing mode of deaths. Although NND cases also have very different modes of death, the duration of death is rapid (see Chapter 4, Table 4.5) and there may be insufficient time for any affects to manifest in the brain. The pathogenic mechanisms occurring within the brains of vCJD patients are less variable than it is within the OND group. For example, the pathological mechanisms involved in Lewy Body dementia and B-cell lymphoma are extremely different. In contrast, >50% of the yield variation is due to the intra-brain effect. The reasons for this difference are unclear as all samples were prepared in the same way.

To determine the amount of variation in RNA quality and yield within a single brain (intra-brain), nine contiguous samples were taken from single frozen OND and vCJD brains and RNA extracted. RNA preparations were measured for quality and quantity. Sample variation was calculated and tabulated (Table 5.7).

A

OND	**1**	**2**	**3**	**4**	**5**	**6**	**7**	**8**	**9**	***Mean ± SD***
RIN values	2.60	2.60	2.70	2.80	2.80	2.90	2.50	2.70	2.60	*2.69 ± 0.13*
28S:18S rRNA ratio	0.3	0.0	0.0	0.2	0.0	0.0	0.0	0.0	0.0	*0.06 ± 0.11*
$A_{260:280}$ ratio	2.12	2.10	2.06	2.07	2.07	2.08	2.09	2.08	2.07	*2.08 ± 0.02*
YIELD (µg)	26.43	38.79	35.99	28.37	36.26	27.96	27.48	43.15	21.36	*31.75 ± 7.05*

B

vCJD	**1**	**2**	**3**	**4**	**5**	**6**	**7**	**8**	**9**	***Mean ± SD***
RIN values	2.6	2.6	2.6	2.3	2.8	2.4	3.2	2.3	2.4	*2.58 ± 0.29*
28S:18S rRNA ratio	0.0	0.0	0.0	0.3	0.1	0.2	0.0	0.0	0.0	*0.07 ± 0.11*
$A_{260:280}$ ratio	2.07	1.67	1.87	2.09	2.11	2.08	2.02	1.98	2.08	*2.00 ± 0.14*
YIELD (µg)	45.12	10.72	28.51	95.91	94.93	104.48	45.39	54.97	49.47	*58.5 ± 32.5*

Table 5.7. Quality metrics from 9 RNA preparations, sampled contiguously from single brains. Each preparation was measured using the Bioanalyzer and the Nanodrop. A. Samples from other neurological diseased brain. B. Samples from a vCJD diseased brain.

Standard deviation of RIN and $A_{260:280}$ ratios show very little variation (< 10%) across each of the two sets of 9 contiguous samples. 28S:18S ratios and total RNA yields (μg) were more variable, although this was expected. Limited intra-patient variation in two main RNA metrics is promising, as this indicates that RNA quality is fairly consistent within a single case. Regional variation of RNA quality can therefore be excluded as a source of variation in subsequent analysis.

If the variation intra-patient is compared to the variation observed inter-patient (see Table 5.6), it shows there is less variation of RNA metrics within a single organ than across many. RIN values for contiguous samples have an average standard deviation of 0.21, whereas the standard deviation for non contiguous samples is much greater (1.45). Total RNA yields vary most, both intra- and inter-patient. Even so, the average standard deviation intra-patient is much less than that observed inter-patient (29.8 and 19.8 respectively). This result would suggest that variation of RNA quality and quantity occurs mainly across patients rather than within a single case.

5.7 INTER-PATIENT VARIATION

One aim of this project is to identify whether any pre- or post-mortem factors are predictive of RNA quality and yield. Initially, factors which were controllable, such as tissue storage method and storage temperature were evaluated. Freezer Interval (FI) was also assessed. Pre- and post-mortem factors out-with the control of the investigator, for example, PMI and age at death, were also assessed.

5.7.1 Effects of Tissue Storage Methods on RNA

Tissues collected at autopsy are stored snap frozen, frozen or fixed. For the RNA profile study, all tissues used were either snap frozen or frozen. In addition to this, it was possible to arrange for additional samples to be collected at autopsy, which were stored in RNAlater then frozen. Quality and quantity of total RNA extracted from 100 mg brain tissue were measured using the Agilent 2100 Bioanalyzer and the

Nanodrop ND-1000 spectrophotometer. Two sample t-test analysis was carried out to determine if storage method affected RNA quality or quantity. RNA that had been isolated from autopsy material has been shown to be of sufficient integrity for RT-PCR analysis. RNA from post-mortem tissue is known to be relatively stable and suitable for RNA research, as long as pre- and post-mortem factors are accounted for (Barton *et al.*, 1993; Brown, 2005; Schramm *et al.*, 1999; Perrett *et al.*, 1988). If RNA quality is poor, measurements of cDNA after reverse transcription cannot be considered accurate (Huggett *et al.*, 2005).

To investigate variability in a relatively homogenous population of RNA preparations, the inter-case variability of all the mouse brain RNA preparations, which were routinely done with the human brain RNA preparations, was determined. A total of 65 samples stored using two different methods (-80ºC freezer and RNAlater) were tested. Mouse RNA preparations were not subjected to much pre- or post-mortem variation. All mice were sacrificed at 10 weeks of age, PMI was approximately 15 mins, brain tissue was not subjected to freeze-thaw cycles and none of the mice were infected with pathogens or had any clinically apparent disease. Figure 5.14 shows the variability of the three RNA metrics in relation to the tissue storage method used.

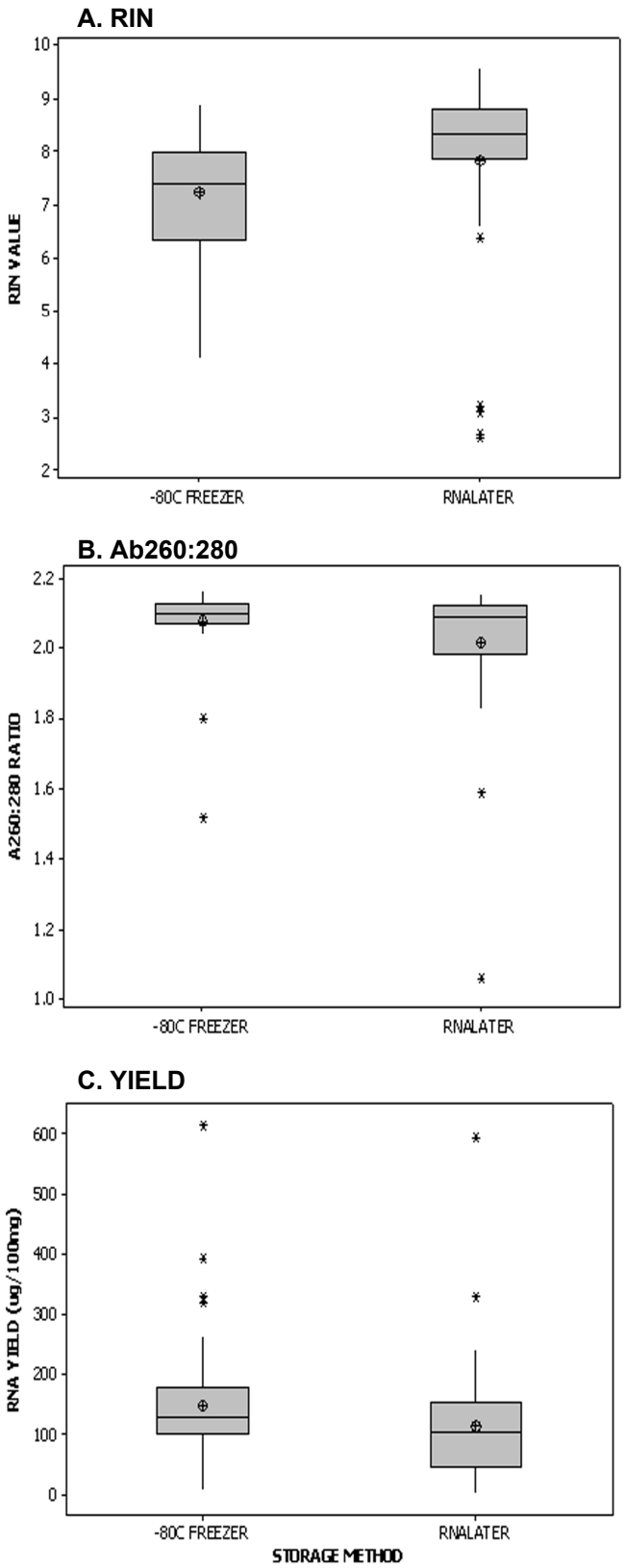

Figure 5.14. Box and whisker plot comparison of storage method of mouse brain tissue and quality and quantity metrics of RNA extracted from brain tissue. The boxes represent the 25th – 75th quartiles, divided horizontally by the median. The whiskers represent the range. The circles represent the mean. Outliers are denoted by (*). Panel A. RIN values. RNAlater; n = 54, mean =7.83, SD =1.73, SEM =0.24. Snap frozen; n =42, mean =7.23, SD =1.04, SEM =0.16, p value =0.051. Panel B. A260:280 absorbance ratios. RNAlater; n = 33, mean =2.02, SD =0.21, SEM =0.037. Snap frozen; n =32, mean =2.08, SD =0.12, SEM =0.02, p value =0.138 (significance level =0.05). Panel C. Total RNA yield from 100 mg starting brain material. RNAlater; n = 55, mean =113, SD =95.4, SEM =13. Snap frozen; n =43, mean =148 SD =114, SEM =17, p value =0.098.

Based on two-sample t-test analysis, mouse brain tissue which has been stored in RNAlater or frozen at -80°C showed no significant difference in the median RIN value, $A_{260:280}$ ratio or the total RNA yield (µg). During mouse tissue harvesting, other factors which may have had an affect on RIN, UV absorption and yield are controlled for, i.e. age, agonal state (and therefore pH) and sex. It is reasonable to assume from these results that, if confounding factors are removed, tissue storage method has no affect on RNA quality and quantity.

For human brain, RNA preparations derived from (i) liquid nitrogen (N_2) stored (referred to as snap frozen), (ii) whole half brains frozen at -80ºC or (iii) from RNAlater stored dissected autopsy brain samples were compared for the quality and yield of the RNA (Figure 5.15).

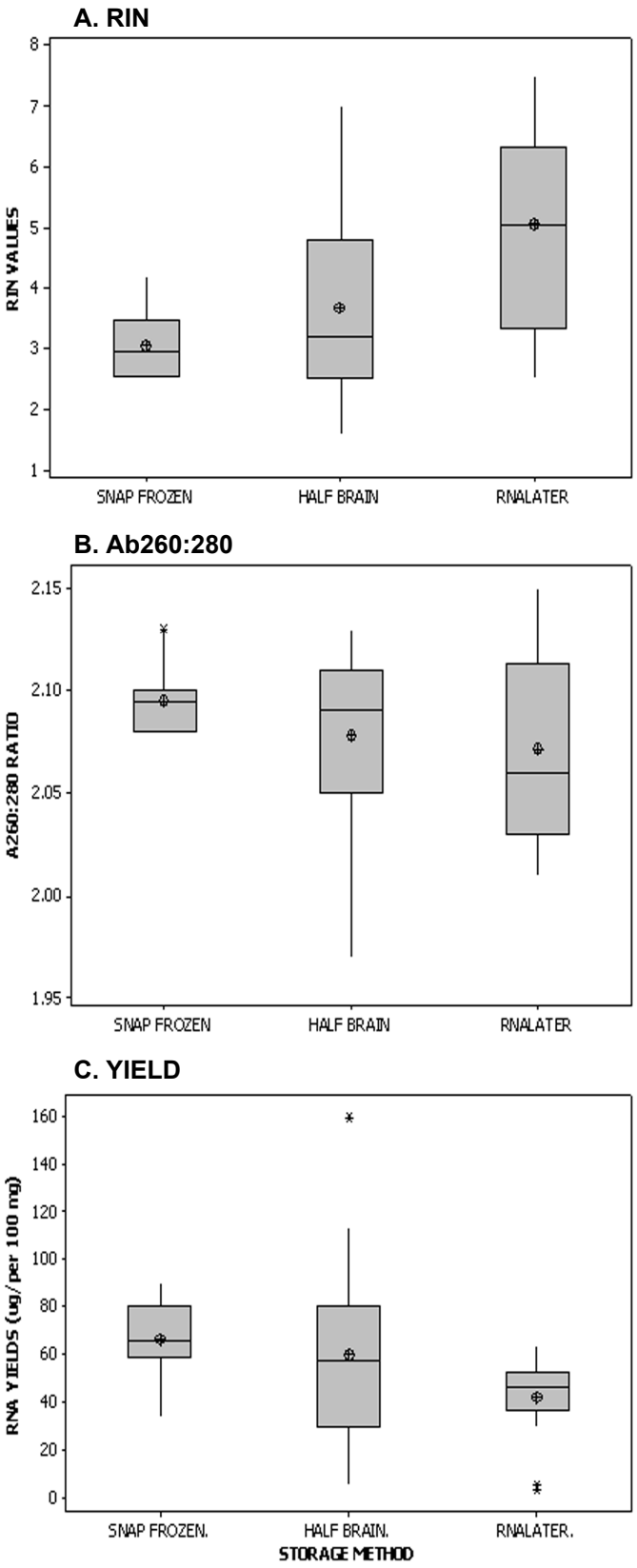

Figure 5.15. Box and whisker plot comparison of storage method of human brain tissue and quality and quantity metrics of RNA extracted from brain tissue. The boxes represent the 25th – 75th quartiles, divided horizontally by the median. The whiskers represent the range. The circles represent the mean. Outliers are denoted by (*). Panel A. RIN values. RNAlater; n = 16 , mean = 5.06, SD = 1.61. Snap frozen; n = 8, mean = 3.05, SD = 0.59. Half brain; n = 37, mean = 3.69, SD = 1.34. p value = 0.001. Panel B. A260:280 absorbance ratios. RNAlater; n = 14 , mean = 2.10, SD = 0.05. Snap frozen; n = 8, mean = 2.10, SD = 0.02. Half brain; n = 37, mean = 2.10, SD = 0.04. p value = 0.341. Panel C. Total RNA yield isolated form 100 mg starting brain material. RNAlater; n = 16 , mean = 42.06, SD = 17.35. Snap frozen; n = 8, mean = 65.97, SD = 17.07. Half brain; n = 41, mean = 59.54, SD = 32.89. p value = 0.072.

One-way ANOVA analysis reveals a significant difference between the RIN values of (i) RNA isolated from dissected samples stored in RNAlater and (ii) liquid nitrogen snap frozen or -80°C half brain stored tissues. 95% CI show similarities between the RIN values of tissues stored in liquid N_2 or as whole half brains. It is preferable to store tissue in RNAlater. There are no significant differences between $A_{260:280}$ readings or total RNA yield (µg) relative to storage method. UV absorbance readings were expected to be unaffected by storage method as $A_{260:280}$ readings are generally an indication of purity not integrity.

5.7.2 Freezer Interval Correlations With RNA Integrity

To determine the effect of F.I. on RNA quality, a large sample of mouse and human brain tissue was taken from a number of different cases. A small sample (~100mg) was used to prepare RNA (t = 0) and the remaining tissue stored at -80ºC. At defined time points, the tissue was again sampled and RNA prepared and measured on the Agilent Bioanalyser and Nanodrop. Figure 5.16 graphically represents the F.I. against the RNA metrics.

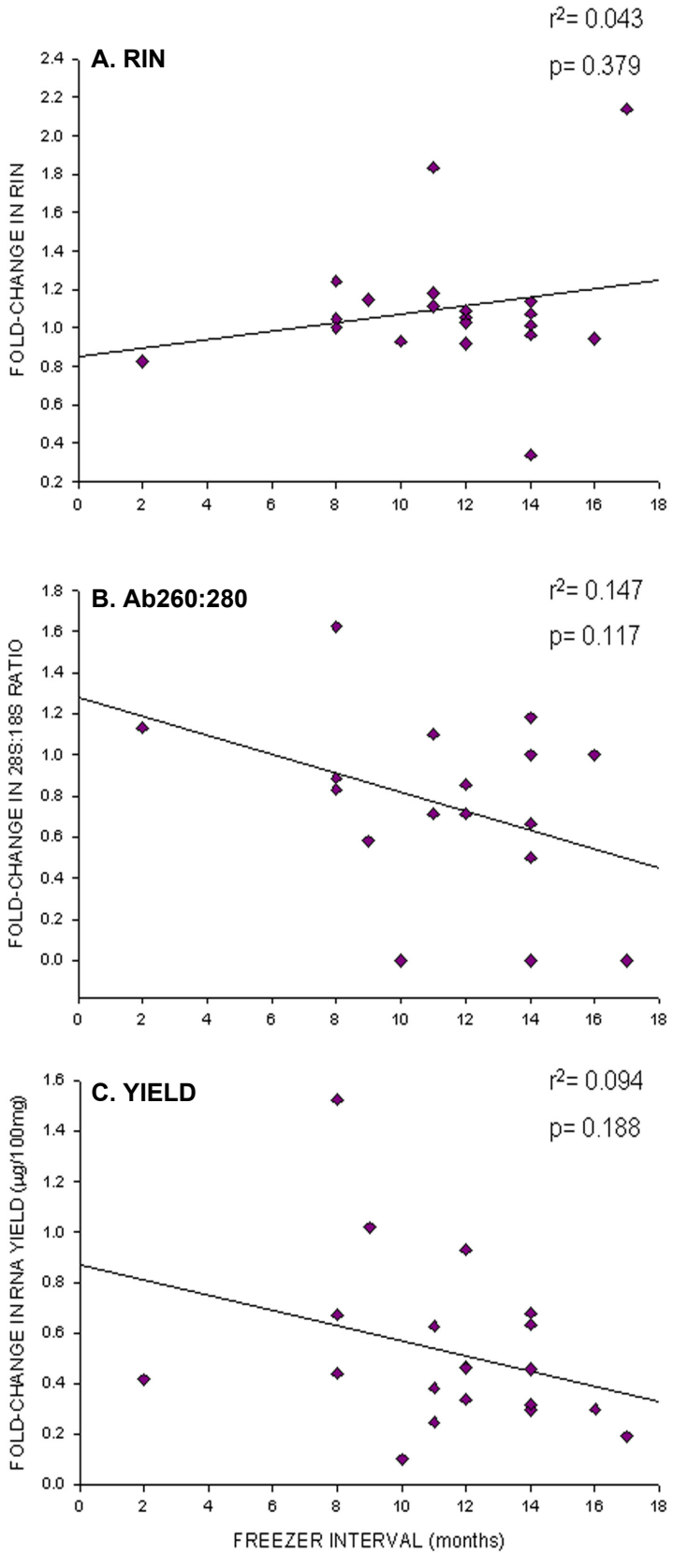

Figure 5.16. Freezer interval (F.I.) and RNA metrics. RNA was extracted from brain tissue and the remaining tissue was frozen at -80ºC (t = 0). At defined time points, tissues were removed from storage and RNA was extracted from a sample and measured. A. Change in RIN value with time. B. Change in 28S:18S ratio with time. C. Change of RNA yield (µg/100mg) with time. Regression coefficient (r2) and p-values are displayed in the figure. n= 20.

Despite trends in the data, multiple regression analysis indicates the variation observed in the RIN value, $A_{260:280}$ and RNA yield cannot be accounted for by the F.I. Although the time range tested is not extensive (17 months), these results are in accordance with the literature, including a 15 year study on AD brain tissue stored at -70ºC (Yasojima *et al.*, 2001; Leonard *et al.*, 1993; Johnson *et al.*, 1986; Schramm *et al.*, 1999). Two-sample t-test analysis between sample metrics before freezing and after a defined period of storage also shows no significant difference ($p > 0.05$). The data shows a lot of variation between different RNA preparations, irrespective of the F.I. This data is in agreement with the data shown in Table 5.3 and Figure 5.13. This result indicates that F.I. has little effect on the quality and yield of RNA preparations.

5.7.3 Storage at -20°C or -80°C Freezer

To investigate whether storage temperature of the RNA preparation has an effect on RNA preparations, aliquots of 7 human RNA preparations were stored at either. -20°C for 12 months or at -80°C for 12 months. After this time, quality and quantity were measured. The results are shown in Table 5.8.

	RIN (-20°C)	**RIN (-80°C)**	**YIELD (µg) (-20°C)[1]**	**YIELD (µg) (-20°C)[2]**	**YIELD (µg) (-80°C)[1]**	**YIELD (µg) (-80°C)[2]**
Mean (range)	5.73 ±0.9 (2.2-9.1)	5.87 ±0.7 (2.2-8.7)	82.3 ± 30 (24.6-252.2)	77.8 ± 30 (19.9-194.5)	60.3 ± 19 (24.3-162.0)	51.5 ± 10 (31.6-90.8)
p-value	*0.907*[a]		*0.545*[b]		*0.438*[c]	

Table 5.8. RIN values and concentration (ng/µl) measurements of tissues stored at -20°C and -80°C.
[1] = Agilent 2100 Bioanalyzer readings. [2] = Nanodrop ND-1000 spectophotometer readings. [a] = RIN value of RNA preparations stored at -20ºC compared to -80ºC. [b]= yield (as measured by Agilent Bioanalyzer) of RNA stored at -20ºC compared to -80ºC. [c]= yield (as measured by Nanodrop) of RNA stored at -20ºC compared to -80ºC. Values are mean ± SEM, with range in parentheses. n=7.

Two-sample t-test analysis reveals no significant difference ($p > 0.05$) between the RIN or yield of RNA (as measured by Agilent Bioanalyzer or Nanodrop spectrophotometer) stored at -20°C or -80°C freezer, for a period of 12 months. Nonetheless all RNA preparations were stored at -80°C, especially if storage time is to be lengthy.

Based on the results from sections 5.7.1-3, it is concluded that tissue storage method or storage time has only a limited affect on RNA quality and quantity. Therefore, all further analysis has assumed that the variation observed within human cases is most likely due to pre- and/or post-mortem factors.

Analysis of two pre-mortem (age and agonal state) and three post-mortem factors (post-mortem interval (PMI), pH of brain, freeze-thaw cycle (FTC)) for human cases with available data were carried out to elucidate any effects these parameters have on the quality or quantity of RNA extracted from human post-mortem brain material. Gender is included as a factor in order to see if mRNA levels are consistent across the sexes.

5.7.4 Affect of Age at Death, Tissue pH, PMI and FT Cycles on RIN

Clinical and autopsy data from all 78 cases were examined and RIN values measured using the Agilent 2100 Bioanalyzer. For cases with all relevant data, correlation analysis was carried out. Figure 5.17 shows four graphs corresponding to the analysis of the four parameters studied; age of patient at time of death (yrs), brain tissue pH at post-mortem, PMI (hrs) and freeze-thaw cycles (FTC), in relation to RIN values.

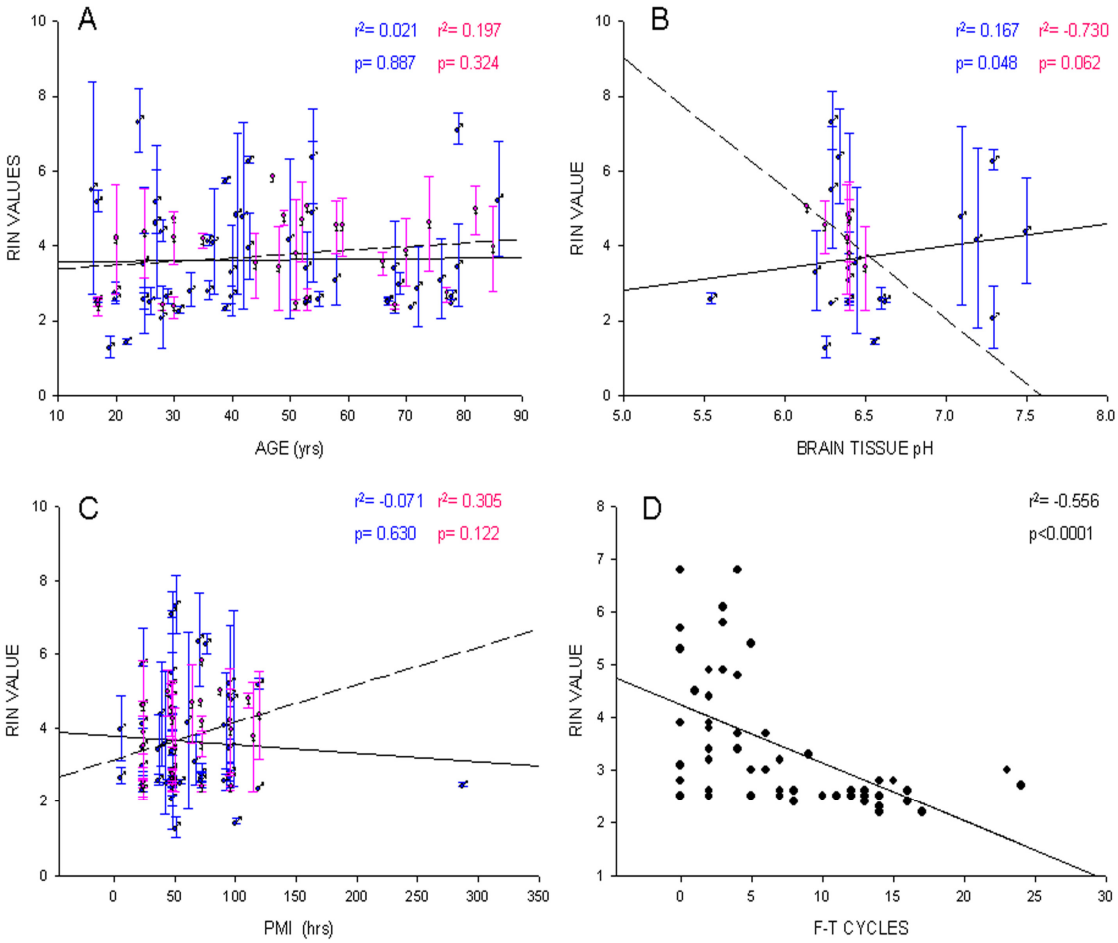

Figure 5.17. Correlation between RIN values and pre- and post-mortem parameters of human cases. A. Age of patient at time of death (yrs). n♂= 50. n♀= 27. B. pH of brain tissue at post-mortem. n♂= 20. n♀= 7. C. Post-mortem interval (hrs). n♂= 49. n♀= 27. D. Freeze-thaw cycles prior to RNA extraction. n= 54. Blue ♂ symbols are male cases. Pink ♀ symbols are female cases. Solid regression line is regression of male data set. Dashed regression line is regression of female data set. Vertical lines are error bars (± 1SD). P-values and correlation coefficients from two-tailed Pearson linear correlation analysis are given.

RNA integrity as assessed by RIN showed no significant correlation with; age of patient at time of death or PMI for either male and female cases (Figure 5.17A, C).

Brain pH at time of autopsy indicated a significant ($p<0.05$) 16.7% positive correlation with RIN in the male data set, and a 73% negative but non-significant correlation within the female data set. It should be noted that the female dataset was small. There were relatively few samples with freeze-thaw data so these were not analysed separately as male and female. There was a highly significant ($p<0.0001$) 56% negative correlation between the number of times the brain tissue had been thawed and the quality (RIN) of the extracted RNA. Freeze-thaw cycles were measured in a discrete manner; only tissue that had been removed from -80°C storage for ~60 minutes were considered to have been subjected to 1 cycle. Minor thaw events (i.e. transferring tissue between freezers) were not taken into account, as this result is based on whole half brains and large organs take time to change temperature. A similar study on AD human brains observed minimal degeneration of specific mRNA's with PMI up to 96hrs or when thawed for 1-2 hours (Yasojima *et al.*, 2001).

On consideration of data in panel A, it is apparent that certain cases, regardless of age, are either variable or not variable. These data points have either very large or very small error bars and occur throughout the dataset. Similar data points can be seen in panels B and C and suggests that the amount of variation of RNA quality (RIN) is intrinsic to the particular sample and does not correlate with age at death, PMI or tissue pH.

5.7.5 Affect of Age at Death, Tissue pH, PMI and FT Cycles on Yield

Figure 5.18 shows the relationship between yield and; age of patient at time of death (yrs), brain tissue pH at post-mortem, PMI (hrs) and freeze-thaw cycles (FTC).

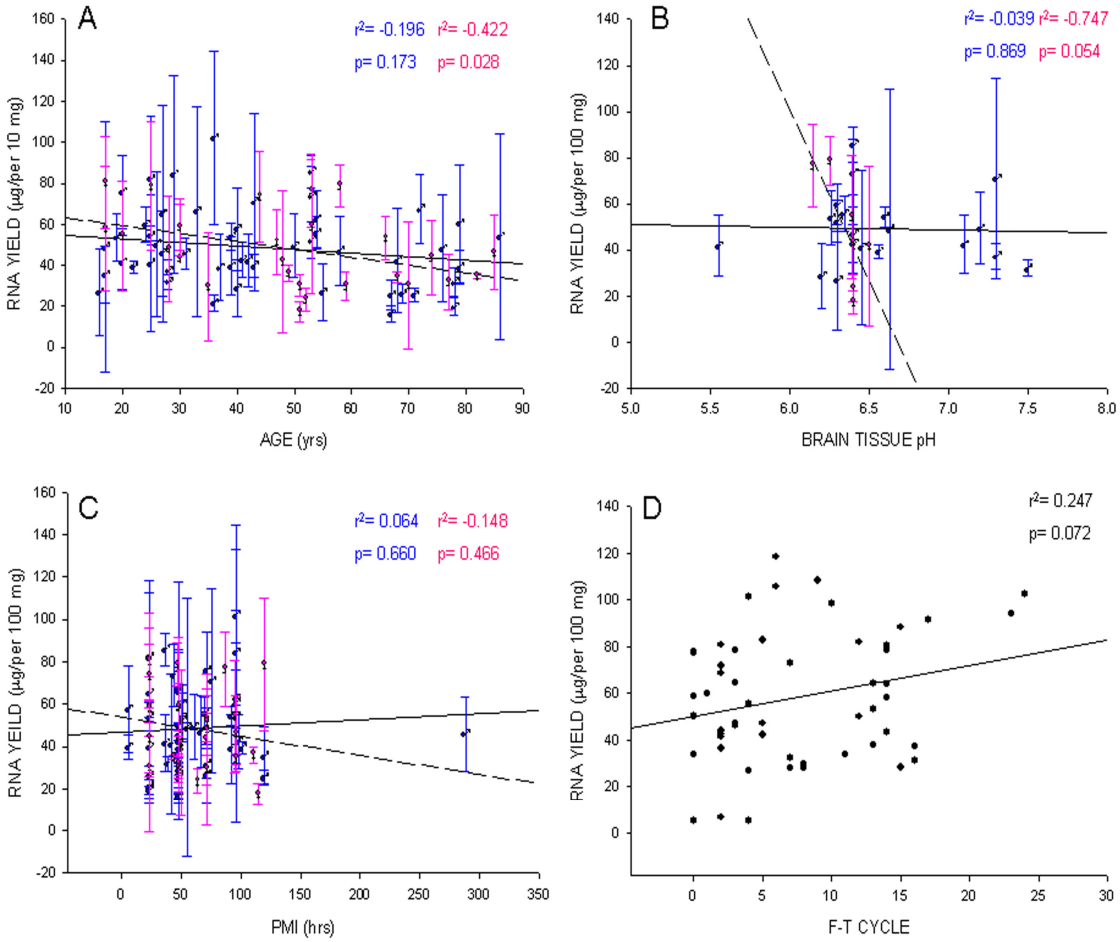

Figure 5.18. Correlation between total RNA yields (µg) extracted from 100 mg starting brain material and pre- and post-mortem parameters of human cases. A. Age of patient at time of death (yrs). n♂= 50. n♀= 27. B. pH of brain tissue at post-mortem. n♂= 20. n♀= 7. C. Post-mortem interval (hrs). n♂= 49. n♀= 27. D. Freeze-thaw cycles at time of RNA extraction. n= 54. Blue ♂ symbols are male cases. Pink ♀ symbols are female cases. Solid regression line is regression of male data set. Dashed regression line is regression of female data set. Vertical lines are error bars (± 1SD). P-values and correlation coefficients from two-tailed Pearson linear correlation analysis are given.

Age, brain pH at post-mortem and PMI had limited correlation with yield within the male data sets (Figure 5.18B, C). Within the female data sets, PMI showed no significant correlation but there was a significant (p = 0.054) negative correlation

with pH (although the p-value was close to the tolerance limit of this experiment). There was a significant 42% negative correlation within the female data set between yield and age. Although figures 5.17D and 5.19D shows a significant negative correlation between the number of freeze-thaw cycle and the quality of the RNA, no such effect was present with yield. No significant correlation between the yield and number of FT cycles may suggest that although the mechanisms of ice crystal formation and re-formation may significantly damage the RNA molecules, the overall amount of RNA within the tissue is unaffected. This suggests that RNA molecules are subjected to mechanical damage due to ice crystal formation and reformation as opposed to degradation by endogenous RNase activity.

5.7.6 Affect of Age at Death, Tissue pH, PMI and FT Cycles on $A_{260:280}$

Figure 5.19 shows the relationship between $A_{260:280}$ ratios and age, pH, PMI and FTC.

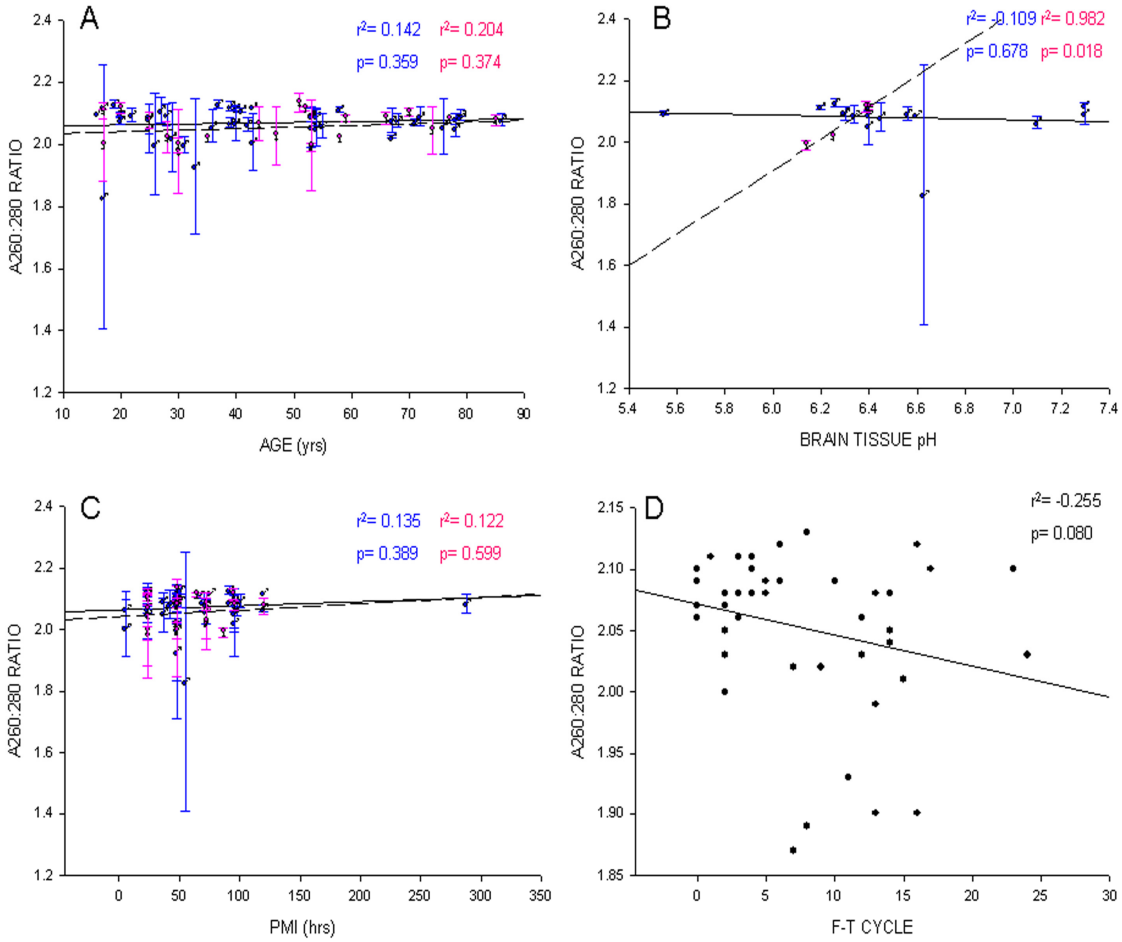

Figure 5.19. Correlation between A260:280 ratios and pre- and post-mortem parameters of human cases. A. Age of patient at time of death (yrs). n♂= 44. n♀= 22. B. pH of brain tissue at post-mortem. n♂= 17. n♀= 4. C. Post-mortem interval (hrs). n♂= 43. n♀= 21. D. Freeze-thaw cycles at time of RNA extraction. n= 48. Blue ♂ symbols are male cases. Pink ♀ symbols are female cases. Solid regression line is regression of male data set. Dashed regression line is regression of female data set. Vertical lines are error bars (± 1SD). P-values and correlation coefficients from two-tailed Pearson linear correlation analysis are given.

With relation to the $A_{260:280}$ ratios; nether age nor PMI showed a correlation within male or female data sets. There was a significant positive correlation between pH and $A_{260:280}$ within the female data set. This effect may be due to the small numbers in

this data set and seems unlikely to be a true correlation. FT cycles do not have a significant effect on the $A_{260:280}$ ratios. This is expected, as RNA molecules of any length will absorb at 260 nm and this agrees with the results seen with FTC and total RNA yield. Quantification of RNA by UV spectrophotometric methods can be compromised by the presence of very short or single-stranded RNA molecules.

5.7.7 Index of Agonal State Correlations with RNA Metrics

Clinical notes, autopsy and histological reports from all 47 NCJDSU cases were examined and an Index of Agonal State (IAS) assigned for each case. Clinical notes were only available for confirmed vCJD cases, autopsy and histological reports were available for all 47 cases. Since only vCJD cases had detailed clinical notes available, the length of time between first symptoms and death (disease duration) was only available for vCJD cases. Therefore analysis was done using two separate scores; one including a score for disease onset (total score) and a second not including disease onset score (histology score).

RNA preparations from these cases were quality and quantity tested using the Agilent Bioanalyzer for RIN values, $A_{260:280}$ ratios and total RNA yield measured using the Nanodrop ND-1000 spectrophotometer. For cases with all relevant data, correlation analysis was carried out. Figure 5.20 shows three graphs corresponding to the analysis of the total IAS scores and histology only IAS scores.

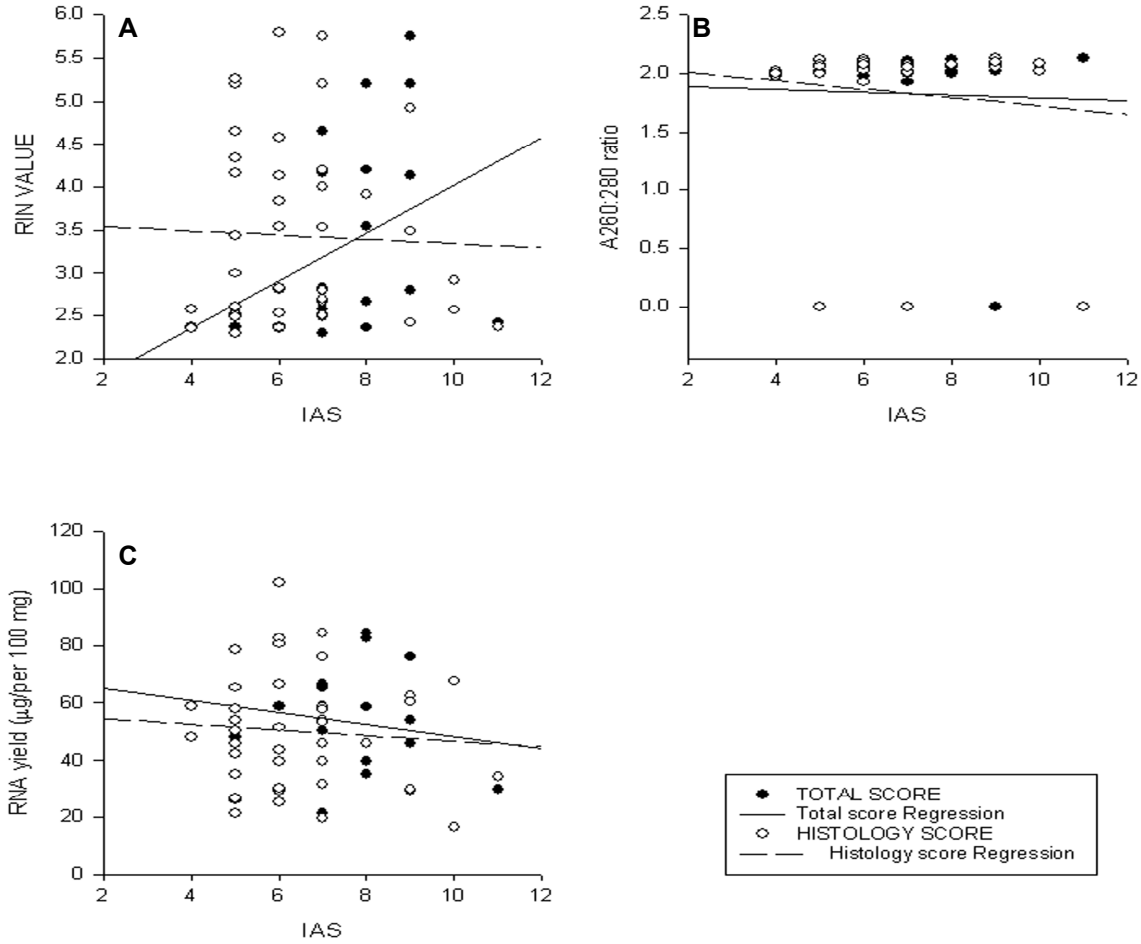

Figure 5.20. IAS correlations (including (total) or excluding (histology) onset score) with RNA metrics as determined by Agilent Bioanalyzer (RIN value) and Nanodrop Spectrophotometer ($A_{260:280}$ ratio and total RNA yield (µg)). A. total: $r^2 = 0.100$. histology: $r^2 = -0.004$. B. total: $r^2 = -0.025$ histology: $r^2 = -0.006$. C. total: $r^2 < -0.001$. histology: $r^2 = -0.009$. n = 19 for total scores. n = 47 for histology scores.

Multiple regression analysis revealed no significant correlation between total IAS scores or histology only IAS scores and any of the three RNA metrics used to measure quality and quantity (Figure 5.20A). The greatest correlation is observed with RIN values but only 12% of the RIN variation can be account for by variation in total IAS score. IAS scores take into account a range of factors (listed in section 4.6.1). It is therefore surprising that there is very limited correlation between RNA quality and agonal state. This data may be limited by its small sample size. In addition, measurement of factors such as degrees of hypoxic and dehydration

damage in the brain, are subjective. However, this analysis suggests that AS does not affect RNA quality or yield.

Inclusion of the disease onset score (Figure 5.20A) had a large effect on the correlation with RNA quality. Therefore further analysis was carried out to determine whether the duration of disease, in months, would have an affect on RNA quality. Relevant data was available from 27 of the NCJDSU cases (Figure 5.21).

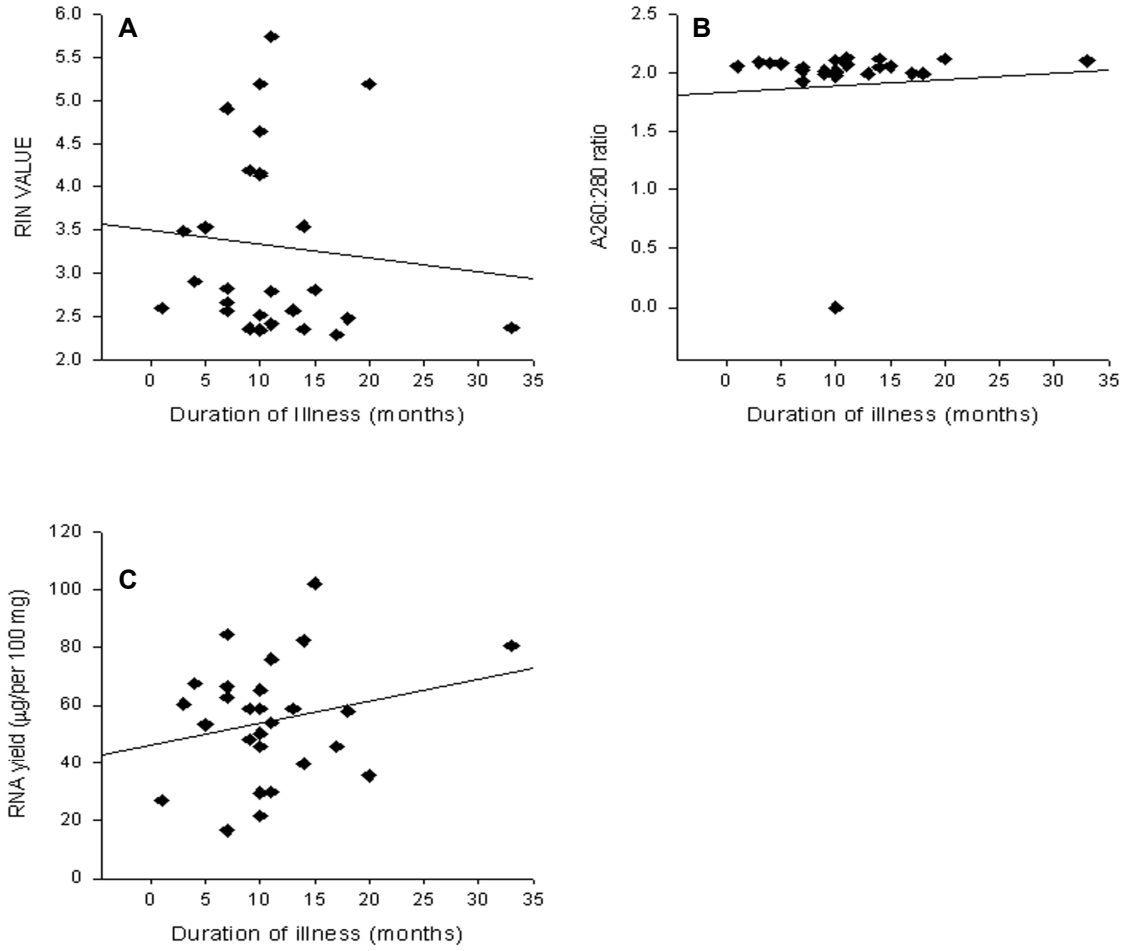

Figure 5.21. Duration of illness (months) correlations with RNA metrics, as determined by Agilent Bioanalyzer (RIN value) and Nanodrop Spectrophotometer (A260:280 ratio and total RNA yield (µg)). A. r2 = -0.008. B. r2 = 0.003. C. r2 = 0.052. .n = 27.

Multiple regression analysis reveals no correlation between the time of disease onset and death and RNA quality or quantity. Individuals, who suffered prolonged agonal states, especially if respiratory arrest or heart failure was involved, would generally

be expected to have had increased levels of plasma acidosis. Build up of lactic acid in the brain can lower the pH environment to neurotoxic levels (pH 6.0-6.5) and cause degradation of RNA. These results do not appear to represent this effect and are contrary to published data (Kingsbury *et al.*, 1995; Harrison *et al.*, 1995; Hardy *et al.*, 1985). Disease onset was not always recorded in clinical notes, in addition, neurological signs can often be subtle, and recollection of disease onset may not be accurate. 78% of the cases included for analysis were vCJD cases, which may explain the difference from previously published data.

5.7.8 Overall Cases

To determine whether gender had an influence on the results in sections 5.7, an overall comparison was carried out between the measured RNA variables and the same pre- and post-mortem factors. The results are summarised in Table 5.9.

	RIN		**YIELD (µg)**		**260:280 RATIO**	
	r^2	p-value	r^2	p-value	r^2	p-value
AGE (yrs)	0.073[a]	0.527	-0.272[a]	***0.017****	0.130[c]	0.303
PMI (hrs)	0.007[b]	0.950	0.008[b]	0.945	0.133[e]	0.294
pH	0.099[f]	0.623	-0.088[g]	0.663	-0.016[h]	0.946

Table 5.9. Correlation between age, post-mortem interval and pH of brain and RIN, 28S:18S ratio, A260:280 ratio and total RNA yield from all cases. n values; a=77. b=76. c=65. d=75. e=64. f=27. g=26. h=21. * = significant.

Two-tailed Pearson correlation analysis shows that there was only a statistically significant correlation between yield and age and this was a slight negative correlation. There were no other statistically significant correlations between any of the investigated parameters when gender effects are removed. In conclusion, RNA levels and quality are relatively consistent under the four investigated conditions. This is in agreement with the majority of published literature (see Chapter 4).

5.8 SUMMARY OF FINDINGS

- Human brain RNA preparations have lower quality and yield than mouse brain preparations.
- The Nanodrop ND-1000 is more reproducible in determining RNA yield than the Agilent Bioanalyzer RNAchip.
- No PrP^{res} was detectable in RNA preparations (10,000-fold less than in brain homogenate).
- No PrP^{res} was detectable in NND brain homogenates or RNA preparations.
- 367 human brain and 102 mouse brain RNA preparations were generated. 20% human RNA preparations and 93% mouse RNA preparations had RIN >5.0 and were potential samples for down-stream gene expression analysis.
- There was considerable variation in quality and quantity of RNA from samples generated from within the same brain and from samples between brains. The RIN variation was greater inter-case.
- RIN, $A_{260:280}$ and yield values showed no correlation with tissue preparation/storage method, including F.I. and storage temperature.
- There was a significant ($p < 0.05$) negative correlation between RNA of RNA preparations and FTC.
- There was no significant ($p > 0.01$) correlation between quality and quantity of the RNA preparations and age, PMI, pH and IAS. There was however a possible correlation between yield and age.

5.9 DISCUSSION

The isolation of intact RNA is integral to reliable transciptome analysis and constitutes the best representation of the steady-state of transcription. For a disease such as CJD, it is essential to investigate gene expression patterns within the post-mortem human brain. This study first determined which methods were most suitable to assess RNA prepared from human brain material. Traditionally, 28S:18S ratio and UV spectrophotometric $A_{260:280}$ ratios have been the accepted techniques for assessing the quality of RNA, but these provide limited information about the degree of RNA degradation.

RNA subjected to electrophoresis separates according to size. The estimated ratio of 28S to 18S rRNA should be approximately two to one in total RNA samples for the mRNA quality to be acceptable (Sambrook & Russel, 2001). Although this method of screening is widely accepted, I have not been able to locate the original data for this premise. Considering there are significant structural differences between mRNA and rRNA, it is perhaps surprising that rRNA is considered a suitable marker for mRNA, as structural difference may elicit differences in stabilities. 18S integrity may more closely reflect mRNA integrity, since the average length of 18S is more closely aligned to the average mRNA length (review; (Noller, 1984; Maden & Hughes, 1997). If transcriptional or maturation processes differ for the 18S and 28S subunits under different conditions, or if degradation events preferentially target the 28S subunit, 28S:18S ratios of ~2.0 could not be an accurate measure for assessing mRNA degradation. Increased RNA length leads to a greater statistical chance of cleavage and 'hidden' breaks can be introduced into the large ribosomal subunits of some eukaryotic organisms *in vivo*, leading to two molecules of equivalent size that cannot be distinguished from the smaller ribosomal subunit (Davis & Mullersman, 1981; Santiago *et al.*, 1986). Evidence that cellular 28S:18S rRNA is not always constant comes from data that shows a decrease in the ribosomal ratio with age in both humans and mice (Payao *et al.*, 1998; Mori *et al.*, 1978). Also it has been

demonstrated that the level of 28S RNA in mouse cell line infected with murine hepatitis virus (MHV) decreases and after 24 hrs practically no intact 28S RNA is left, while there is no observed specific damage to the 18S RNA fraction (Banerjee *et al.*, 2000).

Low rRNA band intensity ratios may be a consequence of post-mortem degradation or to destruction of cellular RNA during purification. There are numerous examples demonstrating that post-mortem changes in tissue do not occur rapidly (Mann *et al.*, 1978; Hardy & Dodd, 1983). RNA damage during purification depends on the nature of the tissue; it is difficult to isolate RNA with 2:1 28S:18S ratio from dense connective tissue (Reno *et al.*, 1997), RNase-rich tissue (Monstein *et al.*, 1995) and some tumours (Skrypina *et al.*, 2003). Certainly RNase activity will eventually lead to the loss of both components, although there are circumstances under which in situ rRNA will be completely degraded but mRNA remains intact (Mayne *et al.*, 1999; Inoue *et al.*, 2002).

Published literature evaluating the fidelity of 28S:18S rRNA ratio to RNA quality is highly contradictory. Weis attempted to identify predictive factors for sample selection of human post-mortem tissues. The quality thresholds for RIN metrics were highly correlated to good quality RNA, whereas 28S:18S was found to be unacceptably variable, although it was still possible to use the 28S:18S ratio as a predictive model for microarray analysis (Weis *et al.*, 2007) The latter outcome is in stark contrast to data published by Miller where no correlation between 28S:18S and the RNA status for RT-PCR was observed (Miller *et al.*, 2006). The reason for this may be due to the specific priming technique requirement for RT-PCR (random-hexamer) and Affymetrix platforms (oligo-dT), the latter being much less forgiving of decrements in the poly-A tail of the mRNA. Furthermore, low 28S:18S rRNA (~0.4) ratio does not preclude correct measuring of individual RNA levels provided that random primer directed cDNA synthesis is used for RT-PCR and that the amplified product does not exceed 700 nucleotides Also the shorter the desired amplicon length, the lower the threshold of 28S:18S ratio can be (Skrypina *et al.*, 2003).

The use of 28S:18S rRNA ratio would have incorrectly excluded a large proportion of the sample set. This finding is particularly important to studies of post-mortem human tissue, which is valuable, difficult to acquire, and necessitates large sample sets to achieve significant results.

Agilent Bioanalyzer RIN calculations are heavily biased towards the electorphoretic profile produced from an RNA sample. Although multiple studies have shown the RIN calculations to be reliable and stable (Copois *et al.*, 2007; Imbeaud *et al.*, 2005; Weis *et al.*, 2007; Atz *et al.*, 2007), certain treatments can significantly change the electoropherogram characteristics and thus the RIN calculation. Concentrating RNA in a SpeedVac has been shown to have a positive impact on the RNA quality measurements derived from the Agilent Bioanalyzer. Weis suggested it was not the extraction process but rather some mechanism which occurred during the concentration process which is likely to alter the RNA structure, facilitating its migration through the capillary chip. As it is highly unlikely that such a structural alteration would result in restoration of degraded mRNA to a nondegraded form, this factor is another variable which must be controlled for when testing RNA quality (Weis *et al.*, 2007).

Spectrophotometric analysis of nucleic acids is highly susceptible to sample contamination. While this is beneficial for excluding substantially contaminated samples, such sensitivity may interfere with obtaining reliable results and lead to high false exclusion rates. A_{260} readings are normally compromised by the presence of genomic DNA, A_{230} readings indicate the level of residual organic contamination whereas A_{280} readings inform of the level of proteinaceous contamination of the sample. $A_{260:280}$ ratios are taken to determine the quality and purity of RNA and $A_{260:230}$ ratios are used as an additional criterion of purity. Individual wavelength readings can easily be misinterpreted and it is more common for ratios to be measured. $A_{260:280}$ and $A_{260:230}$ being roughly equivalent is accepted for pure RNA preparations (Sambrook & Russel, 2001; Manchester, 1995; Manchester, 1996). As discussed in Chapter 4, the RNA extraction protocol used in this project utilises GTC

and phenol-chloroform. These chemicals can contaminate preparations and even minimal residual amounts can give erroneous measurements. The additional chloroform extraction at the end of the procedure should have removed any residual phenol which would alter OD ratios. Tissue-specific variation of UV measurement has not been observed and is invariate relative to purification method and tissue of origin (Imbeaud *et al.*, 2005).

Degradation issues fall under two broad questions; 1) is it possible to determine whether RNA decay has occurred via *in vivo* cellular regulatory mechanisms or processing of extraction? 2) If the later is true, how much RNA destruction due to handling can be tolerated while still retaining the appropriate information concerning the level of expression of the gene of interest?

RNA of any gene, including rRNA, can be specifically degraded due to some specific regulatory process or as a result of response to some external factors within the living cell (Pardue *et al.*, 1994; Taylor *et al.*, 1986; Banerjee *et al.*, 2000; Payao *et al.*, 1998; Mori *et al.*, 1978). If degradation has occurred in an unspecific pattern, where unspecific damage has occurred to many different RNAs in a similar way and to a similar degree, it may be as a result of mishandling, post-mortem degradation, massive cell death or massive infection. One way to overcome this problem is to define a set of well characterised marker RNAs and a methodology to conclude whether most of them are degraded similarly or differently. If damage is randomised along RNA and a number of different RNAs are damaged to approximately the same degree, unspecific degradation can be presumed. The correct data on relative concentration of the RNA of interest will be obtained if the probability of having a cut site within the amplified fragment is low and random primer not oligo-dT is used for RT-PCR. There is published evidence that this is indeed the case (Preece *et al.*, 2003).

The mechanisms of RNA degradation in the *ex vivo* context are not well understood, although mechanical alterations in cell structure following death render organelles physiologically ineffective long before any significant changes in certain constituent

biochemical are detected. Degradation mechanisms are likely to involve different rates and mechanisms for different RNA species (Jacobson & Peltz, 1996; Ross, 1996; Shapiro *et al.*, 1987; Noguchi *et al.*, 1991). It has been reported that an immediate and rapid loss of low molecular weigh RNA species, usually tRNA and mRNA, occurs at death, although there is little alteration in rRNA levels (Mann *et al.*, 1978). Furthermore, Inoue illustrated that total RNA and mRNA isolated from dead rat bodies degrades in the same manner. Degradation rates of three house-keeping genes in the brains of dead rats were identical, suggesting that the mRNA of constitutively expressed genes are degraded via a similar mechanism (Inoue *et al.*, 2002). These finding and the findings from (Castensson *et al.*, 2000) suggest that it is possible to isolated total RNA from autopsy brain tissue that is suitable for mRNA analysis. mRNA of inducible genes is less stable than that of constitutively expressed genes *in vivo*. However, stability of mRNA in inducible gene *ex vivo* is still to be studied.

Gene expression regulation is intrinsically related to mRNA stability. The stability of individual mRNA transcripts are in turn regulated by specific interactions between structural elements (*cis*-elements) and *trans*-acting factors. These interactions are regulated by environmental stimuli such as nutrient levels, cytokines and hormones, as well as environmental stresses like hypoxia and tissue injury, factors which are of particular relevance when studying neurodegenerative disorders (Liebhaber, 1997; Mitchell & Tollervey, 2000; Guhaniyogi & Brewer, 2001; Hollams *et al.*, 2002). The most important structure which determines the stability of the mRNA structure is a destabilizing sequence found in the 3' untranslated region. The general motif is a series of AUUUA pentamers. The greater the number of A + U rich elements (AREs), the greater the vulnerability to decay. In yeast cells, decapping of the 5' structure follows poly(A) shortening to promote nucleolytic decay (Shaw & Kamen, 1986). Highly labile mRNA species such as *c-fos* also contain decay elements within their coding regions. Degradation initiation begins by the progressive deadenylation of the poly(A) tail, thereby reducing the efficacy with which poly(A) binding protein can attach to the mRNA molecule. This therefore permits attack by endonucleases and exonucleases. Direct endonucleolytic decay can also occur (Sachs, 1993). If the

degradation mechanism model proposed by Sachs (Sachs, 1993) is correct, it may be possible to predict genes which are more susceptible to decay by searching for the 3' untranslated region reported in Genbank.

Despite the relative stability of RNA in postmortem tissue studies, human post-mortem brain tissue often yields RNA levels that vary widely among samples. The abundance and integrity of RNA and constituent mRNAs varies markedly between one human brain and another. The average amount of RNA isolated per gram from human post-mortem tissue was ~ 260 µg/g, and was significantly less than the amount routinely isolated from rodent brains, either immediately or after freezing and storing for a length of time (~ 960 µg/g). This is confirmed by other observations (Johnson *et al.*, 1986; Perrett *et al.*, 1988; Sajdel-Sulkowska *et al.*, 1983). The manipulation of brains at time of autopsy (examination for gross anatomy, weighing, slicing and dissection) may contribute to this effect; smaller rodent brains require less handling. Such additional manipulations (especially cutting tissue and disrupting cells) may increase the risk of releasing alkaline ribonucleases as well as the normal lysosomal, acidic ribonucleases. However, one report of RNA yields from a human brain sample taken at biopsy was in the range of 600 µg/g of tissue (Johnson *et al.*, 1986), suggesting that rather than loss due to manipulation, the total amount of RNA in human brains may be less per gram of tissue than in rodents. Variations in brain RNA levels could be the net result of an exceedingly complex set of underlying circumstances.

Screening RNA to exclude samples prior to cDNA synthesis or probe generation saves time and effort on wasted experiments. Gene expression analysis invariably involves cDNA synthesis by RNA reverse transcription and subsequent quantitative evaluation of the DNA product by PCR (Wang *et al.*, 1989) or hybridization (Taylor *et al.*, 1986). Although shorter fragment length or lack of poly(A) tail may reduce efficiency of cDNA synthesis or probe hybridization, a moderate degree of degradation does not exclude the viability of microarray analysis (Schoor *et al.*, 2003). Overall, although an accurate, *in vivo* representation of the transcriptome may

seem difficult to achieve, it is still possible to study mRNA, as these factors are most likely to affect detection of full length mRNA of labile species.

Building a RNA profile for each sample utilising three historically relevant methods of RNA assessment and one recently described computer algorithm ensures a stringent assessment evaluation of all RNA preparations. This is one method of normalization which will improve the quality of the resulting microarray data. Categorisation of borderline samples can still be tricky and can be heavily affected by investigator bias. While an in-depth interpretation of RNA quality is valuable and necessary, it is important that the investigator select what is acceptable in terms of false inclusion and false exclusion. To this end, the experiments were optimized towards correctly identifying good quality sample, at the risk of including some poor quality samples, because the value of post-mortem human brain tissue is so high. Other normalisation strategies applied in the project were; similar sample size/ tissue volume and the use of total RNA instead of alternative RNA species or specific mRNA or rRNA house-keeping genes. Normalisation of tissue volume is a simple first step process which will reduce experimental error, but may be difficult to estimate and/or may not be biologically representative. Total RNA will provide a full picture about the sample integrity, although this greatly depends on the technique used. This method of normalization however, does not control for error introduced at the reverse transcription or PCR stages. It also makes the assumption that there is no variation in the rRNA:mRNA ratio, an assumption known to be incorrect.

While many RNA extraction protocols and recommendations for TSE agent decontamination have been described, there are limited guidelines on how to extract RNA from tissues while simultaneously decontaminating or removing the TSE agent. The majority of decontamination procedures are extremely harsh and are likely to have a detrimental affect on RNA populations. This project has described an RNA extraction protocol for use with TSE infected high-lipid tissues, but it was necessary to determine the level of TSE decontamination or removal achieved. Having established a method for detecting proteinase-K resistant PrP and determining the limit of detection, a random selection of RNA extracts were tested. The RNA extraction protocol was developed specifically for removal of proteins while

conserving the RNA population. Based on the results of the risk assessment, it was considered that the RNA extracts did not contain detectable amounts of infectious PrP^{Sc}. Studies investigating the efficacy of organic solvent extraction protocol for purification of phospholipids from brain tissue concluded that scrapie-like agents can be decontaminated from brain samples, provided only the organic phases are used. *In vitro* results were similar to those seen for this project and the results from the study were confirmed by *in vivo* endpoint titrations (Di Martino *et al.*, 1994). Single exposures to organic solvents are evidently insufficient to inactivate TSE agents, but it is likely that continuous and prolonged exposure may affect infectivity titres (Millson *et al.*, 1976). In this case, extraction by organic solvents using the organic phase only for product purification would be considered a useful procedure for reduction and/or removal of infectivity, especially since scrapie agent is not soluble in many organic solvents. The cessation of solvent extraction for the production of animal feed has been indicated as one of the major concurrent causes for the sudden BSE epidemic (Kimberlin, 1992; Taylor & Woodgate, 1997).

In vitro test methods such as Western blot are only considered useful for studying the initial effects of treatments on prion proteins, since it has been proven that such methods may not be sufficiently sensitive to detect extremely low levels of PrP^{res} and therefore infectivity (Fichet *et al.*, 2004). Conventional *in vivo* assays are widely accepted as being more reliable and able to detect much lower titres of infectivity, although factors such as the presence of species barriers will inevitably lead to a loss in sensitivity. While it is clear that protein western immunoblotting is suitable and reliable for PrP^{res} detection, it remains questionable as to whether this method is sensitive enough to detect low, but still infectious, titres of agents (McLeod *et al.*, 2004). Immunodetection of PrP by western blot has a dynamic range of ~ 100 fold, whereas bioassays measure prions over a ~ 10^9 fold range (Peretz *et al.*, 2006), so although it is possible to state the inadequacy of using Western blot for assessment of decontamination/inactivation of TSE, bioassays were not a viable choice for this project and there are limited alternative methods.

It is possible that the phenol treatment will disassociate or denature the PrP^{Sc} aggregates within a sample, thereby rendering the PrP^{Sc} susceptible to proteinase K treatment. For this safety assessment, it has been assumed that this effect is minimal at best, and these results are consistent with the assumption that PK resistant PrP^{Sc} is indicative of infectivity. If there was significant effect on PrP^{Sc} aggregates, infectious PrP^{Sc} would have been rendered PK sensitive and would not be detected on the western blots. Under these circumstances, if phenol treatment had indeed denatured the PrP^{Sc} aggregates and assuming the prion hypothesis is true, a bioassay would also be unsuitable in detecting PK sensitive PrP^{Sc}.

The findings from this chapter agree with the consensus published data. RIN, 28S:18S rRNA ratio, total RNA yield and $A_{260:280}$ ratio do not correlate with gender, age of patient or post-mortem interval. Based on the IAS, there is also no evidence of agonal state impacting on RNA integrity. Findings from the Tomita study showing that agonal state had a drastic effect on RNA integrity and decreased brain tissue pH were not confirmed in this study (Tomita *et al.*, 2004). It was not possible to study IAS against tissue pH in this study as only NND cases had pH information but did not have clinical notes. The reasons for the different findings may be due to difference in methodology. Tomita used 240 Genechips to test 40 subjects (psychiatric and control) and measured global RNA integrity based on indicators on Affymetric Genechips. However, when specific mRNA levels were tested against a range of agonal variables, no correlation was observed (Burke *et al.*, 1991). Although the IAS is more detailed than the AFS, assessment of degradation was more comprehensive in the Tomita study. The use of the Agilent RIN is a simple assay requiring limited sample, cost and expertise. RNA samples assessed using the RIN have been shown to be suitable for gene expression studies. Therefore, for transcriptome analysis on human tissue, the effect of agonal state is insufficient to affect gene expression results. The pH data does indicate a level of correlation, but this effect is debatable and is probably due to the small sample size rather than to a true correlation. Although Bahn suggests the use of pH of brain tissue as a suitable method for predicting the RNA quality, this has not been confirmed in other studies.

As yet, it has been not been possible to identify a predictive model from which to select suitable cases for molecular genetic analysis (Bahn *et al.*, 2001).

6 GENE EXPRESSION ANALYSIS

6.1 OBJECTIVES

- Select suitable arrays for gene expression analysis.
- Assess reproducibility and specificity of chosen array technology.
- Compare OND, NND and vCJD cases matched cases on selected arrays.

6.2 INTRODUCTION

Molecular methods offer insight into the underlying mechanisms of brain function and in the case of disease, the underlying pathological mechanisms. With the availability of the nearly complete human and mouse genome sequences, the development of genomic tools allows investigators to exploit this valuable information. Such 'gene-centric' approaches permits broad, system-based approaches, while simultaneously obtaining a gene-specific molecular view.

The cellular state is dynamically maintained by a defined set of gene transcripts, or transciptome, which becomes altered at times of stress and disease. In addition, mRNA expression profiles are anatomically specific and because expression levels are influenced by both genetic polymorphisms and environmental input, microarray technologies have the potential to elucidate the underlying molecular changes which occur during the disease state. In contrast to more traditional 'one-gene-at-a-time approaches', large scale parallel views of hundreds of genes allows investigators not just to explain the behavior of a singe gene, but to develop explanations which are consistent and well supported in the context of complementary information on thousands of genes.

A microarray or gene chip is an ordered arrangement of nucleotide molecules representing specific gene coding regions, chemically bonded to a specifically designed spotted or arrayed membrane surface. 'Probes' are the arrayed membrane-tethered nucleic acid of known sequence, whereas the 'target' is the free nucleic acid in the biological sample to be analysed. Microarray analysis of gene expression allows the investigator to analyze the expression level of genes in complementary DNA (cDNA), which is prepared from purified mRNA. RNA transcribed from this is then fluorescently- or radioactively labeled and hybridized to the array. Membranes are washed to remove non-hybridized excess sample and imaged, usually by laser scanning or autoradiographic imaging. At this stage, the data is uploaded onto a database, where the image is recognized and processed, then analyzed by any number of statistical packages currently available.

During the mid 1980's, the first arrays called macroarrays were fabricated by spotting DNA probes of ~300 μm diameter, limiting the density to ~ 2,000 probes per spot, each spot being a single feature. Microarrays created by pin-based robotic systems can dispense an accurate volume of a DNA solution in a spot of about 150 μm, creating much higher density arrays. Stephen Fodor and colleagues produced the world's first microarray using a microscope glass slide and chemically synthesized oligonucleotides (Fodor *et al.*, 1991; Fodor *et al.*, 1993). Since then, variations of this original technique have led to vastly improved genetic array platforms, for example, the most recent Affymetrix GeneChips contains over 1.3 million features, equivalent to over 47,000 RNAs which encompass nearly every known human gene.

The two basic types of microarrays are oligonucleotide and cDNA microarrays. Oligonucleotide microarrays are directly synthesized and arrayed in a discrete regular manner on the chip surface, whereas cDNA microarrays are previously prepared DNA clones (generally a PCR product of longer than 100 nucleotides). The primary commercial DNA microarray providers are Affymetrix and Agilent, aimed at genome wide panels usually with >3,000 features per chip.

Complex diseases often result from both genetic and environmental influences. DNA diagnostics provides a static test of the composition of the genome that does not illustrate the full cellular picture. RNA diagnostics is a more dynamic test, capable of detecting change due to complex environmental factors, in this instance neurological disease state. However, due to cost constraints and due to the subsequent bioinformatics time required to analyse the data, it is not always feasible to monitor all 44,000 different mRNA species transcribed from the human genome for multiple samples simultaneously. To circumvent this problem, 'focused arrays' containing a limited number of mRNAs on a low-density array are also available.

Focused microarrays are smaller versions of whole genome arrays, comprising a thoroughly researched set of relevant, pathway- or disease- focused genes. Generally, such focused microarrays are used to study gene expression associated with a biological pathway or disease state, or to customize the arrays for a selected panel of genes tailored to specific research needs. Because of their focused design, it becomes possible and affordable to process larger number of samples. Also, data handling is easier and more straightforward, allowing research to progress faster.

Commercial availability of focused microarrays is increasing, to accommodate the demand of customized arrays applied to specific clinical disease studies. SuperArray (Bethesda, MD, USA) is one such company with a comprehensive list of focused microarrays. SuperArray OligoArrays have 300–600 bp probes spotted in quadruplicate in 1-mm-diameter "tetrads". These tetrads are arranged in 8 columns and 14 rows, and for the human specific Alzheimer Disease (AD) OligoArray (OHS-057) and Signal Transduction (ST) PathwayFinder OligoArray (OHS-014), there are 96 experimental features per array. Also included on the array design are internal control features consisting of; plasmid (pUC18), blank (no DNA), artificial sequences and biotinylated artificial sequences and four potential normalization genes (Glyceraldehyge-3-phosphate dehydrogenase [GAPDH], β-2- microglobulin [B2M], Heat shock protein 90 [HSP90AB1], and β-actin [ACTB]).

The human AD array has been designed to included genes implicated in amyloid β-peptide (Aβ) generation, clearance and degradation, as well as genes involved in Aβ signal transduction leading to neuronal toxicity and inflammation. The ST array incorporates markers of 18 signal transduction pathways, including the p53, Jak-Stat and calcium and protein kinase C pathways. These arrays were selected as there are pathological similarities between AD and vCJD and evidence of altered expression of genes involved in a number of apoptotic and metabolic signaling pathways in animal models of TSE (Duguid *et al.*, 1989; Diedrich *et al.*, 1991b; Diedrich *et al.*, 1987).

Microarray data in itself is insufficient evidence for gene expression changes and must be independently verified by real-time quantitative polymerase chain reaction (qRT-PCR). Chapter 8 outlines the proof of concept for RT-PCR to verify gene expression changes observed with the microarray results.

Having established that it is possible to extract RNA from human brains of suitable quality for microarray and real time analysis, the next objective was to determine whether it was possible to obtain statistically significant gene expression data. The experimental design included three comparison groups. Each comparison group contained an age and gender matched vCJD, NND and OND case. Each sample was hybridised to the focused AD and ST arrays, where possible, in duplicate. The array data was analysed for;

- Variation between replicate arrays and replicate samples. To determine variability of the RNA preparations and of the arrays.
- Variation between cases of the same status, i.e. vCJD vs vCJD. To determine if gene expression changes were associated with inter-patient variability.
- Variation between cases of different status, i.e. vCJD vs NND control cases. To determine disease associated changes.

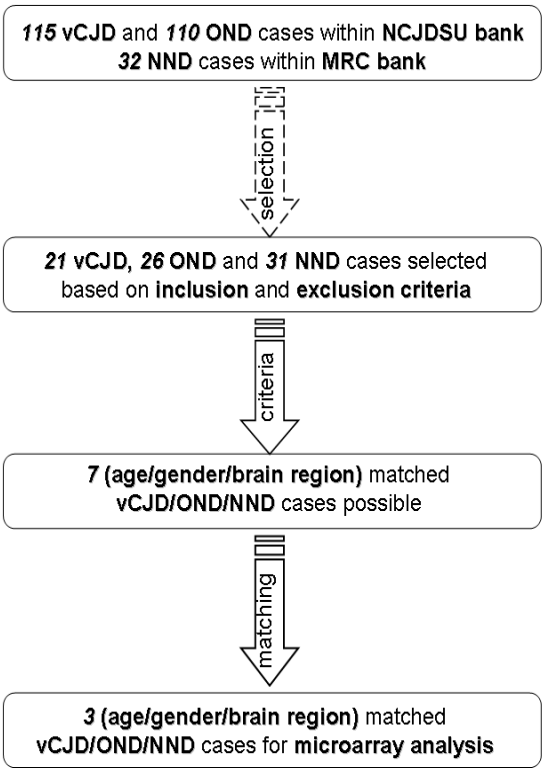

Figure 6.1. Flow chart showing case selection process used to include and then match vCJD/ OND/NND cases used for microarray experiments.

The analysis was also done within the comparison groups, i.e. using age and gender matched cases only, and across all the cases, i.e. using all vCJD hybridised arrays compared to all NND hybridised arrays (see section 6.4). Figure 6.1 shows the total number of cases from which eventually 3 matched cases, one each of vCJD/NND/OND, was selected for microarray analysis. Figure 6.2 illustrates the statistical model used.

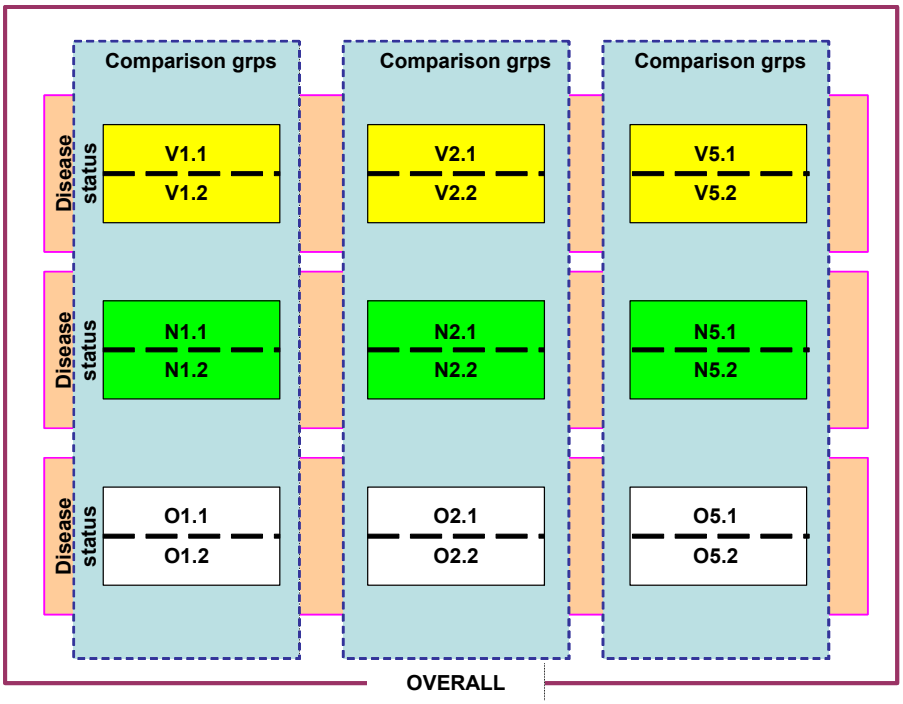

Figure 6.2. Grid model of analysis. Variation may be introduced by; 1) replicates (black dashed lines). 2) intra-status variation (pink box). 3) across comparison groups, i.e. age and/or gender related variation (blue box). These factors must be accounted for before disease associated gene changes can be determined. V1.1= vCJD, comparison group 1, replicate 1. N1.1= NND, comparison group 1, replicate 1. O1.1= OND, comparison group 1, replicate 1. Analysis to determine the degree of variation was done; between replicates (black dashed line), intra-status (pink box), inter-status (blue box) and overall (outer purple box).

In order to determine disease status related changes, replicate effects, intra-status effects and across comparison group effects must be accounted for and/or removed. If replicate effect, intra-status effect and age/gender effects are removed or are minimal, remaining gene expression changes can be considered to be potential disease associated changes.

It must be noted however that the use of focused gene arrays such as the AD OligoArray has biased the study towards the genes printed on the array membrane. The main aim of this experiment was to determine whether RNA isolated from human autopsy brain material from tissues stored at the NCJDSU and the MRC brain banks could be hybridized to cDNA microarrays and whether reliable and reproducible data to be generated. Ideally future work including whole transcriptome anaysis and pathway identification and analysis would be carried out (see Chapter 8).

6.3 CASE COMPARISON GROUPS

From the seven matched comparison groups possible (see Table 4.6), three groups were used for gene expression analysis. These were selected to cover a range of ages and to include both genders; to isolate age- or gender- related gene expression changes. Comparison groups used for gene expression analysis are defined in Table 6.1.

	vCJD	NND	OND
Grp 1	17/M	19/M	18/M
Grp 2	39/M	41/M	54/M*
Grp 5	30/F	31/F	25/F

Table 6.1. Matched comparison groups containing one vCJD case, one NND control and oneOND case. All matched groups were matched for gender and age ±5 years with the exception of *. Refer to Table 4.6

6.4 ALZHEIMER DISEASE OLIGOARRAY

Expression of 113 genes (Appendix 9.10, Table 9.4) implicated in AD pathogenesis were screened on GEarray Q series non-radioactive Alzheimer Disease gene chips (Tebu-Bio, Cambs, UK), using total RNA (1 μg) from brain tissue of vCJD (n=3), OND (n=3) and NND (n=3). Total RNA was amplified and labelled using the Superarray TrueLabeling-Amp 2.0 kit according to the manufacturer's instructions. Membranes were developed using CDP-star as chemiluminescent substrate. Membranes were exposed to X-ray films and developed. Images were digitalised on an Epson Perfection flatbed scanner. Images were acquired at 200 pixels/in and were formatted (squared, cropped, inverted, and saved in TIF format) with Adobe Photoshop version 7.0 (Adobe Systems, Uxbridge, UK). Examples are shown in Figure 6.3. The web-based GEArray Expression Analysis Suite version 1.2 software (Superarray, MD, USA) overlays a grid of spots (10 pixel diameter) on the TIF image, which is centered over each feature tetrad. The average pixel intensity (API)

within each spot was measured and used to calculate gene spot density levels for each feature. The usable range of API values with this instrumentation was 9,000–65,000, as described by the manufacturer's manual. The range was established from determining that the minimum (background) API value detected on the autoradiographs was ~8,000 and the maximum or plateau API was ~65,000. API values that fell within these limits were accepted for analysis. Images were verified by visual comparison with the autoradiographs. Background-corrected densities of each tetra-spot (representing each gene) were averaged across that spot. For normalisation, only the genes between the 25th and 75th quartile from the summation of all spot densities were considered. Regulated genes were identified by ratio changes of ≥ 1.5, unless otherwise stated. All formulae for data analysis can be found in Appendix 9.10.1.

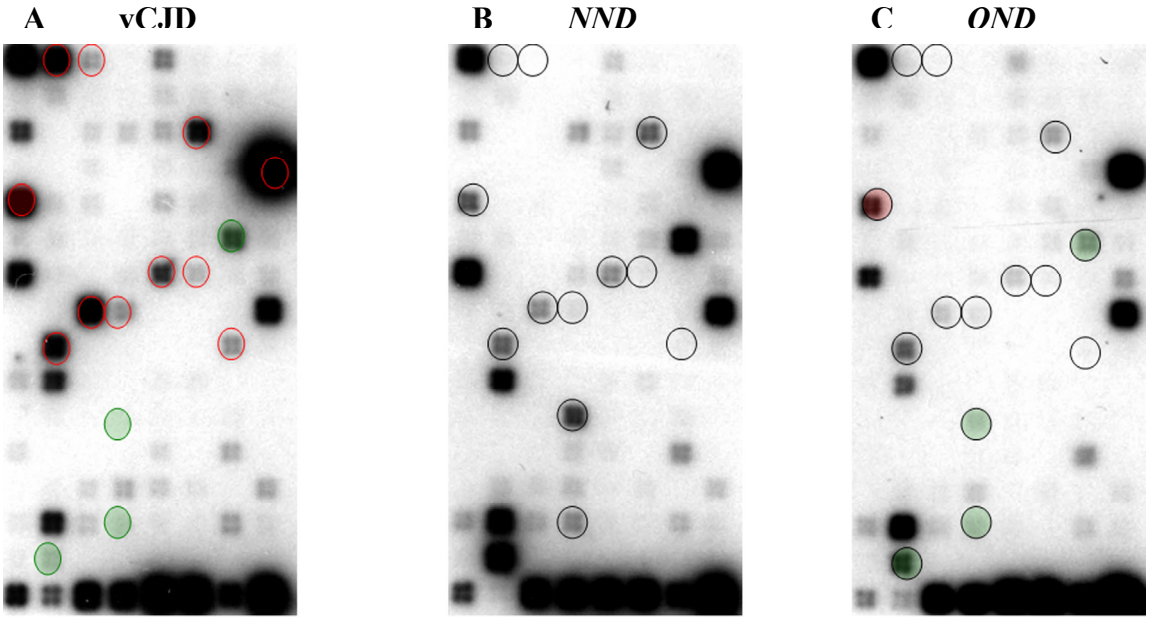

Figure 6.3. Array images (un-edited) of comparison group 1 (see Table 6.1). Total RNA extracted from control cases and vCJD cases was labeled and hybridized to membranes pre-loaded with 96 cDNA representing disease specific genes of interest. Representative images of three membranes hybridized to labeled RNA extracted from vCJD (A), NND control (B) and OND control (C) are shown. Gene spots encased in red circles are induced in vCJD compared to normalized NND and OND controls. Gene spots encased in green squares are reduced. Filled red circles are induced compared to NND controls only. Filled green circles are reduced compared to NND controls only.

6.4.1 Reproducibility and Variation Between Replicates

The variability of technical replicates was determined in two ways; (i) Total RNA from a single RNA preparation was amplified and hybridised to two arrays, to establish the variability of the array analysis. (ii) Two contiguous samples from a single human brain was used to prepare RNA, amplified in parallel and hybridised to two arrays, to establish the variability of RNA preprations and array analysis. All RNA samples were labeled as described in Chapter 2, to generate labelled cRNA target. cRNA quantification and quality assessment was measured by UV spectrophotometry. Samples ≥ 11 ng/µl total RNA, $A_{260:280}$ ratio ≥ 2.0 and $A_{260:230}$ ratio ≥ 1.7 were considered as suitable for hybridization to microarrays. 2 µg of cRNA was hybridised to each of the two separate AD arrays and processed in parallel.This was carried out on all cases in comparison groups 1 and 5. Figure 6.4A represents one such replicate set using two RNA preparations analysed on two separate arrays. It is expected that the combined variability of the RNA preparations and array analysis would be greated than the variability of the array analysis only. However, Figure 6.4B shows the multiple regression analysis which reveals a significant correlation coefficient of 0.97, indicating that replicate arrays assessing the combined variability are highly correlated.

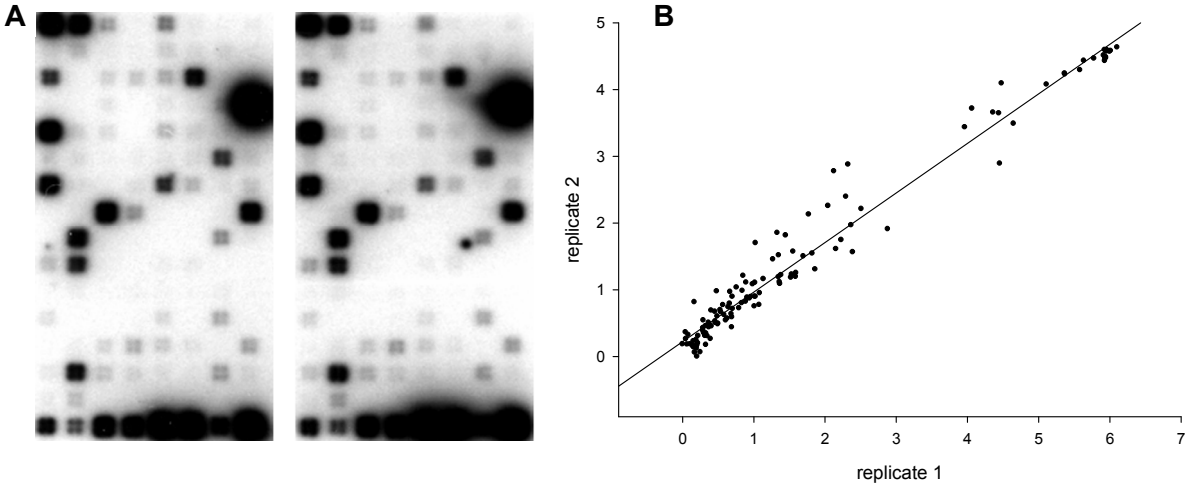

Figure 6.4. A. Replicate array images of case 124. B. Scatter plot of replicate 1 against replicate 2. Axis values are $\log_{10}$ gene spot densities. r2 = 0.969.

Another measure available to compare two samples is the coefficient of variation (CV) which shows the degree of deviation from the mean. The diagonal line in Figure 6.4B indicated how correlated the data is and the CV indicates how close the values are to the line. Replicate AD arrays were hybridized using (i) a single RNA preparation on two separate arrays for all three cases in comparison groups 1 and (ii) two RNA preparations on two separate arrays for all three cases in comparison group 5. Figure 6.5 shows scatter plots of replicate cases of comparison group 1. The average CV value (based on internal chip control spots) for group 1 was 19% and for group 5, 14%. The greater variation observed in comparison group 1 is expected since using two RNA preparations would introduce the variation of the sample as well as the variation of the array analysis. For comparison group 5, the variability of the array analysis is comparable to the Superarray quoted values (CV of 10%) of a single sample on replicate arrays (Fox-Brashears *et al.*, 2000).

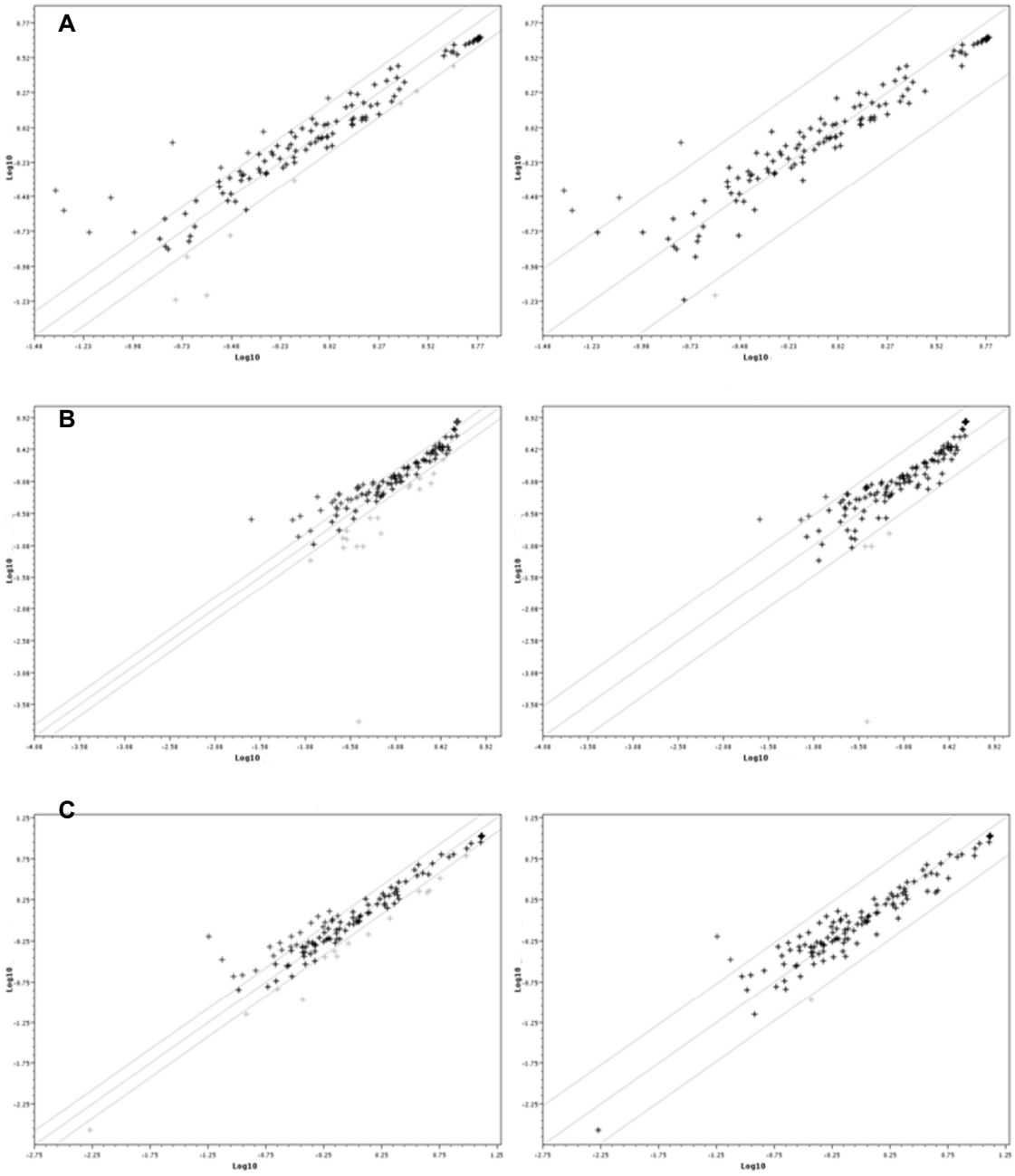

Figure 6.5. Scatter plot of relative spot density of replicate 1 plotted against replicate 2 from comparison group 1. Panel A. vCJD. Panel B. NND. Panel C.OND. All panels show boundaries as lines of 1.5 fold (left) and 3.0 fold (right). Axes are $\log_{10}$ normalised spot density values.

6.4.2 Intra-Status Effects

The next assessment was to determine the degree of variation between cases of the same status (i.e vCJD vs vCJD). In this analysis, CV values were calculated but it should be noted that these have little power due to the small sample sizes and the limitation of not having identical biological replicates. Figures 6.6, 6.8, 6.10 show all possible intra-status combinations. Figures 6.7, 6.9, 6.11 show more detailed examples of individual intra-status comparisons. Table 6.2 gives the correlation coefficients (r^2) and coefficient of variation (CV) for each comparison.

vCJD

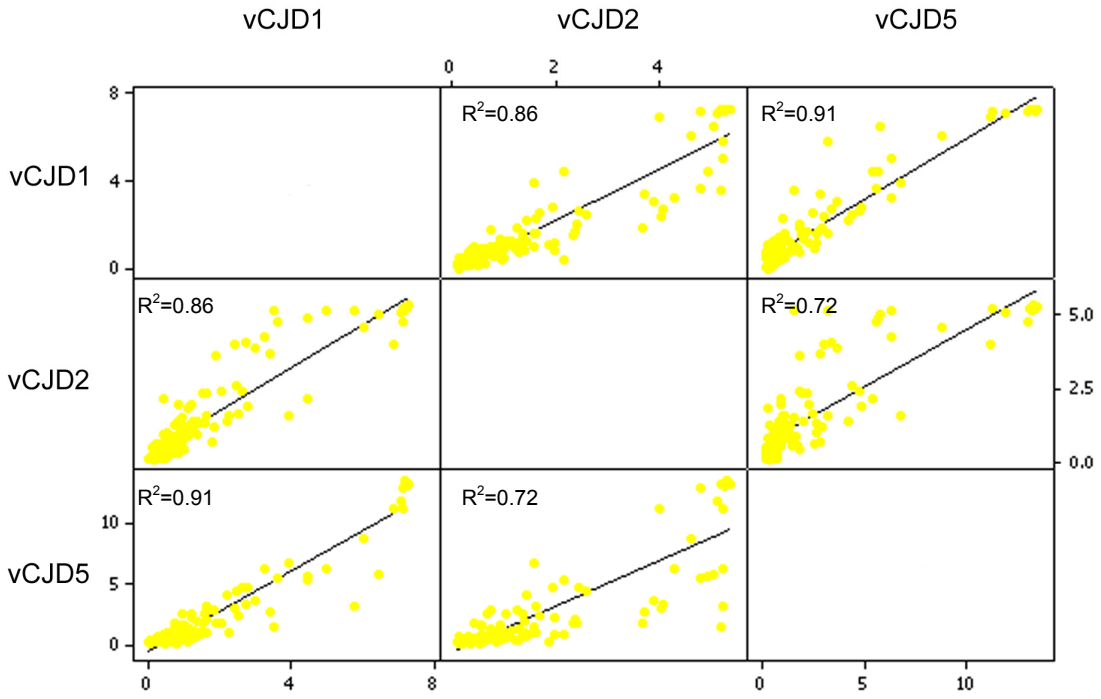

Figure 6.6. Integrated matrix plot of all vCJD cases plotted against each other. Lines represent multiple regression analysis.

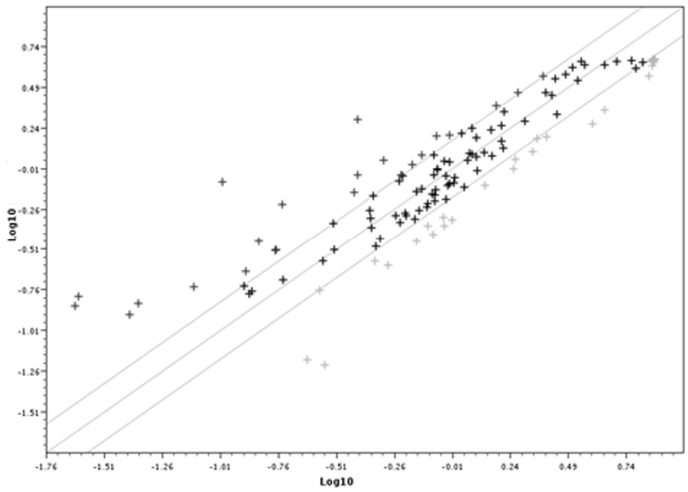

Figure 6.7. Scatter plot of vCJD1 against vCJD2. Outer diagonal lines represent 1.5-fold threshold limits. Axes are $\log_{10}$ spot density values.

OND

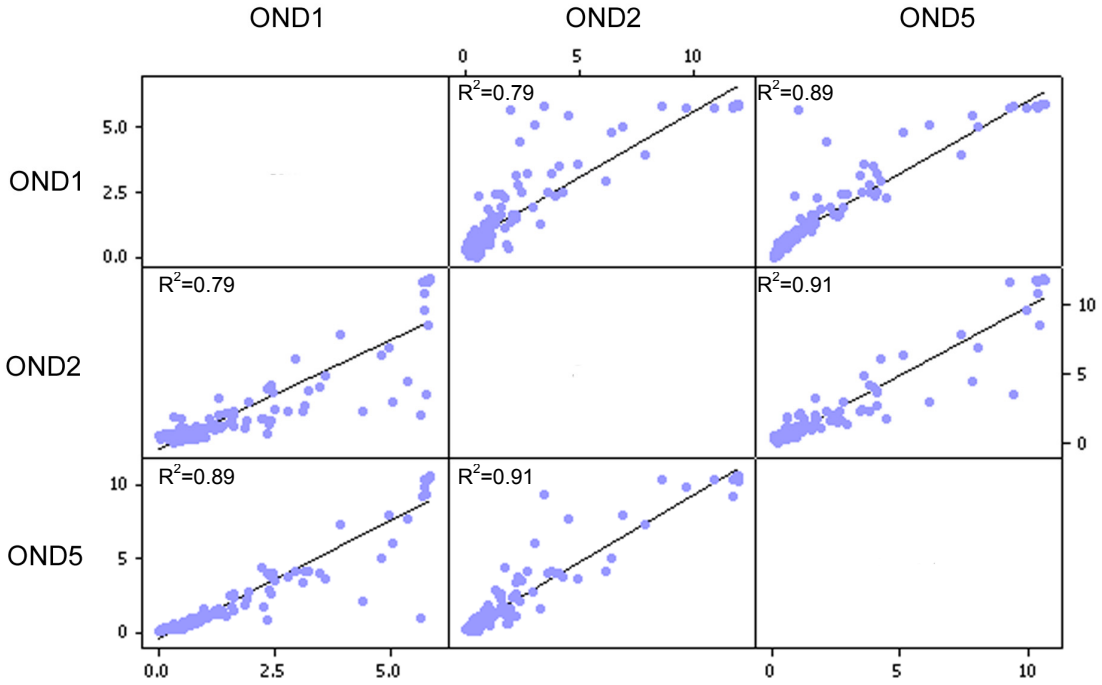

Figure 6.8. Integrated matrix plots of all OND cases plotted against each other. Lines represent multiple regression analysis.

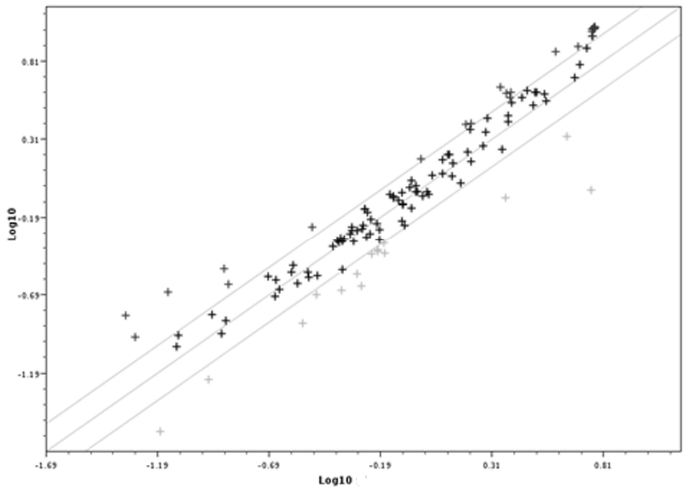

Figure 6.9. Scatter plot of OND2 against OND5. Outer diagonal lines represent 1.5-fold threshold limits. Axes are $\log_{10}$ spot density values.

NND

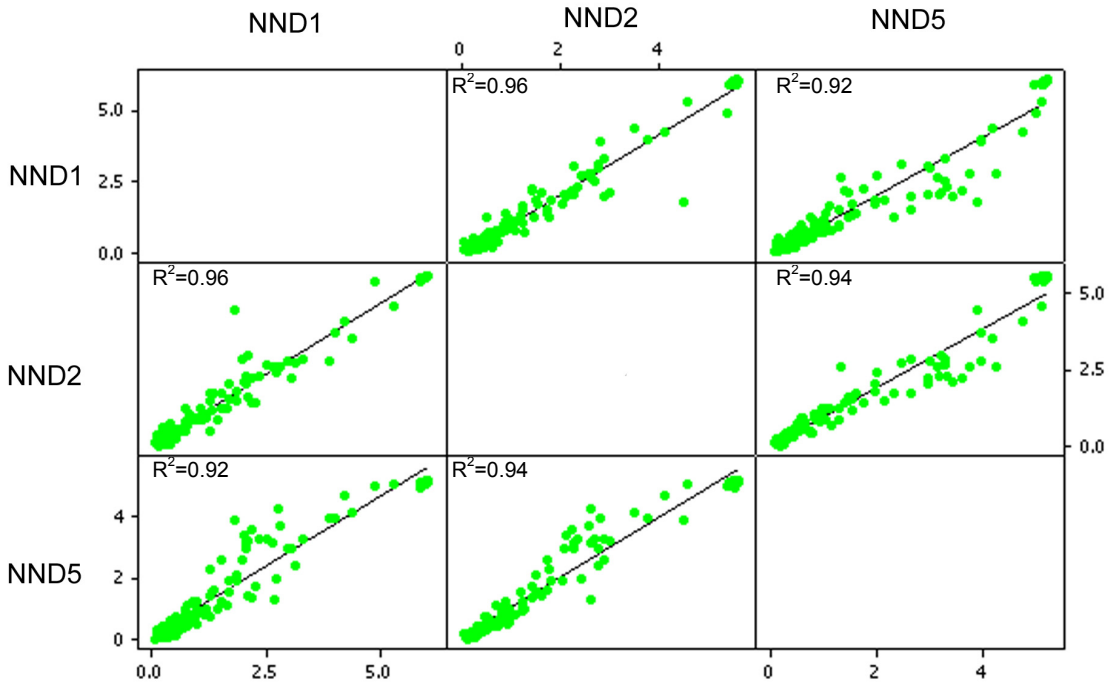

Figure 6.10. Integrated matrix plots of all NND cases plotted against each other. Lines represent multiple regression analysis.

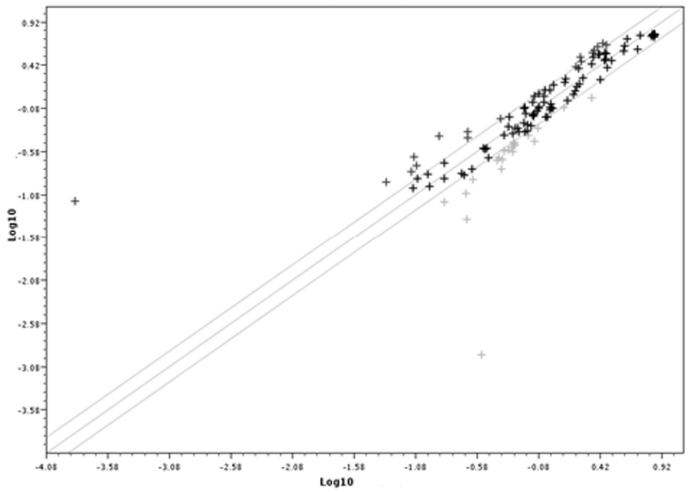

Figure 6.11. Scatter plot of NND1 against NND5. Outer diagonal lines represent 1.5-fold threshold limits. Axes are $\log_{10}$ spot density values.

	Correlation coefficient (r^2)	Coefficient of Variation (CV) (%)
vCJD vs vCJD	0.83	23
OND vs OND	0.86	18
NND vs NND	0.94	23

Table 6.2. Correlation coefficient and coefficient of variation values for all intra-status comparison.

CV and r^2 values were consistent across all intra-status comparison, suggesting that within all 3 disease statuses, there was similar but limited variation between the cases. Single samples run on replicate arrays showed an average CV ~18% and an average r^2 of 0.97. The intra-status comparisons have an average CV of 21% and an average r^2 value of 0.88, suggesting the data is slightly more variable intra-status than for replicates.

6.4.3 Inter-Status, Matched Cases

Variation between vCJD, OND and NND was evaluated. Figures 6.12, 6.13 and 6.14 show vCJD vs NND, OND vs NND and vCJD vs OND for comparison groups 1, 2 and 5 respectively, set at 1.5- (left) and 3-fold (right) boundary threshold limits. Figure 6.15 is a graphical representation of genes observed with ≥ 2- fold changes in gene spot density. Differentially expressed genes observed in vCJD vs NND and in vCJD vs OND but not observed in OND vs NND were considered to be candidate vCJD specific changes.

The average CV across all comparisons in group 1 was 44%. The overall percentage of genes flagged as regulated and the degree of variation observed was greater than the variation observed in the replicate pairs or the intra-status comparisons. This was expected as inter-status comparisons are between different diseased cases and controls.

From these results, the average percentage of genes which were flagged as regulated in comparison group 2 was ~38% at the 2-fold threshold limit, consistent with the result in comparison group 1. An average CV of 40% indicated a greater level of variability in the data than for replicates or intra-status comparison.

The average percentage of genes flagged as regulated in comparison group 5 was ~20% at the 2-fold threshold limit, with an average CV of 37%. The percentage of genes flagged as regulated is slightly lower than observed in comparison group 1 and 2, although the degree of variation is consistent. The reason for this is unclear. In this comparison groups cases were female, but is unlikely that gender affected the results, as previous analysis on gender/age effects were minimal.

6.4.3.1 Comparison group 1

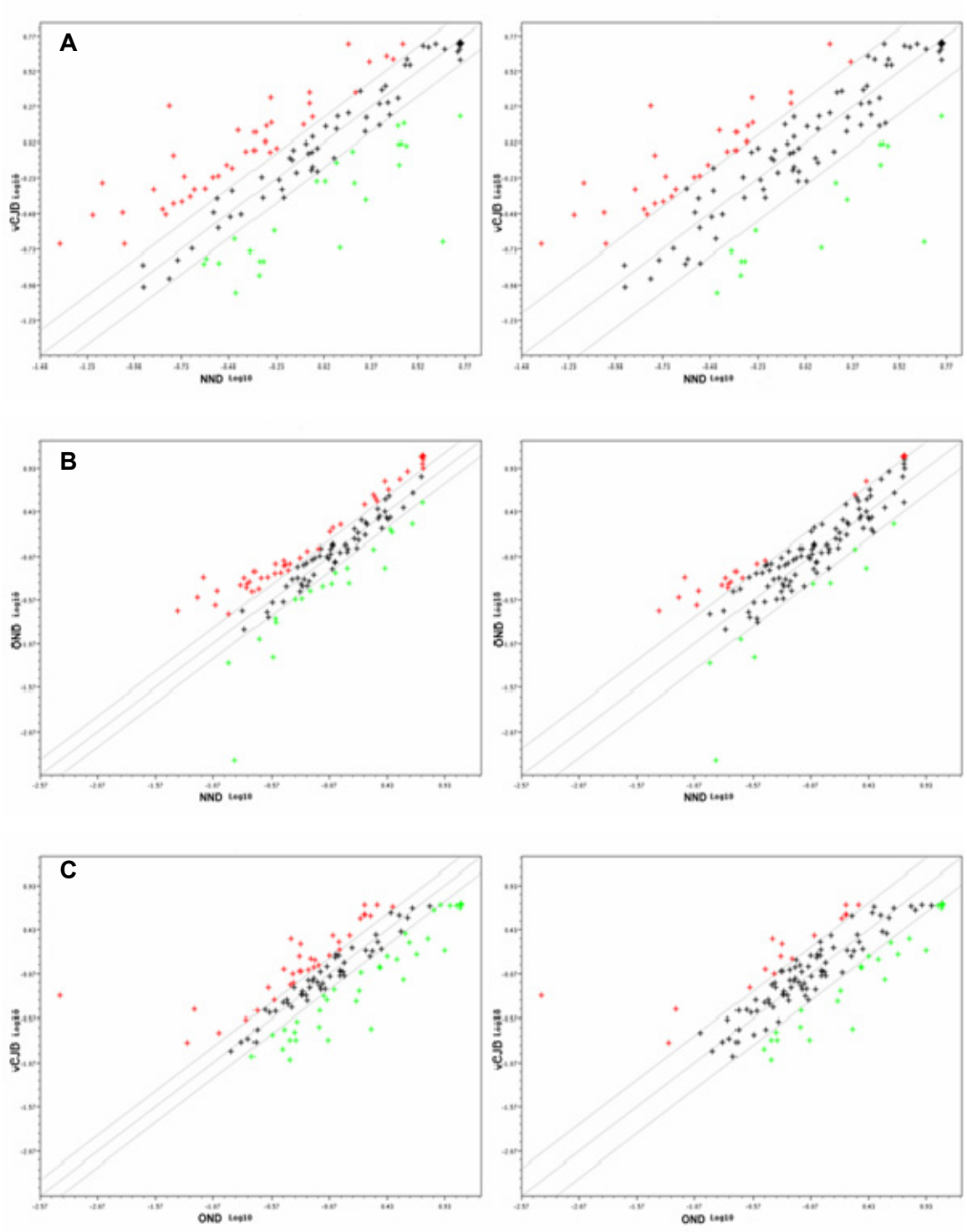

Figure 6.12. Scatter plot of inter-status comparisons of group 1. Panel A. vCJD vs NND. Panel B. OND vs NND. Panel C. vCJD vs OND. Left panels. Outer lines represent 1.5-fold threshold boundary of gene spot density changes. Right panels. Outer lines represent 2- fold threshold boundary of gene spot density changes. Red points represent genes up-regulated; green points represent genes down-regulated on the y-axis sample. Axes are $\log_{10}$ spot density values.

6.4.3.2 Comparison group 2

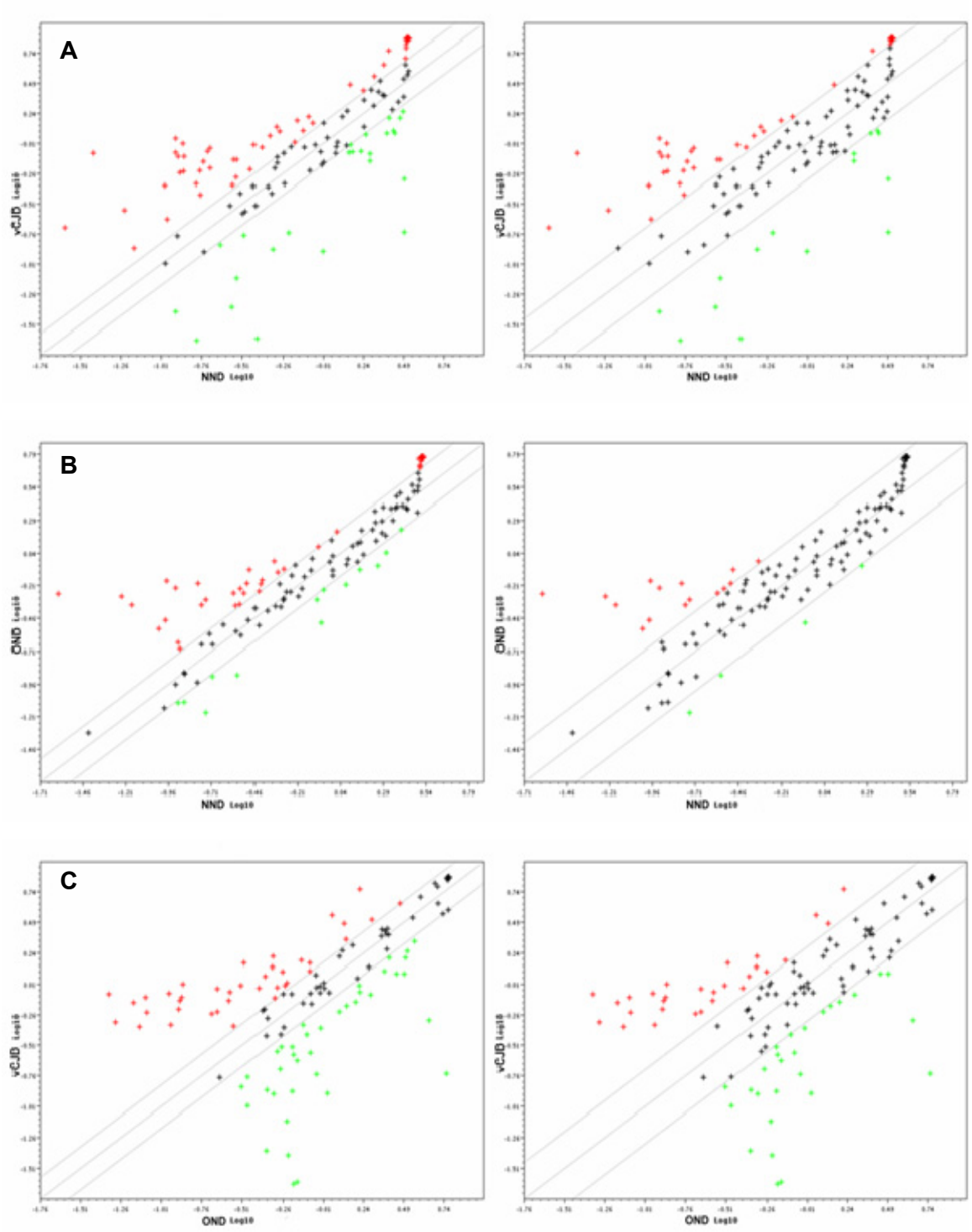

Figure 6.13. Scatter plot of inter-status comparisons for group 2. Panel A. vCJD vs NND. Panel B. OND vs NND. Panel C. vCJD vs OND. Left panel. Outer lines represent 1.5-fold threshold boundary of gene spot density changes. Right panel. Outer lines represent 2-fold threshold boundary of gene spot density changes. Red points represent genes up-regulated; green points represent genes down-regulated on y-axis sample. Axes are $\log_{10}$ spot density values.

6.4.3.3 Comparison group 5

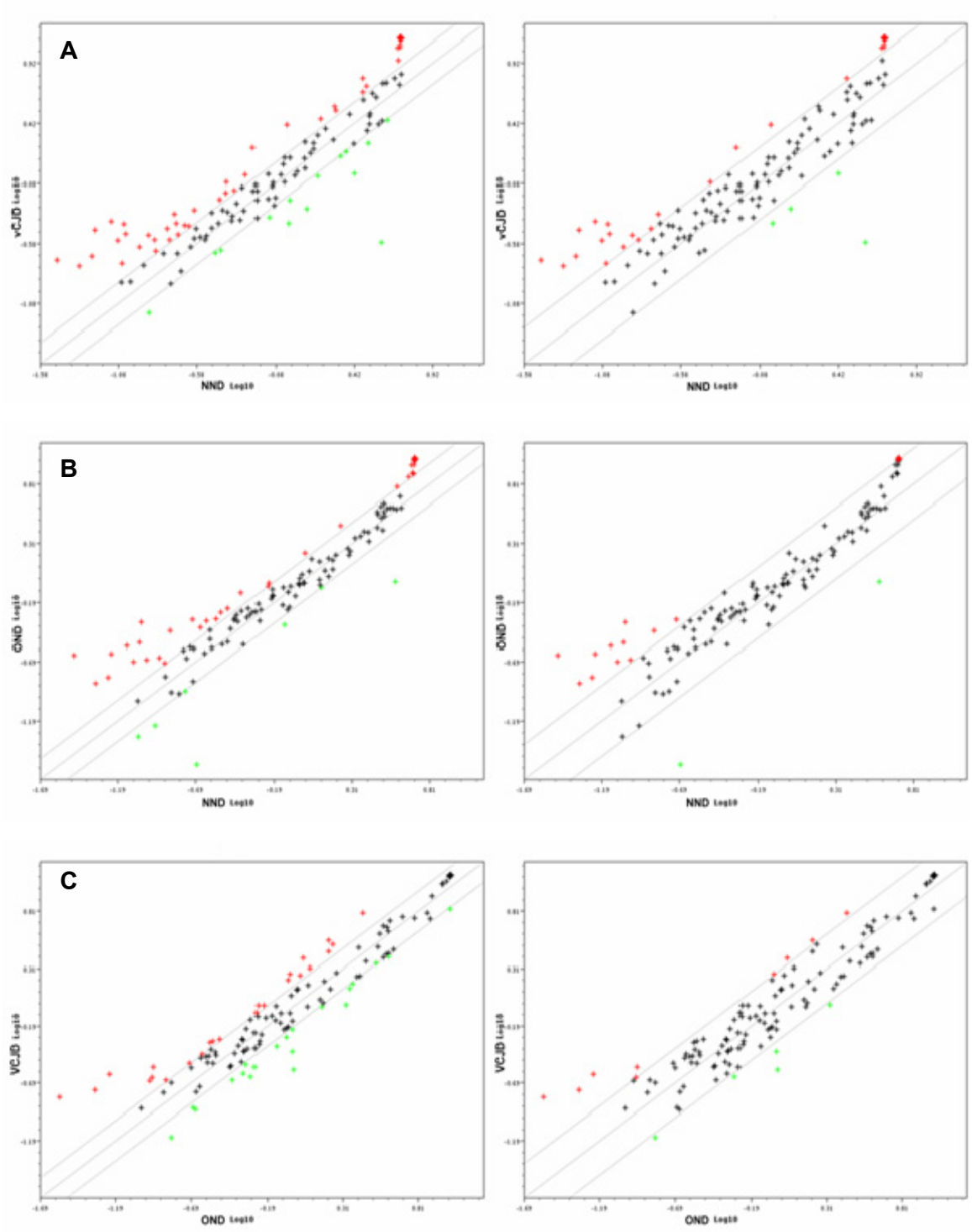

Figure 6.14. Scatter plot of inter-status comparisons for group 5. Panel A. vCJD vs NND. Panel B. OND vs NND. Panel C. vCJD vs OND. Left panel. Outer lines represent 1.5-fold threshold boundary of gene spot density changes. Right panel. Outer lines represent 2-fold threshold boundary of gene spot density changes. Red points represent genes up-regulated; green points represent genes down-regulated on y-axis sample. Axes are $\log_{10}$ spot density values.

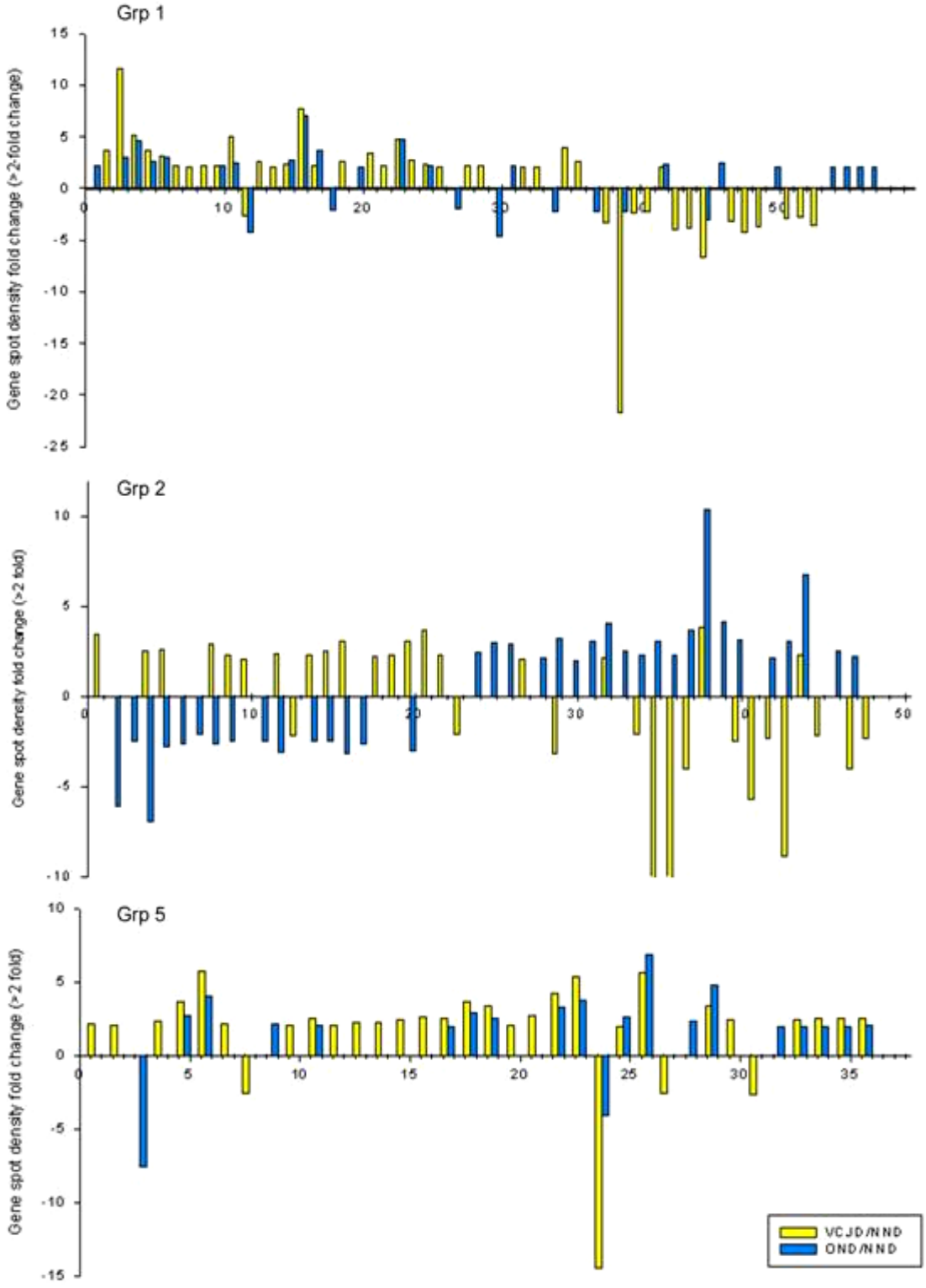

Figure 6.15 Bar chart representing genes with greater than 2-fold change in expression levels, as determined by normalized densitometric analysis of gene arrays. (see Appendix Table 9.6-8 for tabulated gene names). X-axis is the order in which genes showing ≥2-fold change were flagged, based on chip position and may not match across charts.

Differentially expressed genes which were flagged in vCJD vs NND and vCJD vs OND, but not flagged in OND vs NND comparisons were considered to be potential vCJD-specific gene changes. Group 1, 2 and 5 comparisons of vCJD vs NND/OND showed 57, 48 and 36 genes with >2.0-fold change respectively.

Figure 6.16 compares comparison group with one another. If the assumption is made that there is no gender/age effects, the datasets represents the disease status effects across the comparison groups.

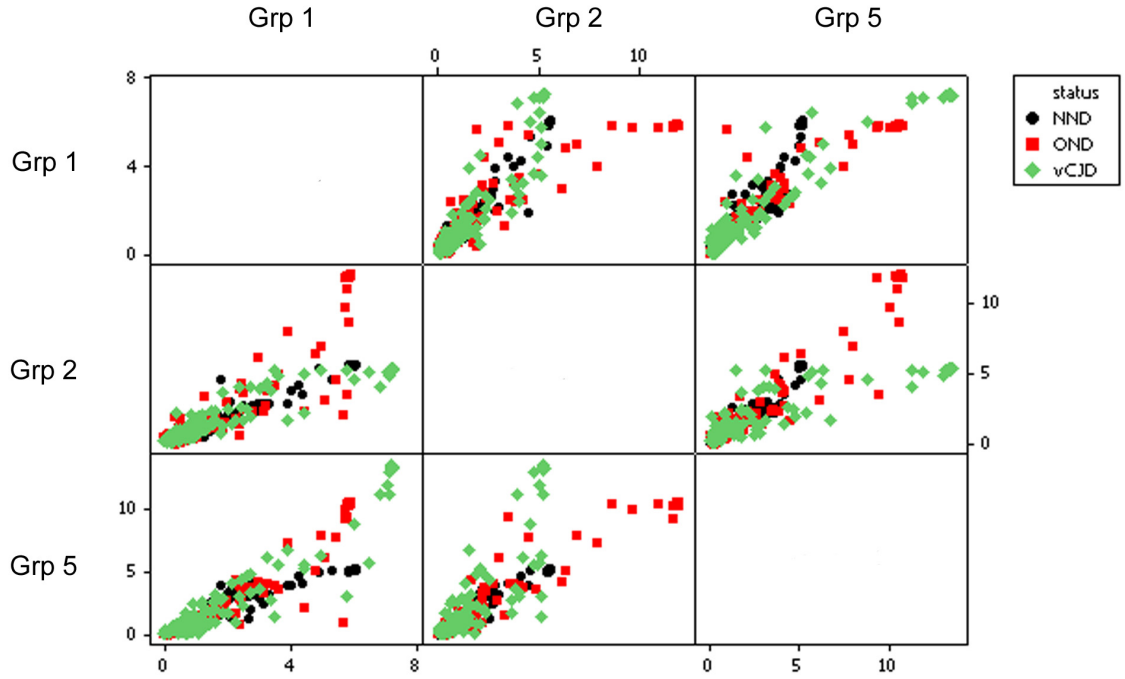

Figure 6.16. Integrated matrix plot of all three comparison groups, separated into status, based on AD array results.

Comparison of the data sets across comparison groups shows whether there were any disease status effects of the case. Looking at each individual scatter, for example, vCJD cases correlate more closely to one another than to OND/NND cases. Due to the lack of biological replicates, it was not possible to determine exactly where the effect was coming from. Sections 6.4.1 and Section 6.4.2 shows there are limited replicate and age/gender effect, so it is reasonable to assume that there are

differences between the different disease status cases, regardless of age/gender. This suggests it will be possible to identify potential disease-specific changes. OND cases in all comparisons were the most scattered indicating the greatest amount of variation when compared across comparison groups. This is to be expected, as the disease of the OND case in each group were not the same disease. NND cases are very closely clustered, suggested very little spread of the data, regardless of comparison group effect. Since NND cases were selected on the same criteria, i.e. short agonal state, no pre-existing disease etc, this clustering is not surprising. This results is in agreement with the data from the clustergram (Figure 6.17).

6.4.4 Clustergram

Hierarchical clustering partitions data points into subsets (clusters), such that points within each cluster are more closely related to one another than points assigned to different clusters. In this case, API was clustered by ratios relative to the central (control) case. Each row represents a specific gene and each column a specific disease status (Figure 6.17). OND and NND cases are more similar to one another than they are to vCJD cases.

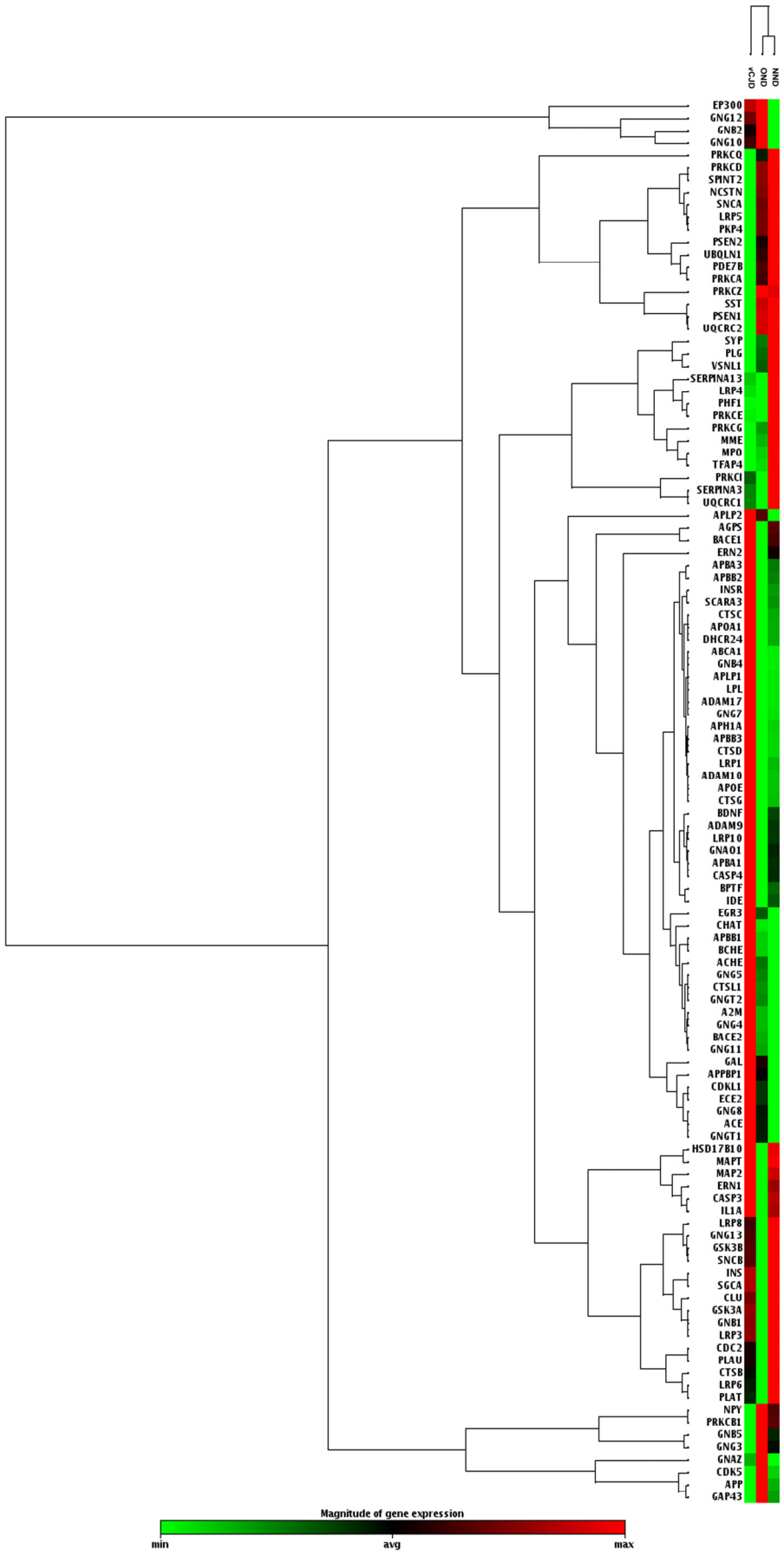

Figure 6.17. Clustergram analysis of all AD Specific oligoarrays, carried out on GEarray Expression Anlaysis Suite web-based software. Genes which are more similar are joined at lower heights in the dendrogam and those that are less similar are joined at higher heights. Average linkage methods were used. The colour-coding legend (below) displays the maximum values as red (furthest right) and minimum values as green (furthest left), as a function of the samples (vertical direction). The vertical dendrogram links the comparison groups according to similarity.

Based on all 16 AD arrays, it was possible to generate volcano-plots for vCJD vs NND and OND vs NND. Volcano plots summarize both fold-change and t-test criteria. Briefly, a volcano plot is a scatter plot of the negative $\log_{10}$-transformed p-values from the gene specific t-test plotted against the $\log_2$ fold-change. Genes with statistically differential expression, according to the gene specific t-test, lie above the horizontal threshold line. Genes with large fold-change values lie outside the pair of vertical threshold lines (set at 1.5-fold here). The significant genes identified by the fold-change and p-value boundaries are located in the upper left (down-regulated) or upper right (up-regulated) sectors of the plot. Figure 6.18A highlights the statistically significant regulated genes in the vCJD vs NND comparisons. Figure 6.18B highlights the statistically significant regulated genes in the OND vs NND comparisons. Figure 6.19 is a graphical representation of the genes observed to have ≥ 2-fold change in expression. Table 6.3, 6.4 and 6.5 list the significantly regulated genes and respective fold-changes.

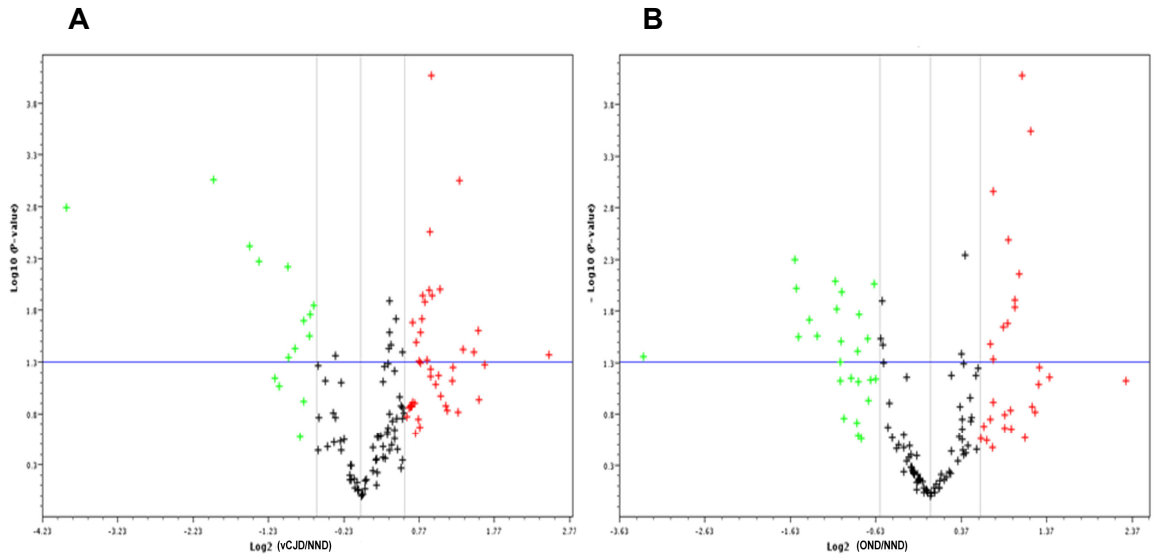

Figure 6.18. Volcano plots of relative gene expression, based on all 16 AD arrays. A. all vCJD vs NND. B. all OND vs NND. Horizontal lines are set at 0.05 significance threshold limits. Vertical lines are set at 1.5-fold change threshold limits. Red points represent genes up-regulated; green points represent down-regulated genes. X-Axis is negative $\log_{10}$-transformed p-values and Y-axis is log2 fold-change.

At the 1.5-fold change threshold (significance level= 0.05), there were 18 up-regulated and 10 down-regulated genes from the vCJD vs NND comparison

(Figure6.18A, Table 6.3). For the same criteria, 19 genes were up-regulated and 2 genes were down-regulated from the OND vs NND comparison (Figure 6.18B, Table 6.4). Only 1 gene was flagged in both comparisons (ERN2). For vCJD vs OND comparisons 11 genes were up-regulated and 13 were down-regulated (graph not shown, see Table 6.5); 16 of these were identical to those flagged in the vCJD vs NND comparison, suggesting these genes are vCJD-specific changes. The GEArray Expression Analysis Suite determines significance using a conservative method which utilizes a logarithmic transformation of the raw data, de-emphasizes the contribution of outliers and noise and facilitates comparisons across experiments. Figure 6.19 shows genes which were significantly regulated with a >2.0 fold change.

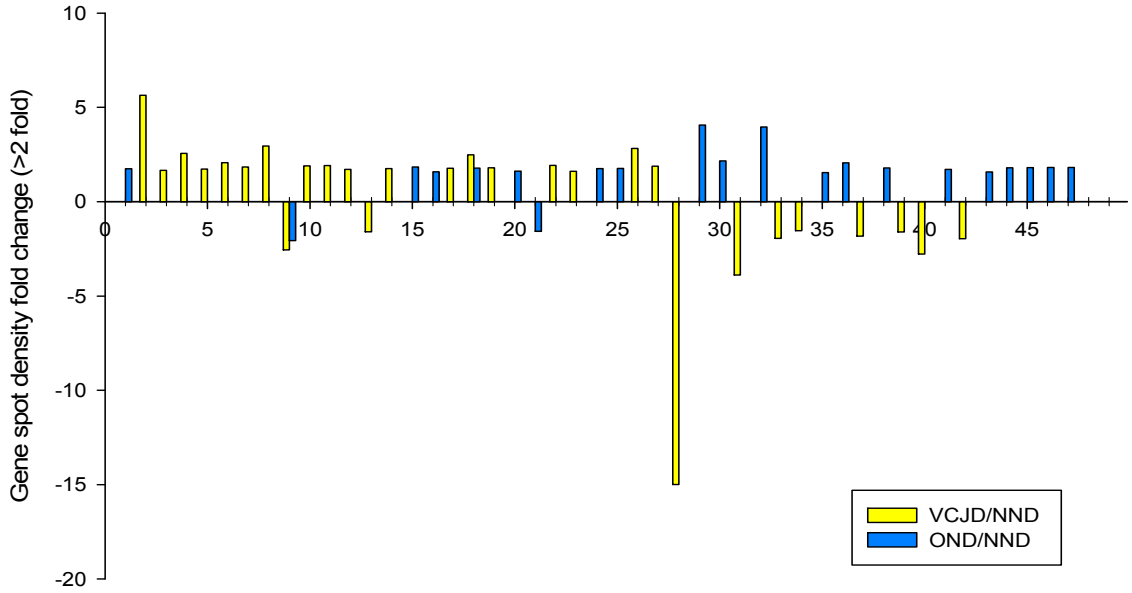

Figure 6.19. Bar chart representing significantly regulated genes with greater than 2-fold change in expression levels, as determined by normalized densitometric analysis of gene arrays. (see Appendix Table 9.9 for tabulated gene names).

Of the 28 significantly ($p<0.05$) regulated genes in vCJD vs NND, 10 were down-regulated and 18 up-regulated. Functional clustering revealed 39% were involved in β-amyloid generation, oligomerization, clearance, and degradation,; 32% in cell signaling, 25% in synaptic formation and 21% in cholesterol or lipid metabolism. There were 21 significantly regulated genes in OND vs NND, of which only 2 were down-regulated. 19% were involved in β-amyloid generation, oligomerization,

clearance, and degradation, but only APP was common to both comparisons. 23% were involved in cell signaling and 9% in lipid metabolism, but these were all unique genes to this particular comparison. There were no synaptic formation genes flagged. The 24 significantly regulated gene in vCJD vs OND showed 13 down-regulated genes (refer to Table 6.4). Of these 24, 15 were also regulated in vCJD vs NND comparison but not in the OND vs NND comparison (refer to Table 6.2, 6.3). That these 15 genes were flagged in these two comparisons (vCJD vs NND and vCJD vs OND) strongly suggests that they are vCJD-specific changes. 33% were involved in β-amyloid generation, oligomerization, clearance, and degradation, none of which were flagged in the OND vs NND comparison, but 5 were also flagged in the vCJD vs NND comparison. 46% of genes were involved in cell signaling, none of which were present in the OND vs NND comparison but 6 were present in the vCJD vs NND comparison.

6.4.5 SAM Analysis of AD Arrays

False discovery rates (FDR) are not calculated by the GEArray software, and CV values are not adjusted. To gain an indication of the FDR, Significance Analysis of Microarrays (SAM) analysis was also carried out. Significance Analysis of Microarrays (SAM) software was used to determine the false discovery rate (FDR) and to avoid problems associated with multiple testing. Software downloads and details on formula and programming are available at http://www-stat.stanford.edu/~tibs/SAM/. Briefly, SAM calculates a test statistic for relative difference in gene expression data and calculates a FDR. This analysis is based on non-parametric statistics which may be more appropriate since gene expression data may not follow a normal distribution. By using a calculated constant to modify the coefficient of variance, SAM analysis accounts for the range of variation and applies a weighting for smaller values. SAM analysis requires a minimum sample size to calculate significance and FDR. Therefore analysis had to be done across all comparison groups. This requires the assumption that there are no differences between cases of the same disease status (i.e.vCJD cases, for example, are the same, irrespective of age/gender). SAM software was used to calculate statistically significant gene expression changes and the FDR of all the AD arrays, using vCJD, OND and NND as three parameters and analyzing in a pair-wise method. Figure 6.20 shows the SAM plot output for AD array results.

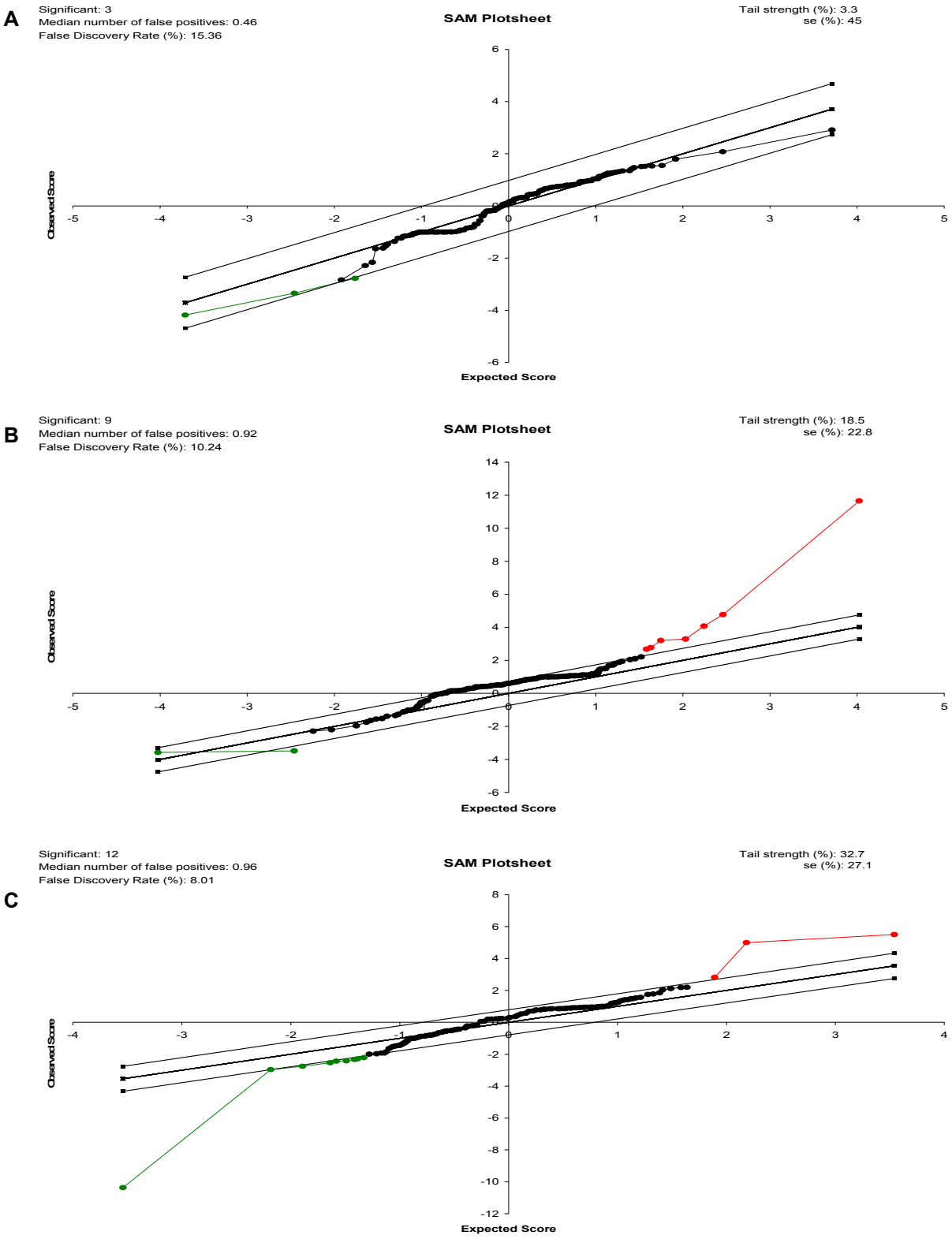

Figure 6.20. SAM analysis of all inter-status comparisons. Panel A. vCJD vs NND. FDR = 15.36%. Significantly up-regulated genes = 0. Significantly down-regulated genes = 3. Panel B. OND vs NND. FDR = 10.24%. Significantly up-regulated genes = 7. Significantly down-regulated genes = 2. Panel C. vCJD vs OND. FDR = 8.01%. Significantly up-regulated genes = 3. Significantly down-regulated genes = 9. Outer lines represent 1.5-fold threshold limit. Red plots represent significantly up-regulated genes. Green plots represent significantly down-regulated genes.

SAM analysis calculated; 0 up- and 3 down-regulated genes in vCJD vs NND, 7 up- and 2 down-regulated genes in OND vs NND and 3 up- and 9 down-regulated genes in vCJD vs OND comparisons. The small sample size of this analysis means that the strength of any findings is limited and the SAM analysis of significance may be too stringent in this case. SAM analysis revealed FDR's of 15%, 8% and 10% for vCJD vs NND, OND vs NND and vCJD vs OND, respectively. Generally FDR thresholds of 5% or less are accepted, in order to limit false-positive identification, but to avoid losing relevant information, FDR thresholds at the 1.5-fold level, were more flexible to allow identification of significance. If the FDRs calculated from SAM analysis is used with the significance as calculated by GEArray Expression Analysis Suite, of the 28 vCJD vs NND significantly modulated genes, potentially 4could be false discoveries, of the 21 OND vs NND flagged genes, 2 may be falsely discovered and of the 24 vCJD vs OND significant genes, 2 potentially are false discoveries.

The number of significantly regulated genes calculated by the SAM analysis was not in good agreement with the numbers calculated by the GEArray Expression Analysis Suite. This was due to differences in statistical formulae and the use of the modified coefficient of variance formulae used by the SAM software. On such small sample sizes, is would be difficult to obtain meaningful significant data. Similar studies on sCJD did not use age/gender matched cases (Xiang *et al.*, 2005), so although the data yielded more significant results, it is not possible to determine whether age or gender affected the expression levels observed. Evidence of gender and age-related changes have been published, therefore it is reasonable to assume that there may be age- or gender- related effects (Galvin & Ginsburgh, 2005; Vawter *et al.*, 2004; Colantuoni *et al.*, 2008).

Gene	UniGene	Description	*Fold-change*	*p-Value*
ABCA1	Hs.429294	ATP-binding cassette, sub-family A (ABC1), member 1	5.64	0.04
APBA1	Hs.592974	Amyloid beta (A4) precursor protein-binding, family A, member 1 (X11)	1.67	0.03
APBA3	Hs.465607	Amyloid beta (A4) precursor protein-binding, family A, member 3 (X11-like 2)	2.57	0.04
APH1A	Hs.108408	Anterior pharynx defective 1 homolog A (C. elegans)	1.73	0.03
APLP1	Hs.74565	Amyloid beta (A4) precursor-like protein 1	2.07	0.01
APOA1	Hs.633003	Apolipoprotein A-I	1.84	0.05
APOE	Hs.515465	Apolipoprotein E	2.95	0.03
BACE2	Hs.529408	Beta-site APP-cleaving enzyme 2	1.89	0.00
BCHE	Hs.420483	Butyrylcholinesterase	1.92	0.00
BDNF	Hs.502182	Brain-derived neurotrophic factor	1.71	0.05
CHAT	Hs.302002	Choline acetyltransferase	1.76	0.02
CTSD	Hs.121575	Cathepsin D	1.77	0.01
ERN2	Hs.592041	Endoplasmic reticulum to nucleus signalling 2	2.48	0.00
BPTF	Hs.444200	Bromodomain PHD finger transcription factor	1.80	0.01
GNB4	Hs.270543	Guanine nucleotide binding protein (G protein), beta polypeptide 4	1.93	0.01

GNG5	Hs.645427	Guanine nucleotide binding protein (G protein), gamma 5	1.61	0.02
LPL	Hs.180878	Lipoprotein lipase	2.83	0.04
LRP10	Hs.525232	Low density lipoprotein receptor-related protein 10	1.88	0.01
APP	Hs.434980	Amyloid beta (A4) precursor protein (peptidase nexin-II, Alzheimer disease)	0.39	0.01
CDK5	Hs.647078	Cyclin-dependent kinase 5	0.63	0.02
NPY	Hs.1832	Neuropeptide Y	0.07	0.00
PRKCB1	Hs.460355	Protein kinase C, beta 1	0.26	0.00
PRKCZ	Hs.496255	Protein kinase C, zeta	0.51	0.05
PSEN1	Hs.592324	Presenilin 1 (Alzheimer disease 3)	0.65	0.01
SNCA	Hs.271771	Synuclein, alpha (non A4 component of amyloid precursor)	0.55	0.04
SPINT2	Hs.31439	Serine peptidase inhibitor, Kunitz type, 2	0.62	0.03
SST	Hs.12409	Somatostatin	0.36	0.00
UQCRC2	Hs.592048	Ubiquinol-cytochrome c reductase core protein II	0.51	0.01

Table 6.3.Differentially expressed genes from vCJD vs NND comparisons revealed by focused AD microarray analysis. Fold-change threshold limit = 1.5. Significance level = 0.05. Red= up-regulated genes. Green = down-regulated genes.

SYMBOL	UniGene	Description	*Fold-change*	*p-Value*
RPS27A	Hs.311640	Ribosomal protein S27a	1.74	0.02
CLU	Hs.436657	Clusterin	1.84	0.01
CTSB	Hs.520898	Cathepsin B	1.59	0.03
ERN2	Hs.592041	Endoplasmic reticulum to nucleus signalling 2	1.79	0.00
GNB1	Hs.430425	Guanine nucleotide binding protein (G protein), beta polypeptide 1	1.62	0.02
GSK3A	Hs.466828	Glycogen synthase kinase 3 alpha	1.75	0.02
IL1A	Hs.1722	Interleukin 1, alpha	1.76	0.02
PLAT	Hs.491582	Plasminogen activator, tissue	4.06	0.04
PLAU	Hs.77274	Plasminogen activator, urokinase	2.17	0.02
PRKCI	Hs.478199	Protein kinase C, iota	3.96	0.00
SERPINA13	Hs.527795	Serpin peptidase inhibitor, clade A (alpha-1 antiproteinase, antitrypsin), member 13 (pseudogene)	1.54	0.02
SERPINA3	Hs.510334	Serpin peptidase inhibitor, clade A (alpha-1 antiproteinase, antitrypsin), member 3	2.06	0.01
SNCB	Hs.90297	Synuclein, beta	1.79	0.01
UQCRC1	Hs.119251	Ubiquinol-cytochrome c reductase core protein I	1.71	0.00
VSNL1	Hs.444212	Visinin-like 1	1.57	0.03

HSP90AB1	Hs.509736	Heat shock protein 90kDa alpha (cytosolic), class B member 1	1.80	0.01
HSP90AB1	Hs.509736	Heat shock protein 90kDa alpha (cytosolic), class B member 1	1.80	0.01
ACTB	Hs.520640	Actin, beta	1.81	0.01
ACTB	Hs.520640	Actin, beta	1.82	0.01
APP	Hs.434980	Amyloid beta (A4) precursor protein (peptidase nexin-II, Alzheimer disease)	0.48	0.03
GNB2	Hs.185172	Guanine nucleotide binding protein (G protein), beta polypeptide 2	0.64	0.02

Table 6.4 Differentially expressed genes from OND vs NND comparisons revealed by focused AD microarray analysis. Fold-change threshold limit = 1.5. Significance level = 0.05. Red = up-regulated genes. Green = down-regulated genes.

SYMBOL	UniGene	Description	*Fold-change*	*p-Value*
APH1A	Hs.108408	Anterior pharynx defective 1 homolog A (C. elegans)	1.63	0.03
APLP1	Hs.74565	Amyloid beta (A4) precursor-like protein 1	1.99	0.01
BACE2	Hs.529408	Beta-site APP-cleaving enzyme 2	2.26	0.00
BCHE	Hs.420483	Butyrylcholinesterase	2.11	0.00
CDKL1	Hs.280881	Cyclin-dependent kinase-like 1 (CDC2-related kinase)	2.06	0.01
CHAT	Hs.302002	Choline acetyltransferase	1.82	0.02
CTSD	Hs.121575	Cathepsin D	1.67	0.05
ECE2	Hs.146161	Endothelin converting enzyme 2	1.67	0.00

EGR3	Hs.534313	Early growth response 3	1.89	0.00
GNB4	Hs.270543	Guanine nucleotide binding protein (G protein), beta polypeptide 4	1.87	0.02
GNG5	Hs.645427	Guanine nucleotide binding protein (G protein), gamma 5	1.99	0.01
NCSTN	Hs.517249	Nicastrin	0.40	0.03
NPY	Hs.1832	Neuropeptide Y	0.10	0.04
PKP4	Hs.407580	Plakophilin 4	0.60	0.03
PLG	Hs.143436	Plasminogen	0.38	0.02
PRKCA	Hs.531704	Protein kinase C, alpha	0.34	0.03
PRKCB1	Hs.460355	Protein kinase C, beta 1	0.34	0.01
PRKCQ	Hs.498570	Protein kinase C, theta	0.49	0.03
PSEN1	Hs.592324	Presenilin 1 (Alzheimer disease 3)	0.63	0.01
SNCA	Hs.271771	Synuclein, alpha (non A4 component of amyloid precursor)	0.46	0.01
SPINT2	Hs.31439	Serine peptidase inhibitor, Kunitz type, 2	0.56	0.02
SST	Hs.12409	Somatostatin	0.33	0.01
UQCRC2	Hs.592048	Ubiquinol-cytochrome c reductase core protein II	0.49	0.01
VSNL1	Hs.444212	Visinin-like 1	0.47	0.02

Table 6.5. Differentially expressed genes from vCJD vs OND comparisons revealed by focused AD microarray analysis. Fold-change threshold limit = 1.5. Significance level = 0.05. Red = up-regulated genes. Green = down-regulated genes.

6.5 SIGNAL TRANSDUCTION PATHWAY FINDER GENE ARRAYS

Signal transduction pathway finder gene arrays were analysed as described for AD arrays. Expression of 113 genes (Appendix 9.10, Table 9.5) representative of 18 signal transduction pathways were screened by a cDNA-based microarray technique using the GEarray Q series nonradioactive Signal Transduction Pathway Finder (Tebu-Bio, Cambs, UK), using total RNA (1 µg) from brain tissue of vCJD (n=3) , OND (n=3) and NND (n=3) controls. Examples are shown in Figure 6.21.

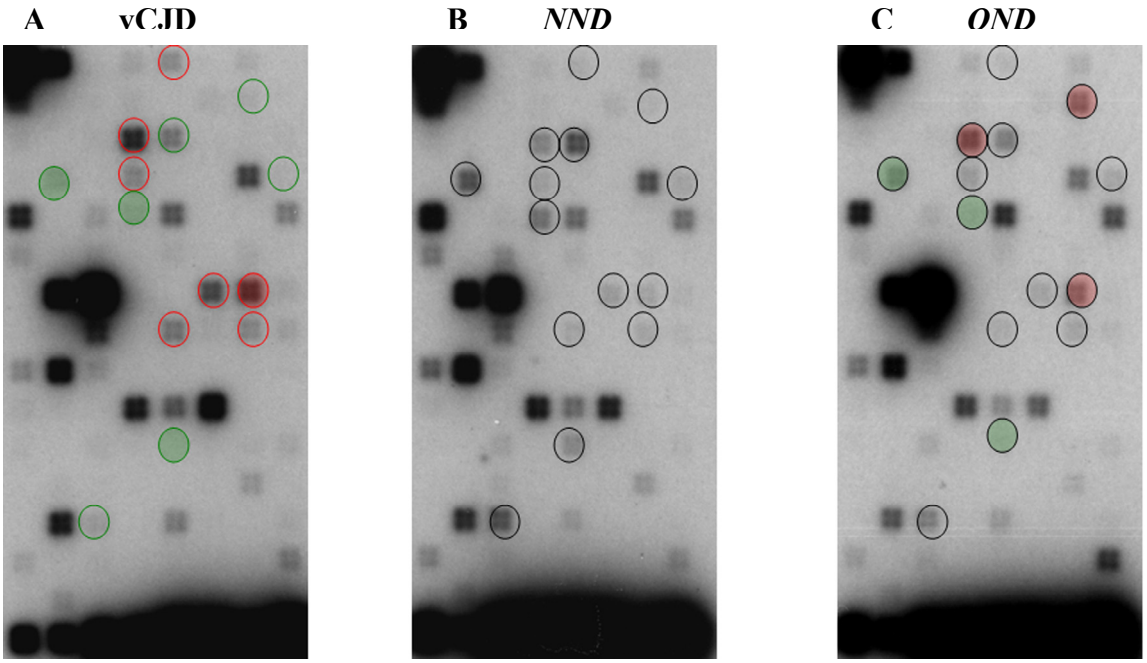

Figure 6.21. Array images (un-edited) of comparison group 2 (see Table 6.1). Total RNA extracted from control cases and vCJD cases was labeled and hybridized to membranes pre-loaded with 96 cDNA representing disease specific genes of interest. Representative images of three membranes hybridized to labeled RNA extracted from vCJD (A), NND control (B) and OND control (C) are shown. Gene spots encased in red circles are induced in vCJD compared to normalized NND and OND controls. Gene spots encased in green squares are reduced. Filled red circles are induced compared to NND controls only. Filled green circles are reduced compared to NND controls only.

6.5.1 Reproducibility and Variation Between Replicates

The reproducibility of replicate arrays was assessed by amplifying a single RNA preparation and hybridizing 2 µg cRNA to two separate ST arrays which were processed in parallel. This was carried out on all cases in comparison group 2 only. Figure 6.22A represents one such replicate set. Figure 6.22B shows the multiple regression analysis of an example replicate set. Figure 6.23 shows scatter plots of replicate cases from comparison group 2.

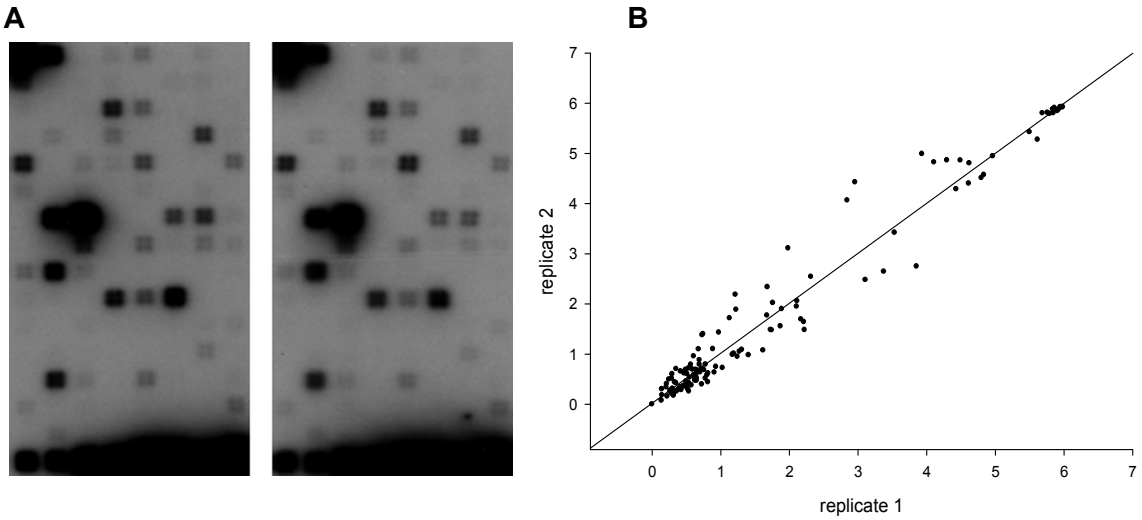

Figure 6.22. A. Replicate array images of case 129. B. Scatter plot of replicate 1 against replicate 2. Axis values are $\log_{10}$ gene spot densities. r2 = 0.963.

Multiple regression analysis reveals a significant correlation coefficient of 0.96, suggesting that replicate arrays are highly correlated. The average CV value (based on internal chip control spots) was 8%. Therefore, reproducibility of hybridization and array processing was considered satisfactory and it was assumed that replicate effect on gene variation for subsequent analyses was minimal. In Figure 6.22B, it is clear that the scatter plot points are clustered tightly for the majority of the genes, indicating good reproducibility.

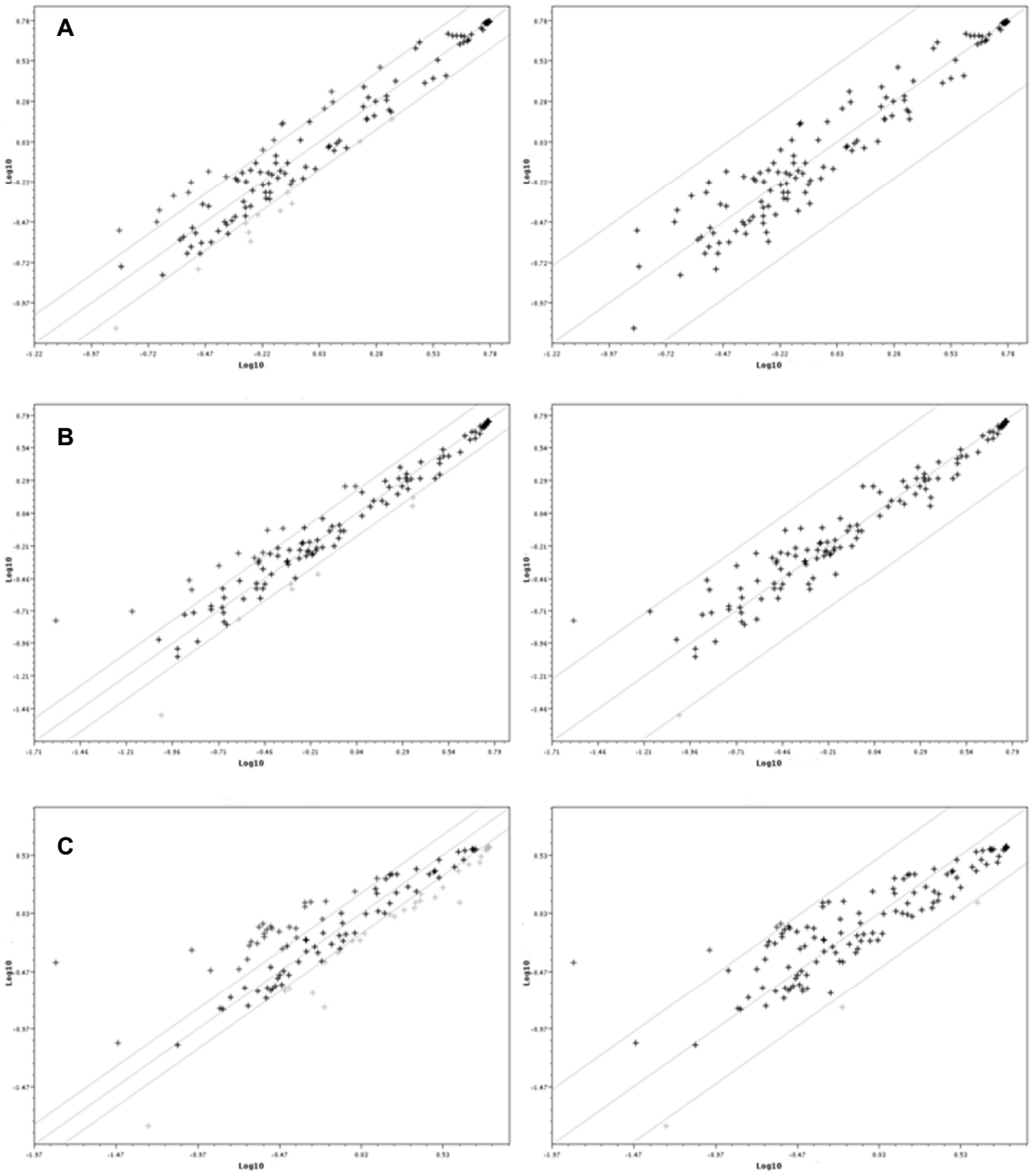

Figure 6.23. Scatter plot of relative spot density of replicate 1 plotted against replicate 2 from comparison group 2. Panel A. vCJD. Panel B. NND. Panel C.OND. All panels show boundaries as outer lines, of 1.5 fold (left) and 3.0 fold (right). Axis are $\log_{10}$ spot density values.

6.5.2 Intra-Status Effect

The next assessment was to determine the degree of variation of gene spot density between same status cases (i.e vCJD vs vCJD). Figures 6.24, 6.26, 6.28 show integrated matrix plots representing all possible intra-status combinations. Figures 6.25, 6.27, 6.29 show more detailed examples of individual intra-status comparisons. Table 6.6 gives the correlation coefficients (r^2) and coefficient of variation (CV) for each comparison.

vCJD

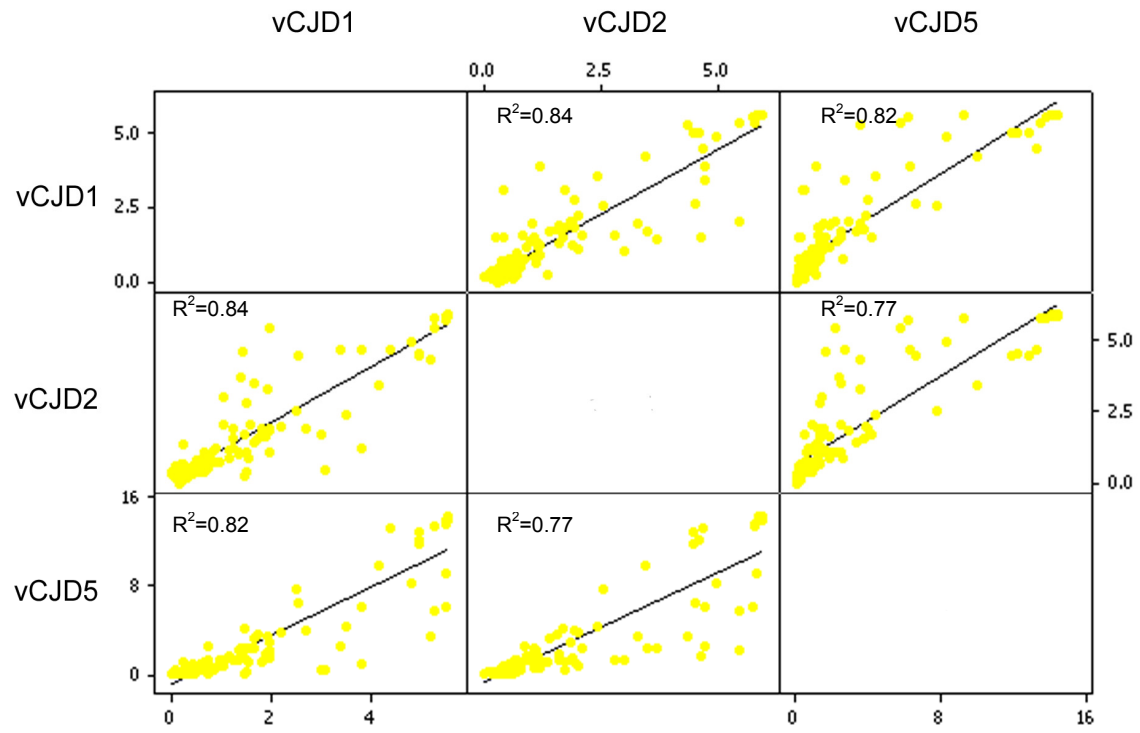

Figure 6.24. Integrated matrix plots of all vCJD cases plotted against each other. Lines represent multiple regression analysis.

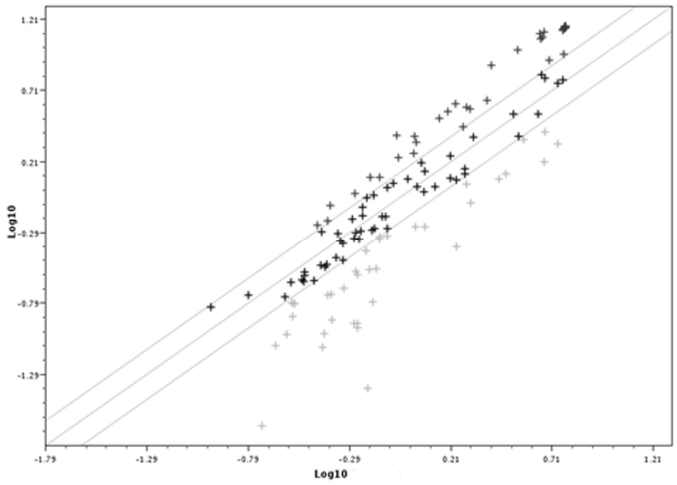

Figure 6.25. Scatter plot of vCJD2 against vCJD5. Outer diagonal lines represent 1.5-fold threshold limits. Axes are $\log_{10}$ spot density values.

OND

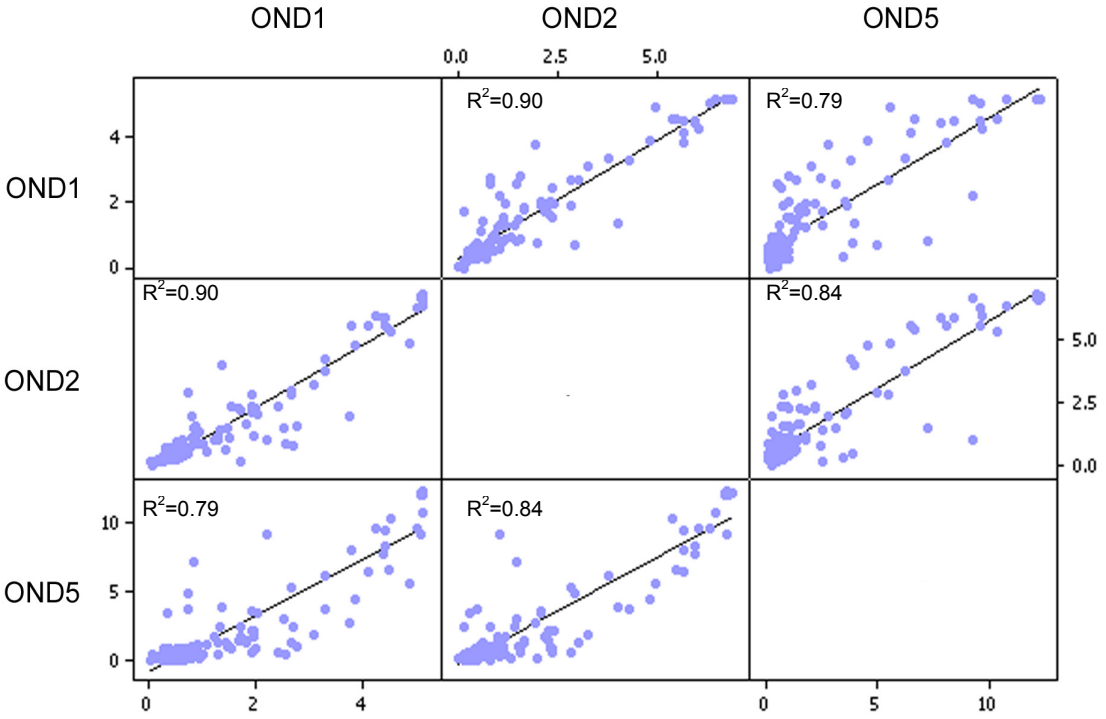

Figure 6.26. Integrated matrix plots of all OND cases plotted against each other. Lines represent multiple regression analysis.

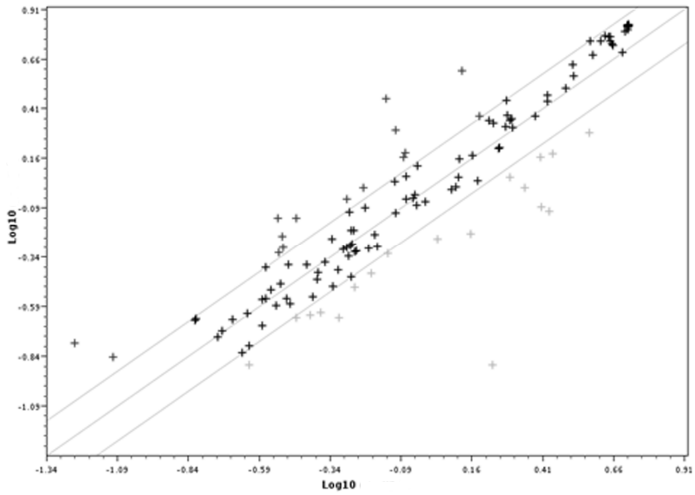

Figure 6.27. Scatter plot of OND2 against OND5. Outer diagonal lines represent 1.5-fold threshold limits. Axes are $\log_{10}$ spot density values.

NND

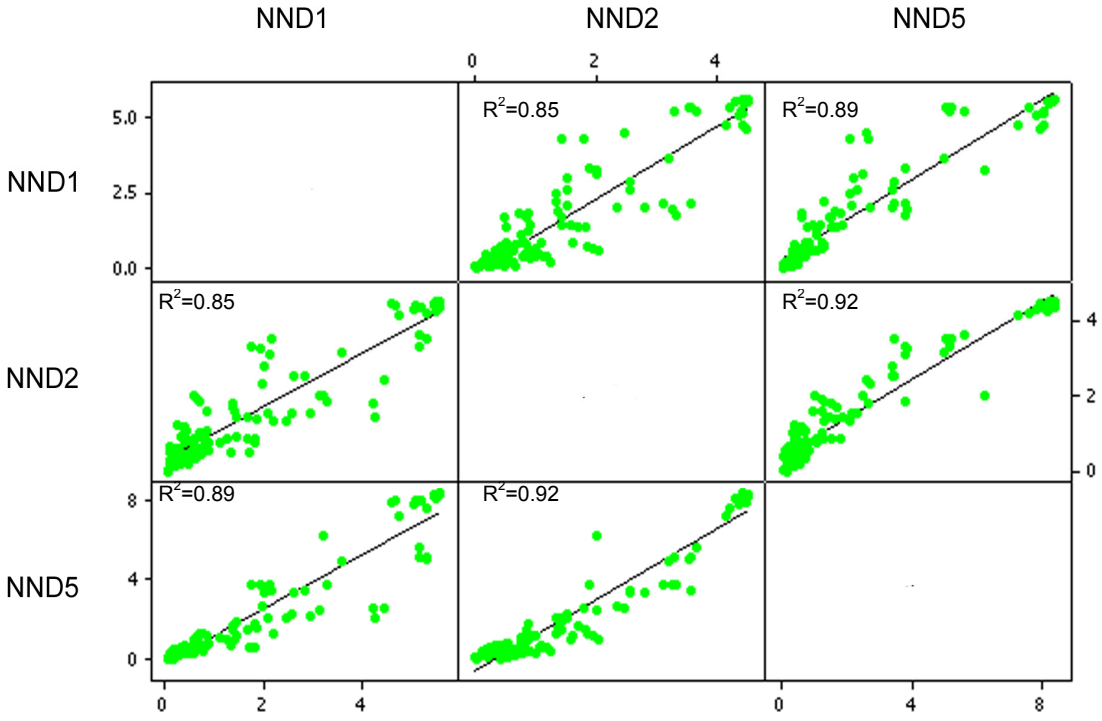

Figure 6.28. Integrated matrix plots of all NND cases plotted against each other. Lines represent multiple regression analysis.

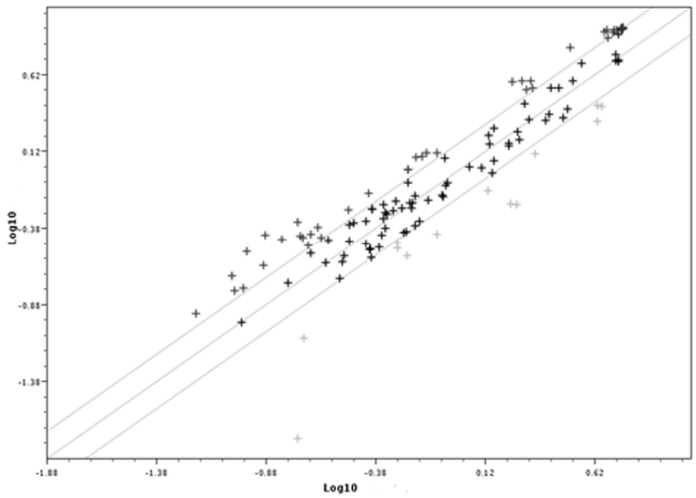

Figure 6.29. Scatter plot of NND1 against NND2. Outer diagonal lines represent 1.5-fold threshold limits. Axes are $\log_{10}$ spot density values.

	Correlation coefficient (r^2)	Coefficient of Variation (CV) (%)
vCJD vs vCJD	0.81	9
OND vs OND	0.84	3
NND vs NND	0.89	4

Table 6.6. Correlation coefficient and coefficient of variation values for all intra-status comparison.

The average CV values (Table 6.6) indicate that the data are closely clustered around the mean and the r^2 values show close correlation between cases of the same status. CV and r^2 values were similar across all intra-status comparisons and are similar to the values calculated from the AD arrays. Taken together, this suggests that age/gender effects are limited.

6.5.3 Inter-Status, Matched Cases

As for the AD array analysis, the level of variation observed between matched disease and control cases was evaluated. This was done by comparing gene spot density between disease-specific (vCJD) vs non-diseased controls (NND) and disease-unspecific (OND) vs non-diseased controls (NND), within the matched comparison groups (see Table 6.1). This method of comparison removes gender-

specific and age-related confounding effects; any variation is likely to be due to disease regulated gene expression. The analysis is broken into comparison groups 1, 2 and 5. Figure 6.30, 6.31 and 6.32 show vCJD vs NND, OND vs NND and vCJD vs OND comparisons respectively, set at 1.5- (left) and 2-fold (right) boundary threshold limits. Figure 6.33 is a graphical representation of genes observed with ≥ 2-fold changes in gene spot density.

The average percentage of genes which were flagged as regulated in comparison grou p1 was ~34%, at the 2-fold threshold limit. The average CV across all comparisons was 49%. This is consistent with the results from comparison group 1 using the AD arrays.

In comparison group 2, the average percentage of genes which were flagged as regulated was ~17% at the 2-fold threshold limit. An average CV of 27% was observed. This result is in contrast to the result observed in comparison group 2 from the AD array results. Less variation in the data may indicate that the selection of genes on the signal transduction array may not be greatly altered during vCJD disease. This is not to suggest there is no relevant results observed, simply that the genes selected for the AD array were more relevant to the pathogenic mechanism of vCJD.

From comparison group 5, the average percentage of genes which were flagged as regulated was ~31% at the 2-fold threshold limit, with an average CV of 48%. This is consistent with comparison group 1 results and also with the AD comparison results. The degree of variability inter-status is greater than is observed intra-status or in replicates, therefore these changes suggest the intre-status comparison is useful for identifying changes in gene expression in signal transduction pathways.

6.5.3.1 Comparison group 1

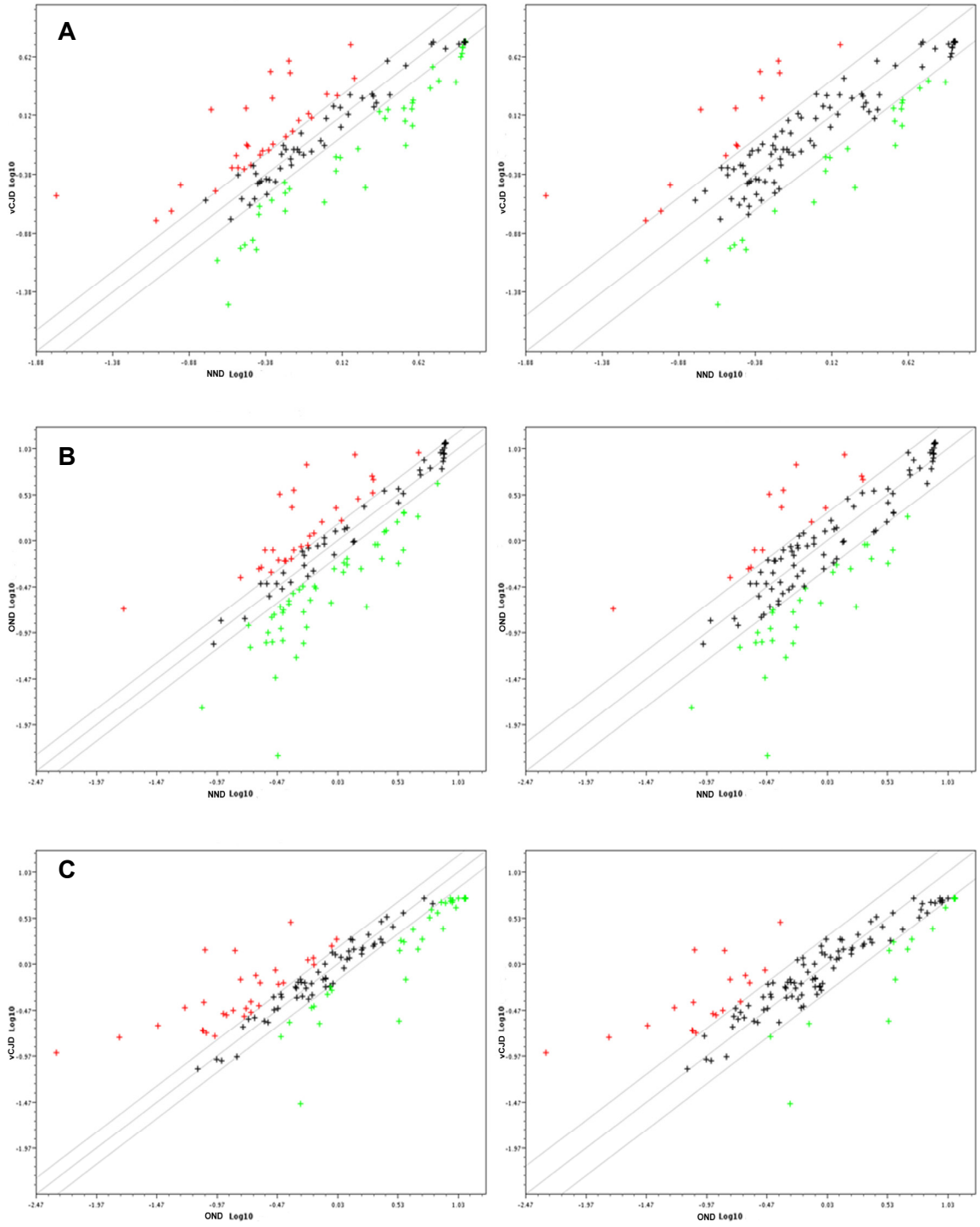

Figure 6.30. Scatter plot of inter-status comparisons of group 1. Panel A. vCJD vs NND. Panel B. OND vs NND. Panel C. vCJD vs OND. Left panels. Outer lines represent 1.5-fold threshold boundary of gene spot density changes. Right panels. Outer lines represent 2- fold threshold boundary of gene spot density changes. Red points represent genes up-regulated; green points represent genes down-regulated on y-axis sample. Axes are $\log_{10}$ spot density values.

6.5.3.2 Comparison group 2

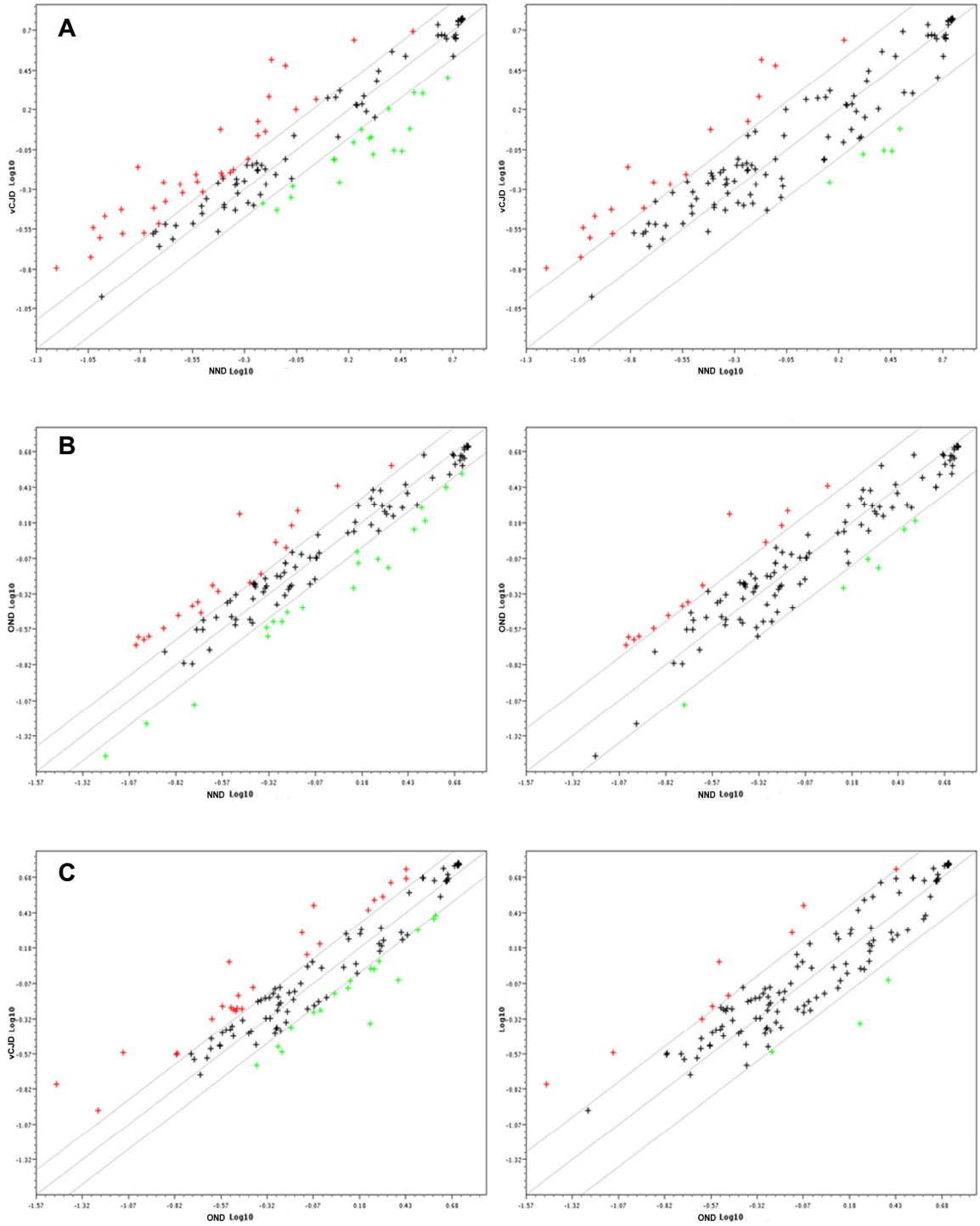

Figure 6.31. Scatter plot of inter-status comparisons of group 2. Panel A. vCJD vs NND. Panel B. OND vs NND. Panel C. vCJD vs OND. Left panels. Outer lines represent 1.5-fold threshold boundary of gene spot density changes. Right panels. Outer lines represent 2- fold threshold boundary of gene spot density changes. Red points represent genes up-regulated; green points represent genes down-regulated on y-axis sample. Axes are $\log_{10}$ spot density values.

6.5.3.3 Comparison group 5

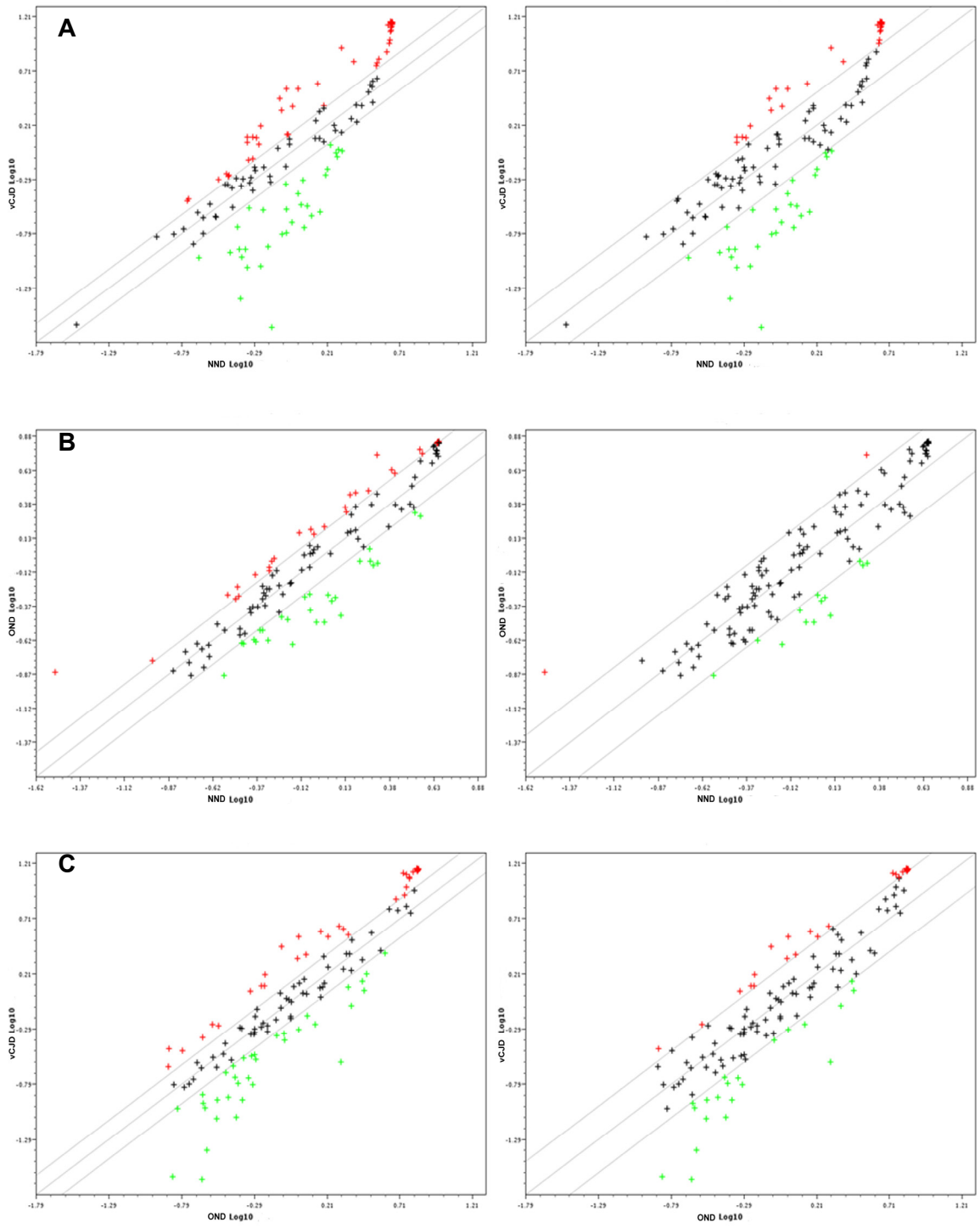

Figure 6.32. Scatter plot of inter-status comparisons of group 5. Panel A. vCJD vs NND. Panel B. OND vs NND. Panel C. vCJD vs OND. Left panels. Outer lines represent 1.5-fold threshold boundary of gene spot density changes. Right panels. Outer lines represent 2- fold threshold boundary of gene spot density changes. Red points represent genes up-regulated; green points represent genes down-regulated on y-axis sample. Axes are $\log_{10}$ spot density values.

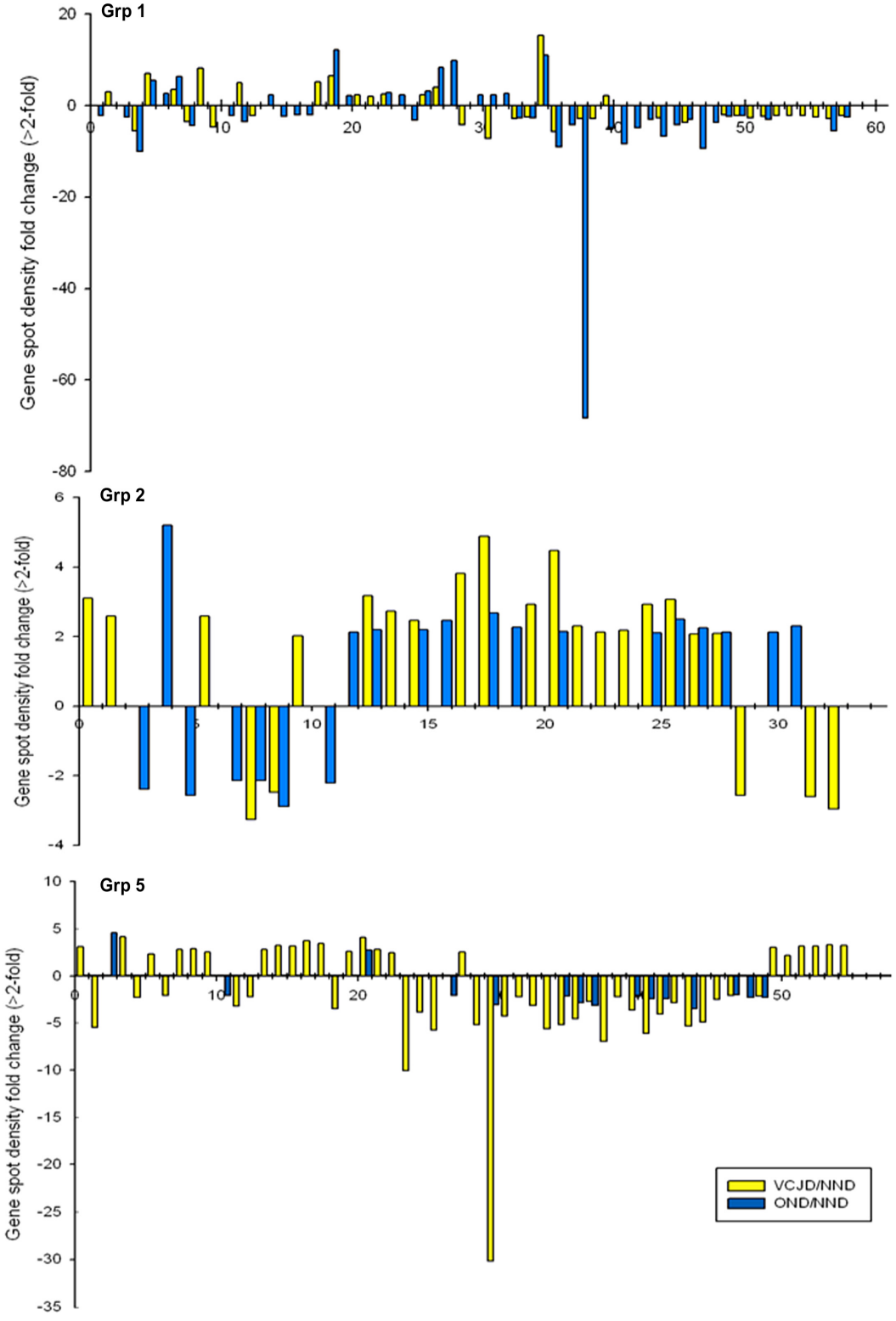

Figure 6.33. Bar chart representing genes with greater than 2-fold change in expression levels from comparison group 5, as determined by normalised densitometric analysis of gene arrays. (see Appendix Table 9.10-12 for tabulated gene names). X-axis is the order in which genes showing ≥2-fold change were flagged, based on chip position and may not match across charts.

Differentially expression genes which were flagged in vCJD vs NND and vCJD vs OND, but not in OND vs NND were considered potential vCJD-specific gene changes. From group 1,2 and 5 comparisons of vCJD vs NND/OND, a total of 58, 33 and 55 genes were observed to have modulated expression levels of >2.0-fold respectively.

Figure 6.34 shows all possible comparison group combinations. The variable on the Y-axis appears at the horizontal, the variable on the X-axis appears on the vertical for each block of plots. This method of analysis assumes equal gender/age effects for all cases and represents the disease status effects across the comparison groups.

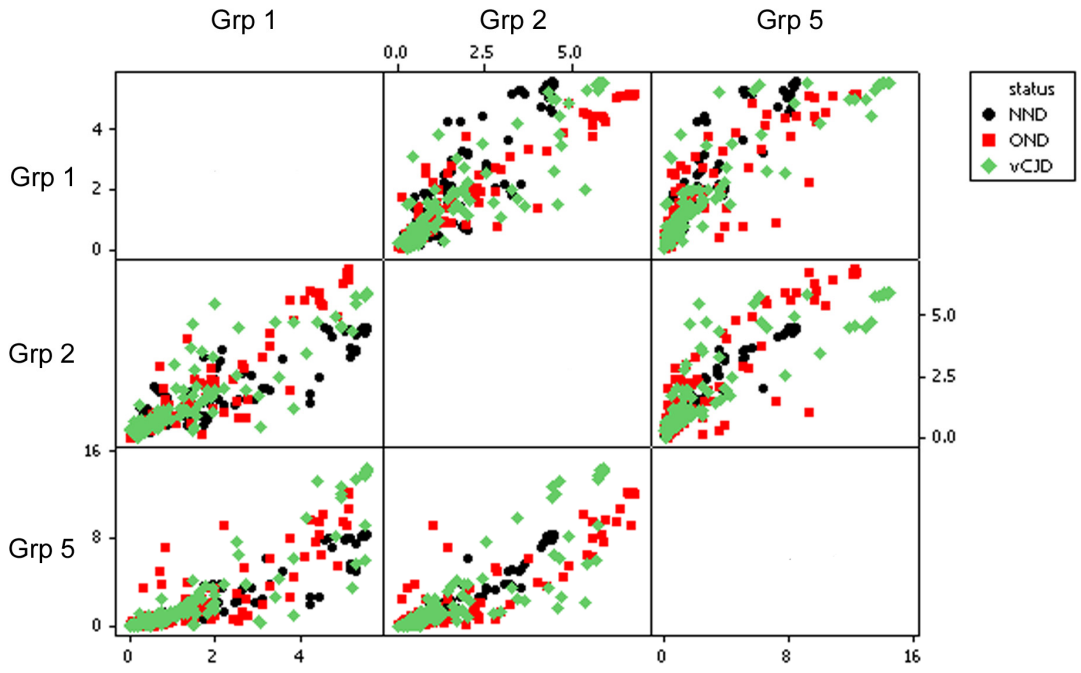

Figure 6.34. Integrated matrix plot of all three comparison groups, separated into status, based on ST array results.

Comparison of the data sets across comparison groups shows whether there were any effects on the disease status of the case. Simultaneous comparisons clearly identifies which comparison is most effected by comparison group effects. The plots are much more scattered than those in the AD integrated matrix plot (see Figure 6.16), suggesting the data from the ST arrays is more variable.

6.5.4 Clustergram

Figure 6.35 shows the average density of each individual gene from group 1, 2 and 5, aligned according to the relative ratios for that gene.The clustergram classifys the data in each subset by expression trait and clustering those with a closer degree of similarity. In this case, average spot density was clustered by ratios relative to the central group.

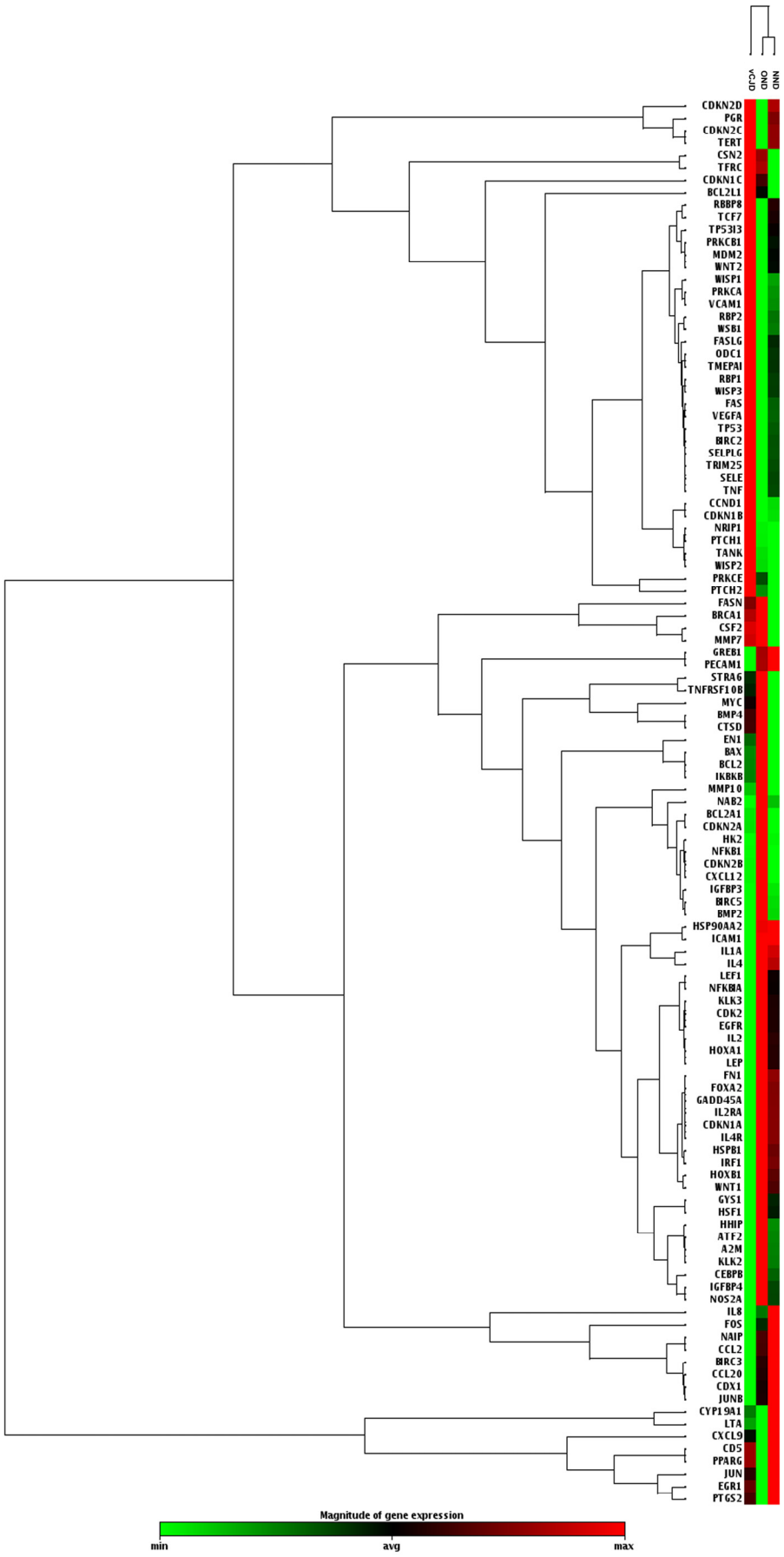

Figure 6.35. Clustergram analysis of all Signal Transduction PathwayFinder oligoarrays, carried out on GEarray Expression Anlaysis Suite web-based software. Genes which are more similar are joined at lower heights in the dendrogam and those that are less similar are joined at higher heights. Average linkage methods were used. The colour-coding legend (below) displays the maximum values as red (furthest right) and minimum values as green (furthest left), as a function of the samples (vertical direction). The vertical dendrogram links the comparison groups according to similarity.

6.5.5 Significant Gene Expression Changes

All 12 arrays used in the ST array analysis, were included for a test of significance. This was done using the GEArray Expression Analysis Suite volcano-plots. Figure 6.36A highlights the statistically significant regulated genes in the vCJD vs NND comparisons. Figure 6.36B highlights the statistically significant regulated genes in the OND vs NND comparisons.

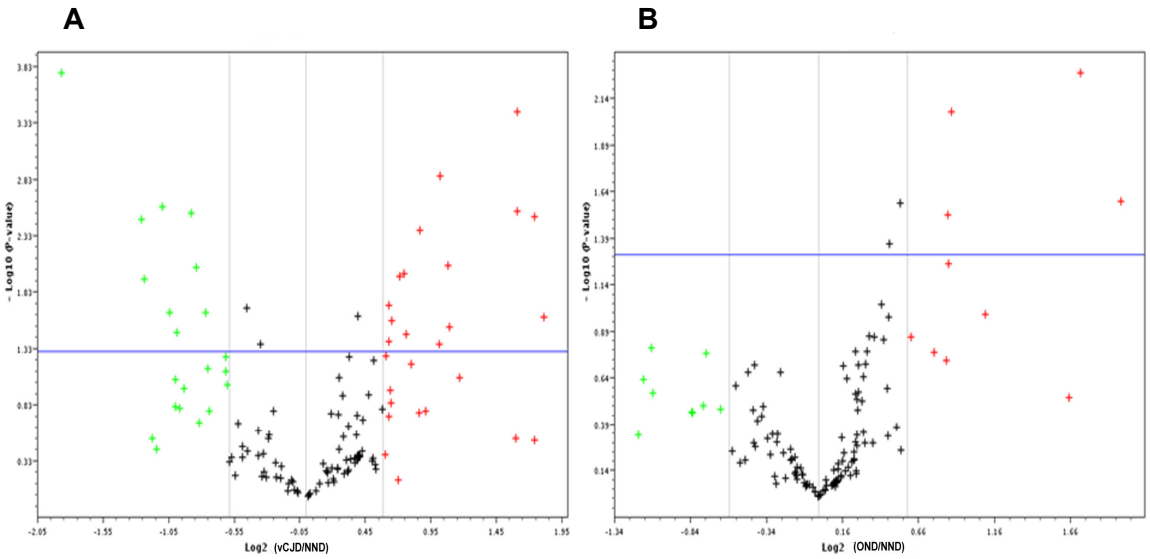

Figure 6.36. Volcano plots of relative gene expression, based on all 12 ST arrays. A. all vCJD vs NND comparisons. B. all OND vs NND comparisons. Horizontal lines are set at 0.05 significance threshold limits. Vertical lines are set at 1.5-fold change threshold limits. Red points represent genes up-regulated in the comparison; green points represent down-regulated genes in the comparison. X-Axis is negative $\log_{10}$-transformed p-values and Y-axis is log2 fold-change, as determined by the GEArray Expression Analysis Suite.

At the 1.5-fold change threshold (significance level= 0.05), there were 15 up-regulated and 9 down-regulated genes from the vCJD vs NND comparison (Figure 6.36A). For the same criteria, 6 genes were up-regulated and only 1 gene was down-regulated from the OND vs NND comparison (Figure 6.36B). Six genes were flagged in both comparisons (GREB1, HOXB1, IGFBP4, IL1A, IL4, CDKN1B), the remaining 18 genes were considered vCJD-specific. For the vCJD vs OND comparison, 4 genes were up-regulated only (graph not shown, see Table 6.9), 2 of which were also observed in vCJD vs NND comparisons (confirming their status as vCJD-specific). One gene was flagged in all three comparisons (IGFBP4).

Figure 6.37 represents significantly regulated (>2.0 fold) gene changes.

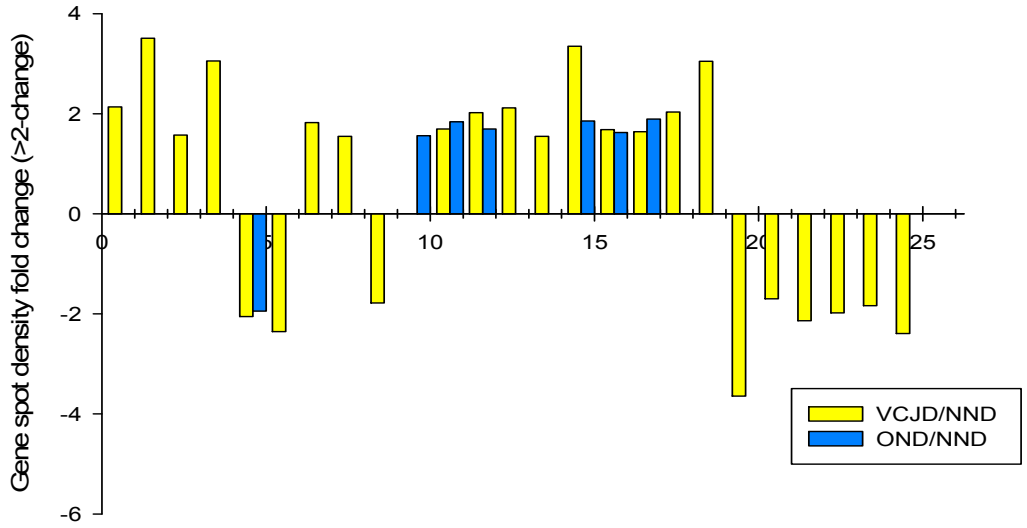

Figure 6.37.Bar chart representing significantly modulated genes with greater than 2-fold change in expression levels, as determined by normalised densitometric analysis of gene arrays. (see Appendix Table 9.13 for tabulated gene names).

Of the 24 significantly regulated genes in the vCJD vs NND comparison, 15 were up-regulated and 9 were down-regulated. Functional clustering revealed 38% of regulated genes were involved in oestrogen and androgen, 21% in the NFκB, 13% in survival (P13 kinase/AKT and Jak/Src) and 13% in the phospholipase C pathways (refer to Table 6.7).

The OND vs NND comparison revealed 7 regulated genes, 6 of which were also flagged in the vCJD vs NND comparison. Therefore those 6 were not considered vCJD-specific. The OND VS NND unique gene was FOXA2, a gene involved in the hedgehog pathway (refer to Table 6.8).

Only 4 genes were significantly regulated in the vCJD vs OND comparison. BCL2 and BCL2A1 were also flagged in vCJD vs NND comparisons, providing confirmation of them being vCJD-specific regulated genes involved in phospholipase C and survival pathways (refer to Table 6.9).

6.5.6 SAM Analysis of ST Arrays

As described in section 6.4.6, GEArray Expression suite software returns significant genes based on modified t-testing methods, but does not adjust the CV values or estimated the FDR. Therefore SAM analysis was also carried out. Figure 6.38 shows the SAM plot output for ST array results of vCJD vs NND and OND vs NND and vCJD vs OND comparisons respectively.

As mentioned in section 6.4.6, generally FDR thresholds are 5% or less are accepted, in order to limit false-positive identification, but to avoid losing relevant information, FDR thresholds at the 1.5-fold level, were more flexible to allow identification of significance. SAM analysis revealed FDR's of 6%, 70% and 8% for vCJD vs NND (5 significant genes), OND vs NND (47 significant genes) and vCJD vs OND (12 significant genes) respectively. The FDR for OND vs NND is significantly higher than the other comparisons, and also higher than the OND vs NND FDR for the AD arrays.

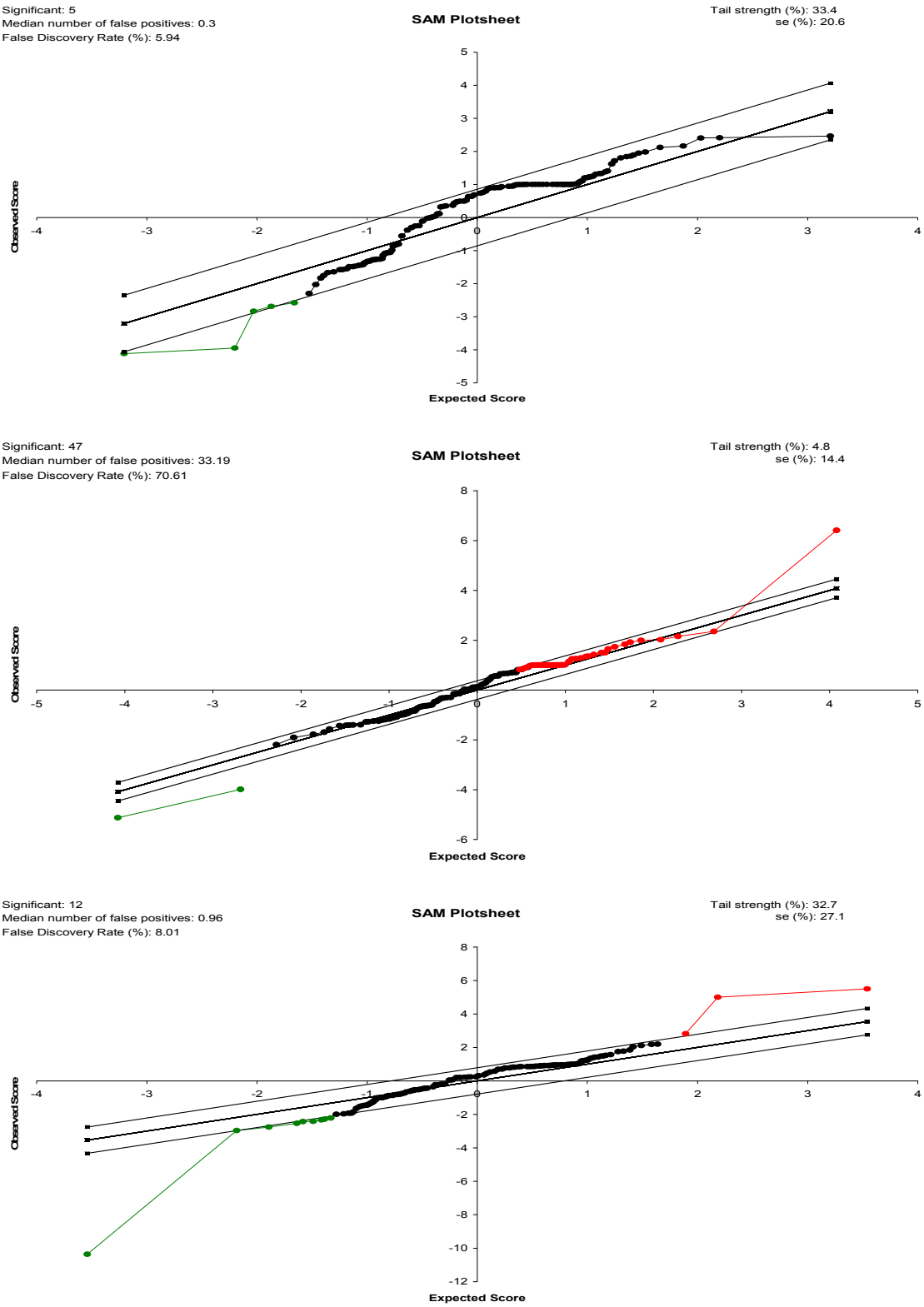

Figure 6.38. SAM analysis of all inter-status comparisons. Panel A. vCJD vs NND. FDR = 5.9%. Significantly up-regulated genes = 0. Significantly down-regulated genes = 5. Panel B. OND vs NND. FDR = 70.6%. Significantly up-regulated genes = 45. Significantly down-regulated genes = 2. Panel C. vCJD vs OND. FDR = 8.01%. Significantly up-regulated genes = 3. Significantly down-regulated genes = 9. Outer lines represent 1.5-fold threshold limit. Red plots represent significantly up-regulated genes. Green plots represent significantly down-regulated genes.

Symbol	UniGene	Description	*Fold-change*	*p-Value*
BCL2	Hs.150749	B-cell CLL/lymphoma 2	2.14	0.03
BCL2A1	Hs.227817	BCL2-related protein A1	3.51	0.02
CDK2	Hs.19192	Cyclin-dependent kinase 2	1.57	0.03
CDKN1A	Hs.370771	Cyclin-dependent kinase inhibitor 1A (p21, Cip1)	3.05	0.00
CEBPB	Hs.517106	CCAAT/enhancer binding protein (C/EBP), beta	1.82	0.00
EGFR	Hs.488293	Epidermal growth factor receptor (erythroblastic leukemia viral (v-erb-b) oncogene homolog, avian)	1.55	0.04
GREB1	Hs.467733	GREB1 protein	1.70	0.04
HOXB1	Hs.99992	Homeobox B1	2.02	0.04
HSP90AA2	Hs.523560	Heat shock protein 90kDa alpha (cytosolic), class A member 2	2.12	0.01
ICAM1	Hs.643447	Intercellular adhesion molecule 1 (CD54), human rhinovirus receptor	1.55	0.02
IGFBP4	Hs.462998	Insulin-like growth factor binding protein 4	3.35	0.00
IL1A	Hs.1722	Interleukin 1, alpha	1.68	0.01
IL2	Hs.89679	Interleukin 2	1.64	0.01
IL4	Hs.73917	Interleukin 4	2.03	0.00
IL4R	Hs.513457	Interleukin 4 receptor	3.05	0.00
CDKN1B	Hs.238990	Cyclin-dependent kinase inhibitor 1B (p27, Kip1)	0.49	0.02

CDKN2D	Hs.435051	Cyclin-dependent kinase inhibitor 2D (p19, inhibits CDK4)	0.42	0.01
EGR1	Hs.326035	Early growth response 1	0.56	0.01
PRKCB1	Hs.460355	Protein kinase C, beta 1	0.27	0.00
RBP1	Hs.529571	Retinol binding protein 1, cellular	0.59	0.02
TMEPAI	Hs.517155	Transmembrane, prostate androgen induced RNA	0.47	0.00
TNF	Hs.241570	Tumor necrosis factor (TNF superfamily, member 2)	0.50	0.03
TRIM25	Hs.528952	Tripartite motif-containing 25	0.54	0.00
WNT2	Hs.567356	Wingless-type MMTV integration site family member 2	0.42	0.00

Table 6.7. Differentially expressed genes from vCJD vs NND comparisons revealed by focused ST microarray analysis. Fold-change threshold limit = 1.5. Significance level = 0.05. Red = up-regulated genes. Green = down-regulated genes.

Symbol	UniGene	Description	*Fold-change*	*p-Value*
FOXA2	Hs.155651	Forkhead box A2	1.56	0.03
GREB1	Hs.467733	GREB1 protein	1.84	0.02
HOXB1	Hs.99992	Homeobox B1	1.70	0.02
IGFBP4	Hs.462998	Insulin-like growth factor binding protein 4	1.86	0.02
IL1A	Hs.1722	Interleukin 1, alpha	1.62	0.04
IL4	Hs.73917	Interleukin 4	1.89	0.04
CDKN1B	Hs.238990	Cyclin-dependent kinase inhibitor 1B (p27, Kip1)	0.51	0.03

Table 6.8. Differentially expressed genes from OND vs NND comparisons revealed by focused ST microarray analysis. Fold-change threshold limit = 1.5. Significance level = 0.05. Red = up-regulated genes. Green = down-regulated genes.

Symbol	UniGene	Description	*Fold-change*	*p-Value*
BCL2	Hs.150749	B-cell CLL/lymphoma 2	3.30	0.01
BCL2A1	Hs.227817	BCL2-related protein A1	3.97	0.03
BRCA1	Hs.194143	Breast cancer 1, early onset	1.83	0.01
IGFBP4	Hs.462998	Insulin-like growth factor binding protein 4	1.80	0.03

Table 6.9. Differentially expressed genes from vCJD vs OND comparisons revealed by focused ST microarray analysis. Fold-change threshold limit = 1.5. Significance level = 0.05. Red = up-regulated genes. Green = down-regulated genes.

6.6 SUMMARY OF FINDINGS

- Replicate arrays were comparable to SuperArray quoted variability for replicates.
- Intra-status variability was only slightly more than observed in replicates.
- Variablity of data inter-status showed a CV of ~38%.
- The overall statisitcal analysis suggests that replicate (13% CV) and intra-status (i.e. age/gender) effects (13% CV) were minimal and that remaining gene expression changes are potential disease associated changes.
- SAM analysis of AD arrays showed a FDR of ~ 11%. ST comparison of OND vs NND gave an anomylous result of a FDR of 70%, and if removed, ST arrays showed a FDR of ~7%.
- From the overall AD comparisons, 37 genes were identified as significantly up-regulated and 17 as significantly down-regulated. Of these, 38 genes were potential vCJD-specific changes (see Table 6.10).
- From the overall ST comparison, 17 genes were identified as significantly up-regualted and 9 as significantly down-regulated. Of these, 15 genes were potential vCJD-specific changes (see Table 6.11).
- 12 of the potential vCJD associated genes identified in this study were also identified in a larger scale gene expression study of sCJD patients (Xiang *et al.*, 2005).
- 25 of the potential vCJD associated genes have previously been described in gene expression studies in experimental models of TSEs (Booth *et al.*, 2004; Brown *et al.*, 2005a; Skinner *et al.*, 2006; Riemer *et al.*, 2004; Sorensen *et al.*, 2008; Xiang *et al.*, 2004)
- 22 genes have not been previously been described in the context of prion disease.
- Functional grouping of modulated genes revealed alterations in a number of pathways including; genes involved in β-amyloid generation, oligomerization, clearance, and degradation; cell signaling; synaptic formation; cholesterol or lipid metabolism; NFκB and survival (P13 kinase/AKT and Jak/Src) and phospholipase C pathways.

6.7 DISCUSSION

In this study, the variability of technical replicates was assessed for, (i) a single RNA preparation run on two separate arrays, this reports the variability of the array analysis and, (ii) separate RNA preparations from the same case run on separate arrays, this reports the variability of the RNA preparation plus the array analysis. These technical replicates had CV values of 10% and 19%, respectively. This first value is close to the SuperArray quoted CV value of 10% for replicate arrays with a single sample. The reproducibility of the microarray analysis also showed a highly significant correlation based on r^2 values.

In the present study, biological (intra-status) replicates are not exactly identical. For example, the vCJD cases are not exact biological replicates, they differ in age and gender. The lack of exact biological replicates has presented challenges for this project. Biological replicates allow increased precision of gene expression measurement and identification of outliers. In clinical and pathological studies, exact biological replicates are rare and require studies of identical twins. The use of non-identical biological replicates, whilst less desirable, is preferable to no replication and still lends statistical power that increases the confidence of the conclusions. However, issues of how the non-identical parameters confound the data remain and need to be taken into account. Intra-status variation revealed an r^2 value >0.8 and a CV of ~13%. This significant correlation and low overall variation is promising. If variation between cases of the same status had been high, it would be more difficult to differentiate between this variation and that between diseased and non-diseased controls.

Overall, inter-status variation (vCJD vs NND vs OND) had a CV value of 44%. This is greater than the overall intra-status variation (13%) or the technical variation (10%) indicating that cases of different status were more different than were cases of the same status or technical replicates. This is as would be expected if the arrays had picked up disease specific gene expression changes. If the arrays had not picked up disease specific gene expression changes, the intra-status variation and the inter-

status variation might have been expected to be similar. Indeed, given that the inter-status cases in each comparison group were age and gender matched whereas the intra-status cases (across comparison groups) were not, the variation might have been expected to be higher intra-status than inter-status. With the exception of vCJD vs OND in the ST arrays, the average FDR (SAM analysis) for the inter-status comparisons was ~9%. This is slightly higher than the generally accepted 5% FDR, but it should be recognised that the project's small sample size places limits on the statistics.

As with all transcriptome analysis studies, two important factors must be taken into account. Firstly, that the stability of the mRNA may not correlate with the stability of the protein it encodes (Hargrove & Schmidt, 1989). Secondly, that intronic regions of genes are also involved in a number of processes related to post-transcriptional control of gene expression (Nakaya *et al.*, 2007). Transcriptome analysis should therefore be followed by proteomics or other work.

While these results have shown in principle that reliable and reproducible microarray data can be collected and processed successfully using RNA preparations isolated from human vCJD autopsy brain material, the use of focused arrays has biased the results towards the identification of relevant genes, especially with the use of an Alzheimer's disease targeted array. The results shown in Chapter 6 will be discussed in the context of the published literature, but as the gene expression data from such focused array lists is insufficiently robust, any interpretations should be done with caution.

Array analysis was carried out for matched cases (within a comparison group: 1, 2 or 5) and across all comparison groups (1, 2 and 5). Criteria A1, A2 and A3 will be used to refer to matched case comparison results (within a single comparison group) where at least one of the comparisons (eg vCJD vs NND) shows a fold-difference greater than 1.5. A1 will refer to genes with altered expression levels within an age/gender matched vCJD vs NND comparison; A2 within a matched OND vs NND comparison and A3 within a matched vCJD vs OND comparison. Criteria B will be

used to refer to genes with significantly (p =< 0.05, threshold change of 1.5) altered expression as identified by analysis (GE software) of the data from all 3 comparison groups (see Tables 6.3-6.5 and 6.7-6.9); again 1, 2 and 3 refer to vCJD vs NND, OND vs NND and vCJD vs OND, respectively. The suffix AD or ST indicates which array type was used. For example, apolipoprotein (APO) (AD:A1) would indicate that regulated expression of APO was observed in one of the vCJD vs NND comparisons on the AD oligoarray, whereas APO (AD:B2) would indicate that significantly regulated expression of APO was observed in OND vs NND when all 3 comparison groups were considered. Tables 6.10 and 6.11 lists those genes with significant changes in gene expression which can be considered to be vCJD specific (vCJD vs NND/OND) or can be considered to be potential vCJD specific changes (vCJD vs NND or OND).

vCJD-specific changes				
SYMBOL	VCJD VS NND		VCJD VS OND	
	FOLD-CHANGE	P-VALUE	FOLD-CHANGE	P-VALUE
APH1A	1.73	0.03	1.63	0.03
APLP1	2.07	0.01	1.99	0.01
BACE2	1.89	0.00	2.26	0.00
BCHE	1.92	0.00	2.11	0.00
CTSD	1.77	0.01	1.67	0.05
GNB4	1.93	0.01	1.87	0.02
GNG5	1.61	0.02	1.99	0.01
CHAT	1.76	0.02	1.82	0.02
BCL2	2.14	0.03	3.30	0.01
BCL2A1	3.51	0.02	3.97	0.03
NPY	0.07	0.00	0.10	0.04
PRKCB1	0.26	0.00	0.34	0.01
PSEN1	0.65	0.01	0.63	0.01
SNCA	0.55	0.04	0.46	0.01

SPINT2	0.62	0.03	0.56	0.02
SST	0.36	0.00	0.33	0.01
UQCRC2	0.51	0.01	0.49	0.01

Table 6.10. Genes identified as having significantly regulated gene expression in vCJD vs NND and OND (i.e. vCJD specific).

Potential vCJD-specific changes					
SYMBOL	**vCJD vs NND**		**SYMBOL**	**vCJD vs OND**	
	FOLD-CHANGE	**P-VALUE**		**FOLD-CHANGE**	**P-VALUE**
ABCA1	5.64	0.04	**CDKL1**	2.06	0.01
APBA1	1.67	0.03	**ECE2**	1.67	0.00
APBA3	2.57	0.04	**EGR3**	1.89	0.00
APOA1	1.84	0.05	**BRCA1**	1.83	0.01
APOE	2.95	0.03			
BDNF	1.71	0.05			
BPTF	1.80	0.01			
LPL	2.83	0.04			
LRP10	1.88	0.01			
CDK2	1.57	0.03			
CDKN1A	3.05	0.00			
CEBPB	1.82	0.00			
EGFR	1.55	0.04			
HSP90AA2	2.12	0.01			
ICAM1	1.55	0.02			
IL2	1.64	0.01			
IL4R	3.05	0.00			
CDK5	0.63	0.02	**NCSTN**	0.40	0.03

PRKCZ	0.51	0.05	**PKP4**	0.60	0.03
PRKCB1	0.27	0.00	**PLG**	0.38	0.02
CDKN2D	0.42	0.01	**PRKCA**	0.34	0.03
EGR1	0.56	0.01	**PRKCQ**	0.49	0.03
RBP1	0.59	0.02			
TMEPAI	0.47	0.00			
TNF	0.50	0.03			
TRIM25	0.54	0.00			
WNT2	0.42	0.00			

Table 6.11. Genes identified has having significantly regulated expression in vCJD vs NND or OND and may be potential vCJD specific gene expression changes.

The etiology and pathogenesis of a number of neurodegenerative disorders appears to be related to the formation and accumulation of an aberrant isoform of an endogenous protein. Common pathologies have been reported between amyloidogenic diseases such as AD, PD, Lewy body and prion diseases, but how aggregation of mutant protein leads to neurodegeneration remains unclear. Gene expression studies have been carried out to identify possible pathways involved in or activated by mutant prion protein aggregation.

A number of gene expression studies of TSE infected brains have been published. There is only one comprehensive study of sCJD in humans (Xiang *et al.*, 2005). There are no previous studies of gene expression in vCJD brain. There are several comprehensive studies of TSE infected mouse brain at terminal disease (Xiang *et al.*, 2004; Riemer *et al.*, 2004) and at earlier time points including preclinical disease (Xiang *et al.*, 2004; Brown *et al.*, 2005a; Skinner *et al.*, 2006; Booth *et al.*, 2004; Sorensen *et al.*, 2008; Xiang *et al.*, 2007). In addition there are many smaller preliminary gene expression studies, studies on specific groups of transcripts or studies on transcripts in TSE infected or PrP treated isolated cell types (Gotz *et al.*,

1994; Quaglio *et al.*, 2001; Jobling *et al.*, 2001; Kovacs *et al.*, 2007; Brown *et al.*, 2004; Brown *et al.*, 2003; Baker *et al.*, 2002; Baker & Manuelidis, 2003; Campbell *et al.*, 1994; Duguid *et al.*, 1989; Riemer *et al.*, 2000; Dandoy-Dron *et al.*, 1998; Dandoy-Dron *et al.*, 2000; Park *et al.*, 2000). Together these have highlighted the following as possible mechanisms for neuronal death and neurodegeneration: oxidative stress, copper, iron and calcium metabolism, endoplasmic reticulum (ER) and mitochondrial dysfunction, endosomal-lysosomal pathways, endocytosis-ubiquitin- proteasomal pathways, apoptosis, cell adhesion, transmembrane signaling, synaptic function or maintenance and cholesterol biosynthesis its the number of genes investigated.

This discussion will concentrate on those genes on the AD and ST arrays which showed a statistically significant change in vCJD vs both OND and NND (B1 & B3) but will mention other genes of potential relevance that fit with putative mechanisms of TSE pathogenesis. It is worth noting that there many genes that showed no significant and specific changes, for example genes associated with cell cycle, the retinoic acid, wnt and hedgehog pathways and cytoskeletal organisation amongst many others.

PROTEIN SYNTHESIS, MODIFICATION AND TRAFFICKING

Protein synthesis occurs on ribosomes either free in the cytosol or attached to the ER. Transmembrane proteins and proteins to be secreted are synthesized on the ER and traffic through the Golgi, where glycosylation occurs before transportation to their final destination. Within the ER proteins fold into their native conformations. Quality-control processes ensure that only correctly folded proteins are exported to the Golgi complex; incorrectly folded proteins are retained within the ER. If retained, one of two mechanisms occur; either the protein completes its folding process, or it is targeted for degradation. ER dysfunction places the ER under stress. In response, signal transduction cascades are initiated to reduce protein synthesis and increase protein folding capacity; this is collectively known as the unfolded protein response (UPR). Generally, two adaptive mechanisms have been recognized, both aimed at

returning the ER to its normal physiological state. 1) Up-regulation of the folding capacity of the ER, by transcriptional activation of genes coding for ER-resident molecular chaperones and foldases and an increase in total ER size. 2) down-regulation of the biosynthetic load of the ER through shut-off of protein synthesis at a transcriptional (Harding *et al.*, 2002) and a translational level and increased clearance of unfolded proteins from the ER through up-regulation of ER associated degradation (Harding *et al.*, 1999; Harding *et al.*, 2001). If physiologically normal function is not recovered after prolonged stress, apoptosis is activated. It is no surprise that the UPR mechanisms have long been linked to diseases such as AD, PD and CJD, which have in common aggregated misfolded proteins. Published comprehensive gene expression studies of TSE infected brains have identified a number of changes relating to ER stress, protein modification and trafficking. ER stress protein genes which are up-regulated include ER chaperones such as FK506 binding protein-2, Erp-29, calnexin and heat shock proteins (Hsp). Genes involved in protein trafficking include Golgi-localised short coiled-coil protein, VAMP4 and AP1s.

Hsps: Only two Hsps were present. (Hsp) 90 kDa alpha, class A member 2 (HSP90AA2) was significantly upregulated in vCJD vs NND and OND vs NND (AD:B1 & B2) (1.6-, 1.8-fold change respectively). This is a molecular chaperone involved in the folding, activation and assembly of a range of proteins, termed Hsp90 client proteins (Pratt & Toft, 2003). Its up-regulation may be due to increased requirement of stress proteins to facilitate correct or re-folding of abnormally folded prion proteins. Hsp27 was not significantly changed in its expression between vCJD and controls. In sCJD brain (Xiang *et al.*, 2005) Hsp (105 kDa/110 kDa) 1 gene expression was down regulated. In mice, gene expression changes have been observed for Hsp1, Hsp90AB1, HSPB3 and HSPA9B (Sorensen *et al.*, 2008; Skinner *et al.*, 2006; Xiang *et al.*, 2004).

ERN/IRE1: In this study, ER to nucleus signaling 2 (ERN2) also known as inositol-requiring enzyme (IRE)-1β was up-regulated (AD: B1 & B2). In the vCJD vs NND comparison, a 2.5-fold increase was seen, however a 1.8-fold increase was also

observed in the OND vs NND comparison ($p<0.05$) and the vCJD vs OND comparison flagged an insignificant change of 1.3-fold. This change cannot therefore be considered to be vCJD-specific. ERN1 was only upregulated in OND vs NND (AD:A2). ERN1 (IRE1α) and ERN2 are transmembrane protein kinase receptors normally suppressed by the binding of the ER chaperone glucose regulated protein 78 (GRP78). During times of ER dysfunction, GRP78 dissociates and binds to unfolded proteins triggering ERN oligomerization, autophosphorylation and activation. IRE1α catalyses the spliceosome-independent processing of the transcription factor XBP1 pre-mRNA and causes a frame shift resulting in a more stable protein ($XBP1^{proc}$). This functions as a transcription factor that specifically activates genes coding for proteins required for ER protein folding and processing (Yoshida *et al.*, 2001). IRE1β cleaves 28S rRNA resulting in a partial attenuation of translation (Imagawa *et al.*, 2008; Iwawaki *et al.*, 2001). The recent discovery of IRE1 mediated degradation of specific ER-localised mRNAs in *Drosophila* presents an additional and novel mechanism by which IRE1 may further decrease the burden of ER stress (Hollien & Weissman, 2006). Up-regulation of proteins that help decrease the burden of proteins imported to the ER would be expected in amyloidogenic diseases. It has been suggested that increases in IRE1 may extend brain cell survival (Lin *et al.*, 2007).

The Superarrays contained a number of genes indicative of other pathways of cell stress. ATF2 activated by a number of stimuli including, ionizing and UV radiation, genotoxic agents and glucose or leucine starvation was not statistically upregulated. TP53 (p53) was not significantly changed.

APOPTOTIC GENES

Both (AD and ST) arrays contain genes associated with cell survival and death responses. These include caspases 3 and 4 (CASP3 & CASP4), BCL2, BCL2A1, BCL2L1 (Bcl-XL) and BAX. Caspases are the executioner enzymes of cell death. Bcl-2 family members are important regulators of apoptosis; Bcl-2 and Bcl-x_L are anti-apoptotic, BAX is pro-apoptotic. Bcl-2 over-expression delays the activation of

caspase activated cell death pathways, by forming complexes with pro-apoptotic Bcl-2 family proteins such as Bax (Oltvai *et al.*, 1993). The intracellular ratio of Bcl-2 or Bcl-x_L to proteins such as Bax and Bad probably determines cell survival or death (Sato *et al.*, 1994).

Caspases: CASP4 showed strong elevation in vCJD (AD:A1 & A3) in two comparison groups, >9-fold and >7-fold up-regulation in vCJD vs OND and in vCJD vs NND, respectively but there was no statistically significant change in expression when all three comparison groups were considered. CASP4 is generally considered to be an inflammatory caspase (Martinon & Tschopp, 2007) CASP4 up-regulation has not been reported in other TSE gene expression studies. Caspases are generally pre-formed in cells and are activated from their pro-caspase in a proteolytic cascade. Cell death responses generally do not involve regulation of caspase gene expression. CASP3 was upregulated (~2-fold) in all inter-status comparisons (AD: A1, A2 & A3) suggesting this was not specific to vCJD pathology.

Bcl2 family genes: BAX (1.5 and 1.8-fold), BCL-2 (2.2 and 3.3-fold) and BCL-2AI (3.5 and 4.0-fold) were all significantly up-regulated (ST:B1, B3) in vCJD brains. In murine scrapie models BCL-2 and BAX were reported to be up-regulated (Riemer *et al.*, 2004; Xiang *et al.*, 2004; Park *et al.*, 2000) but this was not corroborated by another study (Brown *et al.*, 2004) and no change was observed in human sCJD (Xiang *et al.*, 2005). Bcl-2 gene expression has also been reported to be up-regulated in PD (Mogi *et al.*, 1996a). Several studies have discussed the importance of Bcl-2 and Bax in TSE neurodegeneration (Chiesa *et al.*, 2005; Li *et al.*, 2007; Nicolas *et al.*, 2007). Over-expression of Bcl-2 is known to protect neuronal cells against apoptotic cell death (Lawrence *et al.*, 1996). An immunohistochemical study showed Bcl-2 levels to be increased in cells of the cerebellum of CJD patients (Puig & Ferrer, 2001). Misfolded PrP can bind to and aggregate with Bcl-2 thus promoting cell death (Rambold *et al.*, 2006). It has also been suggested that neuronal death in prion disease results from apoptosis via the Bax-pathway and that PrP^c is an anti-apoptotic protein that protects against this independently of Bcl-2 or Bcl-x_L (Sakudo *et al.*, 2003b). In prion disease, the observed induction of Bcl-2 may be an attempt to

attenuate cell death caused by PrP^c deficiency. However, mice null for Bax or over-expressing Bcl-2 challenged with scrapie show no overt difference in disease or survival (Steele *et al.*, 2007; Coulpier *et al.*, 2006). Therefore cell death cannot be solely controlled by Bcl-2/Bax mediated pathways.

TNF (TNFα), (ST: B1, A1, 2, 3) was down-regulated, although it is unclear whether this is biologically relevant since only a 0.5-fold down-regulation was detected. There were no significant changes in levels of TNFβ (LTA). Scrapie and CJD studies have reported TNF family members to be up-regulated (Xiang *et al.*, 2005; Lu *et al.*, 2004; Brown *et al.*, 2003; Xiang *et al.*, 2007). Serum-deprivation can induce death of $Prnp^{-/-}$ neurons; identity of the serum factor(s) essential for cell survival is unclear (Kuwahara *et al.*, 1999). TNFα induces apoptosis in some mitotic cells (Polunovsky *et al.*, 1994) but can be protective for neuronal cells (Cheng *et al.*, 1994), perhaps by induction of anti-apoptotic proteins such as Bcl-2 (Tamatani *et al.*, 1999). TNFα is increased in glial cells following scrapie infection (Kim *et al.*, 1999). Serum-deprivation of $Prnp^{-/-}$ neuronal cells results in a rapid decrease of Bcl-2 and Bcl-x_L eventually leading to cell death, addition of TNFα to serum deprived cultures increases levels of Bcl-2 and Bcl-x_L slowing apoptosis (Sakudo *et al.*, 2003a).

INTERLEUKINS

The ST arrays include interleukins (IL) -1A, -2, -4 and -8, and the interleukin receptors IL-4R and IL-2RA. Transcripts for IL-1α, -2, -4 and -8 and IL-4R and -2RA were elevated in diseased (VCJD & OND) brains. A large number of cytokine profiling studies have previously been carried out. Studies on mouse TSE models generally identify IL-1 as being upregulated (Baker & Manuelidis, 2003; Campbell *et al.*, 1994; Brown *et al.*, 2003; Kim *et al.*, 1999). In contrast, no interleukin genes showed gene expression changes in the only comprehensive sCJD gene profiling study (Xiang *et al.*, 2005). However, both pro-inflammatory (IL-1β and TNFα) and anti-inflammatory (IL-4 and IL-10) cytokines have been detected in the CSF of patients with sCJD and vCJD (Sharief *et al.*, 1999; Stoerck *et al.*, 2005). The best

known source of interleukins (hence the name) are leukocytes but these molecules can also be produced by other cell types. In CJD, histopatholgical examination reveals an absence of inflammatory infiltrates but activated microglia play a prominent role in the atypical inflammatory response releasing both pro- and anti-inflammatory cytokines (Rock *et al.*, 2004). Whether it is the accumulation of toxic prion protein conformers or the augmented release of tissue-toxic cytokines which leads to damage and subsequent neurodegeneration remains unclear.

IL-1α was present on both the AD and ST arrays and was consistently and significantly up-regulated (>1.7-fold) in diseased (vCJD, OND) brains relative to control (NND) brains (ST:B1 & B2, AD:B1 & B2). IL-1 is the prototypic inflammatory cytokine and is known to play a detrimental role in acute neurodegeneration after brain injury (Basu *et al.*, 2005). Certain polymorphisms in the genes encoding IL-1α and IL-1β are considered to increase the risk of early disease onset in AD (Griffin & Mrak, 2002) and the IL-1α allele 2 has an increased frequency in AD (Nicoll *et al.*, 2000). IL-1 is produced by microglial cells on exposure to PrP[106-126] and β-amyloid *in vitro* (Peyrin *et al.*, 1999; Meda *et al.*, 1999) but a link between glial cells, released cytokines and neuronal death has not been established. Increased expression of IL-1 has been reported in numerous murine scrapie models (Kim *et al.*, 1999; Campbell *et al.*, 1994; Brown *et al.*, 2003). IL-1β is the predominant response, an exception being the Chandler/SWRj scrapie model, with IL-1α expression being predominant. IL-1α is generally only observed at terminal disease (Campbell *et al.*, 1994; Kordek *et al.*, 1996; Brown *et al.*, 2003).

IL-2 and IL-2RA (ST:B1) were both up-regulated by 1.6-fold only in the vCJD vs NND ie specifically in vCJD brains. There have been few studies on IL-2 in TSE infected brains. IL-2 activates the PI 3-kinase/Akt signaling pathway which may be activated during prion disease (Mironov *et al.*, 2003). IL-2 was not detected (ELISA) in a study on CSF from both sCJD and vCJD cases (Sharief *et al.*, 1999). Elevated IL-2 levels in certain neuronal regions of PD patients only occur during late disease and are therefore more likely to be a consequence, as opposed to a cause, of neurodegeneration (Mogi *et al.*, 1996b). IL-2 is generally known as a T-cell growth

factor. In the brain, IL-2 is produced in astrocytes and microglial cells and it induces oligodendrocyte proliferation and differentiation and enhances sympathetic neurite outgrowth (Benveniste & Merill, 1986). IL-2 is significantly reduced in copper-deficient animals and could therefore be affected by alterations in copper metabolism associated with loss of PrP^c function in TSE diseases (Brown *et al.*, 1997a; Lukasewycz & Prohaska, 1990).

IL-4 and IL-4R (ST: B1 & B2) showed significantly increased levels of gene expression in diseased (vCJD & OND) compared to non-diseased brains (IL-4, B1 2.0-fold and B2 1.9-fold; IL-4R, B1 3-fold and B2 2.6-fold). IL-4 can be detected in CSF in sCJD (Stoerck *et al.*, 2005). IL-4 is also produced in other neurodegenerative diseases (AD, juvenile PD and PD) and during brain ischemia (Mogi *et al.*, 1996c; Szczepanik *et al.*, 2001). This is in agreement with the finding in the present study that IL-4 transcripts are elevated in both vCJD and OND. It is unlikely to be a CJD specific change. $IL\text{-}4^{0/0}$ mice have comparative survival rates to wild-type controls when challenged with RML scrapie and no other overt differences (Thackray *et al.*, 2004). It is therefore unlikely that IL-4 has a major role in prion disease pathogenesis.

IL-8 (ST:B1 & B2) was significantly up-regulated in diseased cases, by 1.9- and 4.3-fold respectively. IL-8 is classified as a pro-inflammatory cytokine and is a chemokine which attracts neutrophils. TSE neuropathology does not include neutrophil infiltration and the possible relevance of this upregulated gene expression is not apparent.

LIPID METABOLISM

Lipid rafts are membrane microdomains enriched in cholesterol and sphingolipids. They form platforms in the outer leaflet of membranes; these are connected to phospholipids and cholesterol in the inner leaflet. Caveolae are the best characterized lipid rafts and can be differentiated from other lipid rafts by the presence of caveolin protein. The physiological role of lipid rafts is still debated;

signal transduction, molecular transportation and molecular processing have all been suggested as roles (Simons & Toomre, 2000; Parton & Richards, 2003; Salaun *et al.*, 2004). Membrane proteins which are constitutive raft residents include glycophosphatidylinositol-anchored proteins (GPI-anchored) such as PrP^c, cholesterol-linked and palmitate-anchored proteins such as Hedgehog (Jeong & McMahon, 2002) and transmembrane proteins such as β-secretase (BACE) (Simons & Toomre, 2000).

Lipids are transported from the gut to the liver and from the liver to other tissues as high, low or very low density lipoprotein particles known as HDL, LDL and VLDL, respectively. These can be further subdivided and contain various lipids and apolipoproteins (Apo). For example, LDL particles contain ~3,000 lipid molecules and one molecule of ApoB (Segrest *et al.*, 2001). ApoA-1 is the major component of HDL particles and activates cAMP signaling, via protein kinase Cα (PKC) to phosphorylate proteins such as ATP-binding cassette A1 (ABCA1) and other key proteins in signal transduction pathways for lipid transportation (Haidar *et al.*, 2004; Yamauchi *et al.*, 2003). Many apolipoprotein family members have been linked to increased risk for diseases such as hypercholesterolemia and atherosclerosis. ApoE is essential for the normal catabolism of triglyceride-rich lipoprotein constituents. APOE mRNAs are highly concentrated within the CNS (Mahley, 1988). The APOE gene is polymorphic with three major alleles, *ApoE2, ApoE3* and *ApoE4*. Genetic analysis has found a correlation between increased risk of AD and APOE-ε4 (Corder *et al.*, 1993), whereas APOE-ε2 seems to have a protective effect (Corder *et al.*, 1994). APOE-ε4 has been suggested also to be a risk factor for CJD (Amouyel *et al.*, 1994).

Apolipoproteins are taken into cells by a variety of receptors. LDL receptor-related protein (LRP), also known as ApoE receptor 2 (APOER2) is an abundant surface receptor of neurones which recognizes at least 30 different ligands. These include proteinases, molecules associated with regulating proteolytic activity, including members of the Serpin superfamily of serine proteinase inhibitors (eg SERPINA3), the pan-proteinase inhibitor alpha-2 macroglobulin (α_2M, A2M) and

metalloproteinases (MMP) (Herz & Strickland, 2001). Lipoprotein lipase (LPL) binds both ApoE and LRP. It is found at lower levels in the brain than in other tissues but interestingly has increased mRNA, protein and functional activity levels in the CA3 pyrimidal neurons of the hippocampus, the region most affected during AD (Ben-Zeev *et al.*, 1990; Lorent *et al.*, 1995). In the brain, one major function of LPL may be transport of membrane components such as lipids, cholesterol and vitamin E into neurons (Rebeck *et al.*, 1995). This is particularly important because neuronal membranes require a constant supply of components in order to maintain cellular shape and remodel and/or regenerate neuronal processes. ApoE can bind to amyloid β (Aβ) aggregates, and since LPL may promote the binding of ApoE to LRP, it has been suggested that LPL assists in internalisation of ApoE lipoprotein particle components into cells (Rebeck *et al.*, 1995; Strickland *et al.*, 1995). It is thought that through these interactions, LPL protects neurons by clearing Aβ. Mutations in LPL may play a role in AD plaque formation since LPL directly binds amyloid precursor protein (APP) (Lorent *et al.*, 1995), is up-regulated in AD and collects in plaques (Rebeck *et al.*, 1995).

Cholesterol is required for the processing of APP to the amyloidogenic Aβ peptide (De Strooper & Annaert, 2000). Cholesterol plays an essential role in raft assembly (Simons & Ikonen, 1997) and cholesterol depletion abolished the association of proteins with rafts (Cerneus *et al.*, 1993; Keller & Simons, 1998). Taken together, it is therefore reasonable to posit that PrP^{Sc} conversion may be dependent on cholesterol; reduced levels of lipid rafts may affect intracellular transport, reducing intracellular protein targeting efficiency and diminishing PrP aggregation rates. Moreover, it has been shown that PrP^{c}-PrP^{Sc} conversion is likely to occur on lipid rafts (Kaneko *et al.*, 1997; Kazlauskaite & Pinheiro, 2005; Taylor & Hooper, 2006). Changes in cholesterol levels affect PrP^{Sc} formation and prion incubation time in culture (Bate *et al.*, 2004; Borchelt *et al.*, 1992; Baron *et al.*, 2002; Kaneko *et al.*, 1997; Mok *et al.*, 2006; Taraboulos *et al.*, 1995a).

A number of genes involved in cholesterol and lipid metabolism are included on the AD arrays eg ABCA1, APOA1, APOE, LRP8, SYP, LPL and CLU. The

involvement of genes involved in cholesterol and lipid metabolism in TSE diseases has previously been described in scrapie gene expression studies (Brown *et al.*, 2005a; Riemer *et al.*, 2004; Xiang *et al.*, 2007).

Apolipoproteins. There was significant vCJD specific upregulation of APOE and APOA1 (AD:B1 & B3). Although APOE alleles have been linked to the risk of developing AD and CJD, conspicuously expression is not reported as modulated in the sCJD profiling study (Xiang *et al.*, 2005) or in scrapie models. A small study of ApoE proteins in human CSF suggested that detection of ApoE was characteristic of vCJD but not of sCJD (Chloe *et al.*, 2002) however, other studies suggest that APOE may not be suitable as a distinguishing biomarker (Zerr *et al.*, 1996). High levels of ApoE proteins in the CSF have been observed in BSE infected cattle (Hochstrasser *et al.*, 1997). In other TSE gene expression studies, APOD is more commonly reported as up-regulated (Brown *et al.*, 2004; Riemer *et al.*, 2004). APOE and APOD are both expressed by astrocytes and have similar roles in cholesterol transport (Patel *et al.*, 1995; Pitas *et al.*, 1987; Diedrich *et al.*, 1991b). In the diseased brain, astrocytes may assume the role of macrophages and attempt to repair or limit damage within the CNS (Diedrich *et al.*, 1987). APOE is known to be up-regulated in response to generalized neuronal damage (Horsburgh *et al.*, 1997). It could be argued therefore that increased APOE should also have been observed in OND cases. **Clusterin** (CLU), also known as ApoJ, was upregulated in vCJD and OND (AD:A1 & A2; ~3-fold). Expression was also altered in murine scrapie (Xiang *et al.*, 2007; Booth *et al.*, 2004; Skinner *et al.*, 2006; Brown *et al.*, 2004). Clusterin expression is induced by and prevents the aggregation of PrP[106-126] (McHattie & Edington, 1999; Chiesa *et al.*, 1996).

LRP: LRP10 (AD:B1) was significantly up-regulated only in vCJD vs NND (1.9-fold). LRP5 (AD:B1 & B3) was specifically and significantly down-regulated in vCJD. It has been suggested that LRP on neurons mediates uptake of astrocyte-derived cholesterol and other lipids (Simons *et al.*, 1998). PrP^c is constitutively internalized in cell cultures and recycled back to the cell surface (Sunyach *et al.*, 2003). LRP1 facilitates clathrin-coated endocytosis of PrP^c (Taylor & Hooper,

2007). Inhibition of LRP1 causes accumulation of PrP^c in biosynthetic compartments and concomitant lowering of levels of surface PrP^c, indicating that LRP1 facilitates trafficking of PrP^c to the neuronal surface (Parkyn *et al.*, 2008). Currently it is unclear whether LRP also binds to PrP^{sc}, although infectious prion fibrils bind with picomolar affinity to VLDLs and any therefore be cleared from extracellular spaces by LDL receptors (Safar *et al.*, 2006). In scrapie (ME7) infected mouse brain LDL and VLDL receptors were increased in the hippocampus at early time points (Brown *et al.*, 2005a) but decreased in an analysis of whole brain at later stages of disease (Xiang *et al.*, 2007). Interestingly, LRP polymorphisms have been linked to increased risk of late-onset AD (Kang *et al.*, 1997). It would be worthwhile investigating whether LRP polymorphisms are associated with CJD subtypes. LRP

LPL is reported as up-regulated in gene expression studies of 139A-scrapie, ME7-scrapie, RML-scrapie and Fukuoka-CJD infected mouse brains (Riemer *et al.*, 2004; Xiang *et al.*, 2004; Xiang *et al.*, 2007; Baker & Manuelidis, 2003). In the present study, significant LPL up-regulation was observed in vCJD vs OND and vCJD vs NND (both >2.7-fold), a vCJD specific change (AD:B1 & B3).

ABCA1 was vCJD specially and significantly upregulated (AD:B1 & B3; 1.8- and 1.6-fold, respectively. This is in agreement with published data (Xiang *et al.*, 2005; Xiang *et al.*, 2004; Riemer *et al.*, 2004; Xiang *et al.*, 2007). ABCA1 is a membrane-associated protein expressed by neurons, astrocytes and glial cells (Fukumoto *et al.*, 2002). Its main function is to remove cellular cholesterol and phospholipids onto lipid-poor apolipoprotein particles. This process plays a crucial role in the biogenesis of HDL particles and the efflux of cholesterol. Studies have shown increased ABCA1 mRNA levels in the brains of prion infected mice (Riemer *et al.*, 2004; Xiang *et al.*, 2004; Xiang *et al.*, 2007). Although ABCA1 is only one of several genes involved in cholesterol homeostasis differentially expressed in prion infection models, altering its concentration is sufficient to modulate levels of PrP in cultured cells (Kumar *et al.*, 2008). The cause of increased ABCA1 expression in prion disease has not been determined, but it may increase membrane cholesterol concentration, resulting in increased condensation of cholesterol-rich lipid raft

structures, thereby increasing the number or size of lipid rafts. This may augment PrP^{c} bioavailablilty, stability and localization and diminish PrP^{Sc} conversion rates. The observation that over-expression of ABCA1 reduces amyloid deposition in murine models of AD can also be explained within this theory. ABCA1 mediates lipidation of a number of Apolipoproteins. ApoE is one example, and under normal physiological conditions, binds to amyloid proteins and facilitate its clearance and conformation. But if cellular conditions are such that there is more lipid-poor or lipid-free apolipoptoteins, this may in fact promote amyloidogenesis. By mediating lipidation of ApoE, increased ABCA1 increases the ration of correctly lipidated APOE, initiating more clearance than amyloidogenesis (Wahrle *et al.*, 2005; Wahrle *et al.*, 2008).

OTHER GENES OF INTEREST

Protein kinase C (PKC) has many family members. Alpha, beta-1, delta, epsilon, gamma, iota, theta and zeta are on the arrays. Of these, only beta-1 showed a vCJD specific and significant change, it was down-regulated on both (AD and ST: B1 & B3) arrays. PKC-β1 was also down regulated in sCJD brains (Xiang *et al.*, 2005). No PKC changes were reported in gene expression studies of scrapie infected brains (Brown *et al.*, 2005a; Riemer *et al.*, 2004; Booth *et al.*, 2004; Sorensen *et al.*, 2008; Xiang *et al.*, 2007; Xiang *et al.*, 2004; Skinner *et al.*, 2006). PKC-β1 could be involved in CJD pathogenesis in a number of ways. PKCs can phosphorylate ABC transporters affecting cellular lipid metabolism (Mendez *et al.*, 1991). PKC is also a buffer of calcium in the brain. Neuronal cell damage triggers release of calcium ions from intracellular stores such as mitochondria and ER. Reduced levels of PKC could therefore predispose to apoptosis.

Proteinases:

Cathepsin D (CTSD) was up-regulated significantly and specifically in vCJD cases (AD:B1 & B3; 1.8- and 1.7-fold, respectively). CTSD upregulation was only involved in one other comprehensive TSE brain gene profiling study (Riemer *et al.*, 2004). CTSD is a ubiquitously expressed lysosomal protease (Kagedal *et al.*, 2001).

During apoptosis or mild oxidative stress, CTSD is translocated to the cytosol; this is a very early response which happens even before cytochrome *c* release from the mitochondria (Roberg & Ollinger, 1998; Roberg *et al.*, 1999). CTSD mediates programmed cell death induced by TNFα, interferon-γ and Fas (Deiss *et al.*, 1996). In AD, CTSD has been shown to exhibit a beta-secretase-like role and could cleave APP in much the same way resulting in deposition of Aβ and formation of plaques (Chevallier *et al.*, 1997). An alternative role of CTSD could be to cleave Aβ peptides and assist in clearance of aggregated deposits (Hamazaki, 1996). An immunohistochemical study showed CTSD mRNA and protein to be associated with activated astrocytes in both human AD and mouse scrapie infected brains (Diedrich *et al.*, 1991b). In contrast in CJD, CTSD was found to colocalise with the disease associated form of the prion protein in and around neurons with enlarged lysosomes (Kovacs *et al.*, 2007). How CTSD may be involved in CJD pathogenesis is unclear. Enhanced proteolytic cleavage of endocytosed PrP^{c} en route to the ER or Golgi could initiate PrP^{c}-PrP^{Sc} conversion. Alternatively, it has been suggested that increased CTSD activates Bax leading to cell death (Bidere *et al.*, 2003). A recent publication suggests CTSD polymorphisms are a risk factor for vCJD (Bishop *et al.*, 2008). **CTSB** is also known as APP secretase, it is also involved in the proteolytic processing of amyloid precursor protein (APP). Up-regulation of CTSB (AD:B2) was only observed in OND vs NND and it is not therefore a vCJD associated change, although it was found to be upregulated in one study of mouse scrapie(Sorensen *et al.*, 2008). **CTSC and CTSG** were significantly and specifically up-regulated in vCJD (AD:B1 & B3) with > 2-fold change in each case. CTSC upregulation was also observed in the comprehensive gene expression studies of sCJD (Xiang *et al.*, 2005) and one study of scrapie infected mouse brain (Xiang *et al.*, 2004).

The AD array includes probes for a number of genes involved in the processing of APP. APP can be cleaved at three different sites by α- β- and γ-secretases, with cleavage by –β and –γ secretases resulting in the formation of Aβ (Wilquet & De Strooper, 2004). β- and γ-secretases are found in lipid rafts. The α-secretases on the array include ADAMs -9, -10 and -17. These showed no significant change in vCJD. The β–secretases, **β-site APP cleaving enzyme** (BACE) 1 and 2 are both on the AD

array. Only BACE2 was significantly and specifically upregulated in vCJD (AD:B1 & B3; ~2-fold). Prp^{c} in lipid rafts has been reported to bind to β-secretases and its conversion to PrP^{Sc} has been postulated to result in increased Aβ formation (Parkin *et al.*, 2007). γ-secretase is a complex of **presenilins** 1 and 2 (PSEN1 and PSEN2), **nicastrin** (NCSTN), **Aph-1** (APH1A) and presenilin enhancer (PEN-2). Of these, PSEN1 and APH1A were significantly and specifically regulated (down and up, respectively) in vCJD and NCSTN was significantly down regulated (AD:B3) in vCJD vs OND. **β-amyloid precursor-like protein-1** (APLP1) is an APP family member and is also processed by γ-secretase (Wasco *et al.*, 1993; Scheinfeld *et al.*, 2002). APLP1 was significantly and specifically upregulated in vCJD (AD:B1& B3).

Proteinase inhibitors: Alpha-2 macroglobulin (α2M), a general proteinase inhibitor, was upregulated in vCJD (AD:A1 & A3; 3.7- and 3.0-fold, respectively). This was also observed in two studies of mouse scrapie (Xiang *et al.*, 2004; Riemer *et al.*, 2004). Recently, α2M has been suggested to act as an extracellular chaperone binding to unfolded / incorrect folded extracellular proteins (French *et al.*, 2008). Activated α2M binds to Aβ and facilitates its degradation by binding to LRP (LDL-receptor) (Narita *et al.*, 1997). Exogenous addition of α2M to neuronal cultures from APP transgenic mice reduces Aβ as a result of clearance by LRP (Qiu *et al.*, 1999). Genetic polymorphisms of α2M are associated with amyloid diseases including AD (Tanskanen *et al.*, 2008). The serine proteinase inhibitor (SERPIN), Kunitz type 2 (**SPINT2**) was significantly and specifically down-regulated in vCJD (AD: B1 & B3; -0.6- and -0.8-fold, respectively). In other studies, serine peptidase inhibitors are reported to be up-regulated (Riemer *et al.*, 2004; Xiang *et al.*, 2004).

Neuronal proteins: The arrays contain a number of synapse associated proteins; five of these were significantly and specifically changed in vCJD. **Choline acetyltransferase** (CHAT) was upregulated (AD:B1 & B3). This enzyme synthesises acetylcholine. **Butyrylcholinesterase** (BCHE**)** which degrades esters of choline, including acetylcholine, was up-regulated (AD:B1 & B3; 1.9- and 2.1-fold, respectively). BCHE is expressed in neurons and glial cells in the brain and may

participate in neurogenesis and neurite growth (Darvesh & Hopkins, 2003). BCHE expression is significantly increased in AD brains (Perry *et al.*, 1978; Saez-Valero *et al.*, 2003) where it has been associated with neurofibrillar tangles and amyloid plaques (Gomez-Ramos *et al.*, 1994; Carson *et al.*, 1991). S**ynuclein alpha** (SNCA) (AD:B1 & B3; -0.6-, -0.5-fold, respectively) was down regulated. SNCA is also down-regulated in sCJD (Xiang *et al.*, 2005). N**europeptide Y** (NPY) (AD:B1 & B3; -0.1-, -0.1-fold, respectively) was down-regulated. **Somatostatin** (SST) (AD:B1 & B3) was down regulated. That both increases and decreases in the expression of genes coding for synapse and neurotransmitter associated proteins were observed is not surprising given neuronal loss in CJD. At the protein level, decreased levels of synaptic vesicle-associated proteins and neurotransmitters have been observed in CJD and increased levels in AD (Ferrer *et al.*, 1999).

Insulin-like growth factor binding protein (IGFBP3/4) (ST:B1 & B3 / ST:B1, B2 & B3; IGFBP3 = 2.3-,2.1-fold / IGFBP4 = 3.4-,1.9-,1.8-fold change, respectively) is similar to insulin-like growth factor-1 receptor which has been linked to degeneration of scrapie-infected neurons (Ostlund *et al.*, 2001).

Urokinase plasminogen activator (PLAU) (AD:B1 & B2; 1.6-, 2.2-fold change, respectively) has been recently found to bind to the pathological isoform of PrP (Fischer *et al.*, 2000). Plasminogen is a pro-protease that is converted to its active form, plasmin by urokinase-type plasminogen activator systems. Plasmin has been suggested to have a neuroprotective role in AD because it is capable of degrading Aβ fibrils (Tucker *et al.*, 2000). Urokinase-type plasminogen activator receptor (uPAR) bound PLAU elicits intracellular signaling. Up-regulation of PLAU suggests activation of downstream signaling cascades involved in neuronal degeneration.

Three other genes, guanine nucleotide binding protein (G protein)-β4 (GNB4) and guanine nucleotide binding protein (G protein)-γ5 (GNG5) and ubiquinol-cytochrome c reductase core protein-2 (UQCRC2) were also significantly and specifically changed in their expression in vCJD brains but are not discussed further as there is little data available about these genes.

The gene expression changes observed in this study are consistent with much of the recent literature on the neuropathogenesis of TSEs in that they highlight changes in genes associated with the folding, processing and degradation of proteins and in particular PrP and the biochemical and membrane events associated with the formation and turnover of lipid rafts. As is the case for many differentially expressed genes, the significance of modulation in prion disease is not clear. Molecular heterogeneity in which defects in many separate and complicated pathways may account for overlapping diseases has been a challenge in understanding the pathogenic mechanisms in neurodegenerative disorders. Nonetheless, it is encouraging that even on small sample sizes using focused microarray methods, it has been possible to identify a list of 48 up-regulated and 33 down-regulated differentially expressed genes, some of which have previously been published as having links with prion disease or other amyloidogenic diseases. Promisingly, when compared to a recent large-scale Affymetrix genechip study of unmatched (age/gender) sCJD patients, 14 genes were implicated in both studies.

7 CONCLUDING REMARKS

A risk assessment was carried out to develop evidence-based guidelines for an RNA extraction protocol from TSE infected human brain material. Techniques for isolating RNA and retaining RNA quality whilst removing and/or inactivating the TSE agent have not been previously described and are detailed in this project. The use of ~4 M GTC and ~2 M phenol in acidic solution (~pH 5.0) was considered suitable as previous inactivation studies using similar concentrations have observed reduced CJD infectivity titres of ~99.7% (Manuelidis, 1997). For safety and to ensure removal of residual PrP, a further phenol-chloroform extraction was carried out. Assessment of the RNA preparations using western immunoblotting for PrP^{res} detection revealed that the RNA isolation method described in this project reduced the level of PrP^{res} by at least 10^4 fold, and that there was no detectable PrP^{res} in > 0.5µg vCJD brain equivalent. However, to conclusively prove complete inactivation, the protocol must be verified by bioassay for infectivity. Due to time and financial constraints, this was not carried out but based on the results of the risk assessment; it was considered that the RNA extracts did not contain detectable amounts of infectious PrP^{Sc}, although samples were still treated as low risk.

Assessment of relevant inclusion and exclusion criteria for case selection was undertaken. The decision was made to test vCJD vs control and also vCJD vs OND comparisons to verify vCJD-specific modulated genes and differentiate them from generalized neurological alterations. Although a number of relevant criteria were suggested to be matched for, over-zealous matching would have limited the sample strength of the study. Therefore it was necessary to determine which criteria are most have the greatest affect on RNA integrity and whether non-specific alterations correlate with any of the pre- or post-mortem factors investigated and if so, is it possible to match or measure them and account for them by multivariate analysis.

RNA preparations from 78 human cases were tested for quality and quantity as measured by the Agilent Bioanalyzer (giving a 28S:18S rRNA ratio, RIN and

concentration) and Nanodrop spectrophotometer (giving an $A_{260:280}$, $A_{260:230}$ ratio and concentration). RNA metrics were evaluated for their suitability for measuring brain RNA preparations. As observed in previously published studies, the 28S:18S rRNA ratio was not an accurate measure of RNA quality. Quantification was more accurate and reproducible using the Nanodrop spectrophotometer. RIN values and $A_{260:280}$, $A_{260:230}$ gave a good indication of the RNA preparations integrity and purity. Overall, human RNA preparations had lower quality and yield when compared to mouse brain preparations, in agreement with previous findings, an effect which has been suggested to be an intrinsic difference between human and mouse brain tissue. The intra- and inter-case variability of RNA preparations was tested. Although there was some intra-case variation (~10%) of quality and quantity, this effect was greater inter-case, as expected. Variation of RNA quality and quantity occurs mainly across patients rather than within a single case. This finding is promising if further work was to be carried out using the RNA preparations. If RNA sample variablility was so great as to preclude valid transcriptome comparisons, subsequent gene expression analysis would be confounded. Additionally, it suggests that differences between RNA samples were not introduced due to processing and the samples retained the representative in vivo transcriptome situation prior to processing.

Investigation into whether any pre- or post-mortem factors correlated with the quality and/or quantity of isolated RNA from human brain material was also carried out. RIN values of tissues stored in RNAlater was slightly higher when compared to liquid nitrogen or -80ºC storage methods, although this effect was only observed in human and not mouse tissues. No effect on RNA quality or quantity was observed to correlate with FI or storage temperature. Age at death and PMI did not correlate with either RIN or $A_{260:280}$ irrespective of gender, however there was a significant negative correlation between RIN and RNA yields from female cases. Tissue pH and RIN values showed a significant positive correlation in the male data set and a large but insignificant correlation within the female dataset. Tissue pH did not correlate with yield or $A_{260:280}$ in the male data set, but showed a significant negative correlation with yield and a significant positive correlation with $A_{260:280}$ within the female data set. These results were calculated from smaller sample sizes and the p-values are

approaching significance level and therefore cannot be conclusive. FTC did not correlate with yield or $A_{260:280}$, but there was a significant negative correlation with RIN. Repeated freeze-thawing of tissues is known to severely affect cellular molecule integrity. The agonal state of a patient was assessed by reviewing clinical and histopathological notes and scoring the presence and degree of a number of factors. These factors were selected based on a similar system described by Tomita et al and from a literature search for agonal factors have the greatest impact on brain tissue (Tomita *et al.*, 2004). IAS scores were calculated, with and without disease duration, as preliminary results indicated that disease duration may have a prominent effect on RNA quality and quantity. On further assessment, this effect was not significant. The data testify to the high postmortem stability of RNA in general, although the overall low quality of extracted RNA may have occurred during the disease period (pre-mortem) and not as a post-mortem artifact. Overall, age at death, PMI, tissue pH and FI including storage method or storage time does not affect RNA quality, although there may be a potential connection between age at death and RNA quantity. The amount of variation of RNA quality (RIN) is intrinsic to the particular sample and does not correlate with age at death, PMI or tissue pH. This finding is consistent with the finding that variability between RNA samples is greater inter-case than intra-case. Having established that RIN variation is intrinsic, it was decided that sample of high RIN quality would be selected for gene expression analysis.

Ultimately, the aim was to carry out transcriptome analysis and identify potential vCJD-specifically modulated genes. Focused microarrays containing Alzheimer disease related and signal transduction pathway genes were used. Variability due to technical and/or intrinsic case variation was ~13% each and suggests it was reasonable to assume that the remaining gene changes were potential disease associated changes. With the exception of one anomalous result, the overall SAM analysis identified FDR ~9%. While this is slightly higher than the generally accepted 5% FDR threshold, it was still within acceptable limits.

Taking all this into account, 46 genes were identified as potential vCJD-specific changes. 22 have not been previously described in the context of prion diseases. A

comparison of our results with the findings of other groups using similar mouse models and a study of sCJD patients identified 25 genes previously described in experimental models and 12 genes reported as differentially expressed in a sCJD human study (Puig & Ferrer, 2001; Booth *et al.*, 2004; Campbell *et al.*, 1994; Skinner *et al.*, 2006; Riemer *et al.*, 2004; Sorensen *et al.*, 2008; Brown *et al.*, 2005a; Brown *et al.*, 2005b; Xiang *et al.*, 2004; Xiang *et al.*, 2005).

In conclusion, although the use of focused arrays with limited and targeted gene features precludes drawing definitive conclusion regarding gene expression in vCJD human brains, it has been shown that even using robust stastistical comparisons, gene expression measurements can be carried out on relatively degraded RNA samples and preliminary results suggest that differentially expressed gene expression profiles would be identified using microarray techniques. Careful selection of cases is paramount to the experimental design of gene expression studies, especially when using human tissues. However, this study has provided evidence that factors such as PMI, FI and agonal state (as determined by IAS) may not have as large an impact as previously suspected. Based on the findings from this study, improved method of tissue storage, the introduction of RIN assessment of RNA and the introduction of agonal state assessments (IAS) have been proposed to the NCJDSU and MRC brain banks to increase the importance and value of storaging tissues in tissue banks for molecular research.

Overall, this project has shown; that RNA can be safely extracted from CJD brain tissues, that RNA quality and quantity does not correlate with tissue pH, PMI or age at death, it is of sufficient quality for profiling studies and careful comparison of variant CJD and controls can accurately identify disease-specific changes. This provides proof of principle for further, more extensive studies providing a more complete picture of the transcriptome during neurodegenerative disease.

8 FUTURE WORK

8.1 OBJECTIVES

- Design primers for selected genes of interested.
- Optimise primers for real-time polymerase chain reaction (PCR).

8.2 INTRODUCTION

Confirming the veracity of microarray data, while currently not a pre-requiste for acceptance, is quickly becoming expected for publication (Editor in chief and associate editors, 2001; Firestein & Pisetsky, 2002). This has been met with a mixed response from the scientific community, one argument being that rigourous normalization and large sample size are sufficient to preclude corroborative studies (Rockett & Hellmann, 2004). Nonetheless, the inclusion of corroborative data is useful for validating microarray data. For this project, proof of concept for the use of quantitative real-time polymerase chain reaction (qRT-PCR) was carried out to evaluate the technique's appropriateness for validating the microarray data. Time did not permit analysis of samples to verify the array results.

Independent verification of microarray data is generally done by one of four methods; northern blot, *in situ* hybridization, RNase protection assays (RPA) or polymerase chain reaction (PCR). Northern blot and RNase protection assays require a minimum of 5 μg of total RNA and although conventional RT-PCR requires much less total RNA, it is an end-point process which is insufficiently precise for quantitative determination. Quantification by real-time RT-PCR (qRT-PCR) has become the gold standard of nucleic acid quantification.

Polymerase chain reaction is a technique that allows exponential amplification of short, specific DNA sequences (usually 100 to 600 bases) within a longer double

stranded DNA molecule. Since its invention in 1985 by Kary B. Mullis, the technique has been repeatedly refined to be capable of increasingly more accurate and sensitive results (Mullis, 1990; Mullis *et al.*, 1986). RT-PCR is particularly suited to studying the transcriptome, as it is sensitive enough to detect even low-level mRNA levels in different samples. The addition of fluorescene-based kinetics to PCR techniques and real-time quantitation monitoring has meant that qRT-PCR has become the method of choice for quantifying mRNA, due to its simple handling, high reproducibility, large dynamic range, and low total RNA requirement (~1000-fold less than conventional methods) (Bustin, 2000). Figure 8.1 represents the processes involved in generating qRT-PCR results.

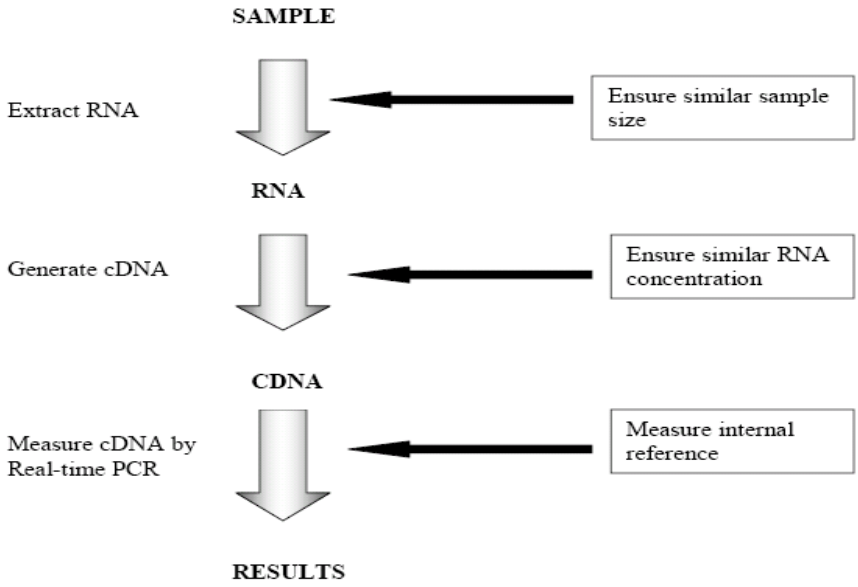

Figure 8.1. Processes required to generate real-time RT-PCR results. Black arrows indicate points of the sample preparation protocol which are suitable for normalization. The three most commonly used strategies for normalization are stated in the boxes on the right and were also used for this project. Modified from (Huggett *et al.*, 2005).

PCR uses a pair of primers, each about 20 nucleotides in length, which are complementary to a defined sequence on each of the two strands of the DNA. These primers are extended by a heat-stable DNA polymerase (i.e. Taq polymerase) to enzymatically assemble a copy of the designated DNA sequence. DNA oligonucleotides are used to initiate the DNA synthesis. Thermal cycling, i.e.

alternately heating and cooling the sample to a defined series of temperature and time steps, physically separates the strands of the DNA double helix (higher temp), to uses as a template during DNA synthesis (lower temp). Amplification happens logarithmically. Real-time modification includes the addition of either florescent dyes that intercalate with double-stranded DNA or modified DNA oligonucleotide probes that fluoresce when hybridized with a complementary DNA. Quantification and amplification are monitored simultaneously. In order to measure messenger RNA (mRNA), the method was extended by introducing the use of reverse transcriptase to convert mRNA into complementary DNA (cDNA) which was then amplified by PCR.

When the sequence of the gene is known, qRT-PCR is well suited for validation of differential expression especially when dealing with low-abundance RNA tissues or when tissue samples are limited and valuable. A quantitative measure of gene expression between different samples requires some form of normalization to a reference that provides a common basis for the comparison. There are a number of alternative strategies; standardizing tissue sample sizes, normalize to an artificial molecule i.e. spiking sample with artificial RNA molecule of known concentration, ensure RT reactions contain equivalent amounts of total RNA, use of internal reference gene/s and use of genomic DNA. There are inherent problems with each of these strategies and in general qRT-PCR data is normalized to an internal control gene. Appropriate genes are typically reference genes whose expression usually does not change under the conditions of the experiment. Traditionally used transcripts included GAPDH, actins, tubulins, cyclophilins and 28S and 18S RNA. These transcripts are historical carryovers and were used for many years as references in northern blots, Rnase protection assays and conventional RT-PCR. While the expression of these historical reference genes in certain cell types or under certain conditions may remain stable, this does not hold true for all cell types or all conditions and can vary considerably (Suzuki *et al.*, 2000; Bustin, 2000; Thellin *et al.*, 1999). qRT-PCR is far more sensitive and as quantitative data becomes an increasingly fundamental part of molecular biology, a re-evaluation of these classic reference genes is required. It was important for this study to choose specifically

relevant reference genes and validate the stability of expression. In addition, a number of recent papers have indicated the inappropriateness of any single reference gene for normalization and highlighted the need for validating the status of reference genes for each type of specimen analyzed (Vandesompele *et al.*, 2002; Huggett *et al.*, 2005).

While qRT-PCR has become more mainstream, there has been increased focus towards pathway analysis and pathway identification. Significance analysis at the single gene level can be affected by limited sample number and experimental noise. To overcome this, analysis may be undertaken at a higher level where genes are categorised into functional groups.Bioinfomatic applications such as, Gene Ontology (GO), Database for Annotation, Visualization and Integrated Discovery (DAVID) and Pathway Studio have streamlined researcher's ability to annotate large gene expression databases and help to understand how lists of individually altered genes are coordinated and interdependently related. Pathway identification based on functional classification of gene sets has been shown to be more robust and reproducible than using single gene results (Manoli *et al.*, 2006). Key changes in gene expression in the vCJD diseased vs control brain could be ranked into categories; biological processes, molecular function and cellular components, to identify whether there is a relationship between differentially expressed sets of genes and to put them into a biologically meaningful context.

8.3 CHOICE OF HOUSE-KEEPING GENES

Different control genes are suitable for different cell types under different conditions. Attention should be paid to the choice of an appropriate control gene or genes used for qRT-PCR for the conditions and tissue/cell type under investigation (Spanakis, 1993). In recent years, a number of large scale studies into appropriate reference genes in a range of tissue types have been published. Barber tested the expression of glyceraldehyde-3-phosphate dehydrogenase (GAPDH) in 72 human pathologically

normal tissue types. Significantly different expression levels were observed between tissue types and between donors for the same tissue, although there was no specific effect of either age or gender on expression levels. GAPDH was selected as a candidate house-keeping gene for this study as its expression is highly stable in neurological tissues (Barber *et al.*, 2005). More recently, Coulson tested a panel of reference genes specifically for use in human post-mortem neuropathological studies and for AD vs control cerebellum, GAPDH, β-2-microglobulin (β2M) and ubiquitin C (UBC) were ranked top for stability (Coulson *et al.*, 2008). β-actin (ACTB) has generally been used as a reference gene for many tissue types, although it has been shown that the human genome contains processed β-actin pseudogenes, which can result in the amplification of fragments from genomic DNA displaying the same size as those generated from the cDNA template (Leavitt *et al.*, 1984). Rigorous testing of 10 neuronal areas of AD and control human brains with PMI's between 6 -96 hrs, showed invariant expression of the cyclophilin gene (Yasojima *et al.*, 2001). For this study, a panel of 9 reference genes were selected from the literature and each was evaluated for its suitability as an internal reference for post-mortem human autopsy brain material (GAPDH, ACTB, B2M, TrkB, PPIA, UBC, HPRT, 18S rRNA and SYP). Details of these genes are given in Table 8.1.

GENE NAME	FUNCTION	PRO	CON
Glyceraldehyde-3-phosphate dehydrogenase (GAPDH)	An important glycolytic enzyme that catalyses the oxidative phosphorylation of glyceraldehyde-3-phosphate to 1,3-diphosphoglycerate.	Historical. Recommended for less sensitive detection methods. Tested for validation in human brains. (Petersen *et al.*, 1990; Coulson *et al.*, 2008; Barber *et al.*, 2005; Tang *et al.*, 1996)	(Suzuki *et al.*, 2000; Schmittgen & Zakrajsek, 2000; Foss *et al.*, 1998; Zhong & Simons, 1999)
β-actin (ACTB)	A major cytoplasmic structural protein and essential for the	Historical. Tested for validation in human brains. (Coulson *et al.*,	Differentially expressed in the brain specimens of both AD and

	kinetics of the cytoskeleton.	2008)	control subjects. (Suzuki *et al.*, 2000; Gutala & Reddy, 2004; Schmittgen & Zakrajsek, 2000; Selvey *et al.*, 2001)
β 2-microglobulin (B2M)	A 11 kDa protein associated with the outer membrane of many cells including lymphocytes. It is the small subunit of the MHC class I molecule. Essential for the structure and kinetics of the cytoskeleton.	Historical. (Schmittgen & Zakrajsek, 2000; Serels *et al.*, 1998)	Altered expression observed in CJD microarray results as well as AD (Carrete *et al.*, 2003) and PD brains (Mogi *et al.*, 1995).
Tyrosine receptor kinase (TrkB/TrkC)	Receptor for neurotrophins; brain derived neurotrophic factors	(Schramm *et al.*, 1999)	Altered expression of BDNF observed in CJD microarray results.
Peptidylprolyl isomerase A/ Cyclophilin A (PPIA)	Involved in cellular protein folding and protein interactions	Highly stable with constant expression in any given organ. (Yasojima *et al.*, 2001)	Under hypoxia, altered expression may occur. (Zhong & Simons, 1999)
Ubiquitin C (UBC)	Highly conversed regulatory protein that is expressed in many tissues types. Functions include labeling of proteins for proteasomal degradation and regulation of the stability and intracellular localization of	Best scoring overall gene from a panel of 9 genes tested in 5 conditions and valid for human brain studies. (Vandesompele *et al.*, 2002; Coulson *et al.*, 2008)	

	proteins.		
Hypoxanthine phosphoribosyltransferase (HPRT)	Enzyme involved in purine metabolism, recycling purine from degraded DNA.	Best scoring overall gene from a panel of 9 genes tested in 5 conditions. (Dheda *et al.*, 2004; Vandesompele *et al.*, 2002)	Low expression level in tissues, although higher in brain. (Krenitsky, 1969)
18S rRNA	Ribosomal subunits.	Historical. (Schmittgen & Zakrajsek, 2000)	
Synaptophysin 1 (SYP)	A membrane glycoprotein of synaptic vesicles that is ubiquitously expressed in all neurons and in many endocrine cells.	neuron-specific gene observed to be remarkably stable following intense neuronal activity. (Chen *et al.*, 2001)	Altered expression in AD human brains. (Gutala & Reddy, 2004)

Table 8.1 Reference gene selected from literature which may be suitable for studying gene expression changes in CJD vs control human brains.

8.4 RESULTS

Primer sequences for the 9 candidate reference genes (Table 8.1) were designed using Primer3 and verified using NetPrimer web-based software applications. The primers were then tested on RNA pooled from 12 human RNA preparations with RIN >6.0, $A_{260:280}$ nm absorbance ≥ 2.0 and $A_{260:230}$ nm absorbance ≥ 1.7.

Only six transcipts were amplified sufficiently to warrant further assessment. Of these, five were successfully cloned in the pGEM®-T Easy vector. For quantification purposes a reference standard is required. PCR amplicons from these 5 genes (refer to Chapter 2, section 2.5.2) were each inserted into pGEM-T Easy vectors (Invitrogen, UK) and ligated using T4 ligase (Figure 8.2). Ligation reactions were then transformed into high-efficiency competent DH5α cells for transformations.

Transformants were screened for inserts by blue/white colony color on IPTG/X-Gal indicator plates. Recombinant plasmid DNA was purified using the Qiaprep Spin Miniprep DNA purification systems and analysed on 1.5% agarose gels. Purified plasmid DNA was restriction digested using ECOR1, and digested and undigested plasmid DNA was analysed on an agarose gel to identify fragment sizes. If the correct sizes were present, the plasmid was sent for sequencing to confirm its identity (Figure 8.3).

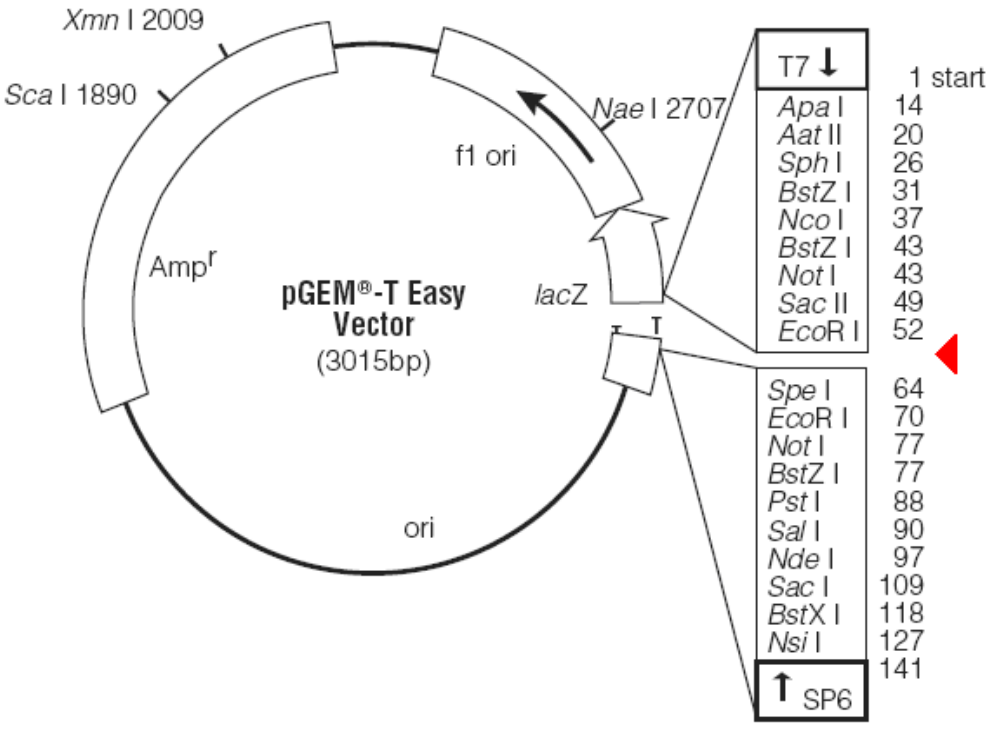

Figure 8.2. pGEM-T Easy vector map. Amplicon were inserted within the multiple cloning region (red arrow). Recombinant clones with the insert within the coding region of β-galactosidase can be identified by white colonies obtained following transformation of competent cells. Restriction enzyme, ECOR1 was used to release the insert in single-enzyme digestion reactions (see Figure 8.3).

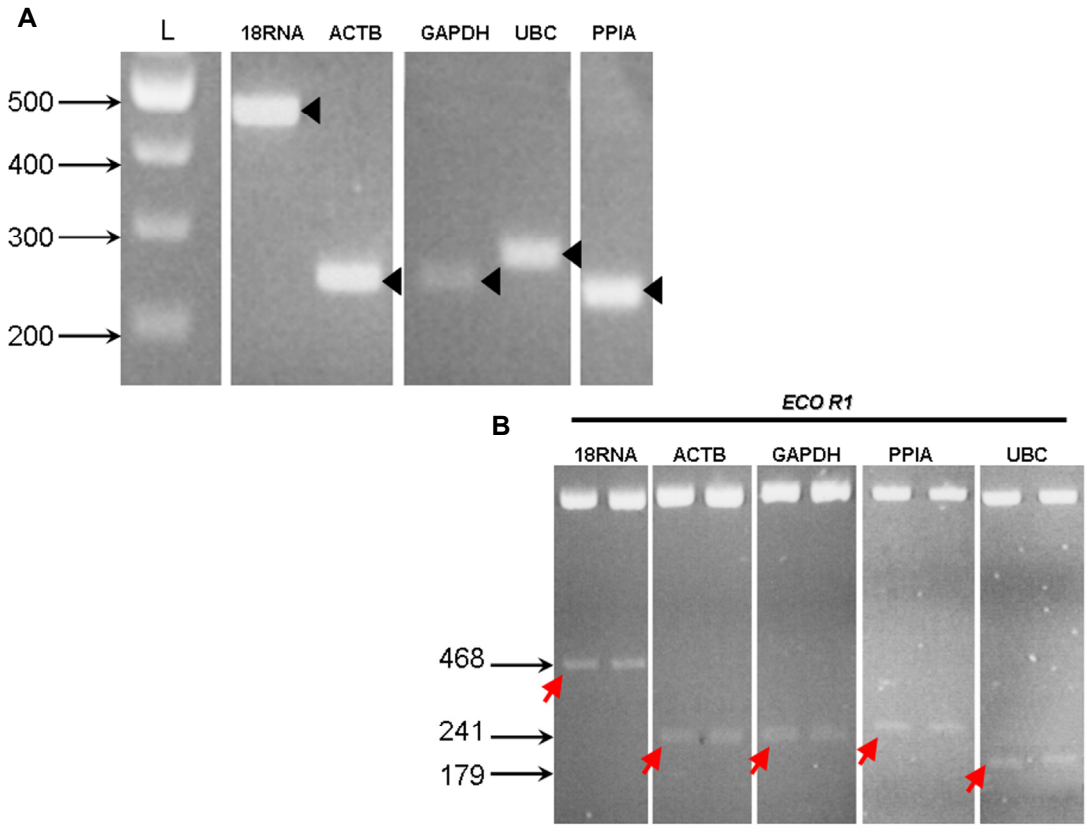

Figure 8.3. Electrophoretic analysis of the amplicons of the 5 selected reference genes. A. PCR-amplified products were analysed on 1.5% agarose gels and visualized with ethidium bromide staining and UV illumination. Specific band of appropriate molecular weight are indicated by the black triangles. Product sizes are; 18SrRNA. 468bp, GAPDH. 241 bp. ACTB. 241bp. UBC. 245 bp. PPIA. 179 bp. L. DNA marker ladder (kb). B. Restriction digest reactions of recombinant plasmids using EcoR 1. Specific bands of the correct molecular weight for PCR product were released from each of the pGEM-T Easy vectors and used for sequencing (red arrows). The extra band seen at the top of each lane corresponds to un-cut plasmid.

These preliminary results have identified a panel of reference genes and primers (Table 8.2) and generated a series of control plasmids to allow their quantification by qRT-PCR. Unfortunately, due to the time constraints of this project, it was not possible to continue this work to validate the use of these reference genes for the comparative analysis of human brain RNA preparations generated in this project. It is intended to carry this work further at a later date.

Gene name	Symbol	GenBank	Sequence	PCR product size
glyceraldehyde-3-phosphate dehydrogenase	GAPDH	NM_002046.3	TCATCATCTCTGCCCCCTCT CCATCACGCCACAGTTTCC	241
Beta-actin	ACTB	NM_001101.2	ATTCCTATGTGGGCGACGAG GCTGGGGTGTTGAAGGTCTC	241
Cyclophilin A	PPIA	NM_021130.3	GGCAAGACCAGCAAGAAGA GGGAGGGAACAAGGAAAAC	179
Ubiquitin C	UBC	NM_021009.4	TGGGTCGCAGTTCTTGTTTG GGGTGGACTCTTTCTGGATGTT	245
18s rRNA	18RNA	X03205	TCAAGAACGAAAGTCGGAGG GGACATCTAAGGGCATCACA	468

Table 8.2. Primer sequences.

Reference List

(1996). World Health Organization consultation on public health issues related to bovine spongiform encephalopathy and the emergence of a new variant of Creutzfeldt-Jakob disease. 45 edn, pp. 295-296.

(2006). World Health Organisation guidelines on tissue infectivity distribution in transmissible spongiform encephalopathies.

(2008). The National Creutzfeldt-Jakob Disease Surveillance Unit.

Advisory Committee on Dangerous Pathogens & Spongiform Encephalopathy Advisory Committee (2003). Transmissible Spongiform Encephalopathy Agents: Safe Working and the Prevention of Infection. Suffolk: HSE Books.

Aguzzi, A. & Heikenwalder, M. (2006). Pathogenesis of prion diseases: current status and future outlook. *Nat Rev Microbiol* **4**, 765-775.

Akowitz, A., Sklaviadis, T., Manuelidis, E. E. & Manuelidis, L. (1990). Nuclease-resistant polyadenylated RNAs of significant size are detected by PCR in highly purified Creutzfeldt-Jakob disease preparations. *Microb Pathog* **9**, 33-45.

Akowitz, A., Sklaviadis, T. & Manuelidis, L. (1994). Endogenous viral complexes with long RNA cosediment with the agent of Creutzfeldt-Jakob disease. *Nucleic Acids Res* **22**, 1101-1107.

Allsopp, T. E. & Fazakerley, J. K. (2000). Altruistic cell suicide and the specialized case of the virus-infected nervous system. *Trends Neurosci* **23**, 284-290.

Alper, T., Haig, D. A. & Clarke, M. C. (1966). The exceptionally small size of the scrapie agent. *Biochem Biophys Res Commun* **22**, 278-284.

Amouyel, P., Vidal, O., Launay, J. M. & Laplanche, J. L. (1994). The apolipoprotein E alleles as major susceptibility factors for Creutzfeldt-Jakob disease. The French Research Group on Epidemiology of Human Spongiform Encephalopathies. *Lancet* **344**, 1315-1318.

Anderson, R. E. & Hill, R. B. (1989). The current status of the autopsy in academic medical centres in the United States. *Am J Clin Pathol* **92**, S31-S37.

Asakura, S., Eguchi, G. & Lino, T. (1966).*Salmonella* flagella: *in vitro* reconstruction and over-all shapes in flagellar filaments. *J Mol Biol* **16**, 302-316.

Asakura, S., Eguchi, G. & Lino, T. (1964). Reconstruction of bacterial flagella *in vitro*. *J Mol Biol* **10**, 42-56.

Asher, D. M., Pomeroy, K. L., Murphy, L., Gibbs, C. J., Jr. & Gajdusek, D. C. (1987). Attempts to disinfect surfaces contaminated with etiological agents of the spongiform encephalopathies.

Asher, D. M., Pomeroy, K. L., Murphy, L., Rohwer, R. g., Gibbs, C. J., Jr. & Gajdusek, D. C. (1986). Practical inactivation of scrapie agent on surfaces.

Atz, M. E., Walsh, D. M., Cartagena, P. & other authors (2007). Methodological considerations for gene expression profiling of human brain. *J Neurosci Methods* **163**, 295-309.

Auer, H., Lyianarachchi, S., NewsoM, D., Klisovic, M. I., Marcucci, U. & Kornacker, K. (2003). Chipping away at the chip bias: RNA degradation in microarray analysis. *Nat Genet* **36**, 292-293.

Baeuerle, P. A. & Henkel, T. (1994). Function and activation of NF-kappa B in the immune system. *Annu Rev Immunol* **12**, 141-179.

Bahn, S., Augood, S. J., Ryan, M., Standaert, D. G., Starkey, M. & Emson, P. C. (2001). Gene expression profiling in the post-mortem human brain -- no cause for dismay. *Journal of Chemical Neuroanatomy* **22**, 79-94.

Baker, C. A. & Manuelidis, L. (2003). Unique inflammatory RNA profiles of microglia in Creutzfeldt-Jakob disease. *PNAS* **100**, 675-679.

Baker, C. A., Martin, D. & Manuelidis, L. (2002). Microglia from Creutzfeldt-Jakob disease-infected brains are infectious and show specific mRNA activation profiles. *J Virol* **76**, 10905-10913.

Baker, D. & Agard, D. A. (1994). Kinetics versus thermodynamics in protein folding. *Biochemistry* **33**, 7505-7509.

Banerjee, S., An, S., Zhou, A., Silverman, R. H., Makino, S. & Abbassi, H. (2000).RNase L-independent specific 28S rRNA cleavage in murine coronavirus-infected cells. *J Virol* **74**, 8793-8802.

Barber, R. D., Harmer, D. W., Coleman, R. A. & Clark, B. J. (2005).GAPDH as a housekeeping gene: analysis of GAPDH mRNA expression in a panel of 72 human tissues. *Physiol Genomics* **21**, 389-395.

Baron, G. S., Wehrly, K., Dorward, D. W., Chesebro, B. & Caughey, B. (2002). Conversion of raft associated prion protein to the protease-resistant state requires insertion of PrP-res (PrP(Sc)) into contiguous membranes. *EMBO J* **21**, 1031-1040.

Barron, R. M., Campbell, S. L., King, D., Bellon, A., Chapman, K. E., Williamson, R. A. & Manson, J. (2007). High titers of transmissible spongiform encephalopathy infectivity associated with extremely low levels of PrP^{sc} i*n vivo*. *J Biol Chem* **282**, 35878-35886.

Barton, A. J., Pearson, R. C., Najlerahim, A. & Harrison, P. J. (1993). Pre- and postmortem influences on brain RNA. *J Neurochem* **61**, 1-11.

Basu, A., Lazovic, J., Krady, J. K., Mauger, D. T., Rothstein, R. P., Smith, M. B. & Levison, S. W. (2005). Interleukin-1 and the interleukin-1 type 1 receptor are essential for the progressive neurodegeneration that ensues subsequent to a mild hypoxic/ischemic injury. *J Cereb Blood Flow Metab* **25**, 17-29.

Bate, C., Salmona, M., Diomede, L. & Williams, A. (2004). Squalestatin cures prion-infected neurons and protects against prion neurotoxicity. *J Biol Chem* **279**, 14983-14990.

Beal, M. F. (1995). Aging, energy, and oxidative stress in neurodegenerative diseases. *Ann Neurol* **38**, 357-366.

Bell, J. E., Alafuzoff, I., Al-Sarraj, S. & other authors (2008). Management of a twenty-first century brain bank:experience in the BrainNet Europe consortium. *Acta Neuropathol* **115**, 497-507.

Bell, J. E. & Ironside, J. W. (1993). Neuropathology of spongiform encephalopathies in humans. *Br Med Bull* **49**, 738-777.

Bellinger-Kawahara, C., Kempner, E., Groth, D., Gabizon, R. & Prusiner, S. B. (1988). Scrapie prion liposomes and rods exhibit target sizes of 55,000 Da. *Virology* **164**, 537-541.

Ben-Shachar, D., Riederer, P. & Youdim, M. B. (1991). Iron-melanin interaction and lipid peroxidation: implications for Parkinson's disease. *J Neurochem* **57**, 1609-1614.

Ben-Zeev, O., Doolittle, M. H., Singh, N., Chang, C. H. & Schotz, M. C. (1990). Synthesis and regulation of lipoprotein lipase in the hippocampus. *J Lipid Res* **31**, 1307-1313.

Benveniste, E. N. & Merill, J. E. (1986). Stimulation of oligodendroglial proliferation and maturation by interleukin-2. *Nature* **321**, 610-613.

Bessen, R. A. & Marsh, R. F. (1994). Distinct PrP properties suggest the molecular basis of strain variation in transmissible mink encephalopathy. *J Virol* **68**, 7859-7868.

Bidere, N., Lorenzo, H. K., Carmona, S., Laforge, M., Harper, F., Dumont, C. & Senik, A. (2003). Cathepsin D triggers Bax activation, resulting in selective apoptosis-inducing factor (AIF) relocation in T lymphocytes entering the early commitment phase to apoptosis. *J Biol Chem* **278**, 31401-31411.

Bischof, J. C. (2000). Quantitative measurement and predicition of biophysical response during freezing in tissues. *Annu Rev Biomed* **2**, 257-288.

Bishop, M., Kovacs, G. G., Sanchez, J.-C. & Knight, R. S. (2008). Cathepsin D SNP associated with increased risk of variant Creutzfeldt-Jakob disease. *BMC Medical Genetics* **9**, 31-36.

Bolton, D. C., McKinley, M. P. & Prusiner, S. B. (1982). Identification of a protein that purifies with the scrapie prion. *Science* **218**, 1309-1311.

Bolton, D. C., McKinley, M. P. & Prusiner, S. B. (1984). Molecular characteristics of the major scrapie prion protein. *Biochemistry* **23**, 5898-5906.

Bonaventure, P., Guo, H., Tian, B. & other authors (2002). Nuclei and subnuclei gene expression profiling in mammalian brain. *Brain Res* **943**, 38-47.

Booth, S., Bowman, C., Baugartner, R., Sorensen, G., Robertson, C., Coulthart, M., Phillipson, G. & Somorjai, R. L. (2004). Identification of central nervous system genes involved in the host response to the scrapie agent during preclinical and clinical infection. *J Gen Virol* **85**, 3459-3471.

Borchelt, D. R., Taraboulos, A. & Prusiner, S. B. (1992). Evidence for synthesis of scrapie prion proteins in the endocytic pathway. *J Biol Chem* **267**, 16188-16199.

Brawerman, G., Mendecki, J. & Lee, S. Y. (1972).A procedure for the isolation of mammalian messenger ribonucleic acid. *Biochemistry* **11**, 637-641.

Breckenridge, D. G., Germain, M., Mathai, J. P., Nguyen, M. & Shore, G. C. (2003). Regulation of apoptosis by endoplasmic reticulum pathways. *Oncogene* **22**, 8608-8618.

Brown, A. R. (2005).

Brown, A. R., Rebus, S., McKimmie, C. S., Robertson, K., Williams, A. & Fazakerley, J. K. (2005a). Gene expression profiling of the preclinical scrapie-infected hippocampus. *Biochem Biophys Res Commun* **334**, 86-95.

Brown, A. R., Webb, J., Rebus, S., Walker, R., Williams, A. & Fazakerley, J. K. (2003). Inducible cytokine gene expression in the brain in the ME7/CV mouse model of scrapie is highly restricted, is at a strikingly low level relative to the degree of gliosis and occurs only late in disease. *J Gen Virol* **84**, 2605-2611.

Brown, A. R., Webb, J., Rebus, S., Walker, R., Williams, A. & Fazakerley, J. K. (2005b). Inducible cytokine gene expression in the brain in the ME7/CV mouse model of scrapie is highly restricted, is at a strikingly low level relative to the degree of gliosis and occurs only late in disease. *J Gen Virol* **84**, 2605-2611.

Brown, A. R., Webb, J., Rebus, S., Williams, A. & Fazakerley, J. K. (2004). Identification of up-regulated genes by array analysis in scrapie-infected mouse brains. *Neuropathol Appl Neurobiol*.

Brown, D. R. (1998). Prion protein-overexpressing cells show altered response to a neurotoxic prion protein peptide. *J Neurosci Res* **54**, 331-340.

Brown, D. R., Clive, C. & Haswell, S. J. (2001). Antioxidant activity related to copper binding of native prion protein. *J Neurochem* **76**, 69-76.

Brown, D. R., Herms, J. & Kretzchmar, H. A. (1994). Mouse cortical cells lacking cellular PrP survive in culture with a neurotoxic PrP fragment. *Neuroreport* **5**, 2057-2060.

Brown, D. R., Nicholas, R. S. & Canevari, L. (2002). Lack of prion protein expression results in a neuronal phenotype sensitive to stress. *J Neurosci Res* **67**, 211-224.

Brown, D. R., Qin, K., Herms, J. W. & other authors (1997a). The cellular prion protein binds copper in vivo. *Nature* **390**, 684-687.

Brown, D. R., Schmidt, B. & Kretzchmar, H. A. (1996). Role of microglia and host prion protein in neurotoxicity of a prion protein fragment. *Nature* **380**, 345-347.

Brown, D. R., Schulz-Schaeffer, W., Schmidt, B. & Kretzchmar, H. A. (1997b). Prion protein-deficient cells show altered response to oxidative stress due to decreases SOD-1 activity. *Exp Neurol* **146**, 104-112.

Brown, D. R., Wong, B. S., Hafiz, F., Clive, C., Haswell, S. J. & Jones, I. M. (1999). Normal prion protein has an activity like that of superoxide dismutase. *Biochem J* **344**, 1-5.

Brown, P. & Abee, C. R. (2005). Working with Transmissible Spongiform Encephalopathy Agents. *Institute for Laboratory Animal Research* **46**, 44-52.

Brown, P., Cathala, F., Raubertas, R. F., Gajdusek, D. C. & Castaigne, P. (1987). The epidemiology of Creutzfeldt-Jakob disease: conclusion of a 15-year investigation in France and review of the world literature. *Neurology* **37**, 895-904.

Brown, P., Gibbs, C. J., Jr., Amyx, H. L., Kingbury, D. T., Rohwer, R. g., Sulima, M. P. & Gajdusek, D. C. (1982). Chemical disinfection of Creutzfeldt-Jakob disease virus. *N Engl J Med* **306**, 1279-1282.

Bruce, M., McConnell, I., Fraser, H. & Dickinson, A. G. (1991). The disease characteristics of different strains of scrapie in Sinc congenic mouse lines: implications for the nature of the agent and host control of pathogenesis. *J Gen Virol* **72**, 595-603.

Bruce, M. E. (2003).TSE Strain Variation. *Br Med Bull* **66**, 99-108.

Bruce, M. E., Will, R. G., Ironside, J. W. & other authors (1997). Transmissions to mice indicate that `new variant' CJD is caused by the BSE agent. *Nature* **389**, 498-501.

Budka, H., Aguzzi, A., Brown, P. & other authors (1995). Neuropathological diagnostic criteria for Creutzfeldt-Jakob disease (CJD) and other human transmissible spongiform encephalopathies (prion diseases). *Brain Pathol* **5**, 459-466.

Bueler, H., Aguzzi, A., Sailer, A., Greiner, R. A., Autenried, P., Aguet, M. & Weissmann, C. (1993). Mice devoid of PrP are resistant to scrapie. *Cell* **73**, 1339-1347.

Burke, W. J., O'Malley, K. L., Chung, H. D., Harmon, S. K., Miller, J. P. & Berg, L. (1991). Effects of pre- and postmortem variables on specific mRNA levels in human brain. *Brain Res Mol Brain Res* **11**, 37-41.

Bustin, S. A. (2000). Absolute quantification of mRNA using real-time reverse transcription polymerase chain reaction assays. *J Mol Endocrinol* **25**, 169-193.

Campbell, I. L., Eddleston, M., Kemper, P., Oldstone, M. B. & Hobbs, M. V. (1994). Activation of cerebral cytokine gene expression and its correlation with onset of reactive astrocyte and acute-phase response gene expression in scrapie. *J Virol* **68**, 2383-2387.

Carrete, O., Demalte, I., Scherl, A., Yalkinoglu, O., Corthals, G., Burkhard, P., Hochstrasser, D. F. & Sanches, J. C. (2003).A panel of cerebrospinal fluid potential biomarkers for the diagnosis of Alzheimer's disease. *Proteomics* **3**, 1486-1494.

Carson, K. A., Geula, C. & Mesulam, M. M. (1991). Electron microscopic localization of cholinesterase activity in Alzheimer brain tissue. *Brain Res* **540**, 204-208.

Castensson, A., Emilsson, L., Preece, P. & Jazin, a. E. (2000). High-resolution Quantification of Specific mRNA Levels in Human Brain Autopsies and Biopsies. *Genome Res* **10**, 1219-1229.

Castilla, J., Saa, P., Hetz, C. & Soto, C. (2005).*In vitro* generation of infectious scrapie prions. *Cell* **121**, 195-206.

Caughey, B. & Baron, G. S. (2006). Prions and their partners in crime. *Nature* **443**, 803-810.

Caughey, B. & Raymond, G. J. (1991). The scrapie-associated form of PrP is made from a cell surface precursor that is both protease- and phospholipase-sensitive. *J Biol Chem* **266**, 18217-18223.

Caughey, B., Raymond, G. J., Ernst, D. & Race, R. E. (1991).N-terminal truncation of the scrapie-associated form of PrP by lysosomal protease(s): implications regarding the site of conversion of PrP to the protease-resistant state. *J Virol* **65**, 6597-6603.

Caughey, B., Raymond, G. J., Kocisko, D. A. & Lansbury, P. T. (1997). Scrapie infectivity correlates with converting activity, protease resistance, and aggregation of scrapie-associated prion protein in guanidine denaturation studies. *J Virol* **71**, 4107-4110.

Cerneus, D. P., Ueffing, E., Posthuma, G., Strous, G. J. & van der Ende, A. (1993). Detergent insolubility of alkaline phosphatase during biosynthetic transport and endocytosis. Role of cholesterol. *J Biol Chem* **268**, 3150-3155.

Chandler, R. L. (1961). Encephalopathy in mice produced by inoculation with scrapie brain material. *Lancet* **1**, 1378-1379.

Chandler, R. L. & Turfrey, B. A. (1972). Inoculation of voles, Chinese hamsters, gerbils and guinea-pigs with scrapie brain material. *Res Vet Sci* **13**, 219-224.

Chen, J., Sochivko, D., Beck, H., Marechal, D., Wiestler, O. D. & Becker, A. J. (2001). Activity-induced expression of common reference genes in individual cns neurons. *Lab Invest* **81**, 913-916.

Cheng, B., Christakos, S. & Mattson, M. P. (1994). Tumor necrosis factors protect neurons against metabolic-excitotoxic insults and promote maintenance of calcium homeostasis. *Neuron* **12**, 139-153.

Chesebro, B. (1998).BSE and Prions: Uncertainties About the Agent. *Science* **279**, 42-43.

Chevallier, N., Vizzavona, J., Marambaud, P. & other authors (1997). Cathepsin D displays in vitro beta-secretase-like specificity. *Brain Res* **750**, 11-19.

Chiesa, R., Angeretti, N., Lucca, E., Salmona, M., Tagliavini, F., Bugiani, O. & Forloni, G. (1996). Clusterin (SGP-2) induction in rat astroglial cells exposed to prion protein fragment 106-126. *Eur J Neurosci* **8**, 589-597.

Chiesa, R., Piccardo, P., Dossena, S., Nowoslawski, L., Roth, K. A., Ghetti, B. & Harris, D. A. (2005). Bax deletion prevents neuronal loss but not neurological symptoms in a transgenic model of inherited prion disease. *PNAS* **102**, 238-243.

Chiesa, R., Piccardo, P., Ghetti, B. & Harris, D. A. (1998). Neurological illness in trangenic mice expressing a prion protein with an insertional mutation. *Neuron* **21**, 1339-1351.

Chirgwin, J. M., Pyzybyla, A. E., MacDonald, R. J. & Rutter, W. J. (1979). Isolation of biologically active ribonucleic acid from sources enriched in ribonuclease. *Biochemistry* **18**, 5294-5299.

Chloe, L. H., Green, A., Knight, R. S., Thompson, E. J. & Lee, K. H. (2002). Apolipoprotein E and other cerebrospinal fluid proteins differentiate ante mortem variant Creutzfeldt-Jakob disease from ante mortem sporadic Creutzfeldt-Jakob disease. *Electrophoresis* **23**, 2242-2246.

Choi, S. I., Ju, W. K., Choi, E. K., Kim, J., Lea, H. Z., Carp, R. I., Wisniewski, H. M. & Kim, Y. S. (1998). Mitochondrial dysfunction induced by oxidative stress in the brains of hamsters infected with the 263 K scrapie agent. *Acta Neuropathol* **96**, 279-286.

Choi, Y. G., Kim, J. I., Lee, H. P., Jin, J. K., Choi, E. K., Carp, R. I. & Kim, Y. S. (2000). Induction of heme oxygenase-1 in the brains of scrapie-infected mice. *Neurosci Lett* **289**, 173-176.

Chomczynski, P. & Sacchi, N. (1987). Single-step method of RNA isolation by acid guanidinium thiocyanate-phenol-chloroform extraction. *Anal Biochem* **162**, 156-159.

Colantuoni, C., Hyde, T. M., Mitkus, S. & other authors (2008). Age-related changes in the expression of schizophrenia susceptibility genes in the human prefrontal cortex. *Brain Struct Funct*.

Colantuoni, C., Purcell, A. E., Bouton, C. M. & Pevsner, J. (2000). High throughput analysis of gene expression in the human brain. *J Neurosci Res* **59**, 1-10.

Collinge, J., Sidle, K. C., Meads, J., Ironside, J. W. & Hill, A. F. (1996). Molecular analysis of prion strain variation and the aetiology of 'new variant' CJD. *Nature* **383**, 685-690.

Collins, P. S., Lawson, V. A. & Masters, P. C. (2004). Transmissible spongiform encephalopathies. *The Lancet* **363**, 51-61.

Come, J. H., Fraser, P. E. & Lansbury, P. T. Jr. (1993).A kinetic model for amyloid formation in the prion diseases: importance of seeding. *PNAS* **90**, 5959-5963.

Copois, V., Bibeau, F., Bascoul-Mollevi, C. & other authors (2007). Impact of RNA degradation on gene expression profiles: Assessment of different methods to reliably determine RNA quality. *J Biotechnology* **127**, 549-559.

Corder, E. H., Saunders, A. M., Risch, N. J. & other authors (1994). Protective effect of apolipoprotein E type 2 allele for late onset Alzheimer disease. *Nat Genet* **7**, 180-184.

Corder, E. H., Saunders, A. M., Strittmatter, W. J., Schmechel, D. E., Gaskell, P. C., Small, G. W., Haines, J. L. & Pericak-Vance, M. (1993). Gene dose of apolipoprotein E type 4 allele and the risk of Alzheimer's disease in late onset families. *Science* **261**, 921-923.

Coulpier, M., Messiaen, S., Hamel, R., Fernandez de Marco, M., Lilin, T. & Eloit, M. (2006). Bax deletion does not protect neurons from BSE-induced death. *Neurobiol Dis* **23**, 603-611.

Coulson, D. T., Brockbank, S., Quinn, J. G., Murphy, S., Ravid, R., Irvine, G. B. & Johnston, J. A. (2008). Identification of valid reference genes for the normalization of RT qPCR gene expression data in human brain tissue. *BMC Mol Biol* **9**, 46.

Cox, R. A. (1968). The use of quanidinium chloride in the isolation of nucleic acids. *Methods Enzymol* **12**, 120.

Creutzfeldt, H. (1920).Über eine eigenartige herdförmige Erkrankung des Zentralnervensystems. *Z Ges Neurol Psychiatr* **57**, 1-18.

Cummings, T. J., Strum, J. C., Yoon, L. W., Szymanski, M. H. & Hulette, C. M. (2001). Recovery and expression of messenger RNA from postmortem human brain tissue. *Mod Path* **14**, 1157-1161.

Dandoy-Dron, F., Benboudjema, L., Guillo, F., Jaegly, A., Jasmin, C., Dormont, D., Tovey, M. G. & Dron, M. (2000). Enhanced levels of scrapie responsive gene mRNA in BSE-infected mouse brain. *Molecular Brain Research* **76**, 173-179.

Dandoy-Dron, F., Guillo, F., Benboudjema, L., Deslys, J.-P., Lasmezas, C., Dormont, D., Tovey, M. G. & Dron, M. (1998). Gene Expression in Scrapie. Cloning of a new scrapie-responsice gene and the identification of increased levels of seven other mRNA transcripts. *J Biol Chem* **273**, 7691-7697.

Darvesh, S. & Hopkins, D. A. (2003). Differential distribution of butyrylcholinesterase and acetylcholinesterase in the human thalamus. *J Comp Neurol* **463**, 25-43.

Davis, F. C. & Mullersman, R. W. (1981). Processing of the ribonucleic acid in the large ribosomal subunits of Urechis caupo. *Biochemistry* **20**, 3554-3561.

De Strooper, B. & Annaert, W. (2000). Proteolytic processing and cell biological functions of the amyloid precursor protein. *J Cell Biol* **113**, 1857-1870.

Deiss, L. P., Galinka, H., Berissi, H., Cohen, O. & Kimchi, A. (1996). Cathepsin D protease mediates programmed cell death induced by interferon-gamma, Fas/APO-1 and TNF-alpha. *EMBO J* **15**, 3861-3870.

Deleault, N. R., Harris, B. T., Rees, J. R. & Supattapone, S. (2007). Formation of native prions from minimal components *in vitro. PNAS* **104**, 9741-9746.

Dheda, K., Huggett, J., Bustin, S., Johnson, M. A., Rook, G. & Zumla, A. (2004). Validation of housekeeping genes for normalizing RNA expression in real-time PCR. *BioTechniques* **37**, 112-119.

Di Martino, A., Safar, J. & Gibbs, C. J., Jr. (1994). The consistent use of organis solvents for purification of phospholipids from brain tissue effectively removes scrapie infectivity. *Biologicals* **22**, 221-225.

Dickinson, A. G. & Fraser, H. (1969). Modification of the pathogenesis of scrapie in mice by treatment of the agent. *Nature* **222**, 892-893.

Dickinson, A. G., Meikle, V. M. H. & Fraser, H. (1968). Identification of a gene which controls the incubation period of some strains of scrapie agent in mice. *J Comp Pathol* **78**, 293-299.

Dickinson, A. G. & Taylor, D. M. (1978). Resistance to scrapie agent to decontamination. *N Engl J Med* **229**, 1413-1414.

Diedrich, J. F., Bendheim, P. E., Kim, Y. S., Carp, R. I. & Hasse, A. T. (1991a). Scrapie-associated prion protein accumulates in astrocytes during scrapie infection. *PNAS* **88**, 375-379.

Diedrich, J. F., Minnigan, H., Carp, R. I., Whitaker, J. N., Race, R., Frey, W. & Haase, A. T. (1991b). Neuropathological changes in scrapie and Alzheimer's disease are associated with increased expression of apolipoprotein E and cathepsin D in astrocytes. *J Virol* **65**, 4759-4768.

Diedrich, J. F., Wietgrefe, S., Zupancic, M., Staskus, K., Retzel, E., Haase, A. T. & Race, R. (1987). The molecular pathogenesis of astrogliosis in scrapie and Alzheimer's disease. *Microb Pathog* **2**, 435-442.

Duguid, J. R., Bohmont, C. W., Liu, N. G. & Toutellotte, W. W. (1989). Changes in brain gene expression shared by scrapie and Alzheimer disease. *PNAS* **86**, 7260-7264.

Editor in chief and associate editors (2001). Suitability Criteria for Manuscripts Utilizing Genomics Array Technology. *Circulation Research* **89**, 469.

Enard, W., Khaitovich, P., Klose, J. & other authors (2002). Intra- and Interspecific Variation in Primate Gene Expression Patterns. *Science* **296**, 340-343.

Ernst, C., Sequeira, A., Klempan, T., Ernst, N., ffrench-Mullen, J. & Turecki, G. (2007). Confirmation of region-specifc patterns of gene expression in the human brain. *Neurogenetics* **8**, 219-224.

Esmonde, T. F., Lueck, C. J., Symon, L., Duchen, L. W. & Will, R. (1993). Creutzfeldt-Jakob disease and lyophilised dura mater grafts: report of two cases. *J Neurol Neurosurg Psychiatry* **56**, 999-1000.

Ferrer, I., Rivera, R., Blanco, R. & Marti, E. (1999). Expression of proteins linked to exocytosis and neurotransmission in patients with Creutxfedlt-Jakob disease. *Neurobiology of Disease* **6**, 92-100.

Fichet, G., Comoy, E., Duval, C. & other authors (2004). Novel methods for disinfection of prion-contaminated medical devices. *Lancet* **364**, 521-526.

Firestein, G. S. & Pisetsky, D. S. (2002).DNA microarrays: boundless technology or bound by technology? Guidelines for studies using microarray technology. *Arthritis Rheum* **46**, 859-861.

Fischer, M., Rulicke, T., Raeber, A. J., Sailer, A., Moser, M., Oesch, B., Brandner, S., Aguzzi, A. & Weissmann, C. (1996). Prion protein (PrP) with amino terminal deletions restoring susceptibility of PrP knockout mice to scrapie. *EMBO J* **15**, 1255-1264.

Fischer, M. B., Roeckl, C., Parizek, P., Schwarz, H. P. & Aguzzi, A. (2000). Binding of disease-associated prion protein to plasminogen. *Nature* **408**, 479-483.

Fleige, S. & Pfaffl, M. W. (2006).RNA integrity and the effect on the real-time qRT-PCR performance. *Molecular Aspects of Medicine* **27**, 126-139.

Fleige, S., Walf, V., Huch, S., Prgomet, C., Sehm, J. & Pfaffl, M. W. (2006). Comparison of relative mRNA quantification models and the impact of RNA integirty in quantitatice real-time RT-PCR. *Biotechnol Lett* **28**, 1601-1613.

Florio, T., Grimaldi, M., Scorziello, A., Salmona, M., Bugiani, O., Tagliavini, F., Forloni, G. & Schettini, G. (1996). Intracellular calcium rise through L-type calcium channels, as molecular mechanism for prion protein fragment 106-126-induced astroglial proliferation. *Biochem Biophys Res Commun* **228**, 397-405.

Fodor, S. P., Rava, R. P., Huang, X. C., Pease, A. C., Holmes, C. P. & Adams, C. L. (1993). Multiplexed biochemical assays with biological chips. *Nature* **364**, 555-556.

Fodor, S. P., Read, J. L., Pirrung, M. C., Stryer, L., Lu, A. T. & Solas, D. (1991). Light-directed, spatially addressable parallel chemical synthesis. *Science* **251**, 767-773.

Forloni, G., Angeretti, N., Chiesa, R., Monzani, E., Salmona, M., Bugiani, O. & Tagliavini, F. (1993). Neurotoxicity of a prion protein fragment. *Nature* **362**, 543-546.

Foss, D. L., Baarsch, M. J. & Murtaugh, M. P. (1998). Regulation of hypoxanthine phosphoribosyltransferase, glyceraldehyde-3-phosphate dehydrogenase and beta-actin mRNA expression in porcine immune cells and tissues. *Anim Biotechnol* **9**, 67-78.

Fountolakis, M. (2004). Application of proteomics technologies in the investigation of the brain. *Mass Spectrom Rev* **23**, 231-258.

Fox-Brashears, H., Quellhorst, G., Blanchard, R., Wang, B. & Yu, S. (2000). Oligo GEArrays: The pathway-focused DNA microarray system for every laboratory.

French, K., Yerbury, J. J. & Wilson, M. R. (2008). Protease activation of alpha2-macroglobulin modulates a chaperone-like action with broad specificity. *Biochemistry* **47**, 1176-1185.

Fukumoto, H., Deng, A., Irizarry, M. C., Fitzgerald, M. L. & Rebeck, G. W. (2002). Induction of the cholesterol transporter ABCA1 in central nervous system cells by liver X receptor agonists increases secreted Abeta levels. *J Biol Chem* **277**, 48508-48513.

Gajdusek, D. C. (1988). Transmissible and non-transmissible amyloidoses: autocatalytic post-translational conversion of host precursor proteins to beta-pleated sheet configurations. *J Neuroimmunol* **20**, 95-110.

Galvin, J. E. & Ginsburgh, S. D. (2005). Expression profiling in the aging brain: a perspective. *Ageing Res Rev* **4**, 529-547.

Gasque, P., Dean, Y. D., McGrral, E. P., VanBeek, J. & Morgan, B. P. (2000). Complement components of the innate immune system in health and disease in the CNS. *Immunopharmacology* **49**, 171-186.

Gauczynski, S., Peyrin, J. M., Haik, S. & other authors (2001). The 37-kDa/67-kDa laminin receptor acts as the cell-surface receptor for the cellular prion protein. *EMBO J* **20**, 5863-5875.

Gerlach, M., Ben Shachar, D., Riederer, P. & Youdim, M. B. H. (1994). Altered Brain Metabolism of Iron as a Cause of Neurodegenerative Diseases? *Journal of Neurochemistry* **63**, 793-807.

Gibbs, C. J. Jr., Gajdusek, D. C., Asher, D. M., Alpers, M. P., Beck, E., Daniel, P. M. & Matthews, W. B. (1968). Creutzfeldt-Jakob disease (spongiform encephalopathy): transmission to the chimpanzee. *Science* **161**, 388-389.

Giese, A., Brown, D. R., Groschup, M. H., Feldmann, C., Haist, I. & Kretzschmar, H. A. (1998). Role of microglia in neuronal cell death in prion disease. *Brain Pathol* **8**, 449-457.

Giese, A. & Kretzchmar, H. A. (2001). Prion-induced neuronal damage--the mechanisms of neuronal destruction in the subacute spongiform encephalopathies. *Curr Top Microbiol Immunol* **253**, 203-217.

Glasel, J. A. (1995). Validity of nucleic acid purities monitored by 260nm/280nm absorbance ratios. *BioTechniques* **18**, 62-63.

Gomez-Ramos, P., Bouras, C. & Moran, M. A. (1994). Ultrastructural localization of butyrylcholinesterase on neurofibrillary degeneration sites in the brains of aged and Alzheimer's disease patients. *Brain Res* **640**, 17-24.

Gorg, A., Weiss, W. & Dunn, M. J. (2004). Current two-dimensional electrophoresis technology for proteomics. *Proteomics* **4**, 3665-3685.

Gotz, M. E., Kunig, G., Rieferer, P. & Youdim, M. B. (1994). Oxidative stress: free radical production in neural degeneration. *Pharmacol Ther* **63**, 37-122.

Graham, D. I. & Lantos, P. L. (1997).*Greenfield's neuropathology.* London: Arnold.

Griffin, W. S. & Mrak, R. E. (2002). Interleukin-1 in the genesis and progression of and risk for development of neuronal degeneration in Alzheimer's disease. *J Leukoc Biol* **72**, 233-238.

Guentchev, M., Voigtlander, T., Haberler, C., Groschup, M. H. & Budka, H. (2000). Evidence for oxidative stress in experimental prion disease. *Neurobiol Dis* **7**, 270-273.

Guhaniyogi, J. & Brewer, G. (2001). Regulation of mRNA stability in mammalian cells. *Gene* **265**, 11-23.

Gutala, R. V. & Reddy, P. H. (2004). The use of real-time PCR analysis in a gene expression study of Alzheimer's disease in post-mortem brains. *Journal of Neuroscience Methods* **132**, 101-107.

Hahn, W. E. & Laird, C. D. (1971). Transcription of nonrepeated DNA in mouse brain. *Science* **173**, 158-161.

Haidar, B., Denis, M., Marcil, M., Krimbou, L. & Genest, J. Jr. (2004). Apolipoprotein A-I activates cellular cAMP signaling through the ABCA1 transporter. *J Biol Chem* **279**, 9963-9969.

Halliwell, B., Gutteridge, J. N. & Cross, C. E. (1992). Free radicals, antioxidants, and human disease: where are we now? *J Lab Clin Med* **119**, 598-620.

Hamazaki, H. (1996). Cathepsin D is involved in the clearance of Alzheimer's beta-amyloid protein. *FEBS Lett* **396**, 139-142.

Hamir, A. N., Kunkle, R. A., Richt, J. A., Miller, J. M. & Greenlee, J. J. (2008). Experimental transmission of US scrapie agent by nasal, peritoneal, and conjunctival routes to genetically susceptible sheep. *Vet Pathol* **45**, 7-11.

Harding, H. P., Calfon, M., Urano, F., Novoa, I. & Ron, D. (2002). Transcriptional and translational control in the Mammalian unfolded protein response. *Annu Rev Cell Dev Biol* **18**, 575-599.

Harding, H. P., Novoa, I., Berolotti, A., Zeng, H., Zhang, Y., Urano, F., Jousse, C. & Ron, D. (2001). Translational regulation in the cellular response to biosynthetic load on the endoplasmic reticulum. *Cold Spring Harb Symp Quant Biol* **66**, 499-508.

Harding, H. P., Zhang, Y. & Ron, D. (1999). Protein translation and folding are coupled by an endoplasmic-reticulum-resident kinase. *Nature* **397**, 271-274.

Hardy, J. A. & Dodd, P. R. (1983). Metabolic and functional studies on post-mortem human brain. *Neurochemistry international* **5**, 253-266.

Hardy, J. A., Wester, P., Winbald, B., Gezelius, C., Bring, G. & Eriksson, A. (1985). The patients dying after long terminal phase have acidotic brains; implications for biochemical measurements on autopsy tissue. *J Neural Transm* **61**, 253-264.

Hargrove, J. L. & Schmidt, F. H. (1989). The role of mRNA and the protein stability in gene expression. *FASEB J* **3**, 2360-2370.

Harries-Jones, R., Knight, R. S., Will, R. G., Cousens, S., Smith, P. G. & Matthews, W. B. (1988). Creutzfeldt-Jakob disease in England and Wales, 1980-1984: a case-control study of potential risk factors. *J Neurol Neurosurg Psychiatry* **51**, 1113-1119.

Harrison, P. J., Heath, P. R., Eastwood, S. L., Burnet, P. W. J., McDonald, B. & Pearson, R. C. A. (1995). The relative importance of premortem acidosis and postmortem interval for human brain gene expression studies: selective mRNA vulnerability and comparison with their encoded proteins. *Neuroscience Letters* **200**, 151-154.

Harrison, P. J., Procter, A. W., Barton, A. J., Lowe, S. L., Najlerahim, A., Bertolucci, P. H., Bowen, D. m. & Pearson, R. C. (1991). Terminal coma affects messenger RNA detection in post mortem human temporal cortex. *Brain Res Mol Brain Res* **9**, 161-164.

Heckmann, J. G., Lang, C. J., Petruch, F., Druschky, F., Erb, C., Brown, P. & Neundorfer, B. (1997). Transmission of Creutzfeldt-Jakob disease via a corneal transplant. *J Neurol Neurosurg Psychiatry* **63**, 388-390.

Heinrich, M., Matt, K., Lutz-Bonengel, S. & Schmidt, U. (2007). Successful RNA extraction from various human postmortem tissue. *Int J Leg Med* **16**, 136-142.

Heller, J., Kolbert, A. C., Larsen, R., Ernst, M., Bekker, T., Baldwin, M., Prusiner, S. B., Pines, A. & Wemmer, D. E. (1996). Solid-state NMR studies of the prion protein H1 fragment. *Protein Sci* **5**, 1655-1661.

Herz, J. & Strickland, D. K. (2001).LRP: a multifunctional scavenger and signaling receptor. *J Clin Invest* **108**, 779-784.

Hetz, C., Castilla, J. & Soto, C. (2007). Perturbation of endoplasmic reticulum homeostasis
facilitates prion replication. *J Biol Chem* **282**, 12725-12733.

Hijazi, N., Kariv-Inbal, Z., Gasset, M. & Gabizon, R. (2005). PrPSc incorporation to cells requires endogenous glycosaminoglycan expression. *J Biol Chem* **280**, 17057-17061.

Hill, A. F., Antoniou, M. & Collinge, J. (1999). Protease-resistant prion protein produced in vitro lacks detectable infectivity. *J Gen Virol* **80**, 11-14.

Hochstrasser, D. F., Frutiger, S., Wilkins, M. R., Hughes, G. & Sanchez, J. C. (1997). Elevation of apolipoprotein E in the CSF of cattle affected by BSE. *FEBS Lett* **416**, 161-163.

Hollams, E. M., Giles, K. M., Thomson, A. M. & Leedman, P. J. (2002).MRNA stbility and the control of gene expression: implications for human disease. *Neurochemical Research* **27**, 957-980.

Hollien, J. & Weissman, J. S. (2006). Decay of endoplasmic reticulum-localized mRNAs during the unfolded protein response. *Science* **313**, 104-107.

Horonchik, L., Tzaban, S., Ben-Zaken, O., Yedidia, Y., Rouvinski, A., Papy-Garcia, D., Barritault, D., Vlodavsky, I. & Taraboulos, A. (2005). Heparan sulfate is a cellular receptor for purified infectious prions. *J Biol Chem* **280**, 17062-17067.

Horsburgh, K., Fitzpatrick, M., Nilsen, M. & Nicoll, J. A. (1997). Marked alteration in the cellular localisation and levels of apopolipoprotein E following acute subdural haematoma in rat. *Brain Res* **763**, 103-110.

Hsiao, K. K., Scott, M., Foster, D., Groth, D. F., DeArmond, S. J. & Prusiner, S. B. (1990). Spontaneous neurodegeneration in transgenic mice with mutant prion protein. *Science* **250**, 1587-1590.

Huber, L. A. (2003). Is proteomics heading in the wrong direction? *Nat Rev Mol Cell Biol* **4**, 74-80.

Hugel, B., Martinez, M. C., Kunzelmann, C., Blattler, T., Aguzzi, A. & Freyssinet, J. M. (2004). Modulation of signal transduction through the cellular prion protein is linked to its incorporation in lipid rafts. *Cell Mol Life Sci* **61**, 2998-3007.

Huggett, J., Dheda, K., Bustin, S. & Zumla, A. (2005). Real-time RT-PCR normalisation; strategies and considerations. **6**, 279-284.

Hunter, G. D. & Millson, G. c. (1967). Attempts to release the scrapie agent from tissue debris. *J Comp Pathol* **77**, 301-7.

Hutter, G., Heppner, F. L. & Aguzzi, A. (2003). No superoxide dismutase activity of cellular prion protein in vivo. *Biol Chem* **384**, 1279-1285.

Hynd, M. R., Lewohl, J. M., Scott, H. L. & Dodd, P. R. (2003). Biochemical and molecular studies using human autopsy brain tissue. *J Neurochem* **85**, 562.

Imagawa, Y., Hosoda, A., Sasaka, S.-I., Tsuru, A. & Kohno, K. (2008).RNase domains determine the functional difference between IRE1a and IRE1b. *FEBS Lett* **582**, 656-660.

Imbeaud, S., Graudens, E., Boulanger, V., Barlet, X., Zaborski, P., Eveno, E., Mueller, O., Schroeder, A. & Auffray, C. (2005). Towards standardization of RNA quality and assessment using user-independent classifiers of microcapillary electrophoesis traces. *Nucleic Acids Res* **33**, 56-68.

Inoue, H., Kimura, A. & Tuji, T. (2002). Degradation profile of mRNA in a dead rat body: basic semi-qualtification study. *Forensic Science International* **130**, 127-132.

Ironside, J. W. (1996). Review: Creutzfeldt-Jakob disease. *Brain Pathol* **6**, 379-388.

Ivanova, L., Barmada, S., Kummer, T. & Harris, D. A. (2001). Mutant prion proteins are partially retained in the endoplasmic reticulum. *J Biol Chem* **276**, 42409-42421.

Iwawaki, T., Hosoda, A., Okuda, T., Kamigori, Y., Nomura-Furuwatari, C., Kimata, Y., Tsuru, A. & Kohno, K. (2001). Translational control by the ER transmembrane kinase/ribonuclease IRE1 under ER stress. *Nature Cell Biology* **3**, 158-164.

Jacobson, A. & Peltz, S. W. (1996). Interrelationships of the pathways of mRNA decay and translation in eukaryotic cells. *Annu Rev Biochem* **65**, 693-739.

Jarrett, J. T. & Lansbury, P. T. Jr. (1993). Seeding "one-dimensional crystallization" of amyloid: a pathogenic mechanism in Alzheimer's disease and scrapie? *Cell* **73**, 1055-1058.

Jeong, J. & McMahon, A. P. (2002). Cholesterol modification of Hedgehog family proteins. *J Clin Invest* **110**, 591-596.

Jobling, M. F., Huang, X., Stewart, L. R. & other authors (2001). Copper and zinc binding modulates the aggregation and neurotoxic properties of the prion peptide PrP106-126. *Biochemistry* **40**, 8073-8084.

John, G. R., Lee, S. C. & Brosnan, C. F. (2003). Cytokines: Powerful Regulators of Glial Cell Activation. *Neuroscientist* **9**, 10-22.

Johnson, S. A., Morgan, D. G. & Finch, C. E. (1986). Extensive postmortem stability of RNA from rat and human brain. *J neurosci Res* **16**, 267-280.

Johnston, N. L., Cerevnak, J., Shore, A. D., Fuller Torrey, E. & Yolken, R. H. (1997). Multivariate analysis of RNA levels from postmortem human brains as measured by three different methods of RT-PCR. *Journal of Neuroscience Methods* **77**, 83-92.

Jones, S., Batchelor, M., Bhelt, D., Clarke, A. R., Collinge, J. & Jackson, G. S. (2005). Recombinant prion protein does not possess SOD-1 activity. *Biochem J* **392**, 309-312.

Ju, W. K., Park, K. J., Choi, E. K., Kim, J., Carp, R. I., Wisniewski, H. M. & Kim, Y. S. (1998). Expression of inducible nitric oxide synthase in the brains of scrapie-infected mice. *J Neurovirol* **4**, 445-450.

Kacharmina, J. E., Crino, P. B. & Eberwine, J. (1999). Preparation of cDNA from single cells and subcellular regions. *Methods Enzymol* **30**, 3-18.

Kagedal, K., Johansson, U. & Ollinger, K. (2001). The lysosomal protease cathepsin D mediates apoptosis induced by oxidative stress. *FASEB J* **15**, 1592-1594.

Kahana, E., Alter, M., Braham, J. & Sofer, D. (1974). Creutzfeldt-Jakob disease: focus among Libyan Jews in Israel. *Science* **183**, 90-91.

Kaneko, K., Vey, M., Scott, M., Pikkuhn, S., Cohen, F. E. & Prusiner, S. B. (1997).COOH-terminal sequence of the cellular prion protein directs subcellular trafficking and controls conversion into the scrapie isoform. *PNAS* **94**, 2333-2338.

Kang, D. E., Saitoh, T., Chen, X., Xia, Y., Masliah, E., Hansen, L. A., Thomas, R. G., Thal, L. J. & Katzman, R. (1997). Genetic association of the low-density lipoprotein receptor-related protein gene (LRP), an apolipoprotein E receptor, with late-onset Alzheimer's disease. *Neurology* **49**, 56-61.

Karlsson, J. O. M. & Toner, M. (1996). Long-term storage of tissues by cryopreservation: critical issues. *Biomaterials* **17**, 243-256.

Kazlauskaite, J. & Pinheiro, T. J. (2005). Aggregation and fibrillization of prions in lipid membranes. *Biochem Soc Symp* **72**, 211-222.

Kazlauskaite, J., Sanghera, N., Sylvester, I., Venien-Bryan, C. & Pinheiro, T. J. (2003). Structural changes of the prion protein in lipid membranes leading to aggregation and fibrillization. *Biochemistry* **42**, 3295-3304.

Keller, P. & Simons, K. (1998). Cholesterol is required for surface transport of influenza virus hemagglutinin. *J Cell Biol* **140**, 1357-1367.

Khaitovich, P., Muetzel, B., She, X. & other authors (2004). Regional patterns of gene expression in human and chimpanzee brains. *Genome Res* **14**, 1462-1473.

Kickhoefen, B. & Buerger, M. (1962). The behaviour of proteins in phenol. I. Ribonuclease. *Biochim Biophys Acta* **65**, 190-199.

Kim, J. I., Choi, S. I., Kim, N. H., Jin, J. K., Choi, E. K., Carp, R. I. & Kim, Y. S. (2001). Oxidative stress and neurodegeneration in prion diseases. *Ann N Y Acad Sci* **928**, 182-186.

Kim, J. I., Ju, W. K., Choi, J. H., Choi, E., Carp, R. I., Wisniewski, H. M. & Kim, Y. S. (1999). Expression of cytokine genes and increased nuclear factor-kappa B activity in the brains of scrapie-infected mice. *Brain Res Mol Brain Res* **73**, 17-27.

Kim, N. H., Park, S. J., Jin, J. K., Kwon, M. S., Choi, E. K., Carp, R. I. & Kim, Y. S. (2000). Increased ferric iron content and iron-induced oxidative stress in the brains of scrapie-infected mice. *Brain Res* **884**, 98-103.

Kimberlin, R. H. (1992). Bovine spongiform encephalopathy. *Rev Sci Tech* **11**, 347-390.

Kimberlin, R. H. (1977). Biochemical approached to scrapie research. *Trends in Biochemical Sciences* **2**, 220-223.

Kimberlin, R. H. & Walker, C. A. (1977). Characteristics of a short incubation period model of scrapie in the golden hamster. *J Gen Virol* **34**, 295-304.

Kimberlin, R. H. & Walker, C. A. (1986). Pathogenesis of scrapie (strain 263K) in hamsters infected intracerebrally, intraperitoneally or intraocularly. *J Gen Virol* **67**, 255-263.

Kimberlin, R. H., Walker, C. A., Millson, G. c., Taylor, D. M., Robertson, P. A., Tomlinson, A. H. & Dickinson, A. G. (1983). Disinfection studies with two strains of mouse-passaged scrapie agent. Guidelines for Creutzfeldt-Jakob and related agents. *J Neurological Sciences* **59**, 355-369.

Kingsbury, A. E., Foster, O. J. F., Nisbet, A. P., Cairns, N., Bray, L., Eve, D. J., Lees, A. J. & David Marsden, C. (1995). Tissue pH as an indicator of mRNA preservation in human post-mortem brain. *Molecular Brain Research* **28**, 311-318.

Klamt, F., Dal-Pizzol, F., Conte da Fronta, M. L. Jr., Walz, R., Andrades, M. E., da Silva, E. G., Brentani, R. R., Izquierdo, I. & Fonseca Moreira, J. C. (2001). Imbalance of antioxidant defence in mice lacking cellular prion protein. *Free Radic Biol Med* **30**, 1137-1144.

Kobayashi, H., Sakimura, K., Kuwano, R., Sato, S., Ikuta, F., Takahashi, Y., Miyatake, T. & Tsuji, S. (1990). Stability of messenger RNA in postmortem human brains and construction of human brain cDNA libraries. *J Mol Neurosci* **2**, 29-34.

Kocisko, D. A., Come, J. H., Priola, S. A., Chesebro, B., Raymond, G. J., Lansbury, P. T. & Caughey, B. (1994). Cell-free formation of protease-resistant prion protein. *Nature* **370**, 471-474.

Kordek, R., Nerurkar, V. R., Liberski, P. P., Isaacson , S., Yanagihara, R. & Gajdusek, D. C. (1996). Heightened expression of tumor necrosis factor alpha, interleukin 1 alpha, and glial fibrillary acidic protein in experimental Creutzfeldt-Jakob disease in mice. *PNAS* **93**, 9754-9758.

Kovacs, G. G., Gelpi, E., Strobel, T., Ricken, G., Nyengaard, J. R., Bernheimer, H. & Budka, H. (2007). Involvement of the endosomal-lysosomal system correlates with regional pathology in Creutzfeldt-Jakob disease. *J Neuropathol Exp Neurol* **66**, 628-636.

Kovacs, G. G., Gasque, P., Strobel, T., Lindeck-Pozza, E., Strohschneider, M., Ironside, J. W., Budka, H. & Guentchev, M. (2004). Complement activation in human prion disease. *Neurobiology of Disease* **15**, 21-28.

Krenitsky, T. A. (1969). Tissue distribution of purine ribosyl- and phosphoribosyltransferases in the Rhesus monkey. *Biochim Biophys Acta* **179**, 506-509.

Kretzchmar, H. A., Stowring, L. E., Westaway, D., Stubblebine, W. H., Prusiner, S. B. & DeArmond, S. J. (1986). Molecular cloning of a human prion protein cDNA. *DNA* **5**, 315-324.

Kristensson, K. (1992). Potential role of viruses in neurodegeneration. *Mol Chem Neuropathol* **16**, 45-58.

Kristiansen, M., Deriziotis, P., Dimcheff, D. E. & other authors (2007). Disease-associated prion protein oligomers inhibit the 26S proteasome. *Mol Cell* **26**, 175-188.

Kumar, A. M., Borodowsky, I., Fernandez, B., Gonzalez, L. & Kumar, M. (2007). Human immunodeficiency virus type 1 RNA levels in different regions of human brain: quantification using real-time reverse transciptase-polymerase chain reaction. *J Neurovirol* **13**, 210-224.

Kumar, R., McClain, D., Young, R. & Carlson, G. A. (2008). Cholesterol transporter ATP-binding cassette A1 (ABCA1) is elevated in prion disease and affects PrPC and PrPSc concentrations in cultured cells. *J Gen Virol* **89**, 1525-1532.

Kuwahara, C., Takeuchi, A. M., Nishimura, T. & other authors (1999). Prions prevent neuronal cell-line death. *Nature* **400**, 225-226.

Kuznetsov, I. B. & Rackovsky, S. (2004). Comparative computational analysis of prion proteins reveals two fragments with unusual structural properties and a pattern of increase in hydrophobicity associated with disease-promoting mutations. *Protein Sci* **13**, 3230-3244.

Lasmezas, C., Deslys, J.-P., Robain, O. & other authors (1997). Transmission of the BSE agent to mice in the absence of detectable abnormal prion protein. *Science* **275**, 402-404.

Lawrence, M. S., Ho, D. Y., Sun, G. H., Steinberg, G. K. & Sapolsky, R. M. (1996). Overexpression of Bcl-2 with herpes simplex virus vectors protects CNS neurons against neurological insults in vitro and in vivo. *J Neurosci* **16**, 486-496.

Lax, A. J., Millson, G. c. & Manning, E. J. (1983). Can scrapie titres be calculated accurately from incubation periods? *J Gen Virol* **64**, 971-973.

Leal-Klevezas, D. S., Martinez-Vazquez, I. O., Cuevas-Hernandez, B. & Martinez-Soriano, J. P. (2000). Antifreeze solution improves DNA recovery by preserving the integrity of pathogen-infected blood and other tissues. *Clinical and Diagnostic Laboratory Immunology* **7**, 945-946.

Leavitt, J., Gunning, P., Porreca, P., Ng, S. Y., Lin, C. S. & Kedes, L. (1984). Molecular cloning and characterization of mutant and wild-type human beta-actin genes. *Mol Cell Biol* **4**, 1961-1969.

Lee, D. W., Sohn, H. O., Lim, H. B., Lee, Y. G., Kim, Y. S., Carp, R. I. & Wisniewski, H. M. (1999). Alteration of free radical metabolism in the brain of mice infected with scrapie agent. *Free Radic Res* **30**, 499-507.

Legname, G., Baskakov, I. V., Nguyen, H.-O. B., Rieser, D., Cohen, F. E., DeArmond, S. J. & Prusiner, S. B. (2004). Synthetic mammalian prions. *Science* **305**, 673-676.

Lehmann, S. & Harris, D. A. (1996). Mutant and infectious prion proteins display common biochemical properties in cultured cells. *J Biol Chem* **271**, 1633-1637.

Leonard, S., Logel, J., Luthman, D., Casanova, M., Kirch, D. & Freedman, R. (1993). Biological stability of mRNA isolated from human postmortem brain collections. *Biological Psychiatry* **33**, 456-466.

Li, A., Barmada, S. J., Roth, K. A. & Harris, D. A. (2007).N-terminally deleted forms of the prion protein activate both Bax-dependent and Bax-independent neurotoxic pathways. *J Neurosci* **27**, 852-859.

Liebhaber, S. A. (1997).mRNA stability and the control of gene expression. *Nucleic Acids Symp Ser* **36**, 29-32.

Lightfoot, S. (2002). Quantitation comparison of total RNA using the Agilent 2100 bioanalyzer, ribo-green analysis and UV spectrometry. *Agilent*.

Lin, J. H., Li, H., Yasumura, D., Cohen, H. R., Zhang, C., Panning, B., Shokat, K. M., Lavail, M. M. & Walter, P. (2007).IRE1 signaling affects cell fate during the unfolded protein response. *Science* **318**, 944-999.

Lipska, B. K., Deep-Soboslay, A., Weickert, C. S., Hyde, T. M., Martin, C. E., Herman, M. M. & Kleinman, J. E. (2006). Critical factors in gene

expression in postmortem human brain: Focus on studies in schizophrenia. *Biological Psychiatry* **60**, 650-658.

Llewelyn, C. A., Hewitt, P. E., Knight, R. S. G., Amar, K., Cousens, S., Mackenzie, J. & Will, R. G. (2004). Possible transmission of variant Creutzfeldt-Jakob disease by blood transfusion. *The Lancet* **363**, 417-421.

Lorent, K., Overberghe, L., Moechars, D., De Strooper, B., Van Leuven, F. & Van Den Berghe, H. (1995). Expression in mouse embryos and in adult mouse brain of three members of the amyloid presursor protein family, of the alpha-2-macroglobulin receptor/low density lipoprotin receptor-related protein and its ligands apolipoprotein E, lipoprotein lipase, alpha-2-macroglobulin and the 40,000 molecular weight recepto-associated protein. *Neurosci* **65**, 1009-1025.

Lu, Z. Y., Baker, C. A. & Manuelidis, L. (2004). New molecular markers of early and progressive CJD brain infection. *J Cell Biochem* **93**, 644-652.

Lukasewycz, O. A. & Prohaska, J. R. (1990). The immune response in copper deficiency. *Ann N Y Acad Sci* **587**, 147-159.

Lukiw, W. J., Wong, L. & McLachlan, D. R. (1990). Cytoskeletal messenger RNA stability in human neocortex: studies in normal aging and in Alheimer's disease. *Int J Neurosci* **55**, 81-88.

Ma, J. & Lindquist, S. (2001). Wild-type PrP and a mutant associated with prion disease are subject to retrograde transport and proteasome degradation. *PNAS* **98**, 14955-14960.

Ma, J., Wollmann, R. & Lindquist, S. (2002). Neurotoxicity and neurodegeneration when PrP accumulates in the cytosol. *Science* **298**, 1781-1785.

Mabbott, N. A. (2004). The complement system in prion diseases. *Current Opinion in Immunology* **16**, 587-593.

Maden, B. E. & Hughes, J. M. (1997). Eukaryotic ribosomal RNA: the recent excitement in the nucleotide modification problem. *Chromosoma* **105**, 391-400.

Madore, N., Smith, K. L., Graham, C. H., Jen, A., Brady, K., Hall, S. & Morris, R. (1999). Functionally different GPI proteins are organized in different domains on the neuronal surface. *EMBO J* **18**, 6917-6926.

Magalhaes, A. C., Silva, J. A., Lee, K. S., Martins, V. R., Prado, V. F., Ferguson, S. S., Gomez, M. V., Brentani, R. R. & Prado, M. A. (2002). Endocytic intermediates involved with the intracellular trafficking of a fluorescent cellular prion protein. *J Biol Chem* **277**, 33311-33318.

Maglio, L. E., Perez, M. F., Martins, V. R., Brentani, R. R. & Ramirez, O. A. (2004). Hippocampal synaptic plasticity in mice devoid of cellular prion protein. *Brain Res Mol Brain Res* **131**, 58-64.

Mahley, R. W. (1988). Apolipoprotein E: cholesterol transport protein with expanding role in cell biology. *Science* **240**, 622-630.

Mallucci, G. R., Dickinson, A. G., Linehan, J., Klohn, P. C., Brandner, S. & Collinge, J. (2003). Depleting neuronal PrP in prion infection prevents disease and reverses spongiosis. *Science* **302**, 871-874.

Mallucci, G. R., Ratte, S., Asante, E. A., Linehan, J., Gowland, I., Jefferys, J. G. & Collinge, J. (2002). Post-natal knockout of prion proteins alters the hippocampal CA1 properties, but does not result in neurodegeneration. *EMBO J* **21**, 202-210.

Manchester, K. L. (1995). Value of A260/280 ratios for measuremetn of purity of nucleic acids. *BioTechniques* **19**, 208-210.

Manchester, K. L. (1996). Use of UV methods for measurement of protein and nucleic acid concentrations. *BioTechniques* **20**, 968-970.

Maniatis, T., Fritsch, E. F. & Sambrook, J. (1982).*Molecular Cloning: a Laboratory Manual.* New York: Cold Spring Habour.

Mann, D. M. A., Barton, C. M. & Davies, J. S. (1978). Post-mortem changes in human central nervous tissue and the effects on quantitation of nucleic acids and enzymes. *Histochemical Journal* **10**, 127-135.

Manson, J. (1996). PrP gene dosage, allelic specificity and gene regulation in the Transmissible Subacute Spongiform Encephalopathies: Prion Diseases. pp. 239-247: Elsevier.

Manson, J., West, J. D., Thomson, V., McBride, P., Kaufman, M. H. & Hope, J. (1992). The prion protein gene- a role in mouse embryogenesis? *Development* **115**, 117-122.

Manson, J. C., Clarke, A. R., Hooper, M. L., Aitchison, L., McConnell, I. & Hope, J. (1994).129/Ola mice carrying a null mutation in PrP that abolishes mRNA production are developmentally normal. *Mol Neurobiol* **8**, 121-127.

Manuelidis, E. E. (1975). Transmission of Creuztfeldt-Jakob disease from man to the guinea pig. *Science* **190**, 571-572.

Manuelidis, E. E., Angelo, J. N., Gorgacz, E. J. & Manuelidis, L. (1977). Transmission of Creutzfedlt-Jakob disease to Syrian hamster. *Lancet* **1**, 479.

Manuelidis, L. (1997). Decontamination of Creutzfeldt-Jakob disease and other transmissible agents. *J Neurovirol* **3**, 62-65.

Manuelidis, L., Murdoch, G. H. & Manuelidis, E. E. (1988). Potential involvement of retroviral elements in human dementias. *Ciba Found Symp* **135**, 117-134.

Manuelidis, L., Sklaviadis, T. & Manuelidis, E. E. (1987). Evidence suggesting that PrP is not the infectious agent in Creutzfeldt-Jakob disease. *EMBO J* **6**, 341-347.

Martinon, F. & Tschopp, J. (2007). Inflammatory caspases and inflammasomes: master switches of inflammation. *Cell Death Differ* **14**, 10-22.

Masters, C. L. & Rishardson, E. P. Jr. (1978). Subacute spongiform encephalopathy (Creutzfeldt-Jakob disease). The nature and progression of spongiform change. *Brain* **101**, 333-344.

Mayne, M., Shepel, P. N. & Geiger, J. D. (1999). Recovery of high integirty mRNA from brains of rats killed by high-energy focused microwave irradiation. *Brain Res Brain Res Protoc* **4**, 295-302.

McGowan, J. P. (1922). Scrapie in sheep. *Scott J Agric* **5**, 365-375.

McHattie, S. & Edington, N. (1999). Clusterin prevents aggregation of neuropeptide 106-126 in vitro. *Biochem Biophys Res Commun* **259**, 336-340.

McLennan, N. F., Brennan, P. M., McNeill, A. & other authors (2004). Prion protein accumulation and neuroprotection in hypoxic brain damage. *Am J Pathol* **165**, 227-235.

McLeod, A. H., Murdoch, H., Dickinson, J., Dennis, M. J., Hall, G. A., Buswell, C. M., Taylor, D. M., Sutton, J. M. & Raven, N. D. (2004). Proteolytic inactivation of the bovine songiform encephalopathy agent. *Biochem Biophys Res Commun* **317**, 1165-1170.

McMahon, H. E., Mange, A., Nishida, N., Creminon, C., Casanova, D. & Lehmann, S. (2001). Cleavage of the amino terminus of the prion protein by reactive oxygen species. *J Biol Chem* **276**, 2286-2291.

Meda, L., Baron, P., Prat, E., Scarpini, E., Scarlato, G., Cassatella, M. A. & Rossi, F. (1999). Proinflammatory profile of cytokine production by human monocytes and murine microglia stimulated with beta-amyloid[25-35]. *J Neuroimmunol* **93**, 45-52.

Mendez, A. J., Oram, J. F. & Bierman, E. L. (1991). Protein kinase C as a mediator of high density lipoprotein receptor-dependent efflux of intracellular cholesterol. *J Biol Chem* **266**, 10104-10111.

Miller, C., Diglisic, S., Leister, F., Webster, M. & Yolken, R. (2006). Evaluating RNA status for RT-PCR in extracts of postmortem human brain tissue. *BioTechniques* **36**, 628-633.

Millson, G. c., Hunter, G. D. & Kimberlin, R. H. (1976). The physio-chemical nature of the scrapie agent. In *Slow virus diseases of animal and man.*, pp. 243-266. Edited by Kimberlin, R. H. Amsterdam: North Holland.

Mironov, A. Jr., Latawiec, D., Wille, H. & other authors (2003). Cytosolic prion protein in neurons. *J Neurosci* **23**, 7183-7193.

Mitchell, C. L. & Tollervey, D. (2000).mRNA stability in eukaryotes. *Curr Opin Genet Dev* **10**, 193-198.

Mogi, M., Harada, M., Kondo, T., Mizuno, Y., Narabayashi, H., Riederer, P. & Nagatsu, T. (1996a).bcl-2 protein is increased in the brain from parkinsonian patients. *Neurosci Lett* **215**, 137-139.

Mogi, M., Harada, M., Kondo, T., Riederer, P. & Nagatsu, T. (1995). Brain beta 2-microglobulin levels are elevated in the striatum in Parkinson's disease. *J Neural Transm Park Dis Dement Sect* **9**, 87-92.

Mogi, M., Harada, M., Kondo, T., Riederer, P. & Nagatsu, T. (1996b). Interleukin-2 but not basic fibroblast growth factor is elevated in parkinsonian brain. *J Neural Transm* **103**, 1077-1081.

Mogi, M., Harada, M., Narabayashi, H., Inagaki, H., Minami, M. & Nagatsu, T. (1996c). Interleukin (IL)-1 beta, IL-2, IL-4, IL-6 and transforming growth factor-alpha levels are elevated in ventricular cerebrospinal fluid in juvenile parkinsonism and Parkinson's disease. *Neurosci Lett* **211**, 13-16.

Mok, S. W., Thelen, K. M., Riemer, C., Bamme, T., Gultner, S., Lutjohann, D. & Baier, M. (2006). Simvastatin prolongs survival times in prion infections of the central nervous system. *Biochem Biophys Res Commun* **348**, 697-702.

Monstein, H. J., Nylander, A. G. & Chen, D. (1995).RNA extraction from gastrointestinal tract and pancreas by a modified Chomsczynski and Sacchi method. *BioTechniques* **19**, 340-344.

Moore, R. C., Redhead, N. J., Selfridge, J., Hope, J., Manson, J. C. & Melton, D. W. (1995). Double replacement gene targeting for the production of a series of mouse strains with different prion protein gene alterations. *Biotechnology (NY)* **13**, 999-1004.

Mori, N., Mizuno, D. & Goto, S. (1978). Increase in the ratio of 18S RNA to 28S RNA in the cytoplasm of mouse tissue during ageing. *Mechanisms of Ageing and Development* **8**, 285-297.

Morrison, M. R. & Griffin, W. S. (1981). The isolation and in vitro translation of undegraded messenger RNAs from human postmortem brain. *Anal Biochem* **113**, 318-324.

Moser, M., Colello, R. J., Pott, U. & Oesch, B. (1995). Developmental expression of the prion protein gene in glial cells. *Neuron* **14**, 509-517.

Mouillet-Richard, S., Ermonval, M., Chebassier, C., Laplanche, J. L., Lehmann, S., Launay, J. M. & Kellermann, O. (2000). Signal transduction through prion protein. *Science* **289**, 1925-1928.

Mullis, K., Faloona, F., Scharf, S., Saiki, R., Hom, G. & Erlich, H. (1986). Specific enzymatic amplification of DNA in vitro: the polymerase chain reaction. *Cold Spring Harb Symp Quant Biol* **51**, 263-273.

Mullis, K. B. (1990). The unusual origin of the polymerase chain reaction. *Sci Am* **262**, 56-61.

Murdoch, G. H., Sklaviadis, T., Manuelidis, E. E. & Manuelidis, L. (1990). Potential retroviral RNAs in Creutzfeldt-Jakob disease. *J Virol* **64**, 1477-1486.

Nakaya, H. I., Amaral, P. P., Louro, R. & other authors (2007). Genome mapping and expression analyses of human intronic noncoding RNAs reveal tissue-specific patterns and enrichment in genes related to regulation of transcription. *Genome Biol* **8**, R43.

Narang, H. K. (2002).A critical review of the nature of the spongiform encephalopathy agent: protein theory versus virus theory. *Exp Biol Med (Maywood)* **227**, 4-19.

Narita, M., Holtzman, D. M., Schwartz, A. L. & Bu, G. (1997). Alpha2-macroglobulin complexes with and mediates the endocytosis of beta-amyloid peptide via cell surface low-density lipoprotein receptor-related protein. *J Neurochem* **69**, 1904-1911.

Nicolas, O., Gvin, R., Braun, N., Urena, J. M., Fontana, X., Soriano, E., Aguzzi, A. & del Rio, J. A. (2007). Bcl-2 overexpression delays caspase-3 activation and rescues cerebellar degeneration in prion-deficient mice that overexpress amino-terminally truncated prion. *FASEB J* **21**, 3107-3117.

Nicoll, J. A., Mrak, R. E., Graham, D. I. & other authors (2000). Association of interleukin-1 gene polymorphisms with Alzheimer's disease. *Ann Neurol* **47**, 365-368.

Noguchi, I., Arai, H. & Iizuka, R. (1991).A study on postmortem stability of vasopressin messenger RNA in rat brain compared with those in total RNA and ribosomal RNA. *J Neural Transm Gen Sect* **83**, 171-178.

Noller, H. F. (1984). Structure of ribosomal RNA. *Annu Rev Biochem* **53**, 119-162.

Nonno, R., Di Bari, M. A., Cardone, F. & other authors (2006). Efficient transmission and characterization of Creutzfeldt-Jakob disease strains in bank voles. *PLos Pathog* **2**, e12.

Oltvai, Z. N., Milliman, C. L. & Korsmeyer, S. J. (1993). Bcl-2 heterodimerizes in vivo with a conserved homolog, Bax, that accelerates programmed cell death. *Cell* **74**, 609-619.

Ostlund, P., Lindegren, H., Pettersson, C. & Bedecs, K. (2001). Up-regulation of functionally impaired insulin-like growth factor-1 receptor in scrapie-infected neuroblastoma cells. *J Biol Chem* **276**, 36110-36115.

Pan, K. M., Bladwin, M., Nguyen, J. & other authors (1993). Conversion of alpha-helices into beta-sheets features in the formation of the scrapie prion proteins. *PNAS* **90**, 10962-10966.

Parchi, P., Capellari, S., Chen, S. G. & other authors (1997). Typing prion isoforms. *Nature* **386**, 232-234.

Parchi, P., Giese, A., Capellari, S. & other authors (1999). Classification of sporadic Creutzfeldt-Jakob disease based on molecular and phenotypic analysis of 300 subjects. *Ann Neurol* **46**, 224-233.

Pardue, S., Zimmerman, A. L. & Morrison-Bogorad, M. (1994). Selective postmortem degradation of inducible heat shock protein 70 (hsp70) mRNAs in rat brain. *Cell Mol Neurobiol* **14**, 341-357.

Park, S. K., Choi, S. I., Jin, J. K., Choi, E. K., Kim, J. I., Carp, R. I. & Kim, Y. S. (2000). Differential expression of Bax and Bcl-2 in the brains of hamsters infected with 263K scrapie agent. *Neuroreport* **11**, 1677-1682.

Parkin, E. T., Watt, N. T., Hussain, I., Eckman, E. A., Eckman, C. B., Manson, J. C., Baybutt, H. N., Turner, A. J. & Hooper, N. M. (2007). Cellular prion protein regulates B-secretase clevage of the Alzheimer's amyloid precursor protein. *PNAS* **104**, 11062-11067.

Parkyn, C. J., Vermeulen, E. G., Mootoosamy, R. C. & other authors (2008).LRP1 controls biosynthetic and endocytic trafficking of neuronal prion protein. *J Cell Sci* **121**, 773-783.

Parton, R. G. & Richards, A. A. (2003). Lipid rafts and caveolae as portals for endocytosis: new insights and common mechanisms. *Traffic* **4**, 724-738.

Patel, S. C., Asotra, K., Patel, Y. C., McConathy, W. J., Patel, R. C. & Suresh, S. (1995). Astrocytes Synthesize Apolipoprotein E and Metabolize Apolipoprotein E-Containing Lipoproteins. *Neuroreport* **6**, 653-657.

Payao, S. L. M., Smith, M. d. A. C., Winter, L. M. F. & Bertolucci, P. H. F. (1998). Ribosomal RNA in Alzheimer's disease and ageing. *Mechanisms of Ageing and Development* **105**, 265-272.

Peden, A. H., Head, M. W., Ritchie, D. I., Bell, J. E. & Ironside, J. W. (2004). Preclinical vCJD after blood transfusion in a PRNP codon 129 heterozygous patient. *Lancet* **364**, 527-529.

Peretz, D., Scott, M., Groth, D., Williamson, D., Burton, D., Cohen, F. E. & Prusiner, S. B. (2001). Strain-specified relative conformational stability of the scrapie prion protein. *Protein Sci* **10**, 854-863.

Peretz, D., Supattapone, S., Giles, K. & other authors (2006). Inactivation of prions by acidic sodium dodecyl sulphate. *J Virol* **80**, 322-331.

Perrett, C. W., Marchbanks, R. M. & Whatley, S. A. (1988). Characterization of mRNA extracted post mortem from the brains of schizophrenic, depressed and control subjects. *J Neurol Neurosurg Psychiatry* **51**, 325-331.

Perry, E. K., Perry, R. H., Blessed, G. & Tomlinson, B. E. (1978). Changes in brain cholinesterases in senile dementia of Alzheimer type. *Neuropathol Appl Neurobiol* **4**, 273-277.

Perry, E. K., Perry, R. H. & Tomlinson, B. E. (1982). The influence of agonal status on some neurochemical activities of postmortem human brain tissue. *Neuroscience Letters* **29**, 303-307.

Petersen, B. H., Rapaport, R., Henry, D. P., Huseman, C. & Moore, W. V. (1990). Effect of treatment with biosynthetic human growth hormone (GH) on peripheral blood lymphocyte populations and function in growth hormone-deficient children. *J Clin Endocrinol Metab* **70**, 1756-1760.

Peyrin, J. M., Lasmezas, C. I., Haik, S., Tagliavini, F., Salmona, M., Williams, A., Ritchie, D., Deslys, J. P. & Dormont, D. (1999). Microglial cells respond to amyloidogenic PrP peptide by the production of inflammatory cytokines. *Neuroreport* **10**, 723-729.

Piccardo, P., Manson, J., King, D., Ghetti, B. & Barron, R. M. (2007). Accumulation of prion protein in the brain that is not associated with transmissible disease. *PNAS* **104**, 4712-4717.

Piccardo, P., Safar, J., Ceroni, M., Gajdusek, D. C. & Gibbs, C. J., Jr. (1990). Immunohistochemical localization of prion protein in spongiform encephalopathies and normal brain tissue. *Neurology* **40**, 518-522.

Pitas, R. E., Boyles, J. K., Lee, S. H., Foss, D. & Mahley, R. W. (1987). Astrocytes synthesize apolipoprotein E and metabolize apolipoprotein E-containing lipoproteins. *Biochim Biophys Acta* **917**, 148-161.

Polunovsky, V. A., Wendt, C. H., Ingbar, D. H., Peterson, M. S. & Bitterman, P. B. (1994). Induction of endothelial cell apoptosis by TNF alpha: modulation by inhibitors of protein synthesis. *Exp Cell Res* **214**, 584-594.

Powell-Jackson, J., Weller, R. O., Kennedy, P., Preece, M., Whitcombe, E. M. & Newsom-Davis, J. (1985). Creutzfeldt-Jakob disease after administration of human growth hormone. *Lancet* **2**, 244-246.

Pratt, W. B. & Toft, D. O. (2003). Regulation of signaling protein function and trafficking by the hsp90/hsp70-based chaperone machinery. *Exp Biol Med (Maywood)* **228**, 111-133.

Preece, P. & Cairns, N. J. (2003). Quantifying mRNA in postmortem human brain: influence of gender, age at death, postmortem interval, brain pH, agonal state and inter-lobe mRNA variance. *Molecular Brain Research* **118**, 60-71.

Preece, P., Virley, D. J., Costandi, M., Coombes, R., Moss, S. J., Mudge, A. W., Jazin, E. & Cairns, N. J. (2003). An optimistic view for quantifying mRNA in post-mortem human brain. *Molecular Brain Research* **116**, 7-16.

Prusiner, S. B. (1998). Prions. *Proc Natl Acad Sci U S A* **95**, 13363-13383.

Prusiner, S. B. & DeArmond, S. J. (1990). Prion diseases of the central nervous system. *Monogr Pathol* **32**, 86-122.

Prusiner, S. B., Groth, D. F., McKinley, M. P., Cochran, S. P., Bowman, K. A. & Kasper, K. C. (1981). Thiocyanate and hydroxyl ions inactivate the scrapie agent. *Proc Natl Acad Sci USA* **78**, 4606-4610.

Prusiner, S. B. (1982). Novel Proteinaceous Infectious Particles Cause Scrapie. *Science* **216**, 136-144.

Prusiner, S. B. (1991). Molecular Biology of Prion Diseases. *Science* **252**, 1515-1522.

Puig, B. & Ferrer, I. (2001). Cell death signaling in the cerebellum in Creutzfeldt-Jakob disease. *Acta Neuropathol* **102**, 207-215.

Qiu, Z., Strickland, D. K., Hyman, B. T. & Rebeck, G. W. (1999). Alpha2-macroglobulin enhances the clearance of endogenous soluble beta-amyloid peptide via low-density lipoprotein receptor-related protein in cortical neurons. *J Neurochem* **73**, 1393-1398.

Quaglio, E., Chiesa, R. & Harris, D. A. (2001). Copper converts the cellular prion protein into a protease-resistant species that is distinct from the scrapie isoform. *J Biol Chem* **276**, 11432-11438.

Rambold, A. S., Miesbauer, M., Rapaport, D., Bartke, T., Baier, M., Winklhofer, K. F. & Tatzelt, J. (2006). Association of Bcl-2 with misfolded prion protein is linked to the toxic potential of cytosolic PrP. *Mol Biol Cell* **17**, 3354-3368.

Rao, R. V. & Bredesen, D. E. (2004). Misfolded proteins, endoplasmic reticulum stress and neurodegeneration. *Current Opinion in Cell Biology* **16**, 653-662.

Ravid, R., Van Zwieten, E. J. & Swabb, D. F. (1992). Brain banking and the human hypothalamus- factors to match for, pitfalls and potentials. *Prog Brain Res* **93**, 83-95.

Rebeck, G. W., Harr, S. D., Strickland, D. K. & Hyman, B. T. (1995). Multiple, diverse senile plaque-associated proteins are ligands of a apolipoprotein E receptor, the alpha-2-macroglobulin receptor/low-density-lipoprotein receptor-related protein. *Ann Neurol* **37**, 211-217.

Reno, C., Marchuk, L., Sciore, P., Frank, C. B. & Hart, D. A. (1997). Rapid isolation of total RNA from small samples of hypocellular, dense connective tissues. *BioTechniques* **22**, 1082-1086.

Rezaie, P. & Lantos, P. L. (2001). Microglia and the pathogenesis of spongiform encephalopathies. *Brain Research Reviews* **35**, 55-72.

Riemer, C., Neidhold, S., Burwinkel, M., Schwarz, A., Schultz, J., Kratzschmar, J., Monning, U. & Baier, M. (2004). Gene expression profiling of scrapie-infected brain tissue. *Biochemical and Biophysical Research Communications* **323**, 556-564.

Riemer, C., Queck, I., Simon, D., Kurth, R. & Baier, M. (2000). Identification of Upregulated Genes in Scrapie-Infected Brain Tissue. *J Virol* **74**, 10245-10248.

Roberg, K., Johansson , U. & Ollinger, K. (1999). Lysosomal release of cathepsin D precedes relocation of cytochrome c and loss of mitochondrial transmembrane potential during apoptosis induced by oxidative stress. *Free Radic Biol Med* **27**, 1228-1237.

Roberg, K. & Ollinger, K. (1998). Oxidative stress causes relocation of the lysosomal enzyme cathepsin D with ensuing apoptosis in neonatal rat cardiomyocytes. *Am J Pathol* **152**, 1151-1156.

Robinson, M. M., Cheevers, W. P., Burger, D. & Gorham, J. R. (1990). Organ-specific modification of the dose-response relationship of scrapie infectivity. *J Infect Dis* **161**, 783-786.

Rock, R. B., Gekker, G., Hu, S., Sheng, W. S., Cheeran, M., Lokensgard, J. R. & Peterson, P. K. (2004). Role of microglia in central nervous system infections. *Clin Microbiol Rev* **17**, 942-964.

Rockett, J. C. & Hellmann, G. M. (2004). Confirming microarray data-is it really necessary? *Genomics* **83**, 541-549.

Rohwer, R. g. (1984a). Scrapie infectious agent is virus-like in size and susceptible to inactivation. *Nature* **308**, 658-662.

Rohwer, R. g. (1984b). Virus like sensitivity of the scrapie agent to heat inactivation. *Science* **223**, 600-602.

Rohwer, R. g. (1991). The scrapie agent: 'a virus by any other name'. *Curr Top Microbiol Immunol* **172**, 195-232.

Ross, J. (1996). Control of messenger RNA stability in higher eukaryotes. *Trends Genet* **12**, 171-175.

Roth, R. B., Hevezi, P., Lee, J., Willhite, D., Lechner, S. M., Foster, A. C. & Zlotnik, A. (2006). Gene expression analyses reveal relationships among 20 regions of the human CNS. *Neurogenetics* **7**, 67-80.

Roucou, X. & LeBlanc, A. C. (2005). Cellular prion protein neuroprotective function: implications in prion diseases. *J Mol Med* **83**, 3-11.

Saborio, G. P., Permanne, B. & Soto, C. (2001). Sensitive detection of pathological prion protein by cyclic amplification of protein misfolding. *Nature* **411**, 810-813.

Sachs, A. B. (1993). Messenger RNA degradation in eukaryotes. *Cell* **74**, 413-421.

Sachs, L. & Bat-Miriam, M. (1957). The genetics of Jewish populations. 1. Finger print patterns in Jewish populations in Israel. *Am J Hum Genet* **9**, 117-126.

Saez-Valero, J., Fodero, L. R., Sjogren, M. & other authors (2003). Glycosylation of acetylcholinesterase and butyrylcholinesterase changes as a function of the duration of Alzheimer's disease. *J Neurosci Res* **72**, 520-526.

Safar, J. G., Wille, H., Geschwind, M. D. & other authors (2006). Human prions and plasma lipoproteins. *PNAS* **103**, 11312-11317.

Sajdel-Sulkowska, E., Coughlin, J. F. & Marotta, C. A. (1983). In vitro synthesis of polypeptides of moderately large size by poly(A)-containing messenger RNA from postmortem human brain and mouse brain. *J Neurochem* **40**, 670-680.

Sakaguchi, S., Katamine, S., Nishida, N. & other authors (1996). Loss of cerebellar Purkinje cells in aged mice homozygous for a disrupted PrP gene. *Nature* **380**, 528-531.

Sakudo, A., Lee, D.-C., Saeki, K., Matsumoto, Y., Itohara, S. & Onodera, T. (2003a). Tumour necrosis factor attenuates prion protein-deficient neuronal cell death by increases in anti-apoptotic Bcl-2 family proteins. *Biochem Biophys Res Commun* **310**, 725-729.

Sakudo, A., Lee, D.-C., Saeki, K., Nakamura, K., Matsumoto, Y., Itohara, S. & Onodera, T. (2003b). Impairment of superoxide dismutase activation by N-terminally truncated prion protein (PrP) in PrP-deficient neuronal cell line. *Biochem Biophys Res Commun* **308**, 660-667.

Salaun, C., Jmaes, D. J. & Chmaberlain, L. H. (2004). Lipid rafts and the regulation of exocytosis. *Traffic* **5**, 255-264.

Sambrook, J. & Russel, D. W. (2001).*Molecular cloning: A laboratory manual.* Cold Spring Harbour, New York: CSH Laboratory Press.

Sanders, V. J., Felisan, S., Waddell, A. & Tourtellotte, W. W. (1996). Detection of herpesviridae in post-mortem multiple sclerosis brain tissue and controls by polymerase chain reaction. *J Neurovirol* **2**, 249-258.

Santiago, T. C., Purvis, I. J., Bettany, A. J. & Brown, A. J. P. (1986). The relationship between mRNA stability and length in Saccharomyces cerevisiae. *Nucleic Acids Res* **12**, 8347-8360.

Santoni, V., Molloy, M. & Rabilloud, T. (2000). Membrane proteins and proteomics: un amour impossible? *Electrophoresis* **21**, 1054-1070.

Sato, T., Hanada, M., Bodrug, S. & other authors (1994). Interactions among members of the Bcl-2 protein family analyzed with a yeast two-hybrid system. *PNAS* **91**, 9238-9242.

Scheinfeld, M. H., Ghersi, E., Laky, K., Fowlkes, B. J. & D'Adamio, L. (2002). Processing of beta-amyloid precursor-like protein-1 and -2 by gamma-secretase regulates transcription. *J Biol Chem* **277**, 44195-44201.

Schmittgen, T. D. & Zakrajsek, B. A. (2000). Effect of experimental treatment on housekeeping gene expression: validation by real-time, quantitative RT-PCR. *Journal of Biochemical and Biophysical Methods* **46**, 69-81.

Schoor, O., Weinschenk, T., Hennenlotter, J., Corvin, S., Stenzl, A., Rammensee, H. G. & Stevanovic, S. (2003). Moderate degradation does not preclude microarray analysis of small amounts of RNA. *BioTechniques* **35**, 1192-1201.

Schramm, M., Falkai, P., Tepest, R., Schneider-Axmann, T., Przkora, R., Waha, A., Pietsch, T., Bonte, W. & Bayer, T. A. (1999). Stability of RNA transcripts in post-mortem psychiatric brains. *Journal of Neural Transmission* **106**, 329-335.

Schroeder, A., Mueller, O., Stocker, S., Salowsky, R., Leiber, M., Gassmann, M., Lightfoot, S., Menzel, S. & Granzow M, R. T. (2006). The RIN: an RNA integrity number for assigning integrity calues to RNA measurements. *BMC Mol Biol*, 3.

Scott, M., Foster, D., Mirenda, C. & other authors (1989). Transgenic mice expressing hamster prion protein produce species-specific scrapie infectivity and amyloid plaques. *Cell* **59**, 847-857.

Segrest, J. P., Jones, M. K., De Loof, H. & Dashti, N. (2001). Structure of apolipoprotein B-100 in low density lipoproteins. *J Lipid Res* **42**, -1346.

Sela, M., Anfinsen, C. B. & Harrington, W. F. (1957). The correlation of ribonuclease activity with specific aspects of tertiary structure. *Biochim Biophys Acta* **26**, 502-512.

Selvey, S., Thompson, E. W., Matthaei, K., Lea, R. A., Irving, M. G. & Griffiths, L. R. (2001).[beta]-Actin--an unsuitable internal control for RT-PCR. *Molecular and Cellular Probes* **15**, 307-311.

Serels, S., Day, N. S., Wen, Y. P., Giraldi, A., Lee, S. W., Melman, A. & Christ, G. J. (1998). Molecular studies of human connexin 43 (Cx43) expression in isolated corporal tissue strips and cultured corporal smooth muscle cells. *Int J Impot Res* **10**, 135-143.

Shaked, G. M., Fridlander, G., Meiner, Z., Taraboulos, A. & Gabizon, R. (1999). Protease-resistant and detergent-insoluble prion protein is not necessarily associated with prion infectivity. *J Biol Chem* **274**, 17981-17986.

Shaked, G. M., Meiner, Z., Avraham, I., Taraboulos, A. & Gabizon, R. (2001). Reconstitution of prion infectivity from solubilized protease-resistant PrP and nonprotein components of prion rods. *J Biol Chem* **276**, 14324-14328.

Shapiro, D. J., Blume, J. E. & Nielsen, D. A. (1987). Regulation of mesenger RNA stability in eukaryotic cells. *Bioessays* **6**, 221-226.

Shapshak, P., Tourtellotte, W. W., Wolman, M. & other authors (1986). Search for virus nucleic acid sequences in post-mortem human brain tissue using in situ hybridization technology with cloned probes; some solutions and results on progressive multifocal leukoencephalopathy and subacute sclerosing panencephalitis tissue. *J Neurosci Res* **16**, 281-301.

Sharief, M. K., Green , A., Dick, J. P., Gawler, J. & Thompson, E. J. (1999). Heightened intrathecal release of proinflammatory cytokines in Creutzfeldt-Jakob disease. *Neurology* **52**, 1289-1291.

Shaw, G. & Kamen, R. (1986).A conserved AU sequence from the 3' untranslated region of GM-CSF mRNA mediates selcetive mRNA degradation. *Cell* **46**, 659-667.

Shyng, S. L., Heuser, J. E. & Harris, D. A. (1994).A glycolipid-anchored prion protein is endocytosed via clathrin-coated pits. *J Cell Biol* **125**, 1239-1250.

Shyng, S. L., Moulder, K. L., Lesko, A. & Harris, D. A. (1995). The N-terminal domain of a glycolipid-anchored prion protein is essential for its endocytosis via clathrin-coated pits. *J Biol Chem* **270**, 14793-14800.

Sigurdson, C. J. & Miller, M. W. (2003). Other animal prion diseases. *Br Med Bull* **66**, 199-212.

Silveira, J. R., Raymond, G. J., Hughson, A. G., Race, R. E., Sim, V. L., Hayes, S. F. & Caughey, B. (2005). The most infectious prion protein particle. *Nature* **437**, 257-261.

Simons, K. & Ikonen, E. (1997). Functional rafts in cell membranes. *Nature* **387**, 569-572.

Simons, K. & Toomre, D. (2000). Lipid rafts and signal transduction. *Nat Rev Mol Cell Biol* **1**, 31-39.

Simons, M., Keller, P., De Strooper, B., Beyreuther, K., Dotti, C. G. & Simons, K. (1998). Cholesterol depletion inhibits the generation of beta-amyloid in hippocampal neurons. *PNAS* **95**, 6460-6464.

Singhrao, S. K., Neal, J. W., Rushmere, N. K., Morgan, B. P. & Gasque, P. (2000). Spontaneous classical pathway inactivation and deficeincy of membrane regulators render human neurons susceptible to complement lysis. *Am J Pathol* **157**, 905-918.

Sitia, R. & Braakman, I. (2003). Quality control in the endoplasmic reticulum protein factory. *Nature* **426**, 891-894.

Skinner, J. P., Abbassi, H., Chesebro, B., Race, R., Reilly, C. & Haase, A. T. (2006). Gene expression alterations in brains of mice infected with three strains of scrapie. *BMC Genomics* **7**, 114.

Skrypina, N., Timofeeva, A. V., Khaspekov, G. L., Savochkina, L. P. & Beabealashvilli, R. Sh. (2003). Total RNA suitable for molecular biology analysis. *Journal of Biotechnology* **105**, 1-9.

Somerville, R. & Carp, R. I. (1983). Altered scrapie infectivity estimates by titration and incubation period in the presence of detergents. *J Gen Virol* **64**, 2050.

Somerville, R., Oberthur, R. C., Havekost, U., MacDonald, F., Taylor, D. M. & Dickinson, A. G. (2002). Characterisation of thermo-dynamic diversity between transmissible spongiform encephalopathy agent strains and its theoretical implications. *J Biol Chem* **277**, 11089.

Sorensen, G., Medina, S., Parchaliuk, D., Phillipson, C., Robertson, C. & Booth, S. (2008). Comprehensive transcriptional profiling of prion infection in mouse models reveals networks of responsive genes. *BMC Genomics* **9**, 114-128.

Soto, C. & Castilla, J. (2004). The controversial protein-only hypothesis of prion propagation. *Nat Med* **10**, S63-S67.

Spanakis, E. (1993). Problems related to the interpretation of autoradiographic data on gene expression using common constitutive transcripts as controls. *Nucleic Acids Res* **21**, 3809-3819.

Sporns, O., Tononi, G. & Edelman, G. M. (2000). Connectivity and complexity: the relationship between neuroanatomy and brain dynamics. *Neural Networks* **13**, 909-922.

Stahl, N., Borchelt, D. R., Hsiao, K. & Prusiner, S. B. (1987). Scrapie prion protein contains a phosphatidylinositol glycolipid. *Cell* **51**, 229-240.

Steele, A. D., King, O. D., Jackson, W. S., Hetz, C. A., Borkowski, A. W., Thielen, P., Wollmann, R. & Lindquist, S. (2007). Diminishing apoptosis by deletion of Bax or overexpression of Bcl-2 does not protect against infectious prion toxicity in vivo. *J Neurosci* **27**, 13022-13027.

Stoerck, K., Bodemer, M., Ciesielczyk, B., Meissner , B., Bartl, M., Heinemann, U. & Zerr, I. (2005). Interleukin 4 and interleukin 10 levels are elevated in the cerebrospinal fluid of patients with Creutzfeldt-Jakob disease. *Arch Neurol* **62**, 1591-1594.

Strickland, D. K., Kounnas, M. Z. & Argraves, W. S. (1995).LDL receptor-related protein:a multiligand receptor for lipoprotein and proteinase catabolism. *FASEB J* **9**, 890-898.

Sunyach, C., Jen, A., Deng, J., Fitzgerald, K. T., Frobert, Y., Grassi, J., McCaffrey, M. W. & Morris, R. (2003). The mechanism of internalization of glycosylphosphatidylinositol-anchored prion protein. *EMBO J* **22**, 2591-3601.

Suzuki, T., Higgins, P. J. & Crawford, D. R. (2000). Control selection for RNA quantitation. *BioTechniques* **29**, 332-337.

Szczepanik, A. M., Funes, S., Petko, W. & Ringheim, G. E. (2001).IL-4, IL-10 and IL-13 modulate A beta(1--42)-induced cytokine and chemokine production in primary murine microglia and a human monocyte cell line. *J Neuroimmunol* **113**, 49-62.

Tamatani, M., Che, Y. H., Matsuzaki, H., Ogawa, H., Okado, H., Miyake, S., Mizuno, T. & Tohyama, M. (1999). Tumor necrosis factor induces Bcl-2 and Bcl-x expression through NFkappaB activation in primary hippocampal neurons. *J Biol Chem* **274**, 8531-8538.

Tang, W. W., Qi, M., Van, G. Y., Wariner, G. P. & Samal, B. (1996). Leukemia inhibitory factor ameliorates experimental anti-GBM Ab glomerulonephritis. *Kidney Int* **50**, 1922-1927.

Tanskanen, M., Peuralinna, T., Polvikoski, T. & other authors (2008). Senile systemic amyloidosis affects 25% of the very aged and associates with genetic variation in alpha2-macroglobulin and tau: a population-based autopsy study. *Ann Med* **40**, 232-239.

Taraboulos, A., Raeber, A. J., Borchelt, D. R., Serban, D. & Prusiner, S. B. (1992). Synthesis and trafficking of prion proteins in cultured cells. *Mol Biol Cell* **3**, 851-863.

Taraboulos, A., Scott, M., Semenov, A., Avrahami, D., Laszlo, L. & Prusiner, S. B. (1995a). Cholesterol depletion and modification of COOH-terminal

targeting sequence of the prion protein inhibit formation of the scrapie isoform. *J Cell Biol* **129**, 121-132.

Taraboulos, A., Scott, M., Semenov, A., Avrahami, D., Laszlo, L. & Prusiner, S. B. (1995b). Cholesterol depletion and modification of COOH-terminal targeting sequence of the prion protein inhibit formation of the scrapie isoform. *J Cell Biol* **129**, 121-132.

Tarraboulos, A., Scott, M., Semenov, A., Avrahami, D., Laszol, L. & Prusiner, S. B. (1995). Cholesterol depletion and modification of COOH-terminal targeting sequence of the prion protein inhibits formation of the scrapie isoform. *J Cell Biol* **129**, 121-132.

Tateishi, J., Koga, M. & Mori, R. (1981). Experimental transmission of Creutsfeldt-Jakob disease. *Acta Pathol Jpn* **31**, 943-951.

Taylor, D. M. & Fernie, K. (1996). Exposure to autocalving or sodium hydroxide extends the dose-response curve of the 263K strain of scrapie agent in hamsters. *J Gen Virol* **77**, 811-813.

Taylor, D. M., Fernie, K., Steele, P. J., McConnell, I. & Somerville, R. A. (2002). Thermostability of mouse-passaged BSE and scrapie is independent of host PrP genotype:implications for the nature of the causal agents. *J Gen Virol* **83**, 3204.

Taylor, D. M. & McBride, P. A. (1987). Autoclaved, formol-fixed scrapie mouse brain is suitable for histopathological examination, but may still be infective. *Acta Neuropathol* **74**, 194-196.

Taylor, D. M. & Woodgate, S. L. (1997). Bovine spongiform encephalopathy:the causal role of ruminant-derived protein in cattle diets. *Rev Sci Tech* **16**, 187-198.

Taylor, D. M., Fernie, K., McConnell, I. & Steele, P. J. (1998). Observation on thermostable subpopulations of the unconventional agents that cause transmissible degenerative encephalopathies. *Vet Microbiol* **64**, 33-38.

Taylor, D. M. & McConnell, I. (1988). Autoclaving does not decontaminate formal-fixed scrapie tissues. *Lancet* **1**, 1463-1464.

Taylor, D. R. & Hooper, N. M. (2007). The low-density lipoprotein receptor-related protein 1 (LRP1) mediates the endocytosis of the celllar prion protein. *Biochem J* **402**, 17-23.

Taylor, D. R. & Hooper, N. M. (2006). The prion protein and lipid rafts. *Mol Membr Biol* **23**, 89-99.

Taylor, G. R., Carter, G. I., Crow, T. J., Johnson, J. A., Fairbairn, A. F., Perry, E. K. & Perry, R. H. (1986). Recovery and measurement of specific RNA species from postmortem brain tissue: A general reduction in Alzheimer's

disease detected by molecular hybridization. *Experimental and Molecular Pathology* **44**, 111-116.

Telling, G. C., Parchi, P., DeArmond, S. J. & other authors (1996). Evidence for the conformation of the pathologic isoform of the prion protein enciphering and propagating prion diversity. *Science* **274**, 2079-2082.

Telling, G. C., Scott, M., Mastrianni, J., Gabizon, R., Torchia, M., Cohen, F. E., DeArmond, S. J. & Prusiner, S. B. (1995). Prion propagation in mice expressing human and chimeric PrP transgenes implicates the interaction of cellular PrP with another protein. *Cell* **83**, 79-90.

Thackray, A. M., McKenzie, A. N., Klein, M. A., Lauder, A. & Bujdoso, R. (2004). Accelerated prion disease in the absence of interleukin-10. *J Virol* **78**, 13697-13707.

Thellin, O., Zorzi, W., Lakaye, B., De Borman, B., Coumans, B., Hennen, G., Grisar, T., Igout, A. & Heinen, E. (1999). Housekeeping genes as internal standards: use and limits. *Journal of Biotechnology* **75**, 291-295.

Thellung, S., Florio, T., Villa, V. & other authors (2000). Apoptotic cell death and impairment of L-type voltage-sensitive calcium channel activity in rat cerebellar granule cells treated with the prion protein fragment 106-126. *Neurobiol Dis* **7**, 299-309.

Tobler, I., Gaus, S. E., Deboer, T. & other authors (1996). Altered circadian activity rhythms and sleep in mice devoid of prion protein. *Nature* **380**, 639-642.

Tomita, H., Vawter, M. P., Walsh, D. M. & other authors (2004). Effect of agonal and postmortem factors on gene expression profile: quality control in microarray analyses of postmortem human brain. *Biological Psychiatry* **55**, 346-352.

Tononi, G., Sporns, O. & Edelman, G. M. (1994).A measure for brain complexity: relating functional segregation and integration in the nervous system. *Proc Natl Acad Sci USA* **91**, 5033-5037.

Trotter, S. A., Brill II, L. B. & Bennett, J. (2002). Stability of gene expression in postmortem brain revealed by cDNA gene array analysis. *Brain Research* **942**, 120-123.

Tucker, H. M., Kihiko, M., Cladwell, J. N. & other authors (2000). The plasmin system is induced by and degrades amyloid-beta aggregates. *J Neurosci* **10**, 3937-3946.

Unterberger, U., Hoftberger, R., Gelpi, E., Flicker, H., Budka, H. & Voigtlander, T. (2006). Endoplasmic reticulum stress features are prominent in Alzheimer disease but not in prion diseases in vivo. *J Neuropathol Exp Neurol* **65**, 348-357.

Vandesompele, J., De Preter, K., Pattyn, F., Poppe, B., Van Roy, N., De Paepe, A. & Speleman, F. (2002). Accurate normalization of real-time quantitative RT-PCR data by geometric averaging of multiple internal control genes. *Genome Biology* **3**, research0034.

Vassallo, N., Herms, J., Behrens, C., Krebs, B., Saeki, K., Onodera, T., Windl, O. & Kretzchmar, H. A. (2005). Activation of phosphatidylinositol 3-kinase by cellular prion protein and its role in cell survival. *Biochem Biophys Res Commun* **332**, 75-82.

Vawter, M. P., Evans, S., Choudary, P. & other authors (2004). Gender-specific gene expression in post-mortem human brain: localization to sex chromosomes. *Neuropsychopharmacology* **29**, 373-384.

Vey, M., Pilkuhn, S., Wille, H., Nixon, R., DeArmond, S. J., Smart, E. J., Anderson, R. G., Taraboulos, A. & Prusiner, S. B. (1996). Subcellular colocalization of the cellular and scrapie prion proteins in caveolae-like membranous domains. *PNAS* **93**, 14945-14949.

Vonsattel, J. P. G., Aizawa, H., Ge, P. & other authors (1995). An improved approach to prepare human brains for research. *J Neuropath Exp Neurol* **54**, 42-56.

Vuong, G. L., Weiss, S. M., Kammer, W., Priemer, M., Vingron, M., Nordheim, A. & Cahill, M. A. (2000). Improved sensitivity proteomics by postharvest alkylation and radioactive labelling of proteins. *Electrophoresis* **21**, 2594-2605.

Waggoner, D. J., Drisaldi, B., Bartnikas, T. B., Casareno, R. L., Prohaska, J. R., Gitlin, J. D. & Harris, D. A. (2000). Brain copper content and cuproenzyme activity do not vary with prion protein expression level. *J Biol Chem* **275**, 7455-7458.

Wahrle, S. E., Jiang, H., Parsadanian, M., Hartman, R. E., Bales, K. R., Paul, S. M. & Holtzman, D. M. (2005). Deletion of Abca1 increases Abeta deposition in the PDAPP transgenic mouse model of Alzheimer disease. *J Biol Chem* **280**, 43236-43242.

Wahrle, S. E., Jiang, H., Parsadanian, M. & other authors (2008). Overexpression of ABCA1 reduces amyloid deposition in the PDAPP mouse model of Alzheimer disease. *J Clin Invest* **118**, 671-682.

Wang, A. M., Doyle, M. V. & Mark, D. F. (1989). Quantitation of mRNA by the polymerase chain reaction. *Proc Natl Acad Sci USA* **86**, 9717-9721.

Wang, X., Wang, F., Arterburn, L., Wollmann, R. & Ma, J. (2006). The interaction between cytoplasmic prion protein and the hydrophobic lipid core of membrane correlates with neurotoxicity. *J Biol Chem* **281**, 13559-13565.

Wasco, W., Gurubhagavatula, S., Paradis, M. D., Romano, D. M., Sisodia, S. S., Hyman, B. T., Neve, R. L. & Tanzi, R. E. (1993). Isolation and characterization of APLP2 encoding a homologue of the Alzheimer's associated amyloid beta protein precursor. *Nat Genet* **5**, 95-100.

Watakabe, A., Sugai, T., Nakaya, N., Wakabayashi, K., Takahashi, H., Yamamori, T. & Nawa, H. (2001). Similarity and variation in gene expression among human cerebral cortical subregions revealed by DNA macroarrays: technical consideration of RNA expression profiling from postmortem samples. *Molecular Brain Research* **88**, 74-82.

Weis, S., Llenos, I. C., Dulay, J. R., Elashoff, M., Martinez-Murillo, F. & MIller, C. L. (2007). Quality control for microarray analysis of human brain samples: The impact of postmortem factors, RNA characteristics, and histopathology. *J Neurosci Methods* **165**, 198-209.

Weise, J., Sandau, R., Schwarting, S., Crome, O., Wrede, A., Schulz-Schaeffer, W., Zerr, I. & Bahr, M. (2006). Deletion of cellular prion protein results in reduced Akt activation, enhanced postischemic caspase-3 activation, and exacerbation of ischemic brain injury. *Stroke* **37**, 1296-1300.

Wells, G. A., Scott, A. C., Johnson, C. T., Gunning, R. F., Hancock, R. D., Jeffrey, M., Dawson, M. & Bradley, R. (1987).A novel progressive spongiform encephalopathy in cattle. *Vet Rec* **121**, 419-420.

Westaway, D., DeArmond, S. J., Cayetano-Canlas, J., Groth, D., Foster, D., Yang, S. L., Torchia, M., Carlson, G. A. & Prusiner, S. B. (1994). Degeneration of skeletal muscle, peripheral nerves, and the central nervous system in transgenic mice overexpressing wild-type prion proteins. *Cell* **76**, 117-129.

Westaway, D., Mirenda, C., Foster, D. & other authors (1991). Paradoxical shortening of scrapie incubation times by expression of prion protein transgenes derived from long incubation period mice. *Neuron* **7**, 59-68.

White, F. A., Ishaq, M., Stoner, G. L. & Frisque, R. J. (1992).JC virus DNA is present in many human brains from patients without progressive multifocal leukoencepahlopathy. *J Virol* **66**, 5726-5734.

Wilesmith, J. W. (1988). Bovine spongiform encephalopathy. *Vet Rec* **122**, 614.

Will, R. G. (1993). Epidemiology of Creutzfeldt-Jakob disease. *Br Med Bull* **49**, 960-970.

Will, R. G., Ironside, J. W., Zeidler, M. & other authors (1996).A new variant of Creutzfeldt-Jakob disease in the UK. *The Lancet* **347**, 921-925.

Will, R. G., Zeidler, M., Stewart, G. E. & other authors (2000). Diagnosis of new variant Creutzfeldt-Jakob disease. *Ann Neurol* **47**, 575-582.

Williams, A., Lucassen, P. J., Ritchie, D. & Bruce, M. (1997). PrP deposition, microglial activation, and neuronal apoptosis in murine scrapie. *Exp Neurol* **144**, 433-438.

Williams, A. E., Lawson, L. J., Perry, V. H. & Fraser, H. (1994). Characterization of the microglial response in murine scrapie. *Neuropathol Appl Neurobiol* **10**, 47-55.

Wilquet, V. & De Strooper, B. (2004). Amyloid-beta presursor protein processing in neurodegeneration. *Curr Opin Neurobiol* **14**, 582-588.

Wong, B. S., Liu, T., Li, R. & other authors (2001). Increased levels of oxidative stress markers detected in the brains of mice devoid of prion protein. *J Neurochem* **76**, 565-572.

Wyatt, J. M., Pearson, G. R., Smerdon, T. N., Gruffydd-Jones, T. J., Wells, G. A. & Wilesmith, J. W. (1991). Naturally occurring scrapie-like spongiform encephalopathy in five domestic cats. *Vet Rec* **129**, 233-236.

Xiang, W., Hummel, M., Mitteregger, G., Pace, C., Windl, O., Mansmann, U. & Kretzchmar, H. A. (2007). Transcriptome analysis reveals altered cholesterol metabolism during the neurodegeneration in mouse scrapie model. *J Neurochem* **102**, 834-847.

Xiang, W., Windl, O., Westner, I. M., Neumann, M., Zerr, I., Lederer, R. M. & Kretzschmar, H. (2005). Cerebral gene expression profiles in sporadic Creutzfeldt-Jakob disease. *Annals of Neurology* **58**, 242-257.

Xiang, W., Windl, O., Wunsch, G., Dugas, M., Kohlmann, A., Dierkes, N., Westner, I. M. & Kretzschmar, H. (2004). Identification of differentially expressed genes in scrapie-infected mouse brains using global gene expression technology. *J Virol* **78**, 11051-11060.

Yamauchi, Y., Hayashi, M., Abe-Dohmae, S. & Yokoyama, S. (2003). Apolipoprotein A-I activates protein kinase C alpha signaling to phosphorylate and stabilize ATP binding cassette transporter A1 for the high density lipoprotein assembly. *J Biol Chem* **278**, 47890-47897.

Yasojima, K., McGeer, E. G. & McGeer, P. L. (2001). High stability of mRNAs postmortem and protocols for their assessment by RT-PCR. *Brain Research Protocols* **8**, 212-218.

Yates, C. M., Butterworth, J., Tennant, M. C. & Gordon, A. (1990). Enzyme activityes in relation to pH and lactate in postmortem brain in Alzheimer-type and other dementias. *J Neurochem* **55**, 1624-1630.

Yoshida, H., Matsui, T., Yamamoto, A., Okada, T. & Mori, K. (2001).XBP1 mRNA is induced by ATF6 and spiced by IRE1 in response to ER stress to produce a highly active transcription factor. *Cell* **107**, 881-891.

Yuan, J., Xiao, X., McGeehan, J. & other authors (2006). Insoluble aggregates and protease-resistant conformers of prion protein in uninfected human brains. *J Biol Chem* **281**, 34848-34858.

Zanata, S. M., Lopes, M. H., Mercandante, A. F. & other authors (2002). Stress-inducible protein 1 is a cell surface ligand for cellular prion that triggers neuroprotection. *EMBO J* **21**, 3307-3316.

Zanusso, G., Petersen , R. B., Jin, T., Jing, Y., Kanoush, R., Ferrari, S., Gambetti, P. & Singh, N. (2000). Proteasomal degradation and N-terminal protease resistance of the codon 145 mutant prion protein. *J Biol Chem* **274**, 23396-23404.

Zerr, I., Helmhold, M., Poser, S., Armstrong, V. W. & Weber, T. (1996). Apolipoprotein E phenotype frequency and cerebrospinal fluid concentration are not associated with Creutzfeldt-Jakob disease. *Arch Neurol* **53**, 1233-1238.

Zhong, H. & Simons, J. W. (1999). Direct Comparison of GAPDH, [beta]-Actin, Cyclophilin, and 28S rRNA as Internal Standards for Quantifying RNA Levels under Hypoxia. *Biochemical and Biophysical Research Communications* **259**, 523-526.

9 APPENDIX

9.1 COMMON REAGENT RECIPES

Water purified with Barnstead NANOpure system (Basingstoke, UK) was used to make up all solutions.

EXTRACTION BUFFER;
0.5% sodium deoxycholate (DOC)
0.5% NP-40
TBS pH 7.4
All reagents obtained from Sigma-Aldrich, UK.

2x SAMPLE BUFFER;
Made up with deionised water or extraction buffer from NuPAGE LDS sample Buffer (4x) (Invitrogen, UK)
Final concentration for use at 2x
212 mM Tris HCL
282 mM Tris base
4% Lithium salt of dodecyl sulphate (LDS)
20% Glycerol
1.02 nM EDTA
0.44 mM SERVA Blue G250
0.35 mM Phenol Red
pH 8.5

NuPAGE MES SDS RUNNING BUFFER 20x STOCK (Invitrogen, UK)
Final concentration of constituents:
50 mM MES
50 mM Tris Base
0.1% SDS
1 mM EDTA

pH 7.3

NuPAGE TRANSFER BUFFER 20x (Invitrogen, UK)
25 mM Bicine
25 mM Bis-Tris (free base)
1 mM EDTA
pH 7.2

For use; 1x NuPAGE Transfer buffer (Invitrogen, UK) with 10% methanol (VWR International, UK) was prepared.

For Superarray GEArray® Focused DNA Microarrays, the following stock buffers were made.

20x SSC
175.3g sodium chloride
88.2g sodium citrate dehydrate
Dilute to 1L with ddH_2O
pH 7.0
All reagents obtained from Sigma-Aldrich, UK.

20% SDS
200g sodium dodecyl sulfate
Dilute to 1L with ddH_2O
All reagents obtained from Sigma-Aldrich, UK.

9.2 NATIONAL CREUTZFELDT-JAKOB DISEASE SURVEILLANCE UNIT DIAGNOSTIC CRITERIA (EDINBURGH)

<table>
<tr><td colspan="2">1. SPORADIC CJD</td><td rowspan="4">I Rapidly progressive dementia.

II A Myoclonus
B Visual or cerebellar problems
C Pyramidal or extrapyramidal features
D Akinetic mutism

III Typical EEG</td></tr>
<tr><td colspan="2">1.1 DEFINITE: neuropahologically/ immunocytochemically confirmed</td></tr>
<tr><td rowspan="2">1.2 PROBABLE:</td><td>1.2.1 I + 2 of II + III</td></tr>
<tr><td>1.2.2.Possible + positive 14-3-3</td></tr>
<tr><td colspan="2">1.3 POSSIBLE: I + 2 of II + duration < 2 years</td></tr>
</table>

<table>
<tr><td colspan="2">2. ACCIDENTALLY TRANSMITTED TSE</td><td rowspan="4">RELEVANT EXPOSURE RISKS FOR THE CLASSIFICATION AS IATROGENIC CJD
The relevance of any exposure to disease causation must take into account the timing of the exposure in relation to disease onset.
Treatment with human pituitary growth hormone, human pituitary gonadotrophin or human dura mater graft.
Corneal graft in which the corneal donor has been classified as definite or probable human prion disease.
Exposure to neurosurgical instruments previously used in a case of definite or</td></tr>
<tr><td colspan="2">2.1 DEFINITE: definite CJD with a recognized iatrogenic risk factor</td></tr>
<tr><td rowspan="2">2.2 PROBABLE:</td><td>2.2.1 progressive predominant cerebellar syndrome in human pituitary hormone recipients</td></tr>
<tr><td>2.2.2 probable CJD with recognized risk factors</td></tr>
</table>

		probable human prion disease. This list is provisional as previously unrecognized mechanisms of human prion disease may occur.

3. GENETIC TSE		PRNP MUTATIONS ASSOCIATED WITH GSS NEUROPATHOLOGICAL PHENOTYPE: P102L, P105L, A117V, G131V, F198S, D202N, Q212P, Q217R, M232T, 192 bpi PRNP MUTATIONS ASSOCIATED WITH CJD NEUROPATHOLOGICAL PHENOTYPE D178N-129V, V180I, V180I+M232R, T183A, T188A, E196K, E200K, V203I, R208H, V210I, E211Q, M232R, 96 bpi, 120 bpi, 144 bpi, 168 bpi, 48 bp*del* PRNP MUTATIONS ASSOCIATED WITH FFI NEUROPATHOLOGICAL PHENOTYPE D178N-129M PRNP MUTATIONS ASSOCIATED WITH VASCULAR PRP AMYLOID Y145s PRNP MUTATIONS ASSOCIATED WITH PROVEN BUT UNCLASSIFIED PRION DISEASE H187R, 216 bpi MUTATIONS ASSOCIATED WITH NEURO-PSYCHIATRIC DISORDER
3.1 DEFINITE:	**3.1.1** definite TSE + definite or probable TSE in 1st degree relative	
	3.1.2 definite TSE with a pathogenic PRNP mutation	
3.2 PROBABLE:	**3.2.1** progressive neuropsychiatric disorder + definite or probable TSE in 1st degree relative	
	3.2.2 progressive neuropsychiatric disorder + pathogenic PRNP mutation	

		BUT NOT PROVEN PRION DISEASE I138M, G142S, Q160S, T188K, M232R, 24 bpi, 48 bpi, 48 bpi + nucleotide substitution in other octapeptides

4. vCJD		I A Progressive neuropsychiatries disorder B Duration of illness > 6 months C Routine investigations do not suggest an alternative diagnosis D No history of potential iatrogenic exposure E No evidence of a familial form of TSE II A Early psychiatric symptoms[a] B Persistent painful sensory symptoms[b] C Ataxia D Myoclonus or chorea or dystonia E Demenitia III A EEG does not show the typical appearance of sporadic CJD[c] (or no EEG performed) B Bilateral pulvinar high signal on MRI scan IV A Positive tonsil biopsy[d] a Depression, anxiety, apathy, withdrawal, delusions.
4.1 DEFINITE: 1A and neuropathological confirmation of vCJD		
4.2 PROBABLE:	**4.2.1** I and 4/5 of II and IIIA and IIIB	
	4.2.2 I and IV A[d]	
4.3 POSSIBLE: I and 4/5 of II and IIIA		

	b This includes both frank pain and/or dysaesthesia. c Generalised triphasic periodic complexes at approximately one per second. d Tonsil biopsy is NOT recommended routinely, nor in cases with EEG appearances typical of sCJD, but may be useful in suspect cases in which the clinical features are compatible with vCJD and MRI does not show bilateral pulvinar high signal. e Spongiform change and extensive PrP deposition with florid plaques, throughout the cerebrum and cerebellum.

Table 9.1. NCJDSU diagnostic criteria.

9.3 CREUTZFELDT-JAKOB DISEASE SURVEILLANCE UNIT, PROTOCOL FOR FULL AUTOPSY (EDINBURGH)

SPECIMENS TO BE RETAINED FROM FULL AUTOPSY (EDINBURGH)

SNAP FREEZING

29 bijou bottles with a small piece of white card in each bottle. "Risk of Infection" sign attached and labelled with patient's name, RU number, date and following specimens:

Adrenal	Kidney	Salivary Gland
Appendix	Liver	Spleen
Bone Marrow	Lung	Spinal cord

Cerebellum	Muscle	Temporal
Cervical lymph node	Occipital	Tendon
Distal Ileum	Ovary/Testes	Thymus
Dorsal root ganglion	Pancreas	Thyroid
Frontal	Parietal (NO)	Tonsil
Heart	Peripheral nerve	Trigeminal Ganglia
Heart Valve	Pituitary	

Put bottles in a "Risk of Infection" specimen bag marked on the outside with patient's name, RU number and "SNAP FREEZE"

PLP FIXED

9 small specimen bottles (PLP to be added just before use). "Risk of Infection" sign, patient's name, RU number, date, PLP and following specimens:

Frontal	Cerebellum	Peripheral nerve
Temporal	Spinal cord	Muscle
Occipital	Spleen	Tonsil

Keep together in "Risk of Infection" bag marked with RU number, patient's name, and PLP

3 Universals - one for CSF, one for spleen and one for blood labelled with "Risk of Infection" sign, patient's name, RU number and specimens. Strip of parafilm for sealing.

1 specimen jar for frozen cerebellar hemisphere - labelled as above and
2 polythene bags (1 labelled) for holding frozen half brain (right hemisphere)

2 specimen bottles (250ml) for microscopic analysis.

9.4 POST MORTEM REQUEST FOR ADDITIONAL AUTOPSY SPECIMENS TO BE TAKEN FROM SUSPECTED CASES OF CJD FOR RNA PROFILING STUDY

AIM

To assess the variation in gene expression profiles within and between brain regions. This will allow us to predict the level of variation that may occur between brain samples from patients with different forms of CJD and with other neurodegenerative diseases. For this study, it is important that the neuroanatomical sites of sampling are recorded as accurately as is possible and that these sites are reproducibly sampled between patients. We are interested in identifying whether there are any disease-specific changes in the expression of selected genes and to relate these to neuropathological features and PrPsc isoform, which would require the samples to be taken adjacent to the samples taken for histopathological analysis. We also wish to test the effects on RNA yield of storing the tissue freshly frozen or frozen in RNALater solution. We understand that the timing, number and final diagnosis of suspected CJD cases is not predictable but if we were able to obtain specimens from three cases (one of which was a case of CJD) over the next six months, this would be sufficient for this part of our study.

SAMPLES

Brain region	Storage	Replicates	Code
Frontal cortex	Freshly frozen	Sample #1	F R 1
		Sample #2	F R 2
		Sample #3	F R 3
	RNALater	Sample #1	RNA 1
		Sample #2	RNA 2
		Sample #3	RNA 3
Cerebellar cortex	Freshly frozen	Sample #1	F R 1
		Sample #2	F R 2
		Sample #3	F R 3
	RNALater	Sample #1	RNA 1

		Sample #2	RNA 2
		Sample #3	RNA 3

If agreed to then we will provide additional containers for the autopsy set as follows:

12 universals:- 6 containing clear, colourless liquid (RNAlater) and 6 empty. All labelled with "Risk of Infection" sign, patient's RU number and specimen code (above), and containing in 2 individual plastic bags. If possible, sample sizes would be ~1-1.5g pieces cut from adjacent areas of the tissue.

9.5 EMERGENCY RESPONSE INFORMATION

These specimens are packed in compliance with IATA packing instructions 650.
There is no immediate hazard to health unless the goods are ingested or injected into the body.
There is no risk of fire or explosion.
In the event of an accident, disposable gloves to be worn for handling the material.
Surfaces that have been in contact with dangerous goods to be wiped with 2M NaOH and left for 1 hour- then wash.
In the event of fire- the infectious agent is destroyed.
Spillage in the absence of fire- wipe areas with 2M NaOH and leave for 1 hour- then wash.
First Aid measures- any skin that has had contact with dangerous goods may be wiped with 2M NaOH for 2 minutes- then washed well.

9.6 Points for basic precautions required for disinfection and decontamination.

	Basic precautions for disinfection and decontamination
1	Clean instruments thoroughly at least twice to remove body fluids prior to disinfection.
2	Use automated decontamination processes where possible, and avoid mixing routine instruments with those used in TSE-related work in the same cycle.
3	Recycle durable items for re-use only after appropriate decontamination- use only stringent autoclaving procedures or recommended chemical disinfection methods.
4	Where possible, cover surfaces with disposable material, which can be removed and incinerated; otherwise clean and decontaminate surfaces thoroughly- use only recommended decontamination procedures.
5	Use absorbent material to soak up spillages, which can then be contained and incinerated.
6	Use leak-proof containers, e.g. double-bagging, for the safe handling of clinical waste.
7	Avoid external contamination of the waste container.
8	Wear protective clothing at all times.

Table 9.2. NCJDSU basic health and safety precautions for work in CL3* (with derogations) laboratory.

9.7 Annex 3 of the WHO infection control guidelines: Decontamination methods for Transmissible Spongiform Encephalopathies

The safest and most unambiguous method for ensuring that there is no risk of residual infectivity on contaminated instruments and other materials is to discard and destroy them by incineration. In some healthcare situations, as described in the guidance, one of the following less effective methods may be preferred. Wherever possible, instruments and other materials subject to re-use should be kept moist between the time of exposure to infectious materials and subsequent decontamination

and cleaning. If it can be done safely, removal of adherent particles through mechanical cleaning will enhance the decontamination process.

The following recommendations are based on the best available evidence at this time and are listed in order of more to less severe treatments. These recommendations may require revision if new data become available.

1. Incineration
2. Use for all disposable instruments, materials, and wastes.
3. Preferred method for all instruments exposed to high infectivity tissues.
4. Autoclave/chemical methods for heat-resistant instruments

WHO Infection Control Guidelines for Transmissible Spongiform Encephalopathies

1. Immerse in sodium hydroxide (NaOH)[20] and heat in a gravity displacement autoclave at 121°C for 30 min; clean; rinse in water and subject to routine sterilization.
2. Immerse in NaOH or sodium hypochlorite[21] for 1 hr; transfer instruments to water; heat in a gravity displacement autoclave at 121°C for 1 hr; clean and subject to routine sterilization.
3. Immerse in NaOH or sodium hypochlorite for 1 hr.; remove and rinse in water, then transfer to open pan and heat in a gravity displacement (121°C) or porous load (134°C) autoclave for 1 hr.; clean and subject to routine sterilization.
4. Immerse in NaOH and boil for 10 min at atmospheric pressure; clean, rinse in water and subject to routine sterilization.
5. Immerse in sodium hypochlorite (preferred) or NaOH (alternative) at ambient temperature for 1 hr; clean; rinse in water and subject to routine sterilization.
6. Autoclave at 134°C for 18 minutes.[22]

[20] Unless otherwise noted, the recommended concentration is 1N NaOH.

[21] Unless otherwise noted, the recommended concentration is 20 000 ppm available chlorine.

[22] In worse-case scenarios (brain tissue bake-dried on to surfaces) infectivity will be largely but not completely removed.

WHO Infection Control Guidelines for Transmissible Spongiform Encephalopathies

4. Chemical methods for surfaces and heat sensitive instruments

1. Flood with 2N NaOH or undiluted sodium hypochlorite; let stand for 1 hr.; mop up and rinse with water.

2. Where surfaces cannot tolerate NaOH or hypochlorite, thorough cleaning will remove most infectivity by dilution and some additional benefit may be derived from the use of one or another of the partially effective methods listed in Section 5.1 (Table 8).

3. Autoclave/chemical methods for dry goods

4. Small dry goods that can withstand either NaOH or sodium hypochlorite should first be immersed in one or the other solution (as described above) and then heated in a porous load autoclave at ≥ 121°C for 1 hr.

5. Bulky dry goods or dry goods of any size that cannot withstand exposure to NaOH or sodium hypochlorite should be heated in a porous load autoclave at 134°C for 1 hr.

WHO Infection Control Guidelines for Transmissible Spongiform Encephalopathies.

5. Notes about autoclaving and chemicals

Gravity displacement autoclaves: Air is displaced by steam through a port in the bottom of the chamber. Gravity displacement autoclaves are designed for general decontamination and sterilization of solutions and instruments. Porous load autoclaves: Air is exhausted by vacuum and replaced by steam. Porous load autoclaves are optimized for sterilization of clean instruments, gowns, drapes, towelling, and other dry materials required for surgery. They are not suitable for liquid sterilization.

Sodium Hydroxide (NaOH, or soda lye): Be familiar with and observe safety guidelines for working with NaOH. 1N NaOH is a solution of 40 g NaOH in 1 litre of water. 1 N NaOH readily reacts with CO_2 in air to form carbonates that neutralize NaOH and diminish its disinfective properties. 10 N NaOH solutions do not absorb CO_2, therefore, 1N NaOH working solutions should be prepared fresh for each use either from solid NaOH pellets, or by dilution of 10 N NaOH stock solutions.

Sodium hypochlorite (NaOCl solution, or bleach): Be familiar with and observe safety guidelines for working with sodium hypochlorite. Household or industrial

strength bleach is sold at different concentrations in different countries, so that a standard dilution cannot be specified. Efficacy depends upon the concentration of available chlorine and should be 20 000 ppm available chlorine. One common commercial formulation is 5.25% bleach, which contains 25 000 ppm chlorine. Therefore, undiluted commercial bleach can be safely used. If solid precursors of hypochloric acid is available, then stock solution and working solutions can be prepared fresh for each use.

WHO Infection Control Guidelines for Transmissible Spongiform Encephalopathies.
6. Cautions regarding hazardous materials
In all cases, hazardous materials guidelines must be consulted.
1. Personnel
NaOH is caustic but relatively slow acting at room temperature, and can be removed from skin or clothing by thorough rinsing with water. Hot NaOH is aggressively caustic, and should not be handled until cool. The hazard posed by hot NaOH explains the need to limit boiling to 10 minutes, the shortest time known to be effective.
Hypochlorite solutions continuously evolve chlorine and so must be kept tightly sealed and away from light. The amount of chlorine released during inactivation may be sufficient to create a potential respiratory hazard unless the process is carried out in a well-ventilated or isolated location.
2. Material
In principle, NaOH does not corrode stainless steel, but in practice some formulations of stainless steel can be damaged (including some used for surgical instruments). It is advisable to test a sample or consult with the manufacturer before dedicating a large number of instruments to decontamination procedures. NaOH is known to be corrosive to glass and aluminum. Hypochlorite does not corrode glass or aluminum and has also been shown to be an effective sterilizing agent; it is, however, corrosive both to stainless steel and to autoclaves and (unlike NaOH) cannot be used as an instrument bath in the autoclave. If hypochlorite is used to clean or soak an instrument, it must be completely rinsed from the surfaces before autoclaving. Other

decontamination methods may need testing, or consultation with the manufacturer to verify their effect on the instrument.

9.8 FUMIGATION OF MICROBIOLOGICAL SAFETY CABINET(S)

The equipment is supplied with a Formalin vaporisor unit (fixed to cabinet).

Switch off cabinet fans.

Switch off cabinet lights.

Fit the night door and ensure properly fitted so there are no leaks into the open laboratory.

Measure approximately 35-40 mls formalin BP, remove screw cap on unit and pour in contents.

Replace the cap and tighten securely.

Press the vaporisor switch on control panel. A lamp on the switch illuminates to show the power on. A second lamp on the vaporisor unit also illuminates indicating that the heating elements are working.

After approximately 10 minutes, the formalin BP will have vaporized.

Leave the cabinet in this condition, preferably overnight, but for a minimum of 3 hours.

Purge the cabinet by simply running the exhaust fan and removing the night door high velocity inlet bung. After a few minutes the night door may be removed and purging allowed to continue for at least 30 minutes.

NOTE: From time to time, the boiling pot should be cleaned of residual Formaldehyde polymers, by heating the pot with water containing a small amount of mild detergent.

9.9 INDEX OF AGONAL STATE SCORES

Table 9.3 details the IAS scored for all 21 vCJD and 26 OND patients for which the NCJDSU had clinical and/or histological reports.

RU No.	CJDU No.	AGE	SEX	DEATH	ONSET	DURATION SCORE-1/9mnths	MODE OF DEATH	SEIZURES	COMA	HYPOXIA	PYREXIA	DEHYDRATION	HYPOGLYCEMIA	MULTIPLE ORGAN FAILURE	HEAD INJURY	NEUROTOXIC SUBSTANCES
01/69	1309	28	F	15/06/01	15/09/00	1	4	0	0	0	0	0	0	0	0	0
01/76	1318	26	M	10/07/01	15/09/00	2	4	0	0	0	0	1	0	0	0	0
01/88	1368	30	F	30/08/01	15/10/00	2	4	0	0	0	0	0	0	0	0	0
00/101	1184	27	M	15/10/00	15/12/99	2	4	0	0	1	0	1	1	0	0	0
00/25	1015	17	F	21/03/00	Sep-98	2	4	0	0	1	0	0	0	0	0	0
00/29	1070	27	M	13/02/00	01/04/99	2	4	0	1	0	0	0	0	0	0	0
00/57	949	17	M	26/02000	Jun-01	3	4	0	0	0	0	0	1	0	0	0
02/103	1553	53	F	25/11/02	Oct-01	2	4	0	0	0/1	0	0	0	0	0	0
96/07	467	30	F	25/05/96	15/08/95	1	4	0	0	0	1	1	1	0	0? multiple falls	0
96/110	571	35	F	13/09/96	15/07/95	2	4	0	0	0	0	1	1	0	head injury 08/96	0
96/45	497	31	M	17/02/96	19/09/94	2	4	0	1	0	0	0	0	0	0	0
97/221	623	25	M	06/02/97	Dec-95	2	4	0	0	0	0	1	1	0	0	0
97/282	707	36	M	20/10/97	Dec-96	2	4	0	0	0	1	0	0	0	0	0

98/148	834	20	M	10/10/98	Nov-97	2	4	1	0	0	0	1	1	0	0	0
98/154	845	36	M	22/10/98	15/07/97	2	4	0		0		1	1	0		
98/155	869	39	M	13/10/98	01/11/97	2	4	1	0	0	0	1	1	0	0	0
99/100	730	17	F	02/09/99	Aug-96	4	4	0		1		1	0			
99/129	1016	33	M	28/11/99	01/04/19	1	4			0		1	1	0	0	
99/15	927	51	F	26/01/99	Feb-98	2	4	0	1	1	1	1	1	0	0	0
99/82	907	39	M	20/07/99	01/05/98	2	4	0	0	1	0	0	0	0	1	0
99/90	1030	29	M	07/08/99	Jan-99	1	4	1	0	2	0	0	0	0	0	0
01/84	\	71	M				4									
07/2006	\	68	M				4			1						
02/14	\	25	F				4	1	0	0	0	0	0	0	0	0
00/49	1135	67	M	02/05/00	Nov-99	1	4	1	0	1	0	1	1	0	1	
03/132	\	40	M				3	0	1	1	0	1	1	0	0	0
24/2005	\	86	M				4				1					
31/2005	\	70	F				4	1	0	1						
33/2005	\	85	F				4	1	0	1	1	0	0	1	0	
67/2004	2270	66	F	18/10/04	01/05/04	1	4		0	1				0	1	

89/2005	\	76	M				1									
93/17	\	43	M				4			2				0	1	
94/132	338	74	F	30/08/94	6yr history of PD		4			2		0	0	0		
94/135	\	?	M				4									
94/140	\	69	M				4			1		0	0	0		
94/154	344	54	M	25/12/94	Jun-94	1	4	0	0	2		1	1	0		
94/75	\	44	F				2			0						
97/03	\	68	F				4	0	0	2	1	2	2	0		
97/14	\	47	F				4			2						
97/265	719	72	M	01/10/97	Jun-97	1	4	1	0	2	0	1	1	0	0	0
98/144	891	77	F	27/09/98			4	0	0	1	1	0	0	0	1	0
98/145	\	67	M				4			1		1				
98/70	828	79	M	15/05/98	01/02/98	1	1	0	0	2	1	0	0	0	1	0
99/118	\	78	M				4			\		\	\			
99/20	\	78	M				4			1		1	1	0		
99/54	995	79	M				4			0		0	0			

99/61	1010	55	M	29/05/99	20/04/99	1	4			0		0	0			

Table 9.3. Index of Agonal State scores for vCJD and OND cases. Yellow shading: vCJD. White/grey shading: OND. Grey shading indicates cases with clinical or histological notes missing. Green shading: factors which were scored 0-absence, 1-evidence, 2-severe. The duration of illness was calculated from the dates of death and onset from the patient notes, and scored 1 for every 9months duration. Mode of death scores are detailed in Chapter 4. All other factors are scored 0-absence, 1-presence.

9.10 GENE EXPRESSION DATA

Table 9.4. Gene table Oligo GEArray® Human Alzheimer's Disease Microarray. Numbers represent gene spot position (p.338).

Table 9.5. Gene table for Oligo GEArray® Human Signal Transduction PathwayFinder Microarray. Numbers represent gene spot position (p.339).

RPS27A 1	A2M 2	ABCA1 3	ACE 4	ACHE 5	ADAM10 6	ADAM17 7	ADAM9 8
AGPS 9	APBA1 10	APBA3 11	APBB1 12	APBB2 13	APBB3 14	APH1A 15	APLP1 16
APLP2 17	APOA1 18	APOE 19	APP 20	NAE1 21	BACE1 22	BACE2 23	BCHE 24
BDNF 25	CASP3 26	CASP4 27	CDC2 28	CDK5 29	CDKL1 30	CHAT 31	CLU 32
CTSB 33	CTSC 34	CTSD 35	CTSG 36	CTSL1 37	DHCR24 38	ECE2 39	EGR3 40
EP300 41	ERN1 42	ERN2 43	BPTF 44	GAL 45	GAP43 46	GNAO1 47	GNAZ 48
GNB1 49	GNB2 50	GNB4 51	GNB5 52	GNG10 53	GNG11 54	GNG12 55	GNG13 56
GNG3 57	GNG4 58	GNG5 59	GNG7 60	GNG8 61	GNGT1 62	GNGT2 63	GSK3A 64
GSK3B 65	HSD17B10 66	IDE 67	IL1A 68	INS 69	INSR 70	LPL 71	LRP1 72
LRP10 73	LRP3 74	LRP4 75	LRP5 76	LRP6 77	LRP8 78	MAP2 79	MAPT 80
MME 81	MPO 82	NCSTN 83	NPY 84	PDE7B 85	PHF1 86	PKP4 87	PLAT 88
PLAU 89	PLG 90	PRKCA 91	PRKCB1 92	PRKCD 93	PRKCE 94	PRKCG 95	PRKCI 96
PRKCQ 97	PRKCZ 98	PSEN1 99	PSEN2 100	SCARA3 101	SERPINA13 102	SERPINA3 103	SGCA 104
SNCA 105	SNCB 106	SPINT2 107	SST 108	SYP 109	TFAP4 110	UBQLN1 111	UQCRC1 112
UQCRC2 113	VSNL1 114	PUC18 115	Blank 116	Blank 117	AS1R2 118	AS1R1 119	AS1 120
GAPDH 121	B2M 122	HSP90AB1 123	HSP90AB1 124	ACTB 125	ACTB 126	BAS2C 127	BAS2C 128

RPS27A 1	A2M 2	ATF2 3	BAX 4	BCL2 5	BCL2A1 6	BCL2L1 7	NAIP 8
BIRC2 9	BIRC3 10	BIRC5 11	BMP2 12	BMP4 13	BRCA1 14	CCL2 15	CCL20 16
CCND1 17	CD5 18	CDK2 19	CDKN1A 20	CDKN1B 21	CDKN1C 22	CDKN2A 23	CDKN2B 24
CDKN2C 25	CDKN2D 26	CDX1 27	CEBPB 28	CSF2 29	CSN2 30	CTSD 31	CXCL12 32
CXCL9 33	CYP19A1 34	EGFR 35	EGR1 36	EN1 37	FASN 38	STRA6 39	FN1 40
FOS 41	FOXA2 42	GADD45A 43	GREB1 44	GYS1 45	HHIP 46	HK2 47	HOXA1 48
HOXB1 49	HSF1 50	HSPB1 51	HSP90AA2 52	ICAM1 53	IGFBP3 54	IGFBP4 55	IKBKB 56
IL1A 57	IL2 58	IL2RA 59	IL4 60	IL4R 61	IL8 62	NOS2A 63	IRF1 64
JUN 65	JUNB 66	KLK2 67	KLK3 68	LEF1 69	LEP 70	LTA 71	MDM2 72
MMP10 73	MMP7 74	MYC 75	NAB2 76	NFKB1 77	NFKBIA 78	NRIP1 79	ODC1 80
PECAM1 81	PGR 82	PPARG 83	PRKCA 84	PRKCB1 85	PRKCE 86	PTCH1 87	PTCH2 88
PTGS2 89	RBBP8 90	RBP1 91	RBP2 92	SELE 93	SELPLG 94	TANK 95	TCF7 96
TERT 97	TFRC 98	TMEPAI 99	TNF 100	TNFRSF10B 101	FAS 102	FASLG 103	TP53 104
TP53I3 105	TRIM25 106	VCAM1 107	VEGFA 108	WISP1 109	WISP2 110	WISP3 111	WNT1 112
WNT2 113	WSB1 114	PUC18 115	Blank 116	Blank 117	AS1R2 118	AS1R1 119	AS1 120
GAPDH 121	B2M 122	HSP90AB1 123	HSP90AB1 124	ACTB 125	ACTB 126	BAS2C 127	BAS2C 128

9.10.1 GEAnalysis Expression Suite Formulae for Data Analysis

CLUSTERGRAM

Clicking the Clustergram menu item generates a simple cluster diagram that calculates the correlation of the genes in a project. The correlation coefficient is used to express similarity. The formula for the correlation coefficient between two-dimensional profiles is:

$$\rho_{X,Y} = \frac{Cov(X,Y)}{\sigma_X \sigma_Y} = \frac{\sum_{i=1}^{n}(X_i - \mu_X)(Y_i - \mu_Y)}{\sqrt{\sum_{i=1}^{n}(X_i - \mu_X)^2 \cdot \sum_{i=1}^{n}(Y_i - \mu_Y)^2}}$$

5. Background correction methods

a. Terms

xk – brightness of k-th pixel in X area (measured but not included to readout).

Nx – number of pixels belonging to X area (measured when building readout).

Ix – sum of brightness of pixels belonging to X area (measured when building readout).

$$I_x = \sum_{k=1}^{N_x} x_k$$

V – spot brightness (total) *q* – average value of *q*

Areas on image: S – spot, C – clover area excluding spots (if applicable), L – local background.

Total Density: $V = I_s$

$$\langle V \rangle = \frac{I_s}{N_s}$$

Average density:

b. No correction

1. No clover:

$V = I_s$,

$$\langle V \rangle = \frac{I_s}{N_s}$$

2. Clover included:

$V = I_v + I_c$,

$$\langle V \rangle = \frac{I_v + I_c}{N_v + N_c}.$$

c. Background correction

1. No clover:

$V = I_s - \langle B \rangle \cdot N_s$,

$$\langle V \rangle = \frac{I_s}{N_s} - \langle B \rangle.$$

2. Clover included:

$V = I_v + I_c - \langle B \rangle \cdot (N_s + N_c)$,

$$\langle V \rangle = \frac{I_v + I_c}{N_v + N_c} - \langle B \rangle.$$

Where *B* is average brightness of background area calculated in the following way:

1. Local background

$$\langle B \rangle = \frac{I_L}{N_L}$$

2. Empty cells

$\langle B \rangle = \frac{\sum I_s}{\sum N_s}$ (no clover), summation by empty cells

3. Global background

$\langle B \rangle = \frac{\sum I_L}{\sum N_L}$, summation by all cells

4. “Brightest” spot

$\langle B \rangle = \langle V \rangle$, $\langle V \rangle$ is the minimum average value for all spots, calculated with the assigned “clover” mode.

6. Normalization

a. Terms

V – raw spot brightness

N – normalized spot brightness

b. Calculation

1. Selected genes:

$$N_I = \frac{V_I}{(\sum_{k=1}^{K} V_k)/K}$$

, where K is number of selected genes.

2. Median:

$$N_I = \frac{V_I}{M}$$

, where M is median of all spots brightness

3. Interquartile:

$$N_I = \frac{V_I}{(\sum_{t=1}^{T} V_t)/T}$$

, where T is number of spots in the interquartile range of all spots brightness's. Summation by all spots in the interquartile range.

c. Dataset Adjustment

1. Adjust to common mean: $A_I = N_I \times D / M$, where M is mean value of all genes brightness's for current sample and D is desired mean value.

2. Adjust minimal positive value: $$E_I = \begin{cases} A_I, & if\ A_I \geq K \\ K, & if\ A_I < K \end{cases}$$,where $K = D/100 \times M$, D is desired minimal value in percents from M, and M is mean of value of all genes brightness's for current sample.

9.10.2 Tabulated gene names for comparison group 1- AD arrays

CHART POSITION	GENE NAME
1	Ribosomal protein S27a
2	Alpha-2-macroglobulin
3	ATP-binding cassette, sub-family A (ABC1), member 1
4	Angiotensin I converting enzyme (peptidyl-dipeptidase A) 1
5	ADAM metallopeptidase domain 17 (tumor necrosis factor, alpha, converting enzyme)
6	Amyloid beta (A4) precursor protein-binding, family A, member 3 (X11-like 2)
7	Amyloid beta (A4) precursor protein-binding, family B, member 1 (Fe65)
8	Anterior pharynx defective 1 homolog A (C. elegans)
9	Amyloid beta (A4) precursor-like protein 1
10	Apolipoprotein A-I
11	Apolipoprotein E
12	Amyloid beta (A4) precursor protein (peptidase nexin-II, Alzheimer disease)
13	Beta-site APP-cleaving enzyme 2
14	Butyrylcholinesterase
15	Caspase 3, apoptosis-related cysteine peptidase
16	Caspase 4, apoptosis-related cysteine peptidase
17	Cell division cycle 2, G1 to S and G2 to M
18	Cyclin-dependent kinase 5
19	Cyclin-dependent kinase-like 1 (CDC2-related kinase)
20	Clusterin
21	Cathepsin C
22	Cathepsin D
23	Cathepsin G
24	Cathepsin L1

25	Endoplasmic reticulum to nucleus signalling 2
26	Bromodomain PHD finger transcription factor
27	Guanine nucleotide binding protein (G protein), alpha z polypeptide
28	Guanine nucleotide binding protein (G protein), beta polypeptide 4
29	Guanine nucleotide binding protein (G protein), gamma 7
30	Guanine nucleotide binding protein (G protein), gamma 8
31	Glycogen synthase kinase 3 beta
32	Insulin-degrading enzyme
33	Interleukin 1, alpha
34	Insulin
35	Lipoprotein lipase
36	Low density lipoprotein receptor-related protein 10
37	Microtubule-associated protein 2
38	Nicastrin
39	Neuropeptide Y
40	Phosphodiesterase 7B
41	Plakophilin 4
42	Plasminogen activator, urokinase
43	Plasminogen
44	Protein kinase C, alpha
45	Protein kinase C, beta 1
46	Protein kinase C, iota
47	Protein kinase C, theta
48	Protein kinase C, zeta
49	Synuclein, alpha (non A4 component of amyloid precursor)
50	Synuclein, beta
51	Somatostatin
52	Ubiquinol-cytochrome c reductase core protein II
53	Visinin-like 1

54	Heat shock protein 90kDa alpha (cytosolic), class B member 1
55	Heat shock protein 90kDa alpha (cytosolic), class B member 1
56	Actin, beta
57	Actin, beta

Table 9.6. Gene names for graph 6.14. Comparison group 1, AD arrays.

9.10.3 Tabulated gene names for comparison group 2- AD arrays

CHART POSITION	GENE NAME
1	ATP-binding cassette, sub-family A (ABC1), member 1
2	Angiotensin I converting enzyme (peptidyl-dipeptidase A) 1
3	ADAM metallopeptidase domain 10
4	ADAM metallopeptidase domain 17 (tumor necrosis factor, alpha, converting enzyme)
5	ADAM metallopeptidase domain 9 (meltrin gamma)
6	Alkylglycerone phosphate synthase
7	Amyloid beta (A4) precursor protein-binding, family A, member 1 (X11)
8	Amyloid beta (A4) precursor protein-binding, family A, member 3 (X11-like 2)
9	Amyloid beta (A4) precursor protein-binding, family B, member 1 (Fe65)
10	Amyloid beta (A4) precursor-like protein 1
11	Apolipoprotein A-I
12	Apolipoprotein E
13	Amyloid beta (A4) precursor protein (peptidase nexin-II, Alzheimer disease)
14	Brain-derived neurotrophic factor
15	Caspase 3, apoptosis-related cysteine peptidase
16	Caspase 4, apoptosis-related cysteine peptidase

17	Cell division cycle 2, G1 to S and G2 to M
18	Cathepsin C
19	Cathepsin D
20	Cathepsin G
21	Endoplasmic reticulum to nucleus signalling 2
22	Bromodomain PHD finger transcription factor
23	Guanine nucleotide binding protein (G protein), gamma transducing activity polypeptide 1
24	Interleukin 1, alpha
25	Insulin
26	Insulin receptor
27	Low density lipoprotein receptor-related protein 10
28	Low density lipoprotein receptor-related protein 4
29	Low density lipoprotein receptor-related protein 5
30	Low density lipoprotein receptor-related protein 6
31	Microtubule-associated protein 2
32	Microtubule-associated protein tau
33	Myeloperoxidase
34	Nicastrin
35	Neuropeptide Y
36	Phosphodiesterase 7B
37	PHD finger protein 1
38	Plasminogen activator, tissue
39	Plasminogen
40	Protein kinase C, alpha
41	Protein kinase C, beta 1
42	Protein kinase C, delta
43	Protein kinase C, epsilon
44	Protein kinase C, iota
45	Protein kinase C, zeta
46	Serpin peptidase inhibitor, clade A (alpha-1 antiproteinase,

	antitrypsin), member 3
47	Somatostatin
48	Ubiquinol-cytochrome c reductase core protein II

Table 9.7.Gene names for graph 6.14. Comparison group 2, AD arrays.

9.10.4 Tabulated gene names for comparison group 5- AD arrays

CHART POSTION	GENE NAME
1	Ribosomal protein S27a
2	ATP-binding cassette, sub-family A (ABC1), member 1
3	Angiotensin I converting enzyme (peptidyl-dipeptidase A) 1
4	ADAM metallopeptidase domain 10
5	ADAM metallopeptidase domain 17 (tumor necrosis factor, alpha, converting enzyme)
6	ADAM metallopeptidase domain 9 (meltrin gamma)
7	Amyloid beta (A4) precursor protein-binding, family A, member 3 (X11-like 2)
8	Amyloid beta (A4) precursor protein (peptidase nexin-II, Alzheimer disease)
9	Caspase 3, apoptosis-related cysteine peptidase
10	Choline acetyltransferase
11	Clusterin
12	Endoplasmic reticulum to nucleus signalling 2
13	Guanine nucleotide binding protein (G protein), alpha activating activity polypeptide O
14	Guanine nucleotide binding protein (G protein), beta polypeptide 1
15	Guanine nucleotide binding protein (G protein), gamma transducing activity polypeptide 1

16	Guanine nucleotide binding protein (G protein), gamma transducing activity polypeptide 2
17	Glycogen synthase kinase 3 alpha
18	Insulin
19	Insulin receptor
20	Lipoprotein lipase
21	Low density lipoprotein-related protein 1 (alpha-2-macroglobulin receptor)
22	Microtubule-associated protein 2
23	Microtubule-associated protein tau
24	Neuropeptide Y
25	PHD finger protein 1
26	Plasminogen activator, tissue
27	Protein kinase C, beta 1
28	Protein kinase C, epsilon
29	Protein kinase C, iota
30	Synuclein, beta
31	Somatostatin
32	Visinin-like 1
33	Heat shock protein 90kDa alpha (cytosolic), class B member 1
34	Heat shock protein 90kDa alpha (cytosolic), class B member 1
35	Actin, beta
36	Actin, beta

Table 9.8. Gene names for graph 6.14. Comparison group 5, AD arrays.

9.10.5 Tabulated gene names for significantly modulated genes- AD arrays

CHART POSITION	GENE NAME
1	Ribosomal protein S27a
2	ATP-binding cassette, sub-family A (ABC1), member 1
3	Amyloid beta (A4) precursor protein-binding, family A, member 1 (X11)
4	Amyloid beta (A4) precursor protein-binding, family A, member 3 (X11-like 2)
5	Anterior pharynx defective 1 homolog A (C. elegans)
6	Amyloid beta (A4) precursor-like protein 1
7	Apolipoprotein A-I
8	Apolipoprotein E
9	Amyloid beta (A4) precursor protein (peptidase nexin-II, Alzheimer disease)
10	Beta-site APP-cleaving enzyme 2
11	Butyrylcholinesterase
12	Brain-derived neurotrophic factor
13	Cyclin-dependent kinase 5
14	Choline acetyltransferase
15	Clusterin
16	Cathepsin B
17	Cathepsin D
18	Endoplasmic reticulum to nucleus signalling 2
19	Bromodomain PHD finger transcription factor
20	Guanine nucleotide binding protein (G protein), beta polypeptide 1
21	Guanine nucleotide binding protein (G protein), beta polypeptide 2
22	Guanine nucleotide binding protein (G protein), beta polypeptide

	4
23	Guanine nucleotide binding protein (G protein), gamma 5
24	Glycogen synthase kinase 3 alpha
25	Interleukin 1, alpha
26	Lipoprotein lipase
27	Low density lipoprotein receptor-related protein 10
28	Neuropeptide Y
29	Plasminogen activator, tissue
30	Plasminogen activator, urokinase
31	Protein kinase C, beta 1
32	Protein kinase C, iota
33	Protein kinase C, zeta
34	Presenilin 1 (Alzheimer disease 3)
35	Serpin peptidase inhibitor, clade A (alpha-1 antiproteinase, antitrypsin), member 13 (pseudogene)
36	Serpin peptidase inhibitor, clade A (alpha-1 antiproteinase, antitrypsin), member 3
37	Synuclein, alpha (non A4 component of amyloid precursor)
38	Synuclein, beta
39	Serine peptidase inhibitor, Kunitz type, 2
40	Somatostatin
41	Ubiquinol-cytochrome c reductase core protein I
42	Ubiquinol-cytochrome c reductase core protein II
43	Visinin-like 1
44	Heat shock protein 90kDa alpha (cytosolic), class B member 1
45	Heat shock protein 90kDa alpha (cytosolic), class B member 1
46	Actin, beta
47	Actin, beta

Table 9.9 .Gene names for graph 6.18 from all significantly modulated genes identified on the AD arrays.

9.10.6 Tabulate gene names for comparison group 1- ST Arrays

CHART POSITION	GENE NAME
1	B-cell CLL/lymphoma 2
2	BCL2-related protein A1
3	BCL2-like 1
4	NLR family, apoptosis inhibitory protein
5	Chemokine (C-C motif) ligand 2
6	Chemokine (C-C motif) ligand 20
7	Cyclin-dependent kinase inhibitor 1A (p21, Cip1)
8	Cyclin-dependent kinase inhibitor 1B (p27, Kip1)
9	Cyclin-dependent kinase inhibitor 2B (p15, inhibits CDK4)
10	Cyclin-dependent kinase inhibitor 2D (p19, inhibits CDK4)
11	Cathepsin D
12	Chemokine (C-X-C motif) ligand 12 (stromal cell-derived factor 1)
13	Chemokine (C-X-C motif) ligand 9
14	Early growth response 1
15	Engrailed homeobox 1
16	Fatty acid synthase
17	Stimulated by retinoic acid gene 6 homolog (mouse)
18	Fibronectin 1
19	V-fos FBJ murine osteosarcoma viral oncogene homolog
20	Forkhead box A2
21	Hexokinase 2
22	Homeobox A1
23	Homeobox B1
24	Heat shock protein 90kDa alpha (cytosolic), class A member 2
25	Inhibitor of kappa light polypeptide gene enhancer in B-cells, kinase beta

26	Interleukin 1, alpha
27	Interleukin 4 receptor
28	Interleukin 8
29	Nitric oxide synthase 2A (inducible, hepatocytes)
30	Interferon regulatory factor 1
31	Lymphotoxin alpha (TNF superfamily, member 1)
32	Nuclear factor of kappa light polypeptide gene enhancer in B-cells inhibitor, alpha
33	Nuclear receptor interacting protein 1
34	Ornithine decarboxylase 1
35	Platelet/endothelial cell adhesion molecule (CD31 antigen)
36	Protein kinase C, beta 1
37	Protein kinase C, epsilon
38	Patched homolog 1 (Drosophila)
39	Patched homolog 2 (Drosophila)
40	Prostaglandin-endoperoxide synthase 2 (prostaglandin G/H synthase and cyclooxygenase)
41	Retinoblastoma binding protein 8
42	Retinol binding protein 2, cellular
43	Selectin E (endothelial adhesion molecule 1)
44	Selectin P ligand
45	TRAF family member-associated NFKB activator
46	Transcription factor 7 (T-cell specific, HMG-box)
47	Telomerase reverse transcriptase
48	Transmembrane, prostate androgen induced RNA
49	Tumor necrosis factor (TNF superfamily, member 2)
50	Fas (TNF receptor superfamily, member 6)
51	Fas ligand (TNF superfamily, member 6)
52	Tripartite motif-containing 25
53	Vascular endothelial growth factor A
54	WNT1 inducible signaling pathway protein 1

55	WNT1 inducible signaling pathway protein 2
56	WNT1 inducible signaling pathway protein 3
57	Wingless-type MMTV integration site family member 2
58	WD repeat and SOCS box-containing 1

Table 9.10. Gene names for graph 6.32. Comparison group 1, ST arrays.

9.10.7 Tabulated gene names for comparison group 2-ST Arrays

CHART POSITION	GENE NAME
1	B-cell CLL/lymphoma 2
2	BCL2-related protein A1
3	Bone morphogenetic protein 4
4	Chemokine (C-C motif) ligand 2
5	Cyclin D1
6	Cyclin-dependent kinase inhibitor 1A (p21, Cip1)
7	Cyclin-dependent kinase inhibitor 1B (p27, Kip1)
8	Cyclin-dependent kinase inhibitor 2D (p19, inhibits CDK4)
9	Early growth response 1
10	Fatty acid synthase
11	V-fos FBJ murine osteosarcoma viral oncogene homolog
12	GREB1 protein
13	Hedgehog interacting protein
14	Hexokinase 2
15	Homeobox A1
16	Heat shock protein 90kDa alpha (cytosolic), class A member 2
17	Insulin-like growth factor binding protein 3
18	Insulin-like growth factor binding protein 4
19	Interleukin 4
20	Interleukin 4 receptor

21	Interleukin 8
22	Nitric oxide synthase 2A (inducible, hepatocytes)
23	Interferon regulatory factor 1
24	Leptin (obesity homolog, mouse)
25	Lymphotoxin alpha (TNF superfamily, member 1)
26	Mdm2, transformed 3T3 cell double minute 2, p53 binding protein (mouse)
27	Ornithine decarboxylase 1
28	Platelet/endothelial cell adhesion molecule (CD31 antigen)
29	Protein kinase C, beta 1
30	Prostaglandin-endoperoxide synthase 2 (prostaglandin G/H synthase and cyclooxygenase)
31	Transcription factor 7 (T-cell specific, HMG-box)
32	Transmembrane, prostate androgen induced RNA
33	Wingless-type MMTV integration site family member 2

Table 9.11. Gene names for graph 6.32. Comparison group 2, ST arrays.

9.10.8 Tabulated gene names for comparison group 5-ST Arrays

CHART POSITION	GENE NAME
1	Ribosomal protein S27a
2	BCL2-related protein A1
3	NLR family, apoptosis inhibitory protein
4	Cyclin-dependent kinase inhibitor 1A (p21, Cip1)
5	Cyclin-dependent kinase inhibitor 1B (p27, Kip1)
6	CCAAT/enhancer binding protein (C/EBP), beta
7	Chemokine (C-X-C motif) ligand 12 (stromal cell-derived factor 1)
8	Forkhead box A2

9	Growth arrest and DNA-damage-inducible, alpha
10	GREB1 protein
11	Hedgehog interacting protein
12	Hexokinase 2
13	Homeobox A1
14	Homeobox B1
15	Heat shock transcription factor 1
16	Heat shock 27kDa protein 1
17	Heat shock protein 90kDa alpha (cytosolic), class A member 2
18	Insulin-like growth factor binding protein 4
19	Inhibitor of kappa light polypeptide gene enhancer in B-cells, kinase beta
20	Interleukin 2
21	Interleukin 2 receptor, alpha
22	Interleukin 4
23	Interleukin 4 receptor
24	Interferon regulatory factor 1
25	Leptin (obesity homolog, mouse)
26	Lymphotoxin alpha (TNF superfamily, member 1)
27	Mdm2, transformed 3T3 cell double minute 2, p53 binding protein (mouse)
28	NGFI-A binding protein 2 (EGR1 binding protein 2)
29	Nuclear receptor interacting protein 1
30	Ornithine decarboxylase 1
31	Platelet/endothelial cell adhesion molecule (CD31 antigen)
32	Progesterone receptor
33	Protein kinase C, alpha
34	Protein kinase C, beta 1
35	Protein kinase C, epsilon
36	Patched homolog 1 (Drosophila)
37	Patched homolog 2 (Drosophila)

38	Prostaglandin-endoperoxide synthase 2 (prostaglandin G/H synthase and cyclooxygenase)
39	Retinol binding protein 1, cellular
40	Retinol binding protein 2, cellular
41	Selectin E (endothelial adhesion molecule 1)
42	Selectin P ligand
43	TRAF family member-associated NFKB activator
44	Transcription factor 7 (T-cell specific, HMG-box)
45	Telomerase reverse transcriptase
46	Tumor necrosis factor (TNF superfamily, member 2)
47	Fas (TNF receptor superfamily, member 6)
48	Fas ligand (TNF superfamily, member 6)
49	Tumor protein p53 (Li-Fraumeni syndrome)
50	Glyceraldehyde-3-phosphate dehydrogenase
51	Beta-2-microglobulin
52	Heat shock protein 90kDa alpha (cytosolic), class B member 1
53	Heat shock protein 90kDa alpha (cytosolic), class B member 1
54	Actin, beta
55	Actin, beta

Table 9.12. Gene names for graph 6.32. Comparison group 5, ST arrays.

9.10.9 Tabulated gene names for significantly modulated genes- ST Arrays

CHART POSITION	GENE NAME
1	B-cell CLL/lymphoma 2
2	BCL2-related protein A1
3	Cyclin-dependent kinase 2
4	Cyclin-dependent kinase inhibitor 1A (p21, Cip1)
5	Cyclin-dependent kinase inhibitor 1B (p27, Kip1)

6	Cyclin-dependent kinase inhibitor 2D (p19, inhibits CDK4)
7	CCAAT/enhancer binding protein (C/EBP), beta
8	Epidermal growth factor receptor (erythroblastic leukemia viral (v-erb-b) oncogene homolog, avian)
9	Early growth response 1
10	Forkhead box A2
11	GREB1 protein
12	Homeobox B1
13	Heat shock protein 90kDa alpha (cytosolic), class A member 2
14	Intercellular adhesion molecule 1 (CD54), human rhinovirus receptor
15	Insulin-like growth factor binding protein 4
16	Interleukin 1, alpha
17	Interleukin 2
18	Interleukin 4
19	Interleukin 4 receptor
20	Protein kinase C, beta 1
21	Retinol binding protein 1, cellular
22	Transmembrane, prostate androgen induced RNA
23	Tumor necrosis factor (TNF superfamily, member 2)
24	Tripartite motif-containing 25
25	Wingless-type MMTV integration site family member 2

Table 9.13. Gene names for graph 6.36 for all significantly modulated genes identified on ST arrays.

9.11 MANUSCRIPTS IN PREPARATION

- **RNA quality assessment from post-mortem human brain material.**
- **Effects of agonal and post-mortem factors on the RNA profile in extracts of post-mortem human brain tissue.**
- **Validating house-keeping genes for normalizing RNA expression in RT-PCR in extracts of post-mortem human brain tissue.**